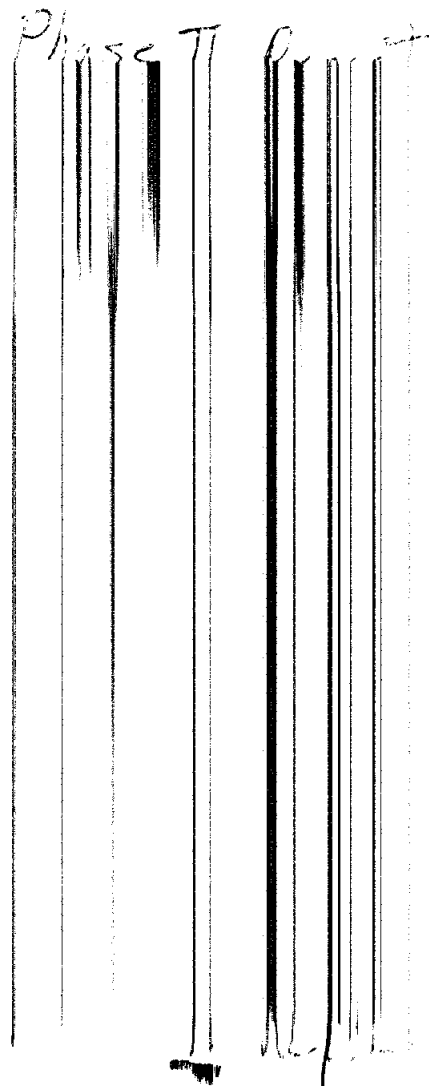


55-41009

ROBERT L. BLUNTZER



November 1954

BUREAU OF ECONOMIC GEOLOGY

THE UNIVERSITY OF TEXAS

AT AUSTIN

W. L. FISHER, DIRECTOR



November 16, 1959

Texas Salt Domes--Aspects Affecting
Disposal of Toxic-Chemical Waste
in Solution-Mined Caverns

S. J. Seni
W. F. Mullican III
H. S. Hamlin

Contract Report for Texas Department of Water Resources
under Interagency Contract No. IAC(84-85)-1019

Bureau of Economic Geology
W. L. Fisher, Director
The University of Texas at Austin
University Station, P. O. Box X
Austin, Texas 78713

TEXAS SALT DOMES--ASPECTS AFFECTING DISPOSAL OF TOXIC-CHEMICAL
WASTE IN SOLUTION-MINED CAVERNS

TABLE OF CONTENTS

INTRODUCTION	1
Organization	1
Recommendations	1
STRUCTURE, STRATIGRAPHY, AND GROWTH HISTORY	2
Structure	3
Stratigraphy	10
Growth Rates for Boling Salt Dome	20
Discussion	22
MECHANICAL BEHAVIOR OF SALT	23
Experimental Procedures	24
Creep Behavior of Salt	25
Survey of Creep Properties	26
Elastic Properties	28
Creep Experiments	28
In Situ Creep	35
Comparison of Strain Rates	43
Creep Laws	47
Steady-State Creep	48
Transient Creep	49
Exponential Creep Law	49
Logarithmic Creep Law	51
Power Creep Law	51
Discussion of Creep Laws	51
Deformation Mechanism	54
Defectless Flow--Regime 1	57
Dislocation Glide--Regime 2	57
Dislocation Limb Creep--Regime 3	57
Diffusional Creep--Regime 4	58
Unknown Mechanism--Regime 5	58
Discussion	59
SALT STOCK PROPERTIES	59
Bryan Mound Salt Dome	60
Discussion	65
CAP ROCK	66
Cap-Rock--Lost-Circulation Zones	67
Discussion	73
ACKNOWLEDGMENTS	74

FIGURE CAPTIONS

Figure 1. Distribution of Texas salt domes and salt provinces in relation to major fault zones and the Stuart City and Sligo reef trends.

Figure 2. Block diagrams of salt domes and structure on top of Cretaceous and Tertiary units in Houston Embayment (modified from Ewing, in preparation).

Figure 3. Block diagram of salt domes and structure of top of Woodbine Group in East Texas Basin (from Jackson and Seni, 1984b).

Figure 4. Structure contour map, Frio Formation around Boling, Markham, and Damon Mound salt domes. Salt-withdrawal basin for Boling dome is closed structural depression southeast of Boling dome. Regional growth faults intercept the northeast flank of Boling dome and the southwest flank of Markham dome.

Figure 5. Cross section, Boling dome and flanking strata. Salt-withdrawal basin has abundant faults in Vicksburg, Jackson, Frio, and Anahuac Formations. Top of Miocene is depressed 500 ft over salt-withdrawal basin owing to post-Miocene (younger than 5 Ma) salt flow into Boling dome.

Figure 6. Cross section, Markham dome and flanking strata. Salt-withdrawal basin is a structural sag north of dome. Major faults are absent in this orientation of cross section.

Figure 7. East-west cross section, Barbers Hill dome and flanking strata. Faulting is common through Frio and Anahuac Formations and at base of Miocene strata. Cap rock is surrounded by Evangeline aquifer.

Figure 8. North-south cross section, Barbers Hill dome and flanking strata. Faulting is common from base of Miocene to deepest control. Faults are typical down-to-the-coast (south) regional growth faults. Salt-withdrawal basin is north of dome.

Figure 9. Isopach map, Miocene and post-Miocene strata, area around Boling, Markham, and Damon Mound domes. Miocene and post-Miocene strata are 2,000 ft thicker in salt-withdrawal basin southeast of Boling dome owing to extensive syndepositional salt flow into Boling dome.

Figure 10. Isopach map, Anahuac Formation, area around Boling, Markham, and Damon Mound domes. Anahuac Formation is approximately 100 percent (600 ft) thicker in salt-withdrawal basin southeast of Boling dome owing to extensive syndepositional salt flow into Boling dome.

Figure 11. Cross section showing map intervals and correlations.

Figure 12. Idealized creep curve depicting behavior of rock salt. Transient (primary), steady-state (secondary), and accelerating (tertiary) stages of creep are separated by inflection points in the curve. The creep curve terminates at the point of brittle (sudden) failure by creep rupture.

Figure 13. In situ creep shown by convergence of floor and ceiling in an underground salt mine (after Empson and others, 1970). Heating of a nearby mine pillar causes acceleration of the rate of convergence.

Figure 14. Creep curve for artificially prepared salt showing the effect of temperature, confining pressure, and axial stress (after Le Comte, 1965).

Figure 15. Creep curves for Avery Island dome salt deformed at temperatures from 24°C to 200°C and stresses from 10.3 MPa to 20.7 MPa. Confining pressures were 3.5 MPa or above (data from Hansen and Mellegard, 1979; Hansen and Carter, 1979, 1980; after Carter and Hansen, 1983).

Figure 16. Stress-strain curve for bedded and dome salt deformed by a differential stress rate of 0.006 MPa to 0.023 MPa s⁻¹ and a confining pressure of 3.45 MPa. There is no systematic variation in creep behavior between bedded and domal salt. However, bedded salt from Lyons, Kansas, is the most creep resistant salt of those tested (after Hansen and Carter, 1980).

Figure 17. Creep curve for artificially prepared salt showing the effect of variations in grain size and axial stress on the creep behavior (after Le Comte, 1965).

Figure 18. Strain rate curve for artificially prepared salt deformed at high temperature (1013 K). Strain rates with a constant stress show a significant increase due to increases in grain size and subgrain size (cited by Hume and Shakoor, 1981; after Burke, 1968).

Figure 19. Convergence in Canadian potash mine as a function of time. Long-term convergence is nearly constant (after Baar, 1977).

Figure 20. Borehole closure of (A) Vacherie and (b) Rayburns salt domes (after Thoms and others, 1982).

Figure 21. Strain rate curve for borehole closure at Vacherie salt dome based on borehole closure data from Thoms and others (1982). Linear closure data were converted to strain data base on a nominal hole diameter of 8-3/4 inches. Strain rates were derived using four points for time control (that is, 0, 163, 413, and 890 days after drilling; see figure 20). At a given depth, strain rates were remarkably linear. Differential stresses were derived from the difference between the lithostatic load exerted by the salt and the load exerted by the borehole filled with saturated brine. Note the exponential increase in strain rate with increasing differential stress or depth.

Figure 22. Exponential creep law behavior (after Herrmann and Lauson, 1981a).

Figure 23. Logarithmic creep law behavior (after Herrmann and Lauson, 1981a).

Figure 24. Power law creep behavior (after Herrmann and Lauson, 1981a).

Figure 25. Predicted long-term closures using different creep law forms (after Wagner and others, 1982).

Figure 26. Deformation-mechanism map for salt, including probable repository and storage cavern conditions in cross-hatched area. Grain size is constant at 3 mm. Solid lines between regimes are confirmed by experimental evidence;

boundaries shown as dashed lines are based on calculations of constitutive equations; boundaries shown as dotted lines are based on interpolation or extrapolation; question marks on boundaries mean the location is based on conjecture only (after Munson, 1979).

Figure 27. Cross section, Bryan Mound dome, showing core locations and foliation. Angle of foliation decreases from vertical in deepest core to 20 to 30 degrees from vertical (no azimuth orientation) in shallow core. Flow direction is inferred to change from near vertical in deep parts of stock to more lateral flow in upper parts of stock.

Figure 28. Photographs of core, Bryan Mound dome, showing variations in grain size and foliation. Core 1A at -1,848 ft is well bedded with dark anhydrite layers and unfoliated; core 110C at -4,173 ft shows no bedding and vertical foliation.

Figure 29. Photographs of core from cap rock, A. Long Point dome, showing mineralogical variations and fractures, B. Long Point dome showing sulfur and fractures, C. Boling dome showing sulfur and vugs.

Figure 30. Map of cap-rock injection zones, Barbers Hill dome. Injection into shallow cap rock is over central part of dome, whereas injection into basal anhydrite sand is around periphery of dome.

Figure 31. Cross section, Barbers Hill dome, and cap rock showing lost-circulation zones and stylized cavern geometries. Appendix 1C lists cavern and injection well names.

TABLE CAPTIONS

Table 1. Growth rates for Boling salt dome.

Table 2. Strain rates for deformation of rock salt (modified from Jackson, 1984).

Table 3. Analysis of salt core--Bryan Mound salt dome.

APPENDICES

- Appendix 1A. List of well information for wells on maps in figures 4, 9, and 10.
- Appendix 1B. List of well information for wells on cross sections in figures 5, 6, 7, and 8.
- Appendix 1C. List of well information for wells on cross section in figure 31.
- Appendix 2. Conversion tables (modified from Paterson, 1978).
- Appendix 3. List of information on cap-rock disposal wells.

INTRODUCTION

This report is Phase II of a one-year contract to analyze technical issues associated with the proposed isolation of toxic-chemical waste in solution-mined caverns in Texas salt domes. A major goal of Phase II research was characterizing properties of salt domes which could affect this type of waste disposal.

Organization

This report is organized along two parallel themes: (1) investigations of dome-related strata--their stratigraphy, structure, and geohydrology and (2) investigations of dome material--salt, cap rock, and mechanical properties of salt. Each theme begins with a regional focus and continues with increasingly narrow investigations.

In Phase II we have (1) block diagrammed regional structure around domes in the Houston diapir province and the East Texas diapir province; (2) mapped and sectioned the structure and stratigraphy locally around four Texas domes; (3) reviewed published data on mechanical properties of salt, concentrating on creep properties; and (4) analyzed site-specific data on cap rocks and salt in 20 cores from six salt domes.

During Phase I, a statewide dome data base was established (Seni and others, 1984b) and natural resources associated with Texas salt domes were detailed with emphasis on brine and storage-cavern industries (Seni and others, 1984a).

Recommendations

It is not possible to fully evaluate in one year all possible technical issues associated with waste disposal in domes. We have concentrated on those

issues with the greatest importance and those which could be completed in the allotted time. A complete characterization of a salt dome for the purposes of waste isolation requires detailed site-specific data on relevant properties of salt, cap rock, and surrounding strata and quantitative data on the hydrogeologic system within the cap rock and the associated strata.

A strong and expanding storage industry is one indication that waste storage in solution-mined caverns in salt is technically feasible. However, long-term (greater than 50 years) containment has not been demonstrated. Critical weak points in a waste-containment system are at the intersection of the cement-casing string and the cap-rock lost-circulation zones. The security of a waste-containment scheme is enhanced by (1) maximizing the number of cemented casing strings, (2) maximizing the safety zone of (a) undisturbed salt around the storage cavern and (b) undisturbed strata around the salt dome, (3) maximizing the viscosity of waste by solidification, (4) minimizing the pressure differential within and outside the cavern, (5) minimizing the contact between the waste-containment system and lost-circulation zones, (6) minimizing contact between the host salt dome and circulating ground water, and (7) choosing a host dome with minimum dome growth rates over the recent geologic span of history.

STRUCTURE, STRATIGRAPHY, AND GROWTH HISTORY

The growth of salt domes typically has a profound influence on the structure, stratigraphy, and depositional systems of surrounding strata. Critical data on the timing of dome growth, rates and volumes of salt flow, and potential for future growth or stability are available through careful analysis of the influence that dome growth has on surrounding strata. Structural, stratigraphic, and depositional systems analysis each provides a part of this

information. However, this technique represents only one approach to reliably predicting the future stability of salt domes or interior caverns. Clearly, aspects of hydrologic stability and geomechanical stability must be integrated to reliably predict future stability.

Structure

Dome growth usually distorts both the local and regional structure around a dome. However, the structural distortion can be very minimal during periods of nongrowth, relatively slow growth, or when the salt source layer has been exhausted. Structurally high areas form over the dome crest and flanks owing to relative upward flow of salt and shear-zone drag. Salt-withdrawal basins are structurally depressed areas that form above zones from which salt is flowing to feed rising diapirs.

A single dome may cause both uplift and subsidence of supradomal strata in different areas of the dome crest. Jackson and Seni (1984a) note that the structural attitude of strata on dome flanks is in part a function of the stage of dome growth and the slope of the sides of the salt stock. The dip of strata around domes commonly varies systematically with increasing depth from dip up toward the dome at the shallow horizons, through horizontal dip, to dip down toward the dome for the deeper strata. The plane where strata near the dome are horizontal or at regional dip is inferred to mark the termination of the stage of active diapiric growth owing to exhaustion of the salt source layer. Apart from shear-zone drag, there is no longer a mechanism to cause the dip of surrounding strata to deviate from regional norms when the salt-source layer is exhausted.

Regional structural patterns around salt domes in the Houston diapir province are illustrated in map view and in a block diagram in figures 1 and 2. Figure 3 is a similar block diagram for domes in the East Texas salt diapir

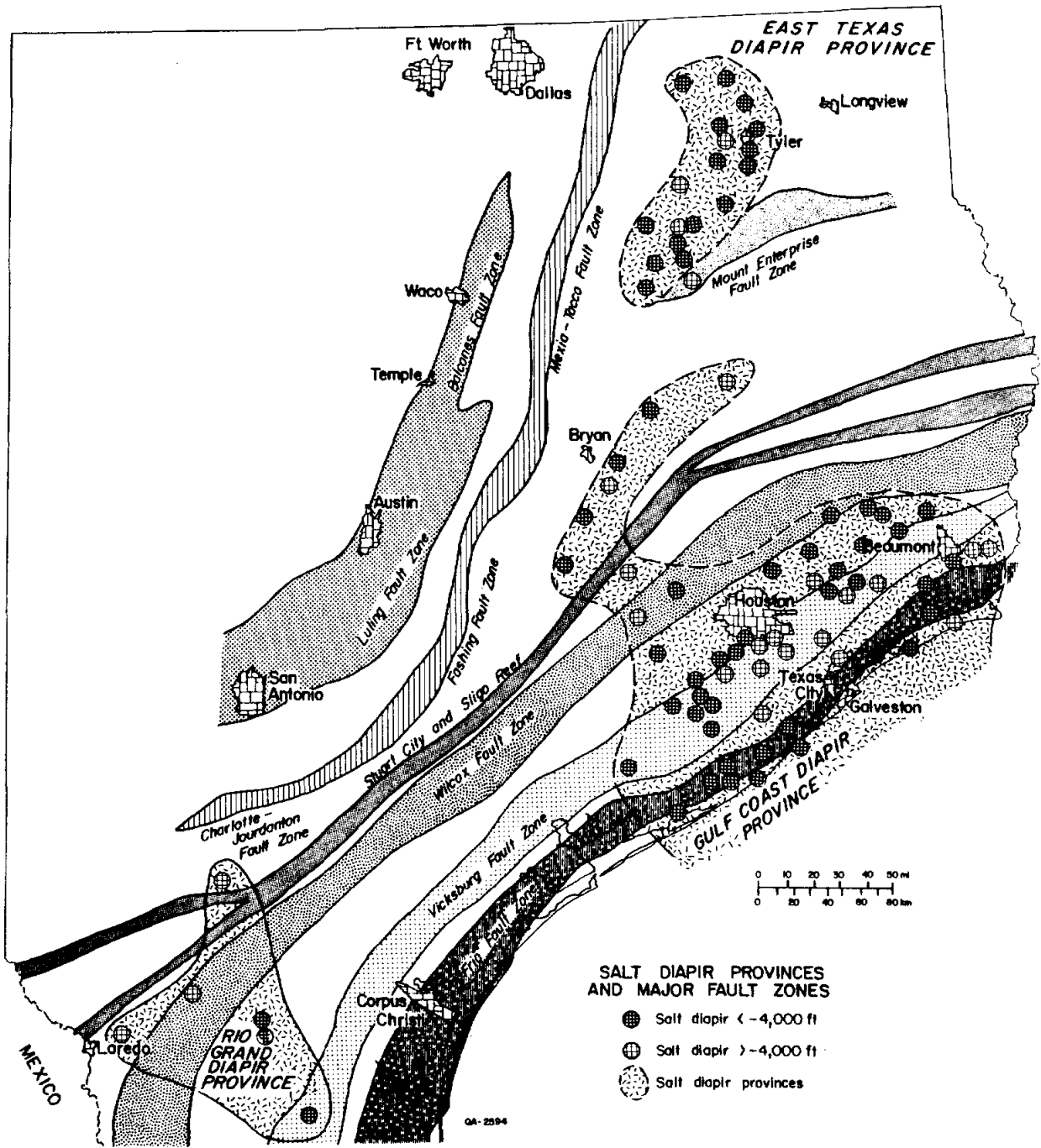


Figure 1. Distribution of Texas salt domes and salt provinces in relation to major fault zones and the Stuart City and Sligo reef trends.

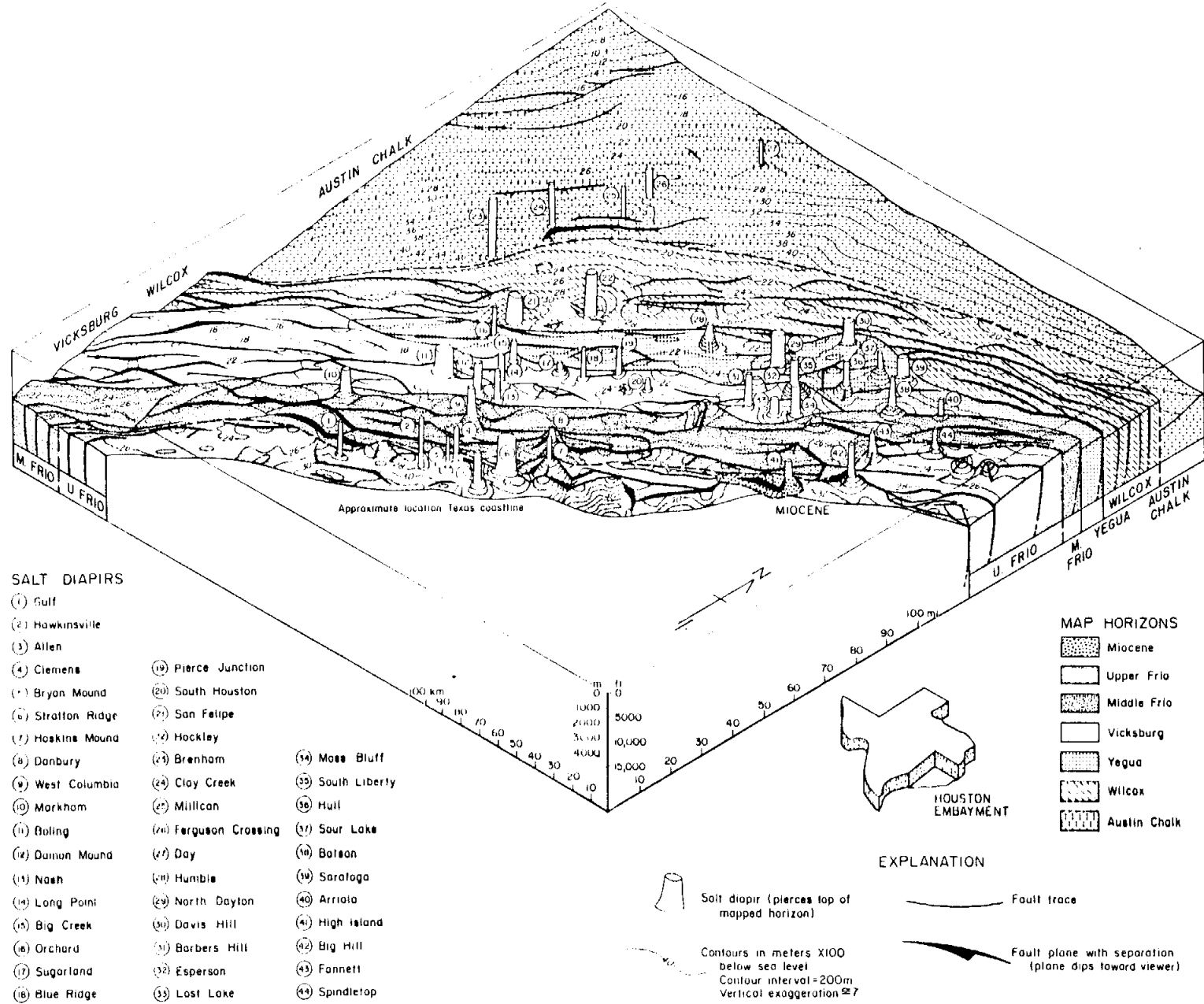
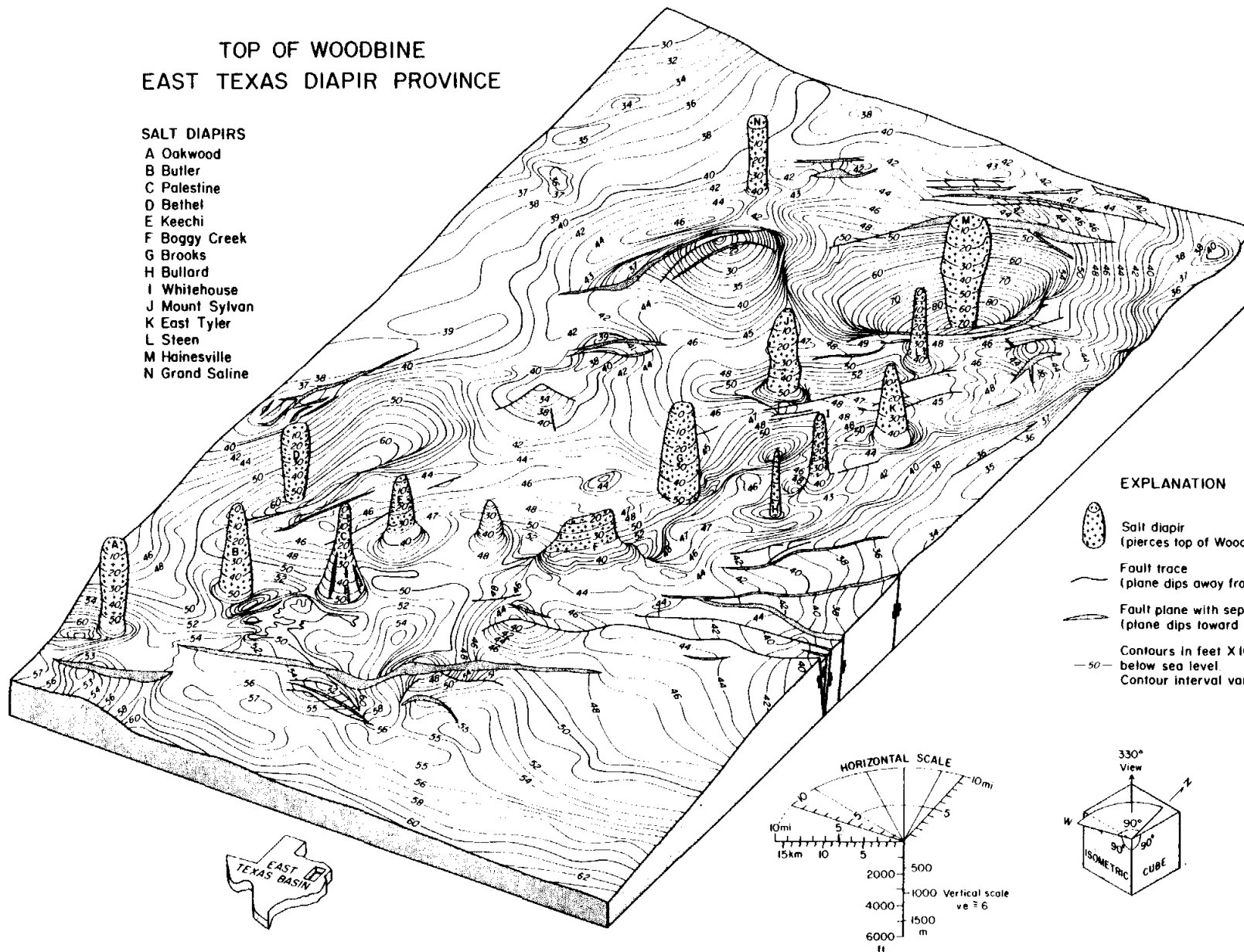







Figure 2. Block diagrams of salt domes and structure on top of Cretaceous and Tertiary units in Houston Embayment (modified from Ewing, in preparation).

TOP OF WOODBINE
EAST TEXAS DIAPIR PROVINCE

- SALT DIAPIRS
 A Oakwood
 B Butler
 C Palestine
 D Bethel
 E Keechi
 F Boggy Creek
 G Brooks
 H Bullard
 I Whitehouse
 J Mount Sylvan
 K East Tyler
 L Steen
 M Hainesville
 N Grand Saline



EXPLANATION

-  Salt diapir (pierces top of Woodbine)
-  Fault trace (plane dips away from viewer)
-  Fault plane with separation (plane dips toward viewer)
-  Contours in feet X100 below sea level
-  Contour interval variable

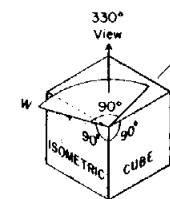
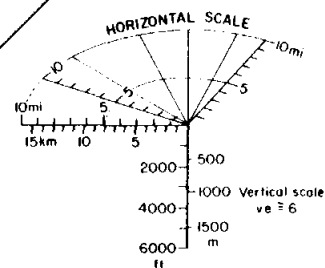


Figure 3. Block diagram of salt domes and structure of top of Woodbine Group in East Texas Basin (from Jackson and Seni, 1984b).

province. Most of the larger faults in the Houston salt diapir province are down-to-the-coast, normal, growth faults. The smaller faults around domes are radial-tear or trap-door faults. The relationship between regional growth faults and salt domes is enigmatic (Ewing, 1983). Whether there is a cause-effect relationship between growth faults and salt diapirism is disputed. Several aspects of salt domes in the Houston diapir province argue against a cause-effect relationship. The regional, parallel, growth-fault trends are highly developed and regularly spaced in the Coastal Bend area, an area without salt domes. But, in the Houston diapir province the fault patterns become more random and fault segments are shorter. There is no strong linear parallel orientation of groups of domes that might be attributed to control of dome distribution by faults or vice versa. The strongest linear arrangement of domes is displayed by the Brenham, Clay Creek, Mullican, Ferguson Crossing, and Day salt domes. These domes are oriented about 30 degrees North of the orientation of regional strike and of the strike of local faults. Note also that these domes have the least effect on the structure of surrounding strata (Austin Chalk). These domes may have terminated the active stage of diapir growth by exhausting their salt source layer in the late Cretaceous.

Major growth faults appear to randomly intercept some domes and to avoid others. Major growth faults intercept Boling, Markham, Hockley, Barbers Hill, Fannett, and Big Hill salt domes. On the other hand, major growth faults are isolated from Damon Mound, Gulf, Allen, Clemens, Big Creek, South Houston, Moss Bluff, Lost Lake, Saratoga, North Dayton, Davis Hill and Arriola salt domes.

The local structure around Boling, Markham, and Damon Mound domes is mapped at the top of the Frio in figure 4. Appendix 1A lists all wells in figures 4, 9, and 10. Major regional faults clearly intercept both Boling and Markham domes but only small radial faults intercept Damon Mound dome. The large oval depression southeast of Boling dome is a salt-withdrawal basin.

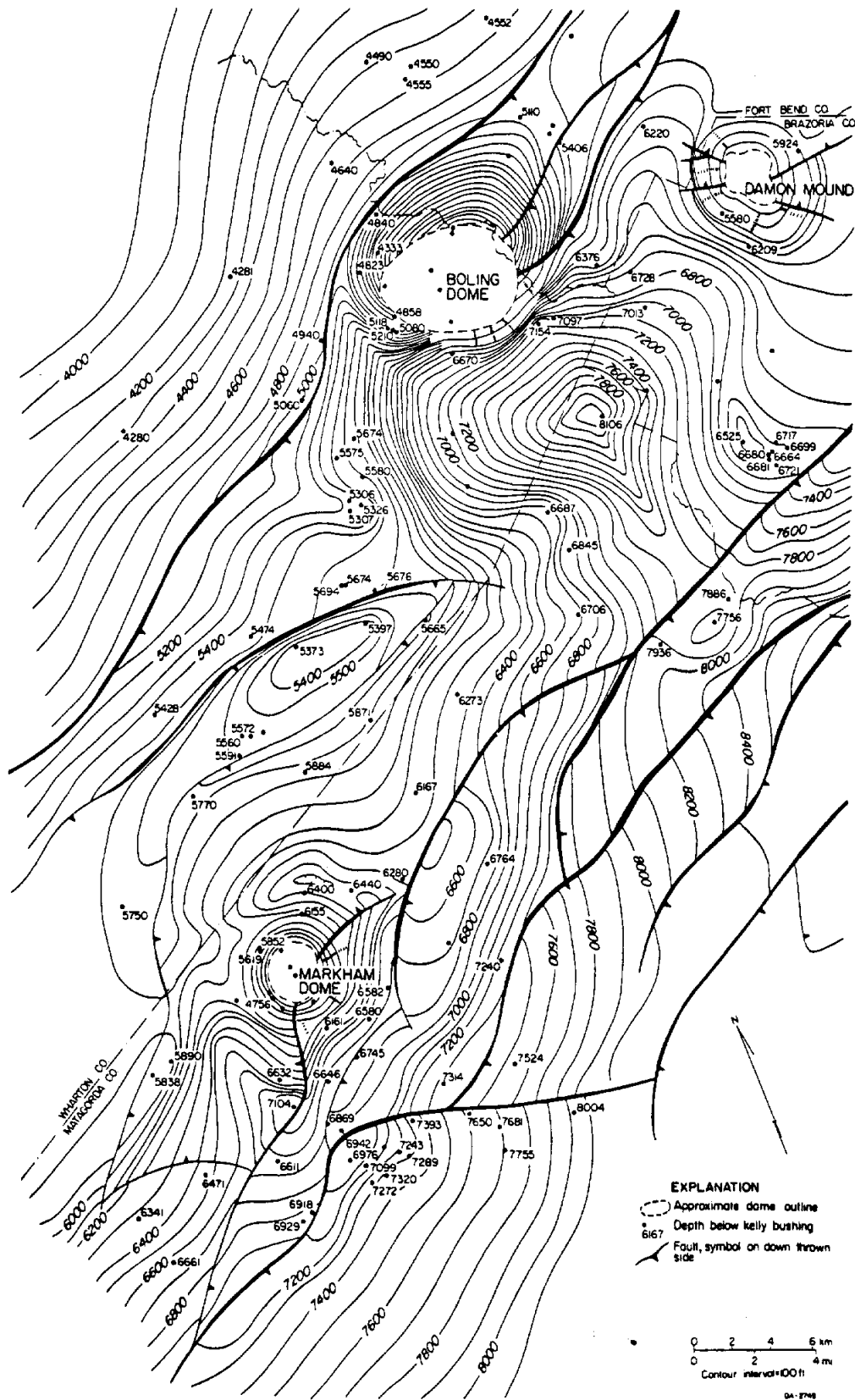
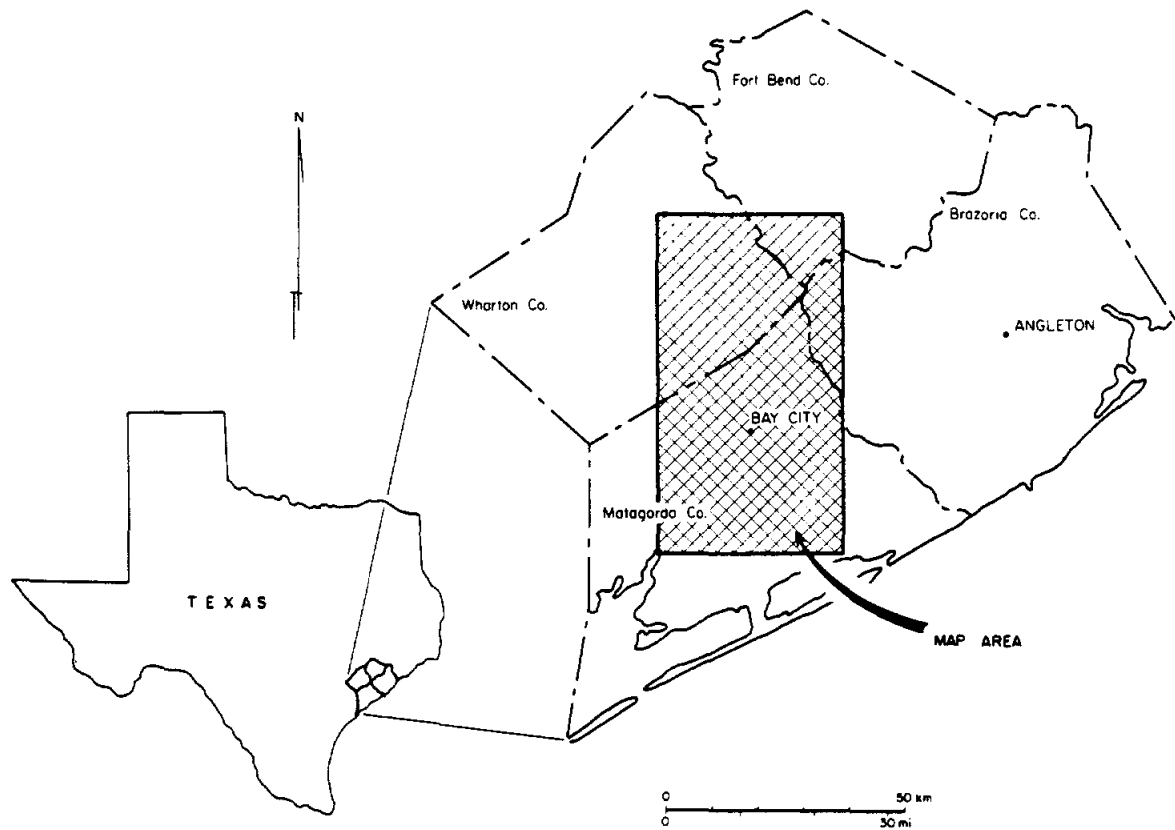


Figure 4. Structure contour map, Frio Formation around Boling, Markham, and Damon Mound salt domes. Salt-withdrawal basin for Boling dome is closed structural depression southeast of Boling dome. Regional growth faults intercept the northeast flank of Boling dome and the southwest flank of Markham dome. Map shows extent of coverage in Fort Bend, Wharton, Matagorda, and Brazoria Counties.



(continued)

Because this structure affects the top of the Frio, the structure must be post-Frio in age.

Radial faults are probably associated with all domes. Only with dense subsurface well or seismic control can the orientation and distribution of these minor faults be determined. Local structure around Boling, Markham, and Barbers Hill domes is also shown in cross section in figures 5, 6, 7, and 8. Appendix 1B lists all wells on cross sections in figures 5, 6, 7, and 8. Salt-withdrawal basins are clearly visible north of Markham, and Barbers Hill domes and southeast of Boling dome. Together with isopach maps, stratigraphic data can be used to help deduce the timing of dome growth.

Stratigraphy

Miocene and post-Miocene strata (fig. 9) and the Anahuac Formation (fig. 10) were mapped around Boling, Markham, and Damon Mound domes. The map interval and correlations are shown in figure 11. Isopach maps are particularly powerful tools for determining the timing of dome growth because syndepositionally growth directly influences isopach patterns and these thickness patterns are preserved in the stratigraphic record with a minimum of complications (Seni and Jackson, 1983a; 1984). Figures 9 and 10 illustrate a large salt-withdrawal basin covering approximately 130 km² (50 mi²) southeast of Boling dome. The isopachous thickening was active during deposition of Anahuac, Miocene, and post-Miocene strata. In contrast, Markham dome has only minor thickening in an ill-defined salt withdrawal basin north and northeast of the dome. The well-formed basin by Boling dome indicates more vigorous growth of Boling dome than for Markham dome during the same time interval.

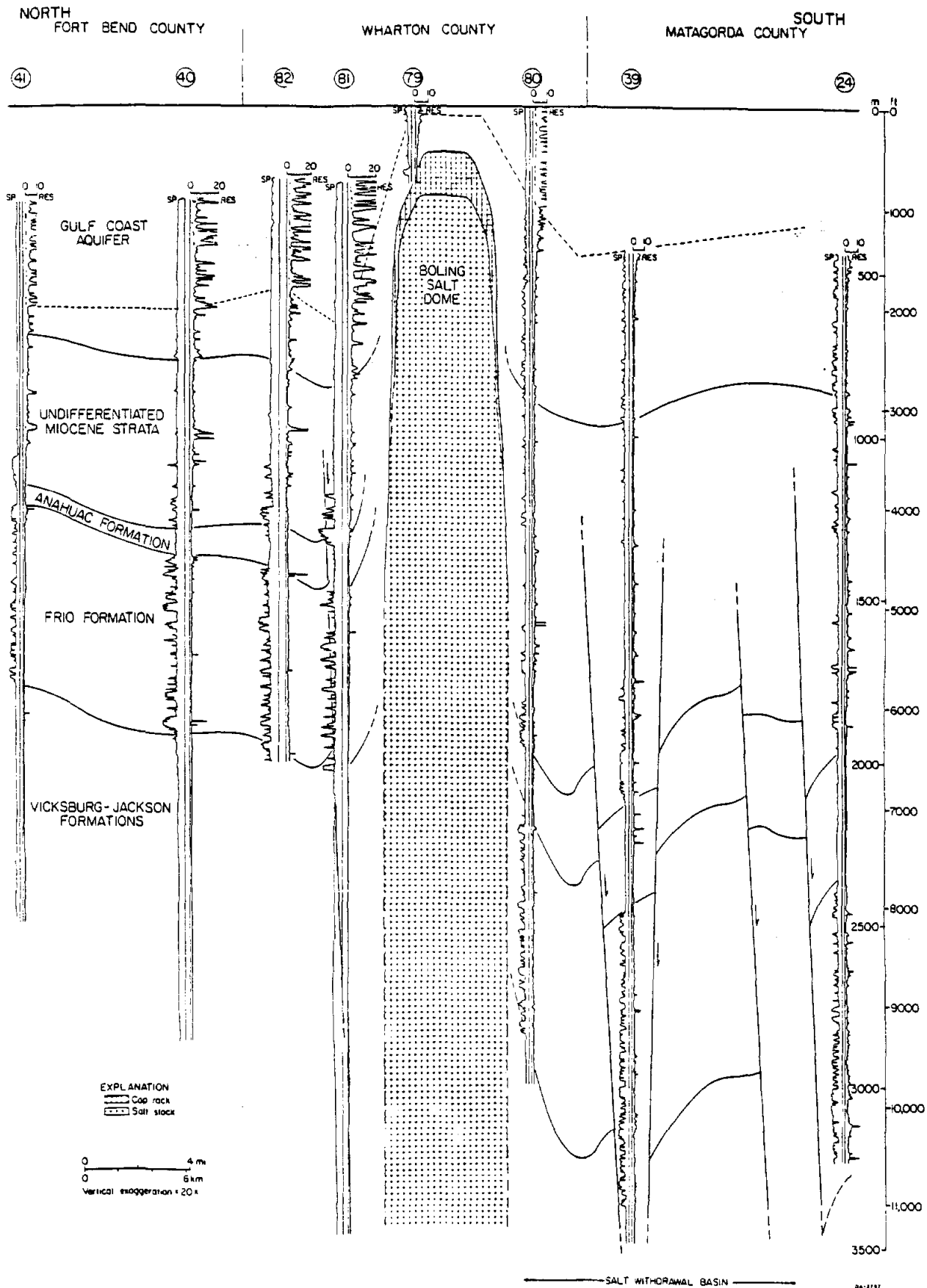
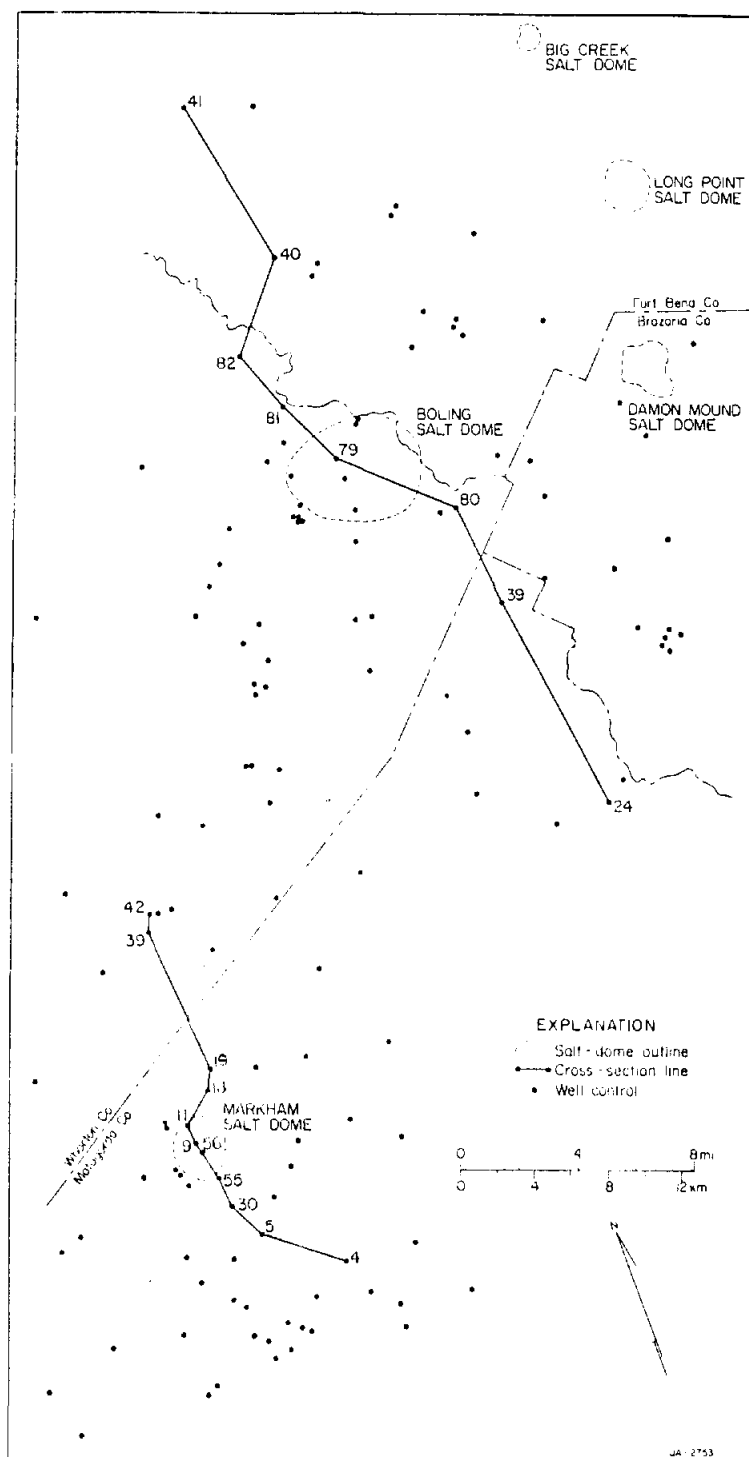


Figure 5. Cross section, Boling dome and flanking strata. Salt-withdrawal basin has abundant faults in Vicksburg, Jackson, Frio, and Anahuac Formations. Top of Miocene is depressed 500 ft over salt-withdrawal basin owing to post-Miocene (younger than 5 Ma) salt flow into Boling dome. Map shows location of wells.



(continued)

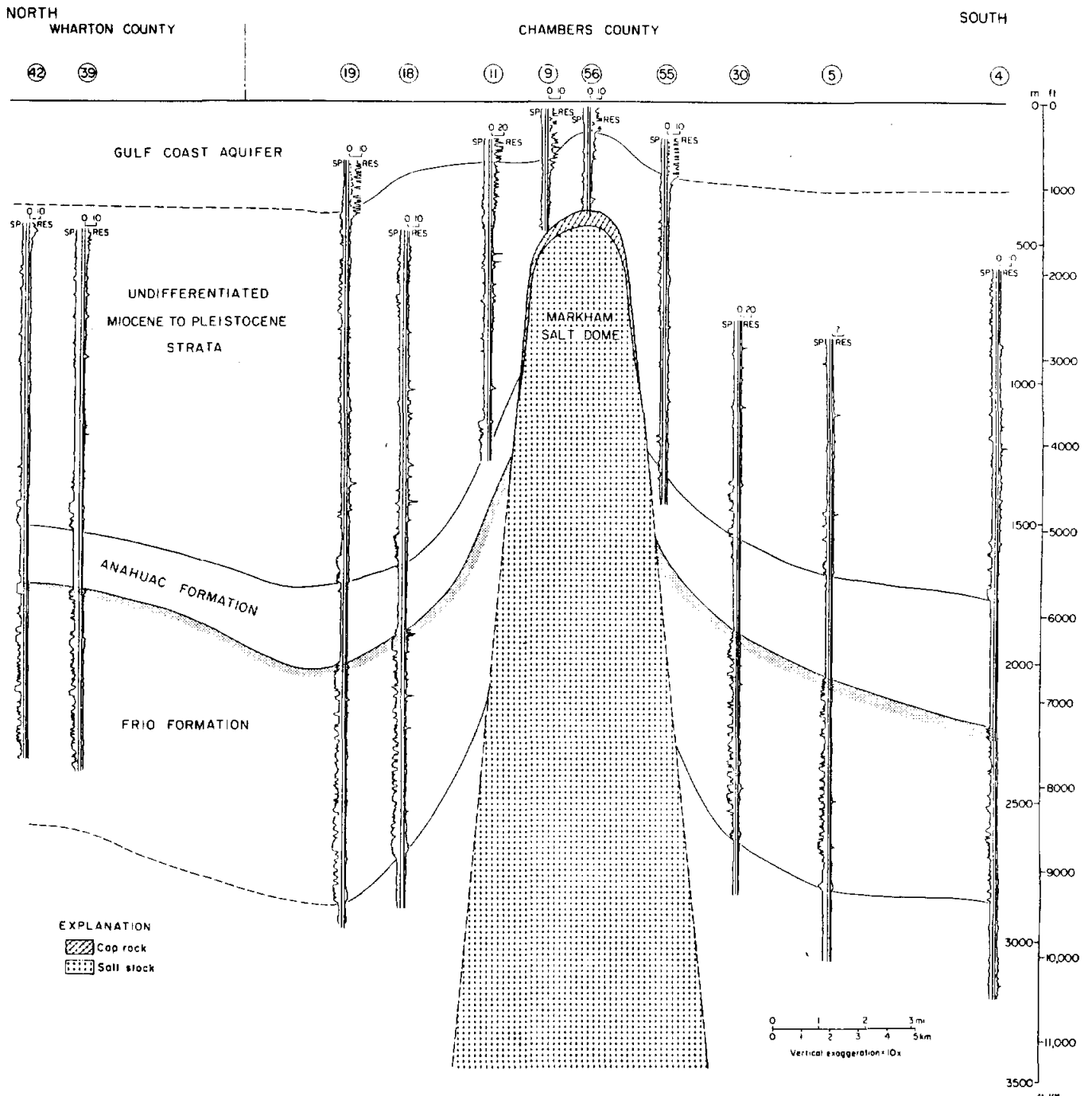


Figure 6. Cross section, Markham dome and flanking strata. Salt-withdrawal basin is a structural sag north of dome. Major faults are absent in this orientation of cross section. See figure 5 for map showing location of wells.

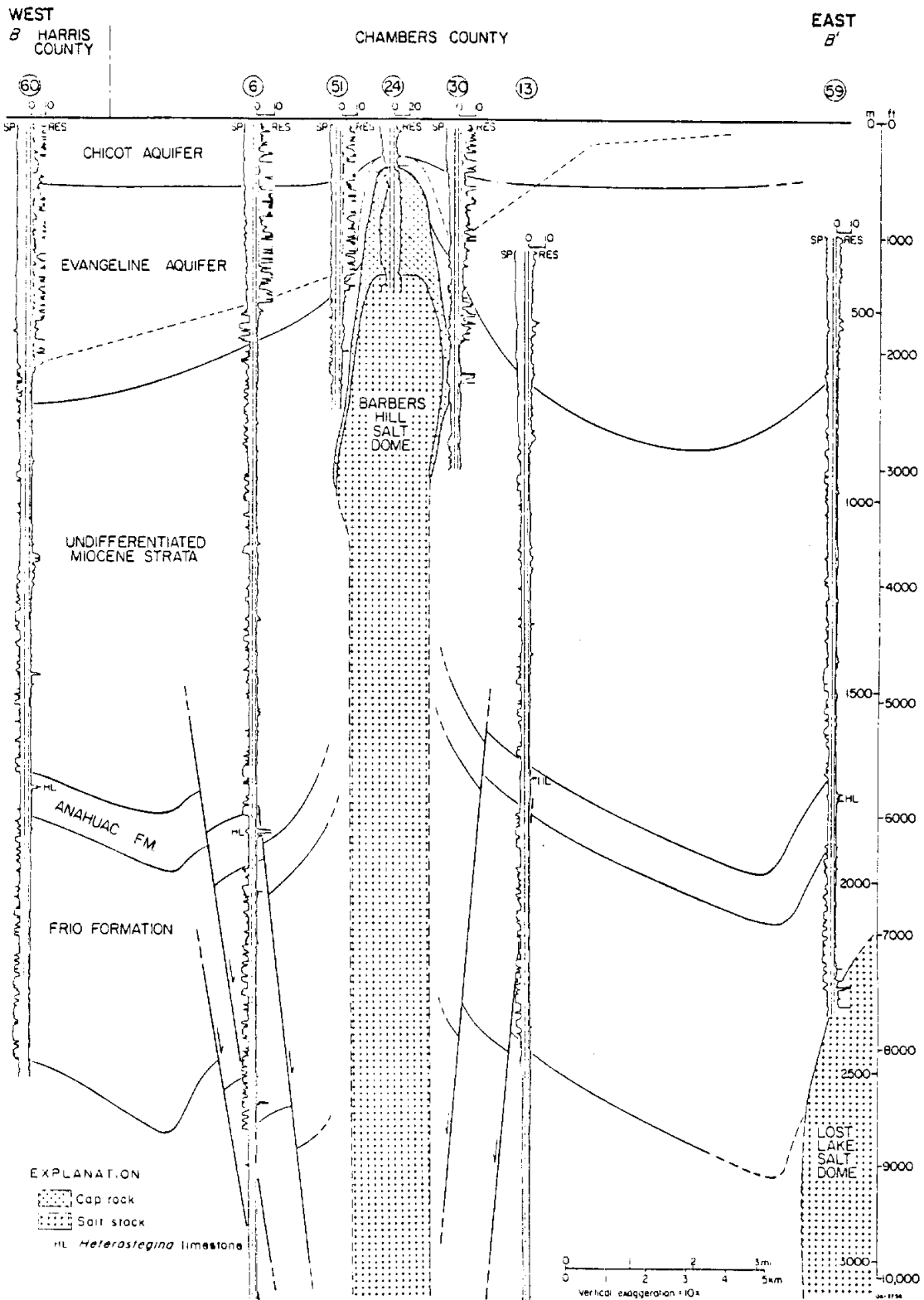
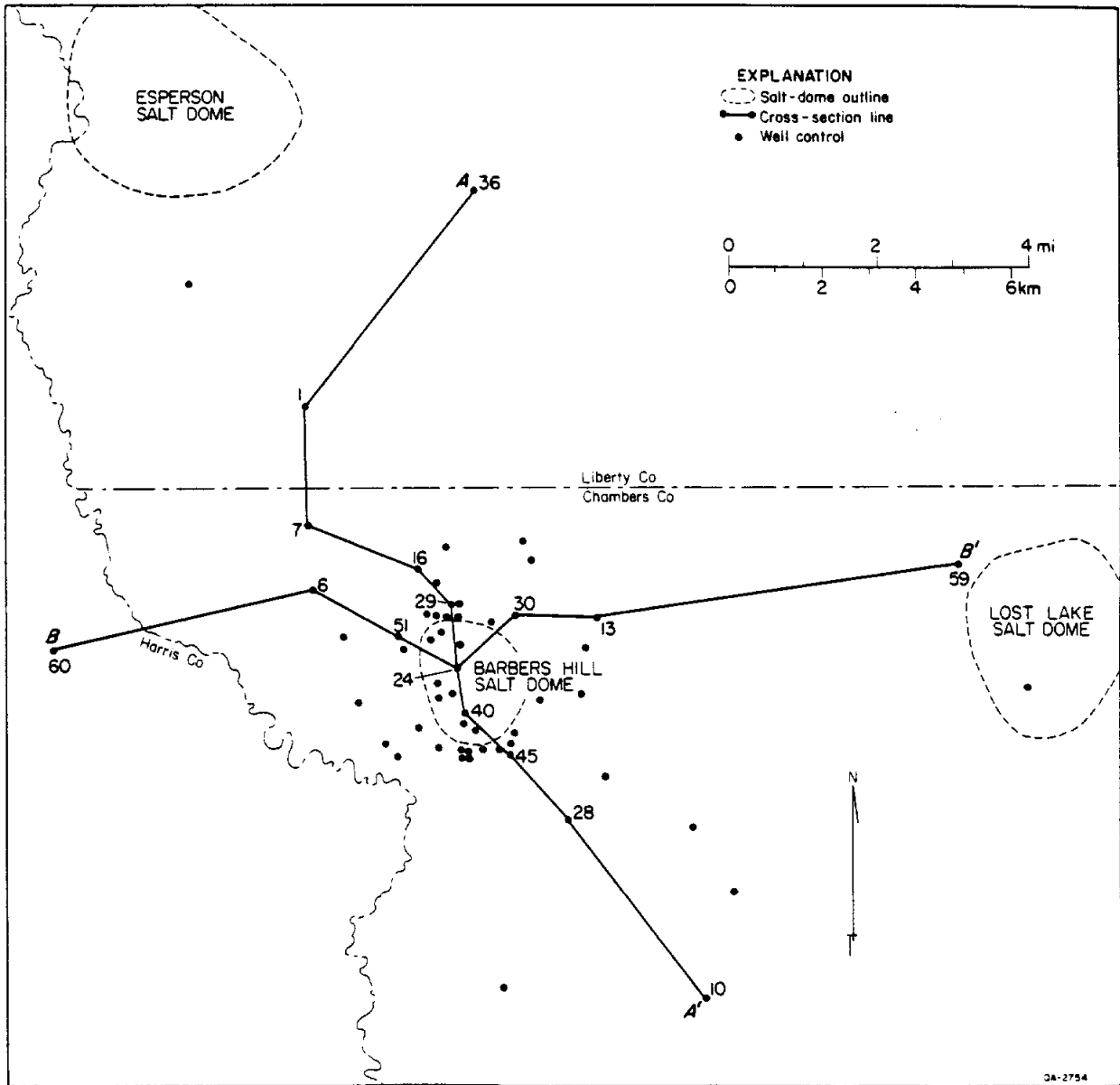


Figure 7. East-west cross section, Barbers Hill dome and flanking strata. Faulting is common through Frio and Anahuac Formations and at base of Miocene strata. Cap rock is surrounded by Evangeline aquifer. Map shows location of wells.



(continued)

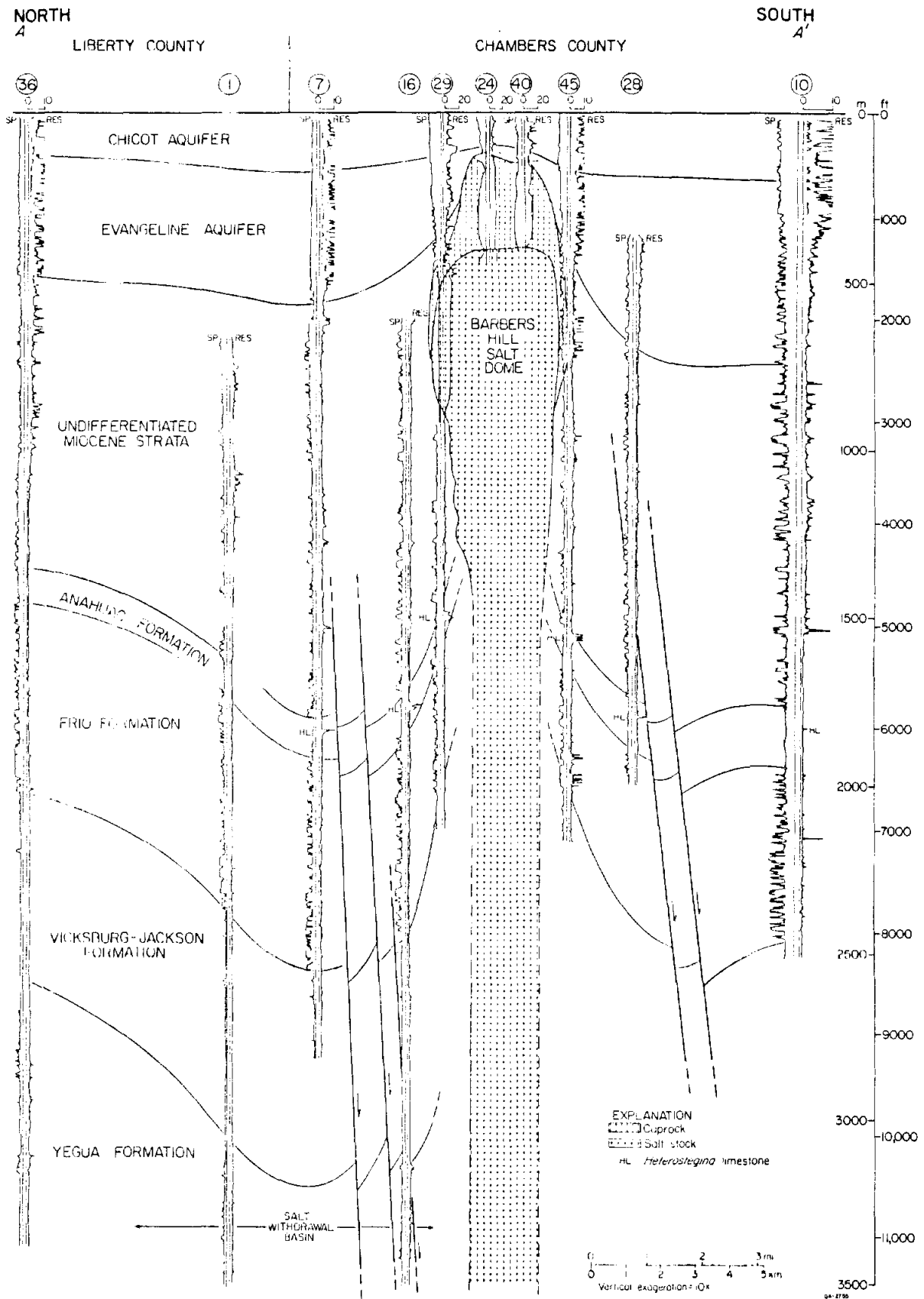


Figure 8. North-south cross section, Barbers Hill dome and flanking strata. Faulting is common from base of Miocene to deepest control. Faults are typical down-to-the-coast (south) regional growth faults. Salt-withdrawal basin is north of dome. See figure 7 for map showing location of wells.

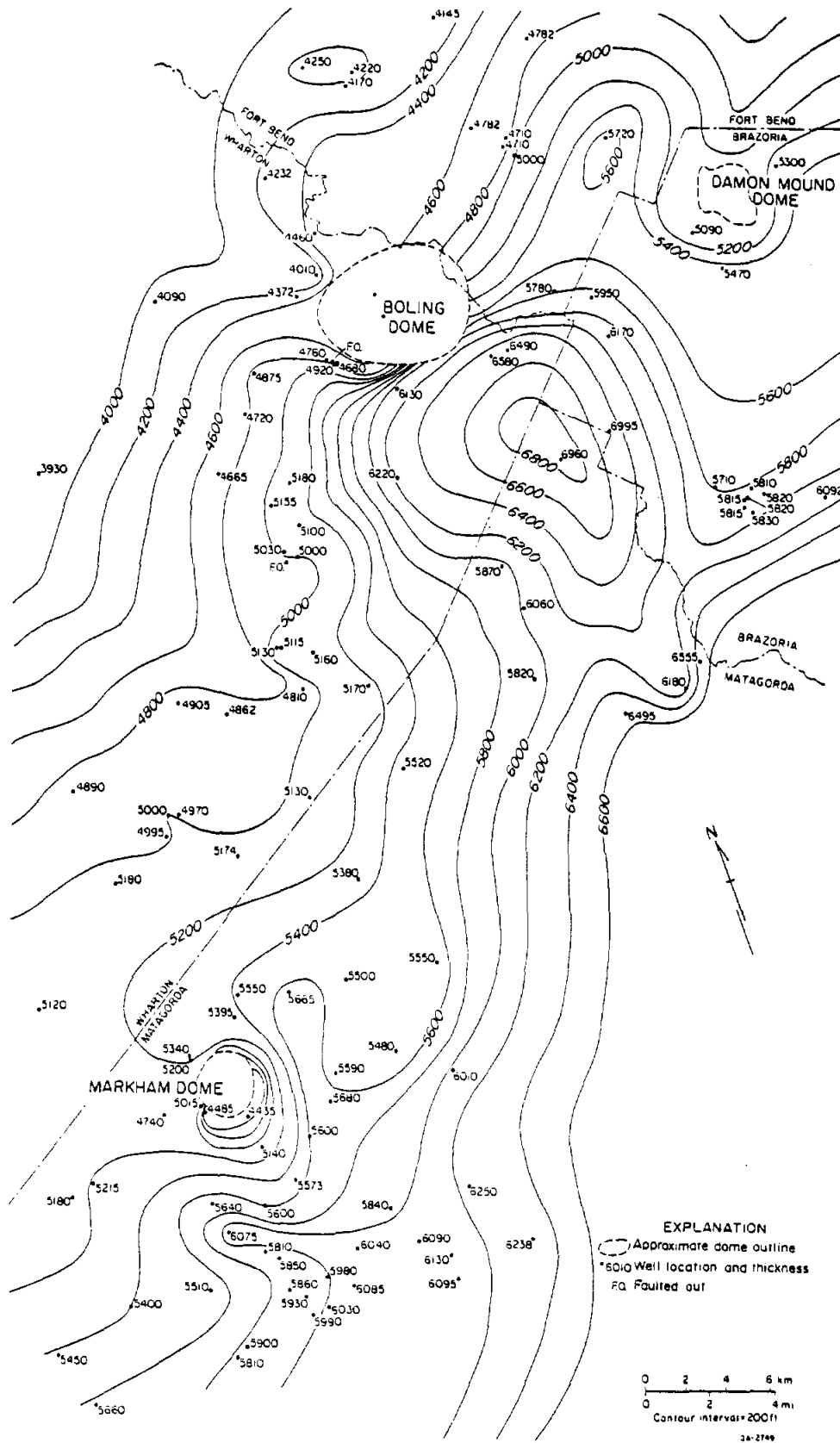


Figure 9. Isopach map, Miocene and post-Miocene strata, area around Boling, Markham, and Damon Mound domes. Miocene and post-Miocene strata are 2,000 ft thicker in salt-withdrawal basin southeast of Boling dome owing to extensive syndepositional salt flow into Boling dome. See figure 4 for mapped area.

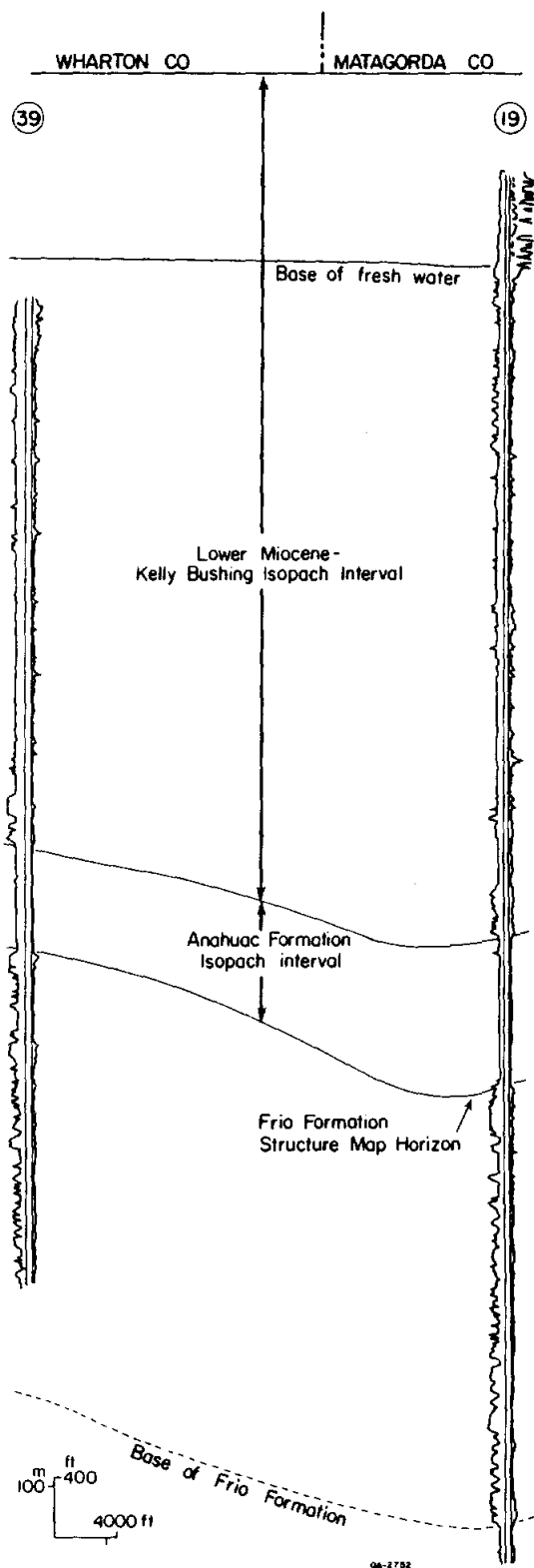


Figure 11. Cross section showing map intervals and correlations.

Growth Rates For Boling Salt Dome

Net and gross rates of growth for Boling dome were calculated following the techniques of Seni and Jackson (1983b; 1984). The growth rates are averaged over the entire Miocene and post-Miocene time interval--22.5 millions of years (Ma). This is a relatively long time interval for measuring rates of dome growth. Actual rates of dome growth over shorter time spans will probably be much greater. Long-term growth rates mask the short-term fluctuations of non-steady-state dome growth.

Gross rates of dome growth measure the rate of movement of salt within the salt stock. The gross rates are calculated by equating the volume of sediment in the salt-withdrawal basin with the volume of salt that migrated into the salt stock during that interval of deposition. The vertical rate of movement within the salt stock is determined by dividing the volume of salt mobilized by the cross sectional area of the neck of the salt stock for the duration of deposition (Table 1). During the past 22.5 Ma, 11.9 km^3 (2.6 mi^3) of salt migrated into Boling salt dome. This yields a gross rate of growth for Boling dome of 16 m/Ma (52 ft/Ma). The gross rates of growth for Boling dome are approximately equal to the gross rates for East Texas salt domes in the East Texas salt diapir province during their growth in the Late Cretaceous and Eocene.

Regional rates of sediment-accumulation were 84 m/Ma (276 ft/Ma) in the vicinity of Boling dome during the Miocene to present. Net rates of sediment accumulation were 94 m/Ma (309 ft/Ma) in the Boling dome salt-withdrawal basin. If Boling dome kept pace with the rate of sediment accumulation and stayed at the same relative position with respect to the depositional interface, then net rates of dome growth averaged 94 m/Ma (309 ft/Ma) for Boling dome from the Miocene to the present. The net rate of growth for Boling is comparable to the net rates of growth for the fastest growing domes in the East Texas diapir

Table 1. Growth Rates for Boling Salt Dome

Gross Rate

Volume of salt-withdrawal basin

Contour Interval (ft)	Area (mi ²)	Thickness (ft)	Volume (mi ³)
6200		200	
6400	40.95	200	1.55
6600	22.73	200	0.86
6800	9.00	200	0.34
6960	3.60	1.60	0.11
		Sum	2.86 mi ³ (11.91 km ³)

Area column is average area of two contour interval.

Area of Boling dome neck 12.83 mi² (32.84 km²)

$$\text{Gross growth of Boling dome} = \frac{\text{Salt-withdrawal volume}}{\text{Salt-neck area}} = \frac{2.86 \text{ mi}^3}{12.83 \text{ mi}^2} = 0.223 \text{ mi} = 1,177 \text{ ft} \text{ (359 m)}$$

$$\text{Growth rate Post-Oligocene to Present} = \frac{\text{Gross growth}}{\text{Duration}} = \frac{1,177 \text{ ft}}{22.5 \text{ Ma}} = 52 \text{ ft/Ma (16 m/Ma)}$$

Net Rate

$$\text{Net rate of growth} = \frac{\text{Domal-sediment accumulation}}{\text{Duration}} = \frac{6960 \text{ ft}}{22.5 \text{ Ma}} = 309 \text{ ft/Ma (94 m/Ma)}$$

$$\begin{aligned} \text{Residual rate of growth} &= \frac{\text{Domal-sediment accumulation} - \text{Regional-sediment accumulation}}{\text{Duration}} \\ &= \frac{6960 \text{ ft} - 6200 \text{ ft}}{22.5 \text{ Ma}} = \frac{760 \text{ ft}}{22.5 \text{ Ma}} = 34 \text{ ft/Ma (10 m/Ma)} \end{aligned}$$

province during the peak periods of diapiric activity in the Early and Late Cretaceous. The discrepancy between net and gross rates of diapirism for Boling dome may be due to incorrect assumptions of the size of the diapir neck during the Miocene and post-Miocene interval and/or to the crest of Boling dome not keeping pace with deposition in this time interval or to incorrect assumptions of the size and volume of the salt-withdrawal basin.

Discussion

Domes grow and are emplaced under a variety of conditions, thus effecting a diversity of structural and stratigraphic styles in the sediments that surround them. These structural and stratigraphic relationships provide data that can be used to assess the suitability of domes for toxic-waste disposal.

This report and Seni and others (1984a,b) describe some of the structural aspects that affect dome and cavern stability. Domes with structural features indicating diapiric movement in the most recent geologic span of time are less suitable for isolating toxic chemical waste than domes that were quiescent. Recent structural distortion from dome growth causes a range of mappable features that are expressed in near-surface strata. Two important features are (1) structurally and topographically elevated areas over dome crests and (2) faults in strata over the domes, on dome flanks, and in cap rocks. These structural discontinuities are expressed in strata that are deeply buried around domes with an older history of growth. The stability problems associated with domes having a recent growth history are not confined to fear that continued domal uplift might expose a waste repository. Calculations on the rate of dome uplift for East Texas domes and for Boling dome show that the amount of uplift required to expose a repository has a low probability of occurring in the foreseeable future. Nor is there a great likelihood that natural faulting will breach a repository. Rather, the concerns are centered

on how these structural discontinuities will affect near-dome hydrogeology. Ground water plays a primary role in salt dome stability. If wastes were to leak from an underground repository, ground water is the likely agent to transport the waste to the biosphere.

The areas over some of the coastal plain domes are topographically elevated 10 to 75 ft (3 to 23 m) above the surrounding plain. These elevated areas are local ground-water recharge zones centered directly over the crest of the dome. Supradomal radial faults, cap-rock faults, and regional growth faults all may act as conduits funnelling meteoric waters toward the upper parts of salt stocks. The geometry and orientation of these faults and their potential for accentuating or inhibiting fluid flow must be analyzed before properly assessing the suitability of a dome for waste isolation. See the CAP ROCK Discussion section for further information on cap-rock faults and hydrogeology.

Stratigraphic relationships around salt domes provide additional means of discriminating among candidate domes. Again, the hydrogeologic aspects are critical. Dome growth strongly influences lithostratigraphy and depositional facies around a dome. This lithostratigraphic framework in turn influences the directions, rates, and flux of ground water around a dome. A diapir encased in a framework of mudstone of low permeability will retard ground-water flow and be a more appropriate candidate for waste isolation than a diapir surrounded by a sandstone characterized by high rates of ground-water flow. These patterns of lithostratigraphy and their influence on ground-water flow are documented around Oakwood dome in East Texas.

MECHANICAL BEHAVIOR OF SALT

Laboratory research on artificial halite and core samples of bedded and domal salt have resulted in substantial strides in our understanding of the

mechanical behavior of salt. Sandia National Laboratories (Herrmann, Wawersik, and Lauson), ReSpec (Senseny, Hansen, and Wagner, under contract to Sandia National Laboratories) and Texas A & M (Carter) are the leaders in this research effort. Despite these advances and advances in computer modeling of salt behavior, as yet there is wide discrepancy between results obtained in the laboratory scale experiments and in situ behavior of rock salt. Baar (1977) asserts much of the technical literature includes erroneous and misleading hypotheses based on laboratory data that cannot be reconciled with the actual behavior of salt rocks around underground excavations. In fact, many laboratory experiments are plagued by small sample size, inadequate test durations, and an absence of many natural geologic variables such as bedding, impurities, and grain size. Herrmann and others (1982) state it is possible that the restricted information obtainable from triaxial tests is not only insufficient but may not dominate behavior involved in mine closing.

In this section we will focus on a review of the creep behavior of salt. Laboratory experiments, results, and in situ observations and experiments will be discussed. Various laws describing creep behavior and possible creep mechanisms will be compared.

Experimental Procedures

Whether testing artificially prepared halite or natural rock salt, the usual test procedure in designing an experiment is to control all variables but one and observe the effects that changing the variable will have on the behavior of the specimen. According to Paterson (1978), the most frequent types of rock mechanical experiments are:

1. A creep test--An axial differential stress is built up rapidly on the specimen and held constant as the specimen deforms. Strain (change in unit length) is then measured as a function of time.

2. A stress-strain test--The differential stress is applied in such a way that the rate of strain is constant and changes in the applied stress are plotted against strain.
3. A strain rate ($\dot{\epsilon}$) test--A constant differential stress is applied and the rate of strain is measured. The results are plotted as differential stress versus strain rate.

Triaxial tests are commonly run on salt samples. The specimen is usually subjected to both confining pressure and axial load. The difference between the axial load and the confining pressure is the differential stress. The axial load is transmitted through a hydraulic jack and confining pressure is supplied by a surrounding fluid, whose temperature can be controlled. Thus, confining pressure, directed stress, and temperature can all be varied.

Creep Behavior of Salt

Salt will undergo deformation by slow creep over long periods of time when subjected to constant load or to differential stress. At low temperatures and low stresses salt will exhibit much less creep deformation than at high temperatures and high differential stress (Hume and Shakoor, 1981). Generally when modeling creep behavior of salt in the laboratory, the following variables are considered: stress-- σ --(force per unit area measured in megapascals [MPa], pounds per square inch [psi], or bars), strain-- E --(ratio of change in length of specimen to its original length), time, and temperature. Appendix 2 is a conversion table for the various units. Most of the units in this section will be Standard International units (SI), because most of the original research and figures use those units. Where non-SI units are used in a cited figure or text, they will be given preference. Creep data are usually presented as some type of time representation. Natural variations in rock salt such as bedding,

impurities, mineral content, moisture content, porosity, permeability, mineral fabric, and grain size are rarely considered. Generally, temperature and stress difference have the greatest effect on creep rate. An increase in either temperature or stress difference increases the creep rate considerably (Le Comte, 1965).

Survey of Creep Properties

Major review articles on creep properties of salt include Le Comte (1965), Odé (1968), Baar (1977), Hume and Shakoor (1981), Herrmann and others (1982), and Carter and Hansen (1983). Government sponsored research for nuclear-waste isolation studies and the Strategic Petroleum Reserve program has produced a wealth of new information often termed "gray literature" because it comes from government laboratories and their contractors. Much of the research on creep modeling is based on laboratory tests and computer modeling of artificially prepared halite and rock salt cores from bedded salts at the Waste Isolation Pilot Project site and domal salt principally from Strategic Petroleum Reserve domes in Louisiana and Texas.

Creep is the basis of salt's ability to flow and heal fractures. Simultaneously, creep causes problems related to closure of mined openings, and surficial and subsurface subsidence. Such plastic behavior is demonstrated by salt glaciers, by flowage patterns within salt domes, and by closure of underground openings in salt.

The idealized creep curve for salt (fig. 12) exhibits four parts:

1. Elastic deformation--An instantaneous deformation which is elastic, thus not time dependent.
2. Transient (or primary) creep--A component of creep deformation that decreases with time.
3. Steady-state creep--A component of creep with a constant rate of deformation.

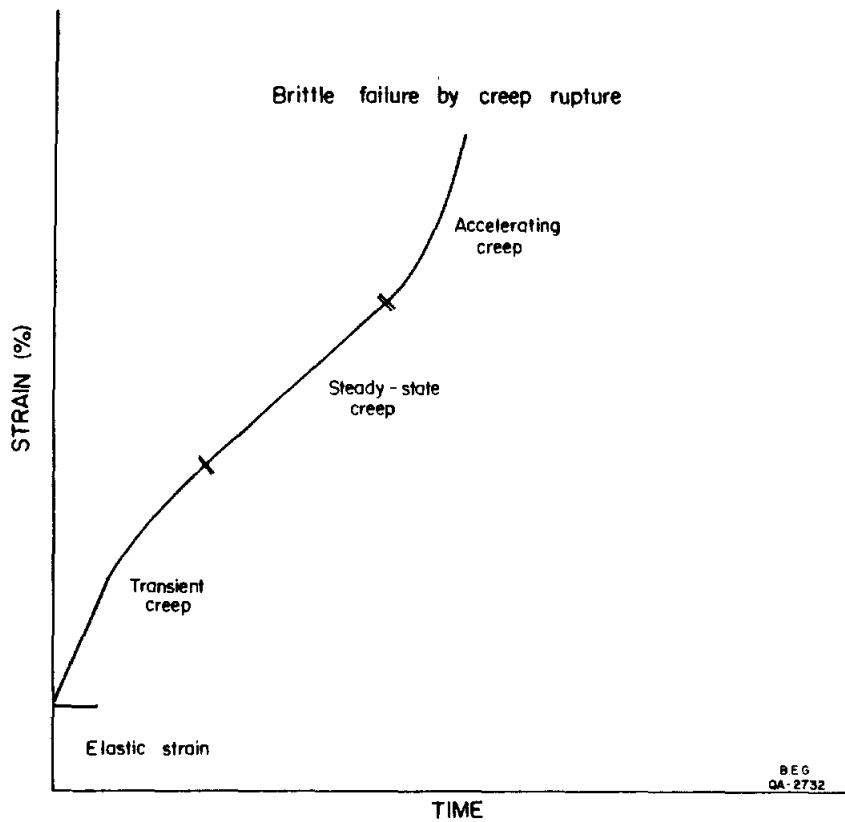


Figure 12. Idealized creep curve depicting behavior of rock salt. Transient (primary), steady-state (secondary), and accelerating (tertiary) stages of creep are separated by inflection points in the curve. The creep curve terminates at the point of brittle (sudden) failure by creep rupture.

4. Tertiary (or accelerating) creep--A component of creep with an increasing rate of deformation leading to brittle failure by creep rupture.

Elastic Properties

Elastic properties of salt include density, compression, Young's modulus, bulk modulus, Poisson's ratio, and wave properties (Hume and Shakoor, 1981). When considering salt properties, from a design viewpoint, elastic properties are of secondary importance because of the extremely low limits of elastic behavior (yield limit) of salt (Odé, 1968). However, shear modulus--the ratio of stress to its corresponding strain under given conditions of load, for materials that deform elastically, according to Hook's Law--is incorporated in various creep laws.

Salt will deform plastically, that is, flow, when the stress difference ($\sigma_1 - \sigma_3$) exceeds the limits of elasticity. According to Odé (1968), if salt does have a yield limit, this limit must be low. The reported values for the true elastic limit of salt vary widely and they are the subject of much acrimonious debate (Baar, 1977). Baar (1977) reports a yield limit of approximately 0.99 MPa whereas other researchers give values ranging from 3.94 to 49.25 MPa (Baar, 1977). With advances in test instrumentation the reported values for the limits of elastic behavior have declined. Some calculations of strain rates for Iranian salt glaciers indicate plastic behavior of salt at very low stresses of 0.03-0.25 MPa (Wenkert, 1979; Talbot and Rogers, 1980).

Creep Experiments

Creep experiments are designed to quantify the effect that changes in stress, confining pressure, temperature, and time will have on creep magnitude (strain) or strain rate. At present the literature on salt rock behavior

contains results that are conflicting and interpretations that are contradictory (Herrmann and others, 1982; Baar, 1977). Behavioral trends that are in general agreement will be shown as well as the contradictory results. Both laboratory experiments and studies with in situ conditions will be reported.

Temperature has the greatest influence on creep rate (Le Comte, 1965). An increase in temperature always increases the creep rate (fig. 13). Le Comte (1965) experimented with artificial halite at moderately elevated temperatures and his studies are still among the most complete. General observations of his experiments include:

1. An increase in temperature and axial stress increases the creep rate.
2. An increase in confining pressure decreases the creep rate.
3. Increasing the grain size by a factor of six (from 0.1-0.65 mm) decreases the creep rate by a factor of two.
4. The creep activation energy increased from about 12.5 kcal/mole at 29°C to about 30.0 kcal/mole at 300°C.

Le Comte (1965) showed (fig. 14) with constant axial stress (69 bars) and confining pressure (1,000 bars) that an increase in temperature from 29-104.5°C increases creep rate by a factor of four to five, whereas an increase in temperature from 20-198.2°C increases creep rate by a factor of about 22. With the same axial stress (69 bars) and much less confining pressure (1 bar), an increase in temperature from 29-104.5°C increases the creep rate by about 10 times. Note that an increase in confining pressure lessens the effect of temperature on the creep rate. Figure 14 also shows an increase in confining pressure will usually cause a decrease in creep rate.

Although the direction that creep rate will change in as a result of changing variables is often predictable, the magnitude of the change is not. Both Herrmann and others (1982) and Verral and others (1977) note a discrepancy

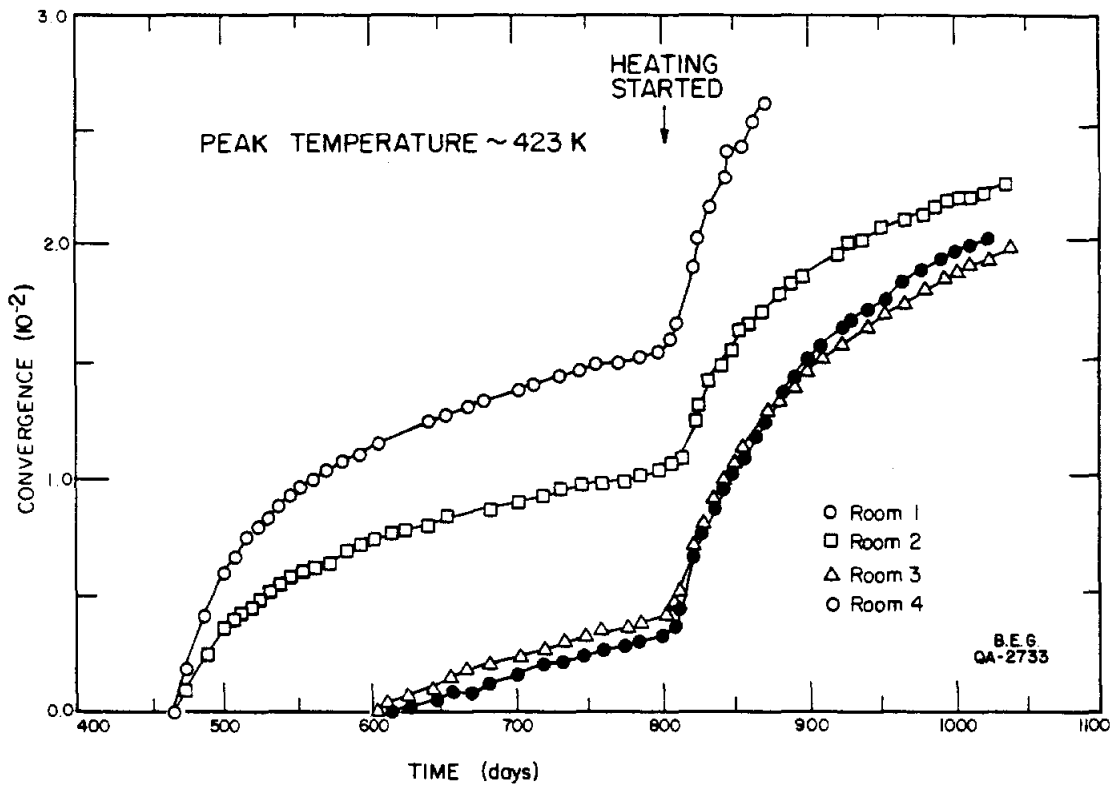


Figure 13. In situ creep shown by convergence of floor and ceiling in an underground salt mine (after Empson and others, 1970). Heating of a nearby mine pillar causes acceleration of the rate of convergence.

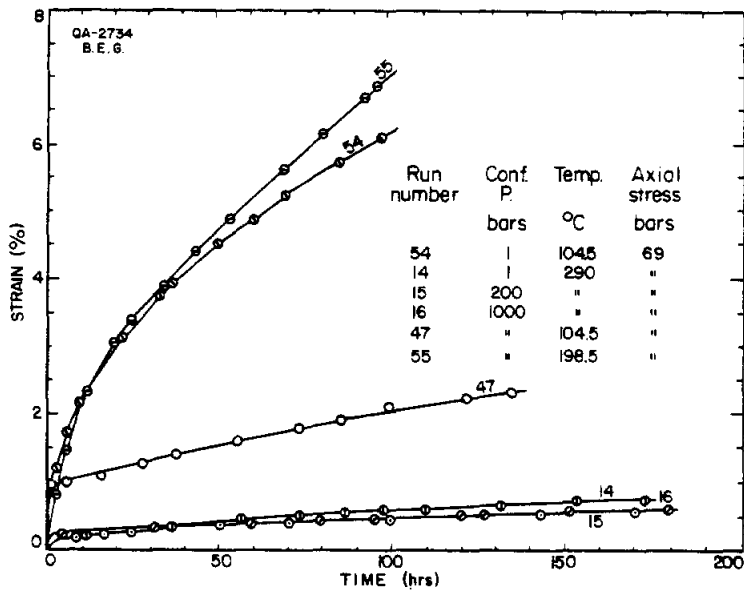


Figure 14. Creep curve for artificially prepared salt showing the effect of temperature, confining pressure, and axial stress (after Le Comte, 1965).

of two orders of magnitude in creep rates between the data of Heard (1972) and Burke (1968).

Strain-rate tests (fig. 15) on natural salt samples from Avery Island salt dome were performed by Hansen and Mellegard (1979) and Hansen and Carter (1980) and are reproduced in Carter and Hansen (1983, their fig. 10). In these experiments a constant differential stress of 10.3 and 20.7 MPa was applied to rock salt at temperatures from 24-200°C. The strain rate curves in figure 15 demonstrate variations in the type of creep behavior with changes in stress and temperature. At differential stress of 10.3 MPa and temperatures less than 115°C the creep is entirely transient, that is, creep decelerates with time. Creep strains are low even as long as ten days (8.6×10^4 s). At higher temperatures there is an appreciable increase in creep rate and steady-state creep behavior is attained. Thus, temperature greatly influences creep rate and the timing of the transition from transient to steady-state creep (Carter and Hansen, 1983).

The influence of differential stress on creep behavior is similar to that of temperature. Higher differential stress produces higher creep rates and causes steady-state flow to begin at a much earlier time.

Natural rock salt exhibits wide variations in fabric, crystal size, and impurity content. These variations are especially pronounced between domal salt (relatively nonbedded, highly foliated, and pure) and bedded salt (highly bedded, relatively impure). Recent tests have attempted to quantify differences in creep behavior of natural rock salts including bedded Lyons salt from Kansas, bedded Salado salt from New Mexico, and dome salt from Avery Island and Weeks Island, Louisiana. Results of stress-strain tests on these salts are shown in figure 16. Initial behavior of the salts was nearly identical, except for Lyons salt which is appreciably stronger. The results were unexpected by Hansen and Carter (1980). Lyons salt would have been predicted to be the

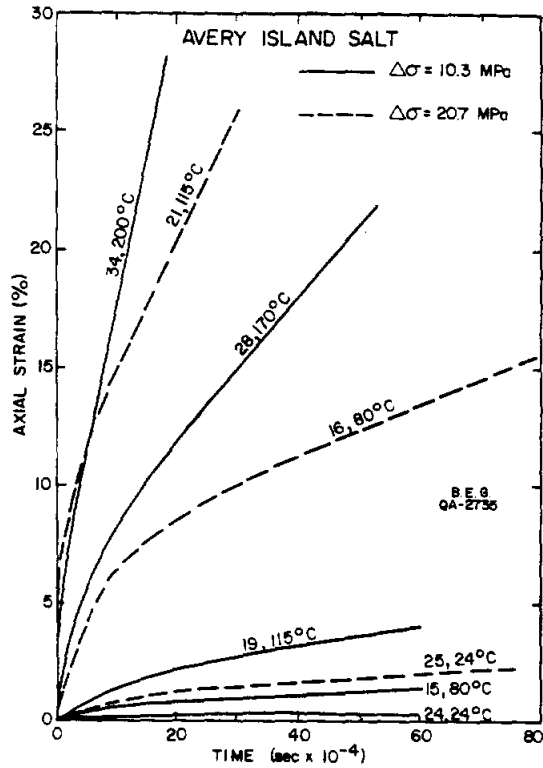


Figure 15. Creep curves for Avery Island dome salt deformed at temperatures from 24°C to 200°C and stresses from 10.3 MPa to 20.7 MPa. Confining pressures were 3.5 MPa or above (data from Hansen and Mellegard, 1979; Hansen and Carter, 1979, 1980; after Carter and Hansen, 1983).

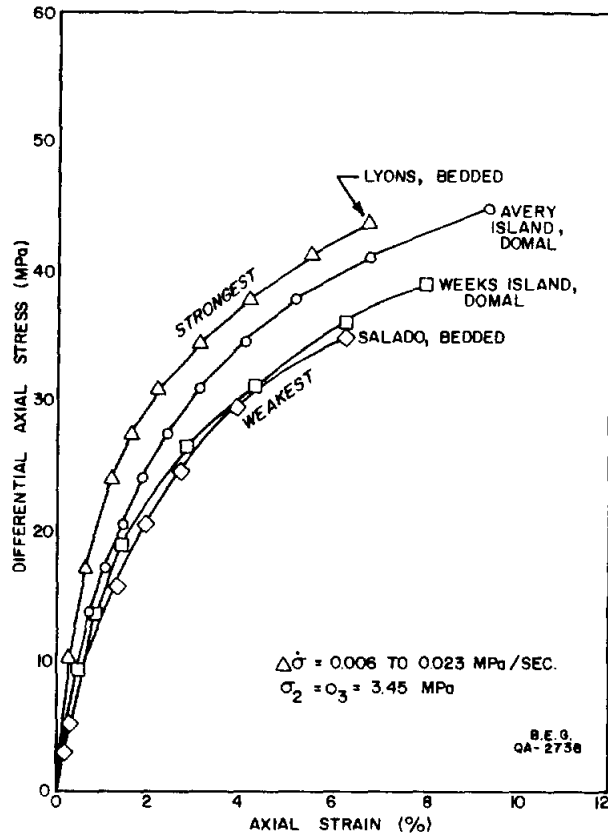


Figure 16. Stress-strain curve for bedded and dome salt deformed by a differential stress rate of 0.006 MPa to 0.023 MPa s⁻¹ and a confining pressure of 3.45 MPa. There is no systematic variation in creep behavior between bedded and domal salt. However, bedded salt from Lyons, Kansas, is the most creep resistant salt of those tested (after Hansen and Carter, 1980).

weakest on the basis of the orientation of crystal fabric in which the Lyons salt contained the largest number of primary slip planes oriented with the orientation of high shearing stress.

The influence of grain size on the behavior of salt has been reported by Le Comte (1965), Burke (1968), Reynolds and Gloyna (1961), and Serata and Gloyna (1959). These results are especially contradictory. Le Comte (1965) showed that with all other conditions constant, increasing the grain size by a factor of six decreased the creep rate by a factor of two (fig. 17). Burke (1968) also worked on artificial salt but at higher temperature (1013 K), and his data show the opposite behavior (fig. 18). Increasing the grain size by a factor of 2.5-10 increased the creep rate by about an order of magnitude when the stress is held constant at 1 MPa. The results from in situ observations of mine openings reported by Reynolds and Gloyna (1961) and cited by Odé (1968) documents the exact opposite behavior to that displayed by artificial salt in the laboratory. Reynolds and Gloyna (1961) found that at low temperature fine-grained salt is more creep resistant than coarse-grained salt and that at higher temperatures this effect is reversed (Odé, 1968, p. 584). One possible explanation for the discrepancy between laboratory and in situ results is that under in situ conditions grain-size variations of salt are not the cause of differences in salt behavior but merely a reflection of different stress states which caused the grain-size variations.

In Situ Creep

In situ creep and creep rates have been measured directly in salt and potash mines (Baar, 1977; Dreyer, 1972; Obert, 1964; Reynolds and Gloyna, 1961) and indirectly in boreholes (Thoms and others, 1982; Fernandez and Hendron, 1984), and in solution-mined caverns (Preece and Stone, 1982). Baar (1977) is especially critical of applying laboratory-derived creep curves to in situ

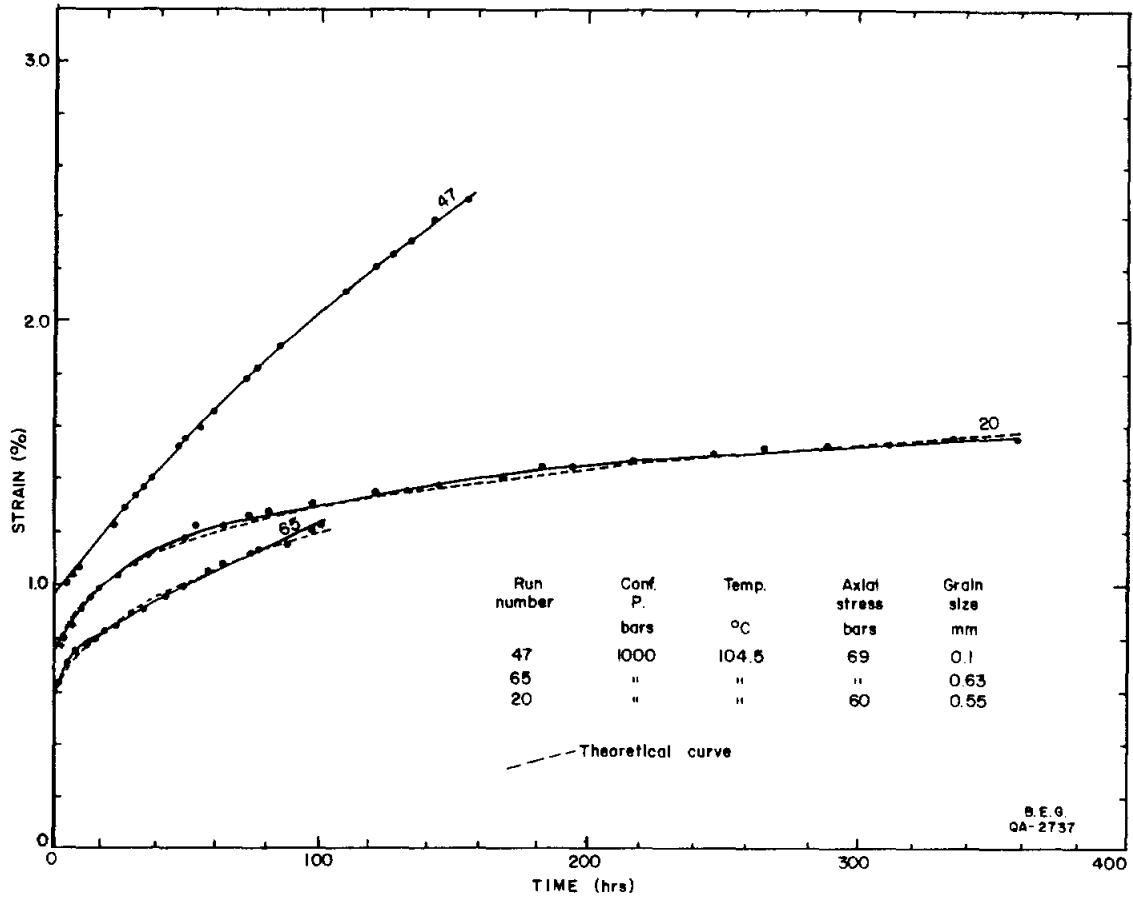


Figure 17. Creep curve for artificially prepared salt showing the effect of variations in grain size and axial stress on the creep behavior (after Le Comte, 1965).

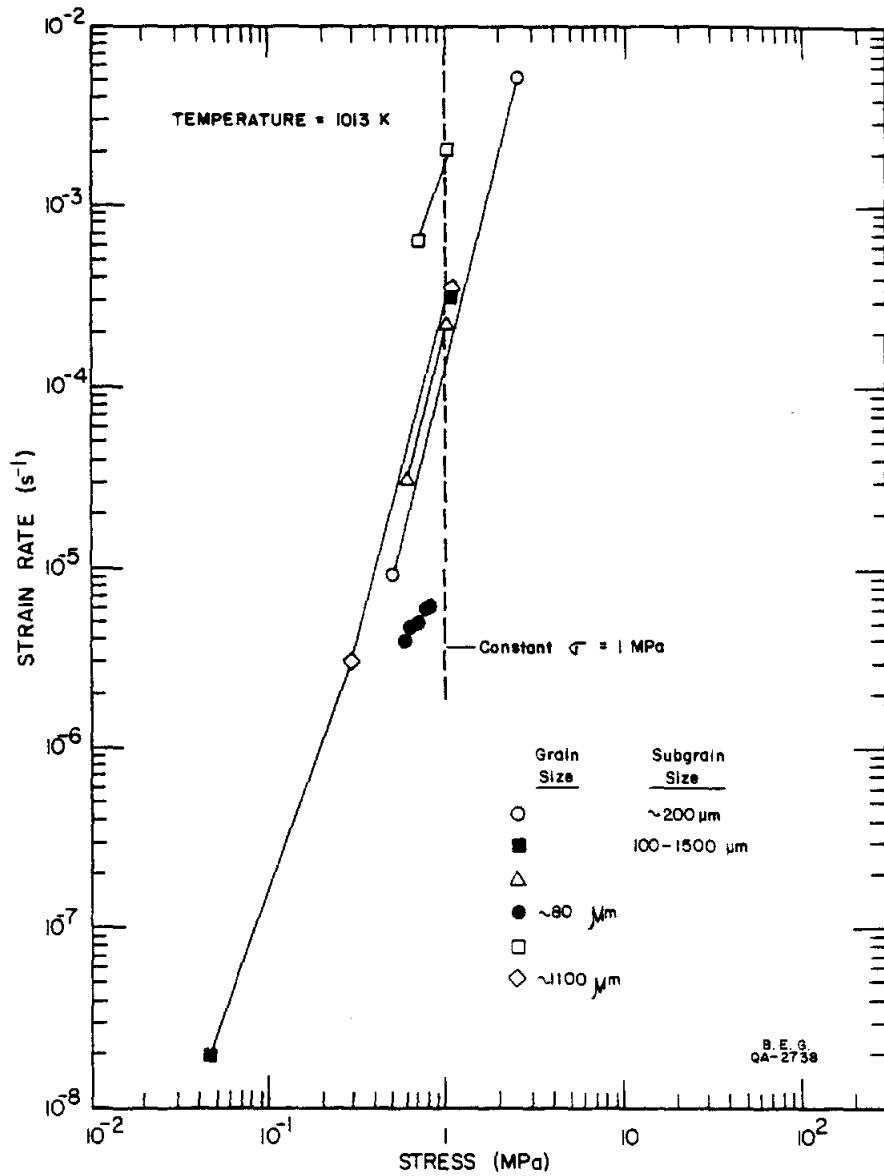


Figure 18. Strain rate curve for artificially prepared salt deformed at high temperature (1013 K). Strain rates with a constant stress show a significant increase due to increases in grain size and subgrain size (cited by Hume and Shakoor, 1981; after Burke, 1968).

conditions. Baar (1977) specifically denies the applicability of the transient part of creep curves to in situ salt behavior. He ascribes the decreasing rate of salt creep with time in laboratory experiments to strain (or work) hardening which he insists only occurs in laboratory scale experiments. A critical review of Baar's data (Baar, 1971, 1977) reveals short initial periods of declining rate of creep with time. This initial period of declining rate is referred to by Baar as "stress-relief creep." Baar (1971, 1977) concentrated on German and Canadian potash mines, and his observations include data of up to five years duration (fig. 19). The results of Dreyer (1972) and Baar (1977) characteristically showed that long-term creep rates are constant. Obert (1964) studied the convergence of rock-salt pillars in Kansas and described both transient and steady-state creep behavior. Reynolds and Gloyna (1961) cited by Odé (1968) summarized convergence measurements from domal salt mines in Louisiana and Texas and from bedded salt in Kansas. Their observations and those of previous workers include:

1. The rate of creep decrease with time.
2. The rate of creep is temperature dependent.
3. The rate of creep depends on the location where the measurement was conducted.
4. The rate of creep increases with depth.
5. Fine-grained materials at low temperature are more creep resistant than coarse-grained material; at higher temperatures the effect is reversed.
6. Impurities can increase the cohesive force of salt.

Borehole closure studies are another potentially powerful means of studying in situ salt behavior (Fernandez and Hendron, 1984; Thoms and others, 1982). Borehole closure at Rayburns and Vacherie salt domes, Louisiana, was studied by simply repeating caliper surveys in a hole filled with saturated

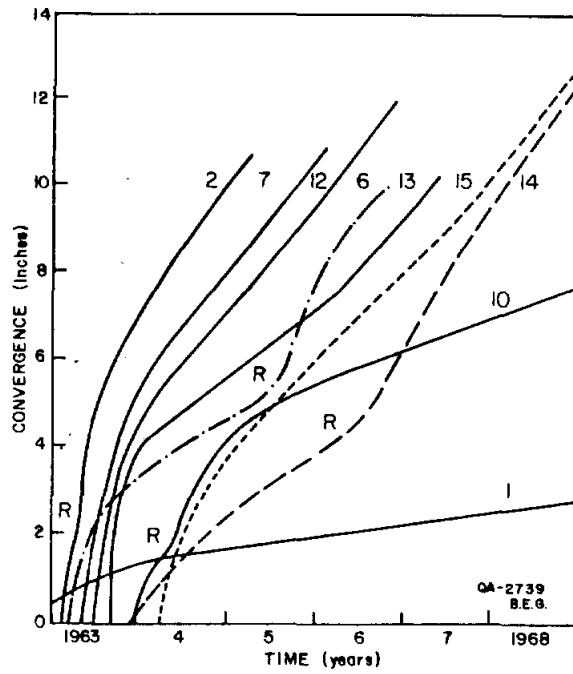


Figure 19. Convergence in Canadian potash mine as a function of time. Long-term convergence is nearly constant (after Baar, 1977).

brine at 387 and 864 days and at 163, 413, and 890 days, respectively, after drilling (figs. 20A, 20B). Note that after 864 days Rayburns borehole closure at a depth of 4,000-5,000 ft was fairly constant, but at Vacherie dome the borehole continued to close throughout the entire depth range. For both domes the closure was very small (percent closure = 0.5) above depths of 2,500 ft.

Borehole closure data for Vacherie dome were recalculated in order to see how strain rates varied with time, stress, and depth and to see how these data compared with data derived from laboratory analysis. The strain rate was calculated by dividing the linear closure (strain) for the borehole (using a nominal hole diameter of 8-3/4 inches) by the duration in seconds of time since drilling. Strain rates were nearly constant at any given depth after a transient initial period of approximately 163 days. The strain rate (fig. 21) clearly increases exponentially with stress and depth and ranges from $7.4 \times 10^{-11} \text{ s}^{-1}$ at 1,150 ft to $3.5 \times 10^{-9} \text{ s}^{-1}$ at 4,950 ft. The range of known environmental conditions were temperature (100 to 165°C), axial stress (4.2-18.1 MPa), and strain (0.1 to 27 percent).

Fernandez and Hendron (1984) studied borehole closure over a moderately long term (three test segments of approximately 100 days duration each) in bedded salt at a depth of 6,000 ft. They analyzed wellbore closure of a bedded salt section by daily observation of the volume of saturated brine (stage 1) or oil (stage 2) expelled from an uncased salt section. The expulsion was inferred to have been due solely to hole closure. Three different levels of constant pressure (9.0, 15.2, and 20.7 MPa) were induced by the weight of fluids in the borehole to evaluate the response to various stress levels. The authors concluded:

1. Creep rates continued to decline for the duration of the test segments.

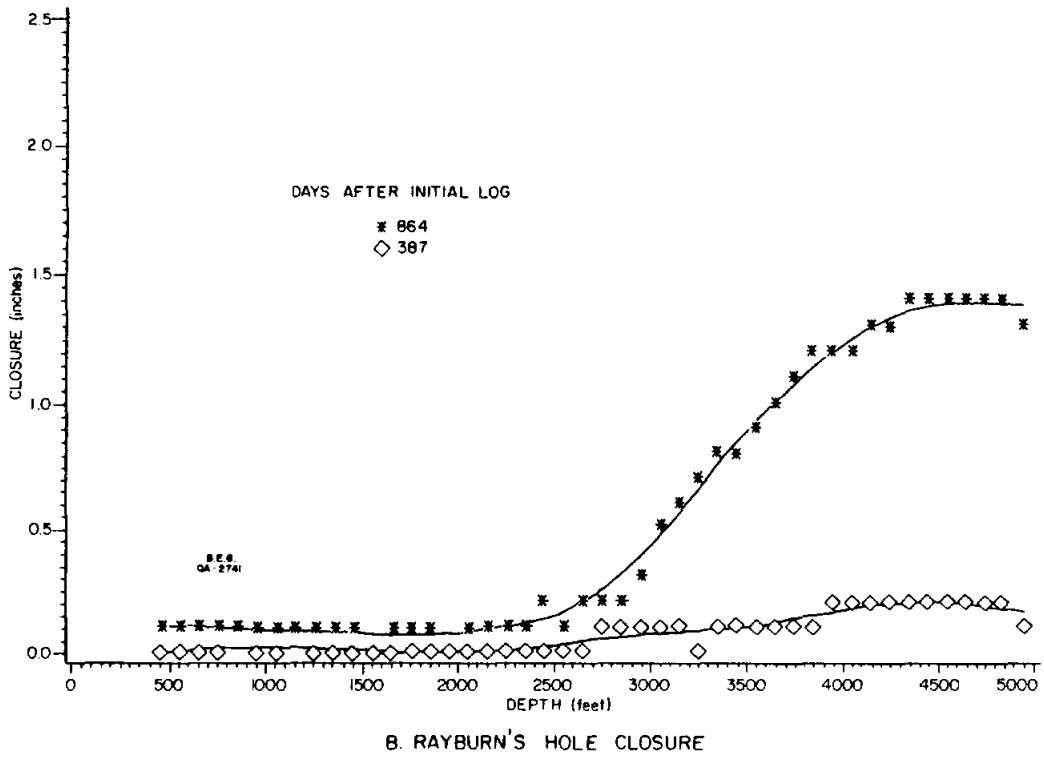
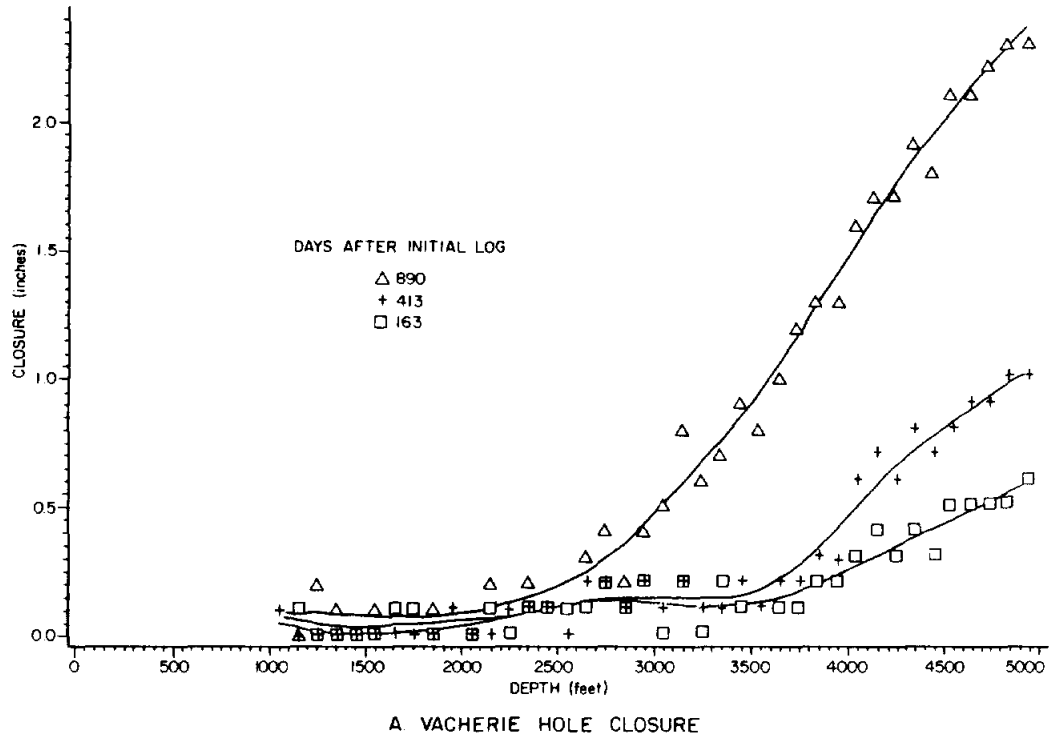


Figure 20. Borehole closure of (A) Vacherie and (b) Rayburns salt domes (after Thoms and others, 1982).

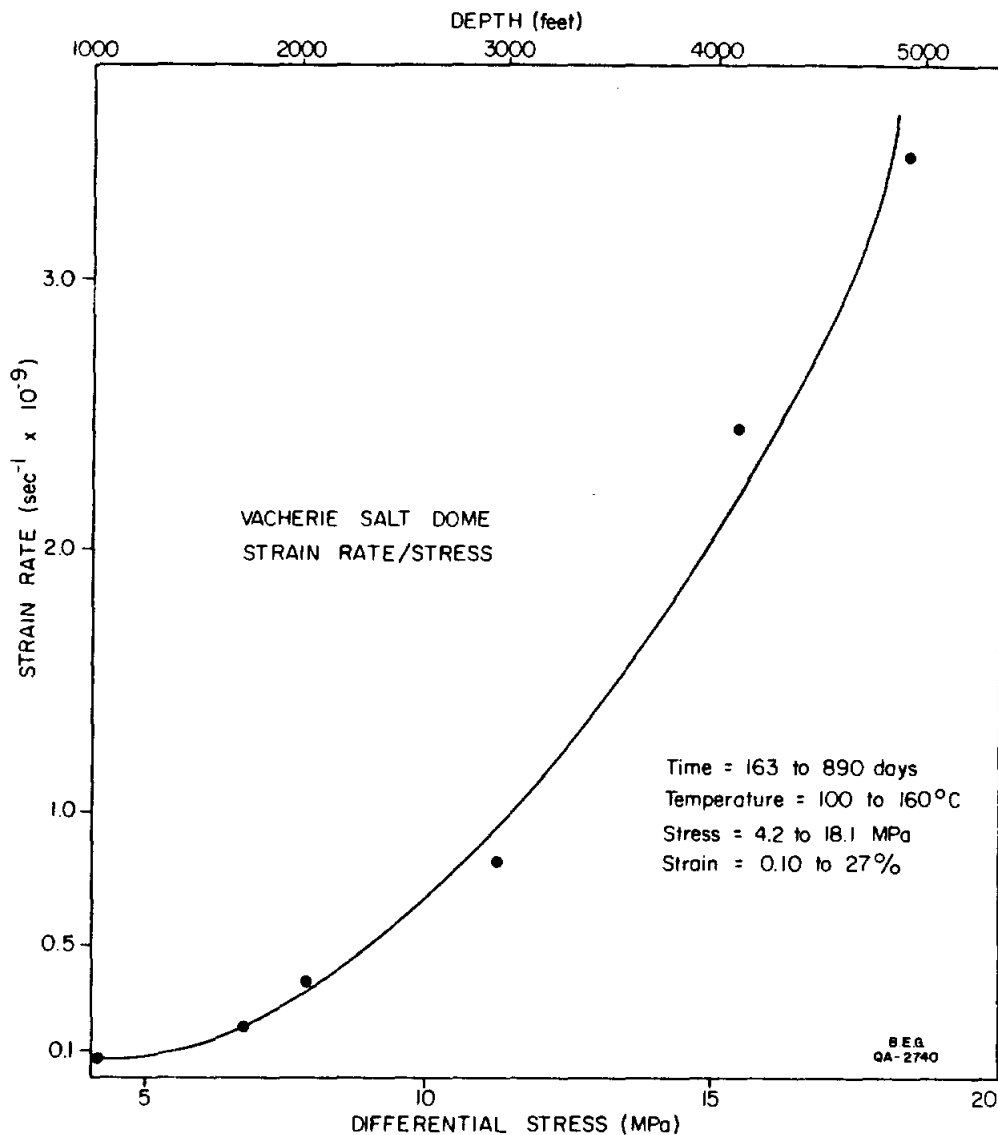


Figure 21. Strain rate curve for borehole closure at Vacherie salt dome based on borehole closure data from Thoms and others (1982). Linear closure data were converted to strain data base on a nominal hole diameter of 8-3/4 inches. Strain rates were derived using four points for time control (that is, 0, 163, 413, and 890 days after drilling; see figure 20). At a given depth, strain rates were remarkably linear. Differential stresses were derived from the difference between the lithostatic load exerted by the salt and the load exerted by the borehole filled with saturated brine. Note the exponential increase in strain rate with increasing differential stress or depth.

2. The magnitude of well closure was greater for higher shear stress (differential stress).
3. The rate of well closure was greatest for higher shear levels (differential stress).

Comparison of Strain Rates

Strain rates ($\dot{\epsilon}$) of domal-rock salt are compared in Table 2 for three fields of data--salt domes and salt glaciers, boreholes and mine openings, and laboratory experiments on rock salt. Only steady-state strain rates were used from laboratory tests (Mellegard and others, 1983; Carter and Hansen, 1983; Spiers and others, 1984). Strain rates for rock salt vary through 11-12 orders of magnitude. Among the fastest strain rates ($1.25 \times 10^{-6} \text{ s}^{-1}$) were those from laboratory runs on Avery Island dome salt with differential stress of 10.3 MPa and a temperature of 200°C. Mean long-term strain rates for fastest growing salt domes in the East Texas salt diapir province were 2.3×10^{-15} - $6.7 \times 10^{-16} \text{ s}^{-1}$ (Seni and Jackson, 1984). Natural stress difference within salt domes is very low, on the order of 0.03-0.25 MPa, thus natural strain rates are expected to be much lower than laboratory rates.

Strain rates for domal salt in laboratory experiments are three orders of magnitude faster than the strain rates calculated from borehole closure and mine closure observations. There is a general equivalence in temperature and stress conditions between these two fields of data. Both sets of data are principally on dome salt. The discrepancy in strain rates is thought to be partially related to differences between in situ and test conditions or observation duration. The duration of laboratory tests usually ranges up to three months. Maximum in situ observations of boreholes and mine openings range from three to thirty years, respectively. Therefore, in situ tests are over a time

Table 2. Strain Rates for Deformation of Rock Salt
(Modified from Jackson 1984)

TEST DATA	STRAIN RATE ^a (per second)
Natural Conditions of Dome Salt	
Diapiric Salt	
Measurement of topographic mound ^b	2×10^{-14}
Comparison of dome profiles ^c	8.4×10^{-13}
Estimates from thickness variations in strata around domes ^d	3.7×10^{-15} to 1.1×10^{-16}
Average growth of Zechstein domes ^e	2×10^{-15}
Glacial Salt	
Direct measure of flow ^f	1.9×10^{-9} to 1.1×10^{-11}
Comparison of glacial profile ^c	6.7×10^{-13} to 9.0×10^{-13}
Estimates from glacial morphology ^g	2×10^{-8} to 2×10^{-13}
In Situ Conditions of Dome and Bedded Salt	
Direct measure of mine-opening closure ^h	1×10^{-9} to 9×10^{-12}
Direct measure of peak-borehole closure ⁱ	3×10^{-8}
Direct measure of long-term borehole closure ^j	3.5×10^{-9} to 7.4×10^{-11}
Laboratory Strain Rate Tests	
Strain-rate test ^k	1.25×10^{-6} to 9.5×10^{-9}
Strain-rate test ^l	2.04×10^{-9} to 3.61×10^{-9}
Strain-rate test ^m	1.35×10^{-6} to 3.45×10^{-9}
Strain-rate test ⁿ	4×10^{-4} to 1×10^{-9}

Table 2. (cont.)

- a. Conventional strain rate $\dot{E} = E/t$, where elongation E = change in length/original length at t = duration in seconds (s).
- b. Ewing and Ewing (1962), Sigsbee Knolls Gulf of Mexico abyssal plain. Calculation based on salt stock height of 1,300 m; duration of strain 3.5×10^{11} s (11,000 years).
- c. Talbot and Jarvis (in press) comparison of observed profile of Kuh-e-Namak stock and glacier to profile of numerical model of viscous fluid extruding from a narrow orifice.
- d. Seni and Jackson (1984) based on dome growth rates over 9.5×10^{14} s to 1.8×10^{15} s (30 Ma to 50 Ma).
- e. Sannemann (1960) based on stratigraphic-thickness data and salt stock height of 4 km; duration of strain 1.14×10^{15} s to 4.1×10^{15} s (35 Ma to 130 Ma).
- f. Talbot and Rogers (1980) based on displaced markers on salt duration of strain 2.5×10^7 s (292 days); calculated stress (σ) \leq 0.25 MPa. Maximum flow after 5 mm rainfall.
- g. Wenkert (1979) for five Iranian glaciers, assumed steady-state equilibrium between extrusion and wasting; with erosion rates of 0.08 cm/yr to 0.25 cm/yr; calculated stress (σ) = 0.03 MPa.
- h. Serata and Gloyna (1959), Reynolds and Gloyna (1960), and Bradshaw and McClain (1971) based on observations in Grand Saline dome in Texas and Lyons bedded salt in Kansas; upper limit corresponds to wall temperature 100°C; estimated stress difference 10 MPa; duration of strain 3.2×10^8 s to 9.5×10^9 s (10 to 30 years).
- i. Martinez and others (1978) Vacherie dome, Louisiana; duration 7.8×10^6 s (3 months).
- j. Thoms and others (1982), Vacherie dome, Louisiana; duration of strain 7.7×10^7 s (890 days); slowest rate at 100°C, 351 m depth, stress difference 42 MPa; fastest rate at 160°C, 1,509 m depth, stress difference 18.1 MPa.
- k. Carter and Hansen (1983), from data of Hansen and Carter (1982), Avery Island dome, Louisiana; temperature 24°C to 200°C; differential stress 10.3 MPa and 20.7 MPa; duration 4×10^4 to 30×10^4 s.
- l. Wawersik and others (1980), Bryan Mound dome, Texas; temperature 22°C to 60°C; differential stress 20.7 MPa; duration 9.72×10^4 to 1.44×10^6 s (27 to 400 hrs).
- m. Mellegard and others (1983), Avery Island dome, Louisiana; temperature 24°C to 200°C; differential stress 6.9 MPa to 20.7 MPa.
- n. Spiers and others (1984), Asse dome, Germany; temperature 150°C; confining pressure 2.5 MPa (SP 124) to 10 MPa (SP 125,129). SP125 brine added, SP129 inherent brine 0.05% only.

period from one to two orders of magnitude longer than laboratory tests. Natural strain rates are very low when measured over the period of dome growth which are up to seven orders of magnitude longer than test durations in the laboratory.

The short duration of laboratory tests may be a serious shortcoming of this type of strain experiment, both from the rapid application of stress and from the inadequate test duration.

Some very exciting data have just come to light (Spiers and others, 1984) which offer a mechanistic explanation for discrepancies observed between previous laboratory data and long-term mechanical properties inferred from geological studies. Salt core from Asse salt dome, Germany, was subjected to laboratory tests exceeding three years duration. Further, brine content, a previously ignored but important variable, was included in the testing. Salt cores were compressed under triaxial load and then studied dilatometrically (under dilation) using stress relaxation techniques. Essentially the conditions may be visualized as a mirror reversal of borehole closure studies. Both "dry" samples with inherent (very small but unspecified) brine concentrations and "wet" (>0.25-0.5 weight percent brine added under pressure of 1.0-10 MPa) samples were evaluated.

The salt deformation was sensitive to both brine content and to strain rates. Above very rapid strain rates of 10^{-7} s^{-1} (normal laboratory rates), both wet and dry samples exhibited dislocation creep behavior in agreement with previous studies. Dry samples weakened (that is, less differential stress yielded the same strain rate) when subjected to slower strain rates less than 10^{-7} s^{-1} and when dilatancy was suppressed ($\sigma_3 = 5-10 \text{ MPa}$). Wet samples also displayed weakened behavior at strain rates slower than 10^{-7} s^{-1} , but dilatancy was suppressed naturally ($\sigma_3 = 2 \text{ MPa}$). The weakened behavior of wet salt was

due to fluid-film-assisted grain boundary diffusion. The brine greatly facilitated recrystallization. Spiers and others (1984) concluded that flow laws obtained from dry salt at rapid strain rates or low pressures cannot be extrapolated to predict long-term behavior of wet or dry salt. Wet salt under natural low stress conditions displays long-term creep rates much faster than previously predicted particularly if relatively small amounts of brine (>0.25-0.5 weight percent) are present.

Creep Laws

Creep laws are one kind of the many constitutive laws that model the rate-dependent deformation of materials. Creep laws are applied to the design of underground storage caverns, radioactive waste repositories, and to salt mines where the combination of stress, temperature, and time gives rise to significant time-dependent deformation. A number of creep laws have been proposed to describe the behavior of rock salt. These laws have been used in a variety of ways in evolving creep and creep-plasticity theory, creep mechanisms, and in various finite element computer codes for analyzing nuclear-waste isolation studies and in Strategic Petroleum Reserve facilities. Reviews of various creep laws include Dawson (1979), Herrmann and Lauson (1981a, 1981b), Wagner and others (1982), Herrmann and others (1982), Senseny (1981), and Carter and Hansen (1983).

The total strain in any given material is given by Carter and Hansen (1983) as:

$$E = E_e + E_p + E_t + E_s + E_a \quad (1)$$

where E_e is the elastic strain ($\Delta\sigma/E$) upon loading,

E_p is the plastic strain during loading,

E_t is the transient or primary creep strain,

E_s is the steady state or secondary creep strain, and

E_a is the accelerating or tertiary creep strain.

The contributions of E_t and E_s are expected to contribute the bulk of the creep strain. For the purposes of this discussion, E_e , E_p , and E_a will be neglected, although some creep laws do include terms for these variables.

Most researchers agree that both transient and steady-state creep behavior are likely to be encountered in rock salt at the pressure and temperature range in a waste repository or storage cavern. Various equations used to describe these two aspects of creep behavior will be described and compared.

Steady-State Creep

The Weertman expression (Weertman, 1968; Weertman and Weertman, 1970) is the equation most commonly used to describe steady-state creep behavior of rock salt at 1/4 to 1/2 salt's homologous temperature (the ratio of temperature to the melt temperature in degrees Kelvin). The Weertman expression for creep rate is:

$$\dot{E}_s = A \exp\left(\frac{-Q}{RT}\right) \left(\frac{\sigma}{\mu}\right)^n \quad (2)$$

where T is absolute temperature, σ is shear stress or principal stress difference under triaxial load, μ is shear modulus, R is the universal gas constant, and A , Q , and n are constants which depend on the creep mechanism that is operating in the given stress-temperature region.

Carter and Hansen (1983) show a somewhat simpler form of the equation

$$\dot{E}_s = A \sigma^n \exp\left(\frac{-Q}{RT}\right) \quad (3)$$

where A is a slightly temperature and structure-sensitive material parameter.

The temperature dependence of the creep rate is strong, being given by the exponential term in both (2) and (3). Similarly, the stress dependence is also strong. The influence of various creep mechanisms will be described in later sections. Both (2) and (3) tacitly imply that steady-state creep is not dependent on the mean stress of hydrostatic pressure.

Transient Creep

Transient creep is not well understood and various creep laws have been proposed to describe and predict creep rates that decrease with time (Herrmann and Lauson, 1981a). These laws include exponential, logarithmic, power law, and Munson and Dawson equations.

Exponential Creep Law

An exponential (on time) creep law is of the form:

$$E = E_e + E_s t + E_\infty (1 - \exp(-\xi t)) \quad (4)$$

where E is strain, E_e is elastic strain, t is time, and

E_s , E_∞ , and ξ are fitting parameters.

This equation first proposed by McVetty (1934) for high temperature creep of metals is also widely used for rock salt. It is the baseline creep law used for numerical analysis of potential nuclear repositories in salt (Senseny, 1981).

As t approaches infinity in equation (4) the bracketed term approaches zero. Thus, when the steady-state terms E_e and E_s are ignored, the transient creep rate decays linearly from the initial value of ξE_∞ to zero as the transient creep rate approaches its limiting value E_∞ (fig. 22).

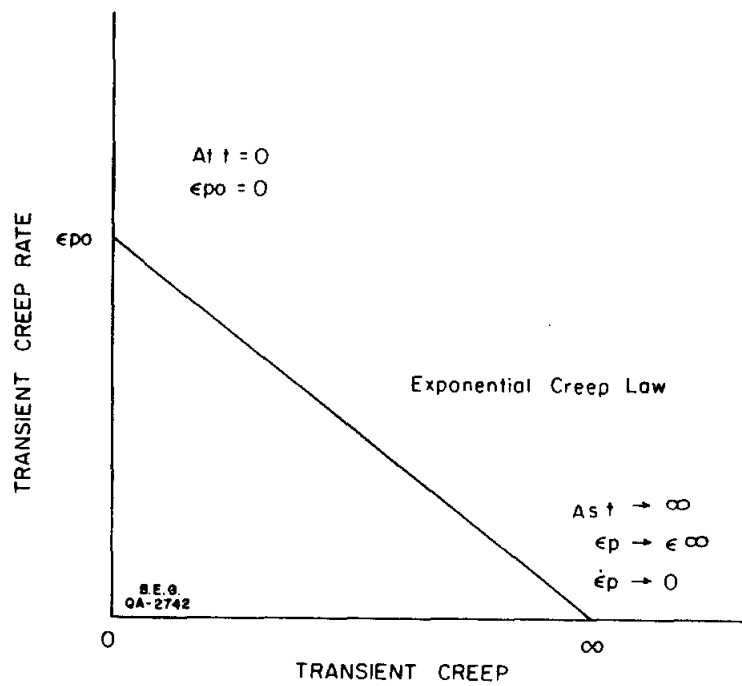


Figure 22. Exponential creep law behavior (after Herrmann and Lauson, 1981a).

Logarithmic Creep Law

The logarithmic (on time) law is given as:

$$E = E_e + \dot{E}_s t = \gamma \ln(1 + \mu t) \quad (5)$$

where E is strain, E_e is elastic strain, t is time, μ is shear modulus, \dot{E}_s and γ are fitting parameters.

The logarithmic law has been used to fit low temperature creep data in both metal and rock salt (Herrmann and Lauson, 1981a). Herrmann and Lauson (1981a) showed the creep rate decays exponentially to zero from its initial finite value with the logarithmic creep law, but the transient creep strain becomes unbounded as t approaches infinity (fig. 23).

Power Creep Law

A power creep law is of the form:

$$E = E_e t + K \sqrt{J_2}^m t^n \quad (6)$$

where E is strain, E_e is elastic strain, t is time, $\sqrt{J_2}$ is the square root of the second invariant of the deviator stress, and K , m , and n are creep fitting parameters.

According to Herrmann and Lauson (1981a), the transient creep rate is infinite initially and decays to zero with time, whereas the creep strain grows without limit as time goes to infinity (fig. 24).

Discussion of Creep Laws

Both Herrmann and Lauson (1981a) and Wagner and others (1982) applied these creep laws to a single set of laboratory data and compared the resulting fit. Herrmann and Lauson (1981a) also derived the laws and examined interrelations between the laws. In both the articles, the laws were found to fit the data base equally well, although the duration of the laboratory data was quite short (9 to 72 days). Major conclusions were very different. Wagner and

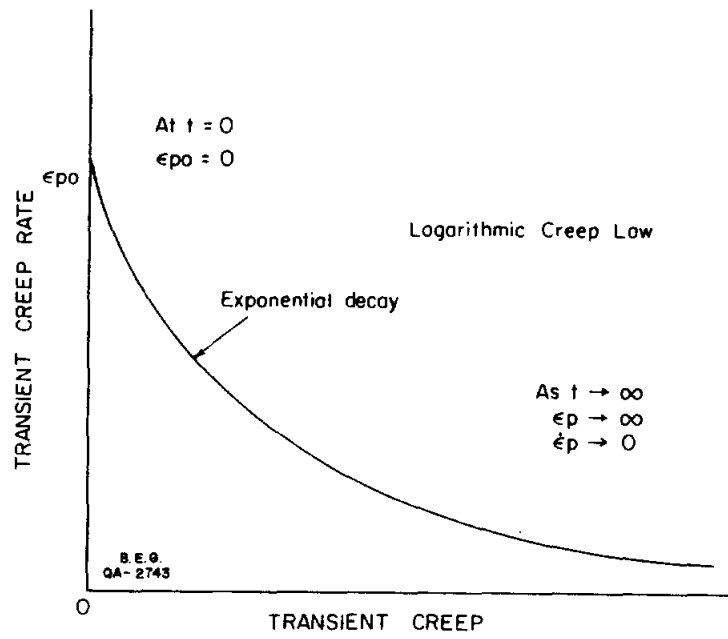


Figure 23. Logarithmic creep law behavior (after Herrmann and Lauson, 1981a).

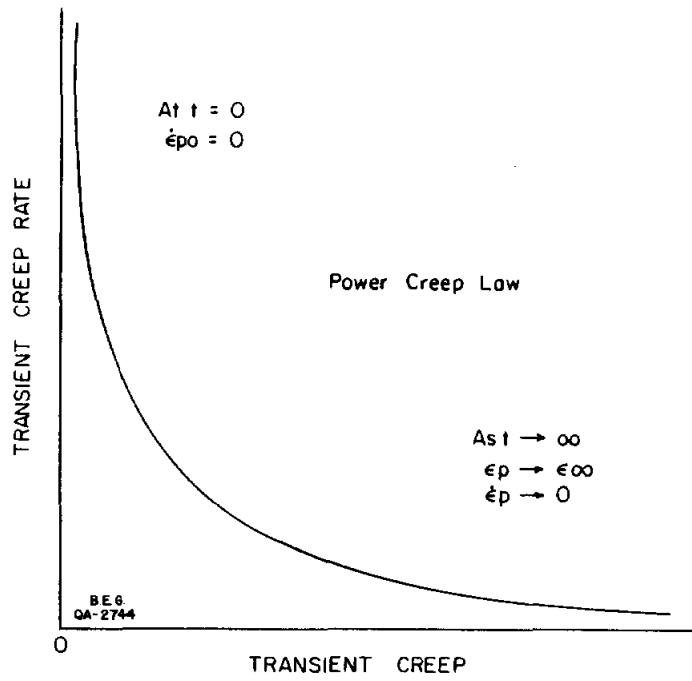


Figure 24. Power law creep behavior (after Herrmann and Lauson, 1981a).

others (1982) emphasized long-term extrapolation of the results (up to 25 years). They found that the amount of predicted closure was very sensitive to the form of the creep law. They found that the exponential (on time) creep law yielded the least closure and the power law the greatest (fig. 25). Herrmann and Lauson (1981a) emphasized the fact that all the creep laws fit the creep data satisfactorily for the duration of the lab tests. Herrmann and Lauson (1981a) used a power law that did not have a steady-state term. Because transient creep became negligible in extrapolations greater than a few months, the three creep laws with steady-state terms essentially coincided while the power law yielded much lower rates of creep. The power law predicted creep strains about two orders of magnitude less than the other laws at 30 years duration. In contrast, Wagner and others (1982) found their power law equation yielded the greatest creep over the long term (4 months) (fig. 25).

Deformation Mechanism

Munson (1979) and Verrall and others (1977) have produced a preliminary deformation mechanism map for salt based on theoretical and experimental results (fig. 26). According to Munson (1979), the deformation-mechanism map is a representation in non-dimensionalized space of regimes of stress (stress/shear modulus) and homologous temperature. Munson defined five stress and temperature regimes where a single deformation mechanism predominates in controlling the strain rate. These regimes include (1) defectless flow, (2) dislocation glide, (3) dislocation climb creep, (4) diffusional creep, and (5) an undefined mechanism. The two high stress regimes (defectless flow and dislocation glide) are controlled by flow processes, whereas the other three regimes (dislocation climb, diffusional creep, and the undefined mechanism) are thermally activated equilibrium processes (Munson, 1979). Although Munson (1979)

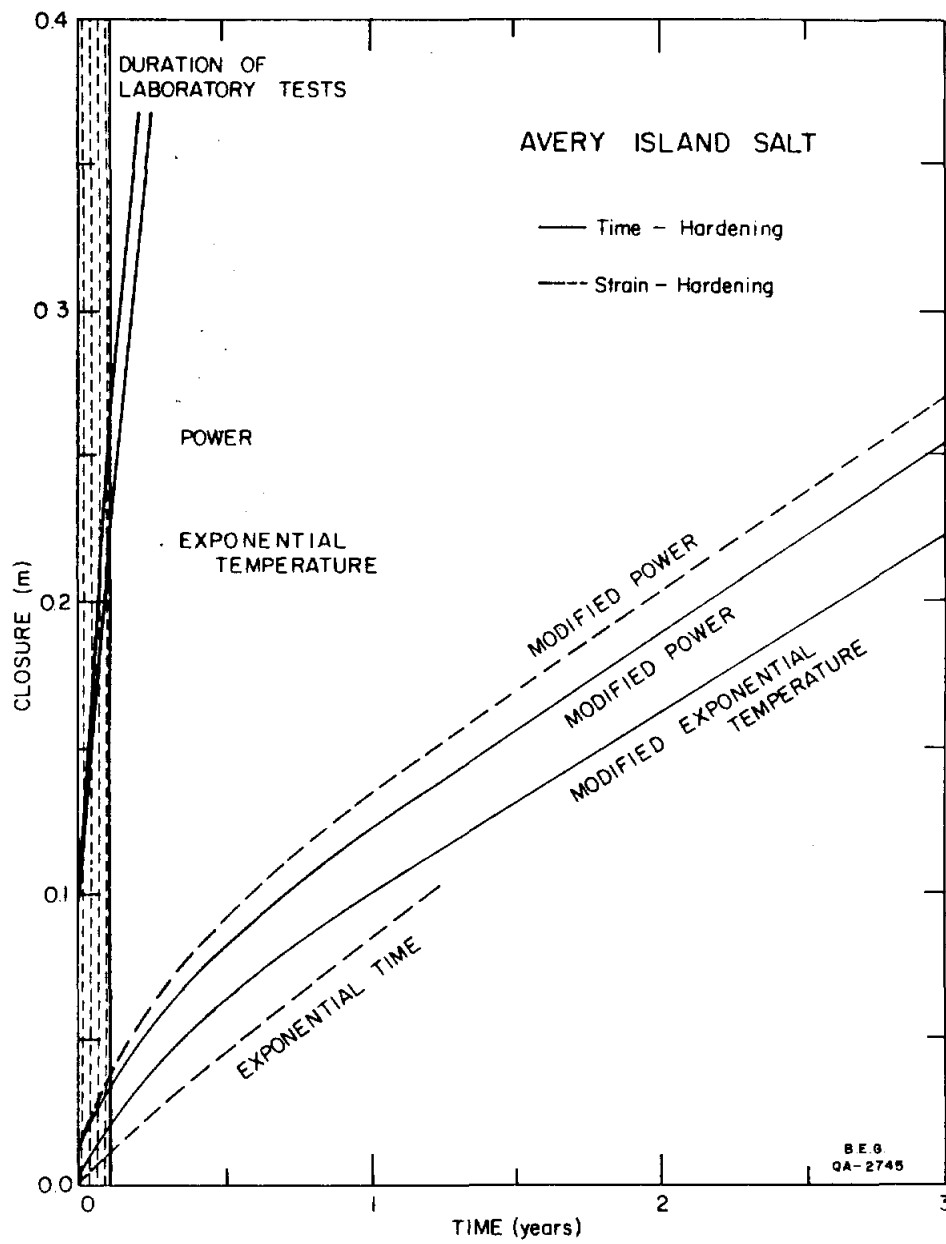


Figure 25. Predicted long-term closures using different creep law forms (after Wagner and others, 1982).

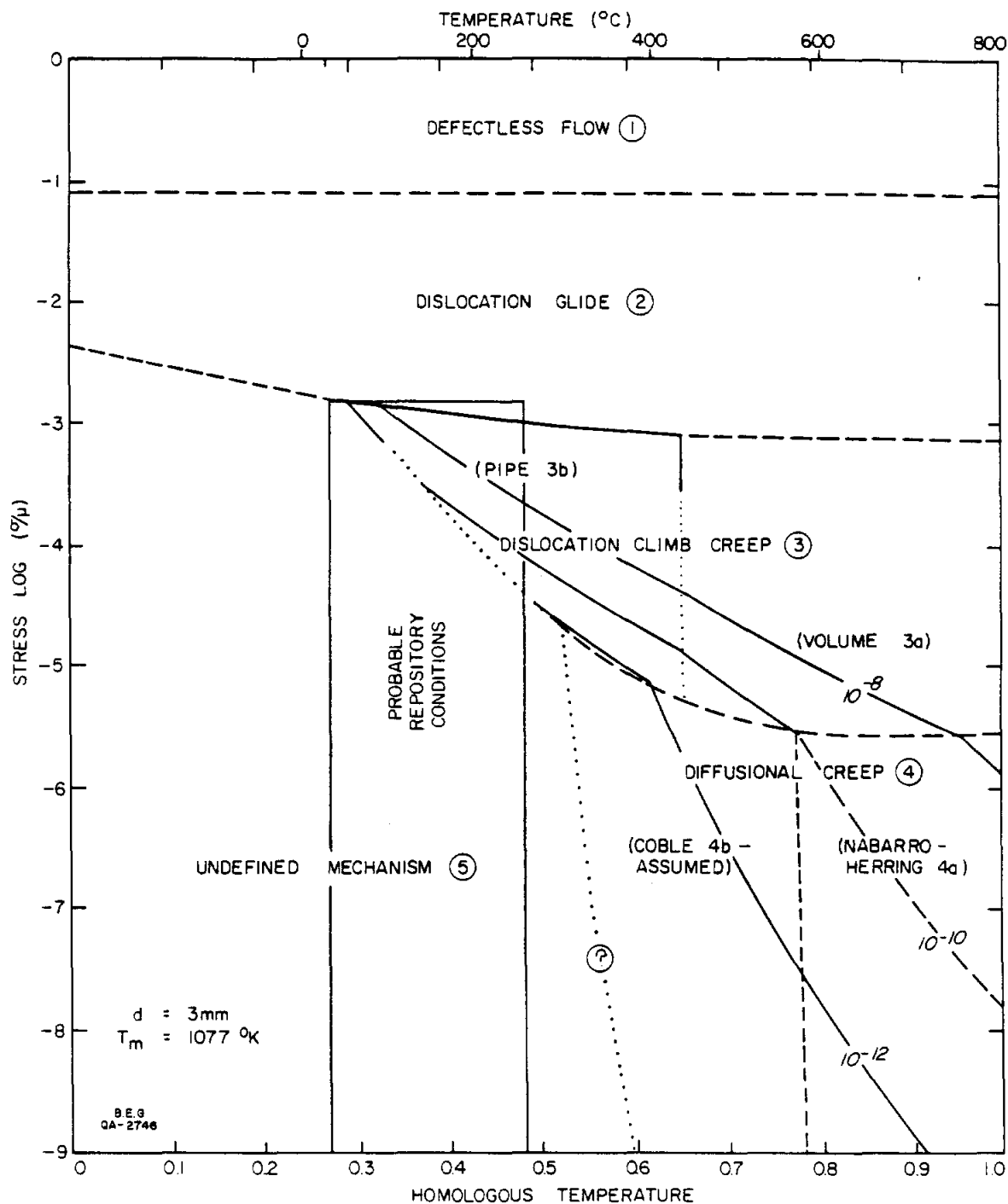


Figure 26. Deformation-mechanism map for salt, including probable repository and storage cavern conditions in cross-hatched area. Grain size is constant at 3 mm. Solid lines between regimes are confirmed by experimental evidence; boundaries shown as dashed lines are based on calculations of constitutive equations; boundaries shown as dotted lines are based on interpolation or extrapolation; question marks on boundaries mean the location is based on conjecture only (after Munson, 1979).

provided constitutive equations for each regime, a complete treatment of those equations is beyond the scope of this report and is largely repetitive with the preceding section.

Defectless Flow--Regime 1

At the theoretical shear strength (derived from calculations of atomic bonding strengths), a crystal of salt will deform even though it is initially without defects. Stress above the theoretical shear strength will produce infinite strain rates and therefore deformation will occur simultaneously throughout the crystal. This stress regime is of little consequence to problems of designing salt storage space or waste repositories because of the very high stress levels in regime 1.

Dislocation Glide--Regime 2

Salt deformation by dislocation glide occurs along several slip systems that permit deformation by dislocation motion. Slip systems listed in decreasing order of importance are $\{110\}\langle\bar{1}10\rangle$, $\{100\}\langle\bar{1}10\rangle$, $\{111\}\langle\bar{1}\bar{1}0\rangle$. Dislocation glide along these systems is hindered by particles of other mineralogical phases, grain boundaries, and by forest dislocations (Munson, 1979). As glide continues, dislocations stack up at locations where flow is hindered; this results in work (or strain) hardening and an increase in flow stress.

Dislocation Climb Creep--Regime 3

Dislocation climb creep is controlled by the equilibrium processes of dislocation climb and polygonization that leads to steady-state creep. Munson (1979) further defined two subregimes of higher and lower temperatures--volume diffusion and pipe diffusion, respectively. At higher temperatures, the creep processes are controlled by volume diffusion of Cl^- ions. For dislocation climb in salt both Na^+ and Cl^- ions must be supplied to the dislocation jog,

but the slower diffusing ion Cl^- controls the rate of the process. This is the reason why the Weertman expression (1) uses the gas constant R in the equation for steady-state creep. At lower temperatures the limiting factor of volume diffusion of Cl^- ions is replaced by a more rapid pipe diffusion of Cl^- ions along dislocations as the controlling process.

Diffusional Creep--Regime 4

Diffusional creep is grain shape changes--strain--by selective transportation of material (Munson, 1979). According to Munson (1979) diffusional creep includes two mechanisms: (1) Nabarro-Herring creep (stress-induced bulk vacancy diffusion of Carter and Hansen, 1983) if transport is by volume diffusion and (2) Coble creep (grain-boundary diffusion of Carter and Hansen, 1983) if transport is by grain-boundary diffusion. Carter and Hansen (1983) note that fine-grained metals and ceramics undergo these processes at low stresses when near melting. However, they say these processes have not been observed in rocks. The boundary between subregimes is a function of grain size. The Nabarro-Herring regime of creep vanishes in favor of Coble creep for grains with a diameter less than 0.33 mm (Munson, 1979).

Undefined Mechanism--Regime 5

The undefined mechanism(s) falls into the low stress, low temperature region of greatest interest to designing storage facilities and waste repositories. The mechanism is difficult to analyze and its boundaries are poorly constrained. There is a clear and pressing need for additional laboratory and in situ studies to understand the nature of the mechanism and the stress/temperature conditions of its activity, especially at the low temperature and stress field of repository or storage cavern conditions.

Discussion

The preceding section of the behavior of rock salt points out how poorly understood are the mechanical properties of salt and creep mechanisms under in situ conditions. Predictions of cavern closure that were based on empirical calculations are not universally applicable. There is no consensus on how salt grain size, salt-stock permeability, and foliation within the stock influence creep properties. Recently recognized is the critical role that small amounts of intercrystalline water play in weakening salt (that is, accelerating salt creep) by recrystallization through fluid-film-assisted-grain boundary diffusion.

Even the best laboratory experiments are seriously flawed by inadequacies in experiment duration, sample size, and in the ability of the experiment to mimic in situ conditions. There is an obvious need for refined experiments based on in situ and site-specific data. Such data are available from core studies, from analysis of structures and textures within core, and from borehole and cavern closure studies.

SALT STOCK PROPERTIES

The in situ structure, stratigraphy, and physical properties of salt in Texas salt domes are known from a few cores and from observations at two salt mines (Kleer Mine--Grand Saline dome, and Hockley salt mine--Hockley dome). Internal boundary-shear zones, foliation, bedding, associated mineral phases, moisture content, grain size, porosity, and permeability are properties that will influence the geometry and long-term stability of solution-mined caverns. In this section we discuss aspects on internal geometry of salt structures from analysis of core from Bryan Mound salt dome.

Bryan Mound Salt Dome

Thirteen cores (with 610 ft [180 m] of recovered salt) from Bryan Mound dome are housed at the Bureau of Economic Geology Well Sample Library. The U.S. Department of Energy is storing crude oil in preexisting brine caverns at Bryan Mound dome. Future plans include creating 12 additional storage caverns. The cores were recovered for site-specific data on mechanical and physical properties of salt at Bryan Mound dome (Bild, 1980; Wawersik and others, 1980; Price and others, 1981).

Bryan Mound dome is in Brazoria County 0.5 mi (1.2 km) from the Gulf of Mexico. Bryan Mound dome is circular with a nearly planar salt stock--cap-rock interface at a depth of 1,100 ft (335 m). Table 3 lists the core holes and data on foliation, grain size, bedding, and depth.

Salt grain size varied from 0.04 inches (1 mm) to 4.0 inches (100 mm). Bild (1980) reports average grain size is 0.33 inches (8.5 mm). Dark laminations, owing to disseminated anhydrite crystals, were common in cores 1A, 106B, 106C, 109A, 110A, but were rare to absent in cores 104A, 108B, 108C, 109B, and 110C. Bild (1980) reports the cores contain 1.9 to 6.1 weight-percent anhydrite.

The orientation and intensity of foliation (schistosity) of halite crystals were studied to better understand flow patterns within the salt stock and the extent of recrystallization (fig. 27). Two trends are clear: (1) in shallow cores (above a depth of 2,500 ft; 762 m) the foliation tends to be weak or absent, whereas in deep cores (below a depth of 3,000 ft; 914 m) the foliation is strong and (2) preferred orientation of foliation changes from near vertical below a depth of 3,500 ft (1,067 m) to an inclination of 20 to 30 degrees (measured from vertical axis of the core) above a depth of 3,000 ft (914 m). The average dip in the seven deepest wells is 12 degrees, whereas the

Table 3. Analysis of Salt Core--Bryan Mound Salt Dome

CORE	FOLIATION	ORIENTATION (degrees)	GRAIN SIZE Fine = <6 mm Medium = 6-20 mm Coarse = 21-50 mm Very Coarse = > 50 mm	BEDDING	DEPTH (FT)
1A	absent		medium-coarse	dark anhydrite common; inclined 15-30 ⁰	1800-1850
104A	strong	30 ⁰	coarse	absent	3063-3095
106B	strong	20 ⁰	medium	gray anhydrite; vertical	3275-3314
106C	weak-strong	25 ⁰	medium	gray anhydrite; vertical	3660-3692
107B	strong	20 ⁰	medium-coarse	gray anhydrite; rare, vertical	2520-2589
107C	strong	05 ⁰	medium-very coarse	gray anhydrite; rare, vertical	3367-3427
108B	absent		fine	absent	3480-3483
108C	strong	10 ⁰	medium	absent	3920-3977
109A	absent-weak	0?	medium	thin, gray anhydrite; inclined 10 ⁰	2324-2384
109B	weak to strong	0	coarse-very coarse	absent	3133-3251
110A	weak	25 ⁰	medium	thin, gray, anhydrite; inclined 10-35 ⁰	2660-2712
110B	strong	25 ⁰	medium	rare anhydrite; vertical	3740-3777
110C	strong	0	medium	absent	4139-4180

average dip of the foliation in the three shallowest cores is 25 degrees. Photographs of the whole core illustrate some of these features (fig. 28).

Two processes are considered to be important with respect to foliation in salt domes. Foliation is basically the elongation of individual crystals. The long axis of foliation is oriented along the axis of least principal stress. The direction of salt flow within the diapir controlled the orientation of the resultant foliation. Recrystallization tends to destroy foliation by removing the accumulated strain history.

The record of foliation at Bryan Mound salt dome can be fit into a simple flow model based on near vertical salt flow from deeper areas of the diapir where foliation is near vertical. Lateral spreading of salt at shallower levels near the diapir crest causes foliation to depart from the vertical. Jackson and Dix (1981) presented a more complex model of salt flow at Oakwood dome which is also applicable to Bryan Mound dome. Lateral salt flow near the diapir crest is by multiple emplacement of salt tongues. The salt tongues progressively refold older salt tongues. True azimuth orientation of the foliation at Bryan Mound dome could not be determined because the cores were unoriented. The absence of any definable salt stratigraphy also made it impossible to determine the nature of the folding.

Foliation is absent or weak in shallow salt samples because recrystallization has removed the strain (E). The strong foliation of the deep samples indicates these deep samples are at present still highly strained (elongation may approach 20 percent). The timing of the strain application is unknown. Recrystallization at Bryan Mound dome occurs down to a depth of 2,000 ft (610 m) to 2,500 ft (762 m). This depth is 750 ft (220 m) to 1,250 ft (381 m) below the cap rock-salt interface. A similar recrystallization phenomenon was described for salt core from Oakwood dome (Dix and Jackson, 1982). At Oakwood

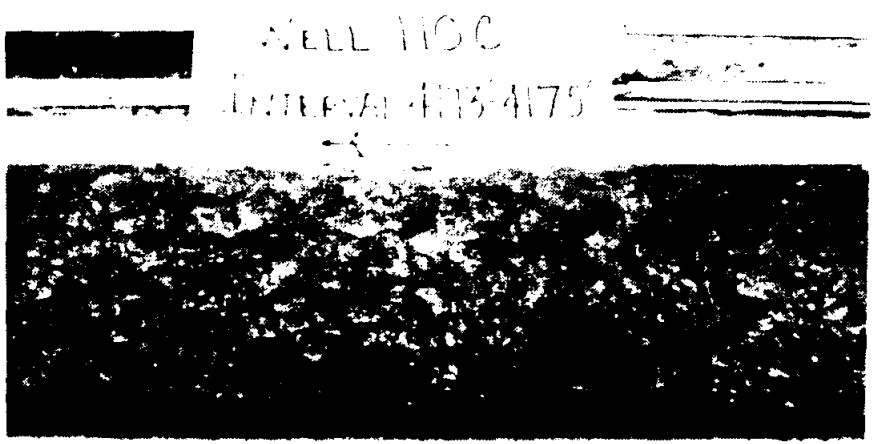


Figure 28. Photographs of core, Bryan Mound dome, showing variations in grain size and foliation. Core 1A at -1,848 ft is well bedded with dark anhydrite layers and unfoliated; core 110C at -4,173 ft shows no bedding and vertical foliation.

dome, recrystallization occurred at depth of 1,168 ft (356 m), only about 2 ft (0.6 m) below the cap-rock--salt-stock interface.

Discussion

The stability of a solution-mined cavern undoubtedly would be influenced by foliation owing to the elongation of grain boundaries and cleavage planes in the direction of foliation. These boundaries and planes are the avenues for fluid flow. However, the magnitude of the influence is unknown. The absence of foliation would seem to be more favorable for stability of underground openings than highly foliated and strained rock salt. The absence of foliation indicates recrystallization under relatively strain-free conditions. Minute amounts of intercrystalline water are thought to promote halite recrystallization by grain boundary diffusion (Spiers and others, 1984). Thus, if recrystallization was facilitated by small amounts of water, then this water must have penetrated a substantial distance through the upper part of the salt stock. Our data indicate that at Bryan Mound dome this ingress seeped down the 750 ft to 1,250 ft from the cap-rock contact or migrated in laterally from the dome flanks. Aufrecht and Howard (1961) noted that the addition of small amounts of water to rock salt reduced the permeability in most cases to near zero. However, this positive aspect of moisture content in salt is also saddled with a negative aspect. Water greatly increases the plasticity (creep) of rock salt. Salt glaciers in Iran show peak strain rates of $1.9 \times 10^{-9} \text{ s}^{-1}$ after rainfall events (Talbot and Rogers, 1980). There has only recently been controlled laboratory experiments on the influence of moisture in salt creep and viscosity (Spiers and others, 1984).

CAP ROCK

Domal cap rocks have a significant effect on the stability of a salt dome and an intradomal solution-mined cavern (Dix and Jackson, 1982). Lost-circulation zones especially at the cap-rock--salt-stock interface are among the aspects of cap rocks which could negatively affect dome and cavern stability. In this section we will provide data on cap-rock mineralogy and lost-circulation zones.

Cap rocks are primarily a residual accumulation of anhydrite particles left after a portion of the crest of the salt stock was dissolved. Cap rocks are mineralogically complex and in addition to anhydrite they contain calcite, gypsum, sulfur, celestite, dolomite, Zn-, Pb-, and Fe-sulfides, petroleum, and other minor constituents. This mineralogical complexity stems from a number of cap-rock forming processes (Bodenlos, 1970) in addition to simple salt solution. These processes include (1) hydration of anhydrite to gypsum; (2) reaction of anhydrite and/or gypsum with petroleum and sulfate-reducing bacteria to produce calcite and hydrogen sulfide; (3) vertical migration of metalliferous deep-basin brines into porous cap rock precipitating metallic sulfides (marcasite, sphalerite, pyrite, and other minerals) in reduced zones owing to the presence of hydrogen sulfide (Price and others, 1983); and (4) oxidization of hydrogen sulfide to sulfur.

Examples of the complex mineralogy of domal cap rock are seen in core from Hockley, Long Point, and Boling domes. Massive Zn- and Pb-sulfide concentrations at Hockley dome triggered a significant exploration effort (Price and others, 1983). The Bureau of Economic Geology will receive from Marathon Minerals approximately 40,000 ft (12,000 m) of core from this exploration. Long Point dome was cored for sulfur exploration (M and S Lease Wells 5, 14, 15). These cores show a similar mineralogical complexity with that of Hockley

dome. Four mineralogical zones are recognized in core from Long Point dome: (1) a calcite zone with sulfur (depth 628-644 ft; 191-196 m), (2) an anhydrite-gypsum zone with rare sulfur (depth 644-815 ft; 196-248 m); (3) a broken calcite zone containing sulfur and sulfides (depth 815-855 ft; 248-261 m), and (4) an anhydrite sand and gypsum zone (depth 855-865 ft; 261-264 mm).

Banding and fractures in the anhydrite-gypsum zone (depth 719-720 ft; 219.2-219.5 m) are shown in figure 29A. Mineralogical relationships and vuggy fractures in the broken calcite zone (depth unknown) are shown in figure 29B. Vugs and fracture porosity are especially common in the calcite zones. Visual estimates of effective porosity range from 5 to 15 percent. Fractures are 0.02-0.2 inches (0.5-5 mm) wide, but weathering during outdoor storage has enlarged fractures. Some fractures are orthogonal sets oriented 45 degrees to the vertical axis of the core.

Sulfur is a secondary fracture- and vug-filling mineral. Unidentified metallic sulfide minerals are also concentrated in the calcite zones. The paragenesis and diagenesis of cap rocks remain to be examined in detail. An especially critical need is identification of factors controlling formation and distribution of fractures and vugs in the cap rocks.

Cap-Rock--Lost-Circulation Zones

Cap-rock--lost-circulation zones are areas of enhanced porosity and permeability within cap rocks. The porosity in these zones may be either fracture controlled, cavernous, or intergranular. These zones are common in cap rocks of salt domes in the Houston diapir province and are particularly thick in cap rock of Barbers Hill dome. Wells are completed through lost-circulation zones with a series of procedures designed to mitigate the problem of lost circulation. However, 137 storage caverns in Barbers Hill salt dome indicate successful completion through this problem area. The long-term effect of fluids

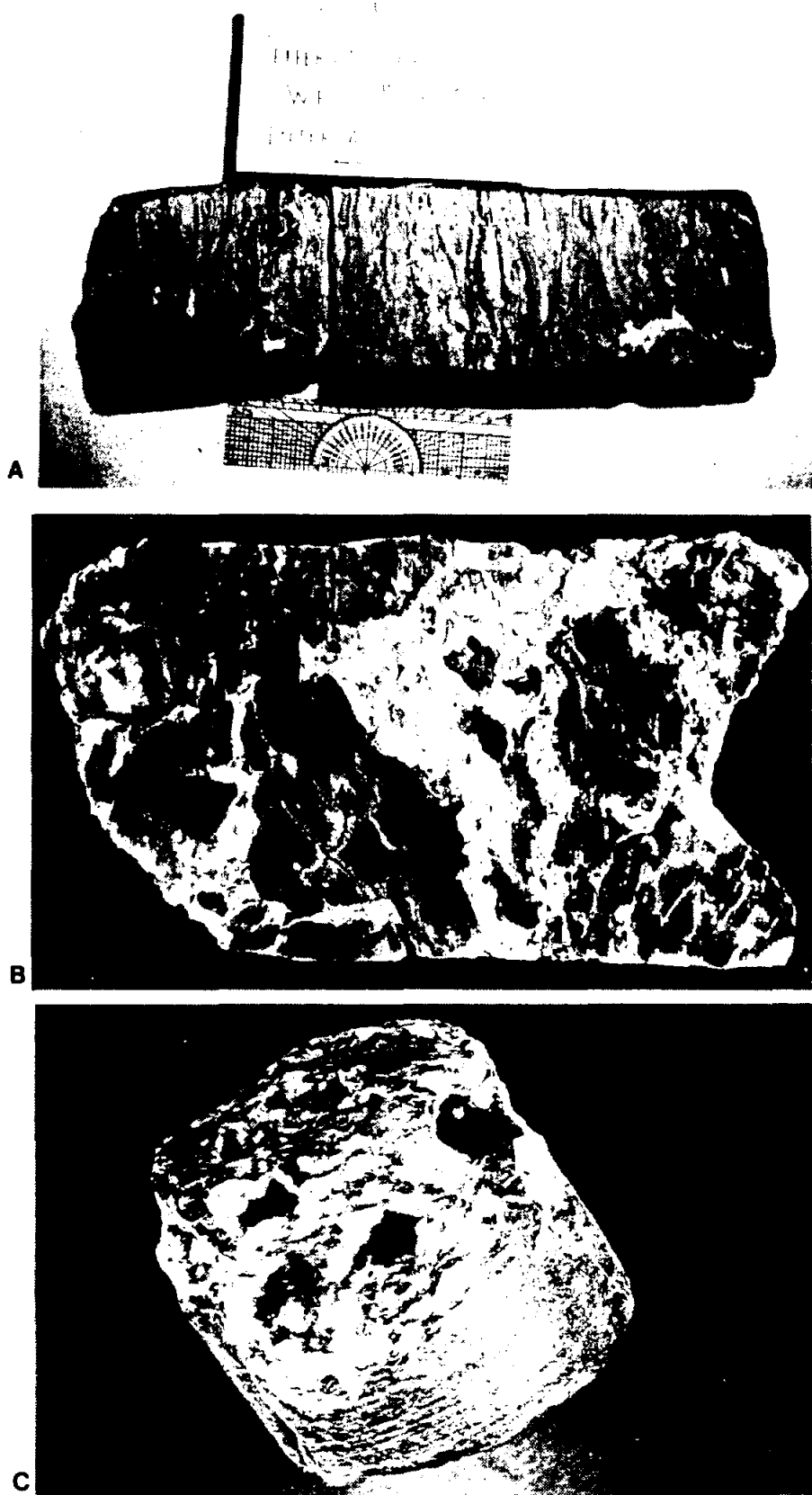
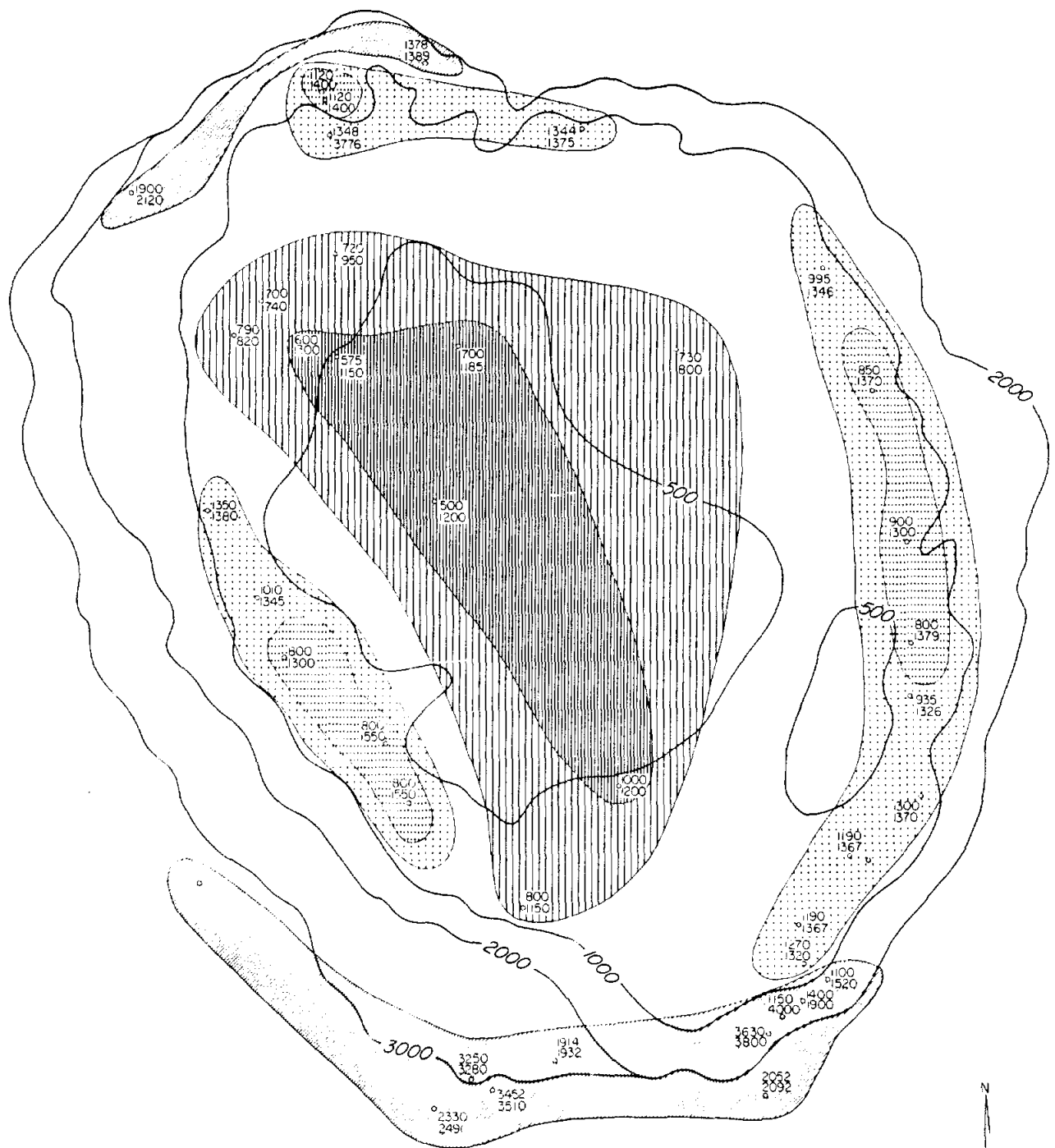


Figure 29. Photographs of core from cap rock, A. Long Point dome, showing mineralogical variations and fractures, B. Long Point dome showing sulfur and fractures, C. Boling dome showing sulfur and vugs.

within lost-circulation zones on the cements of casing strings remains unknown. The following section covers lost-circulation zones in Barbers Hill dome cap rock. The information is from cap rock-injection wells for brine disposal. Appendix 3 lists cap-rock injection wells with injection interval and the year the injection permit was approved by the Texas Railroad Commission. Lithology of the actual injection interval is often unspecified. Well depth and location are used to infer the lithology of the injection zone. Most wells clearly inject into cap rock; however, some wells that inject into supradomal or flank sandstones may be included.

Barbers Hill dome is in northwest Chambers County 30 mi (50 km) east of Houston. Barbers Hill dome is nearly circular, with a very planar contact (salt mirror) between the salt and cap rock. A thick (greater than 20 ft; 6 m) anhydrite sand comprises the lost-circulation zone over the flat crest of the salt-cap-rock interface.

An estimated 1.5 billion barrels of salt water have been disposed by injection into lost-circulation zones at Barbers Hill dome. Various zones within the cap rock have been permitted to receive this brine including (1) upper cap-rock gypsum zone, (2) upper and lower cap rock, (3) upper cap-rock gypsum zone and basal anhydrite sand, (4) basal anhydrite sand, and (5) deep flank cap rock and deep flank sandstone. The distribution of these injection intervals is shown in figure 30. The shallowest injection is into the upper cap-rock gypsum zone in the area over the central part of the dome. Brine is injected at a depth of 800-1,560 ft (244-475 m) into the basal anhydrite sand around the periphery of the salt dome. The vertical extent of these lost-circulation zones is shown with stylized cavern geometries in figure 31. Appendix 1C lists well information for caverns and disposal wells.



- EXPLANATION**
- | | |
|--|--|
| <p>INJECTION ZONES</p> <ul style="list-style-type: none"> Upper and lower cap rock Upper cap rock gypsum zone Basal anhydrite sand and upper cap rock-gypsum zone | <ul style="list-style-type: none"> Basal anhydrite sand Deep flank sandstone and deep flank cap rock Top cap rock (ft below sea level) Injection interval (ft) |
|--|--|

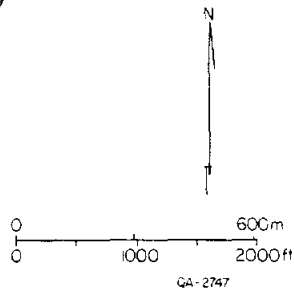


Figure 30. Map of cap-rock injection zones, Barbers Hill dome. Injection into shallow cap rock is over central part of dome, whereas injection into basal anhydrite sand is around periphery of dome.

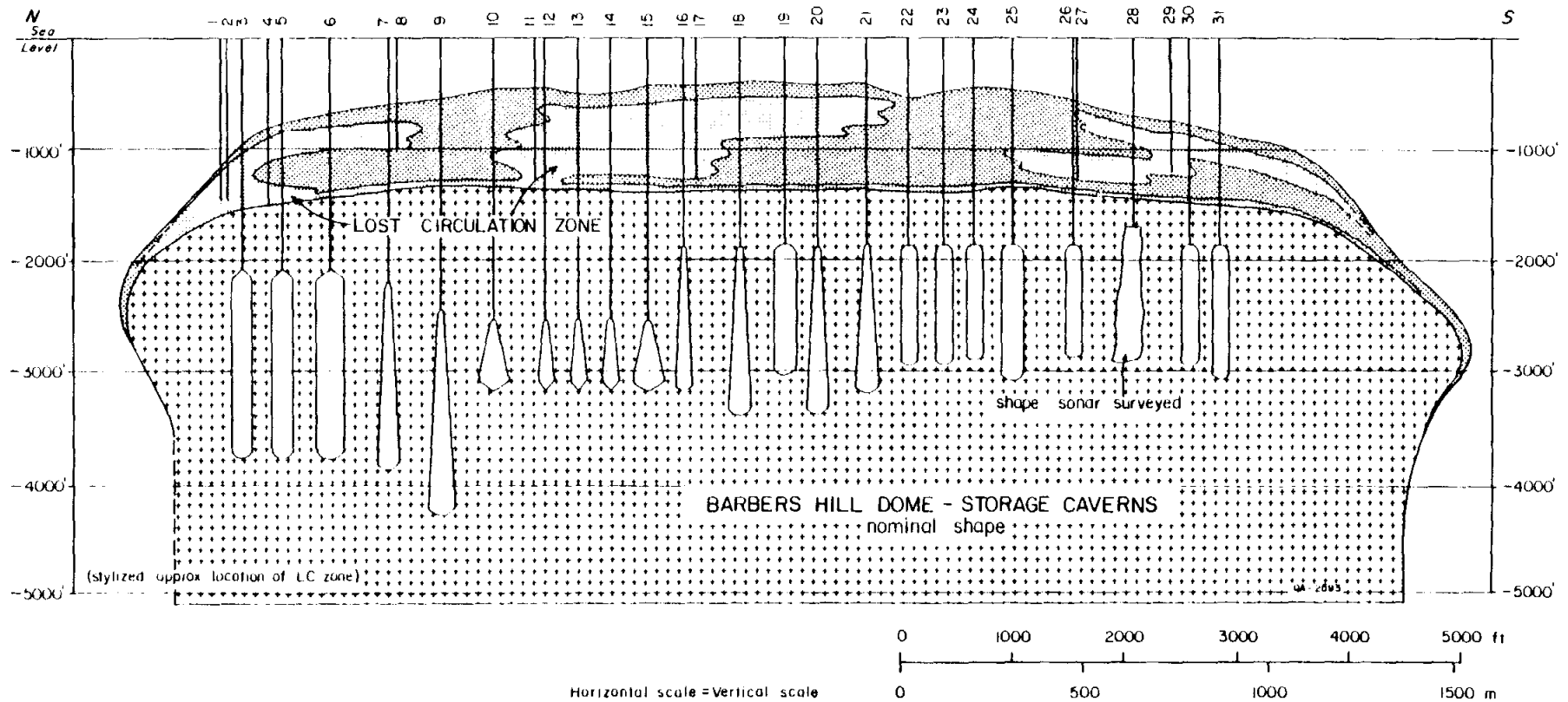
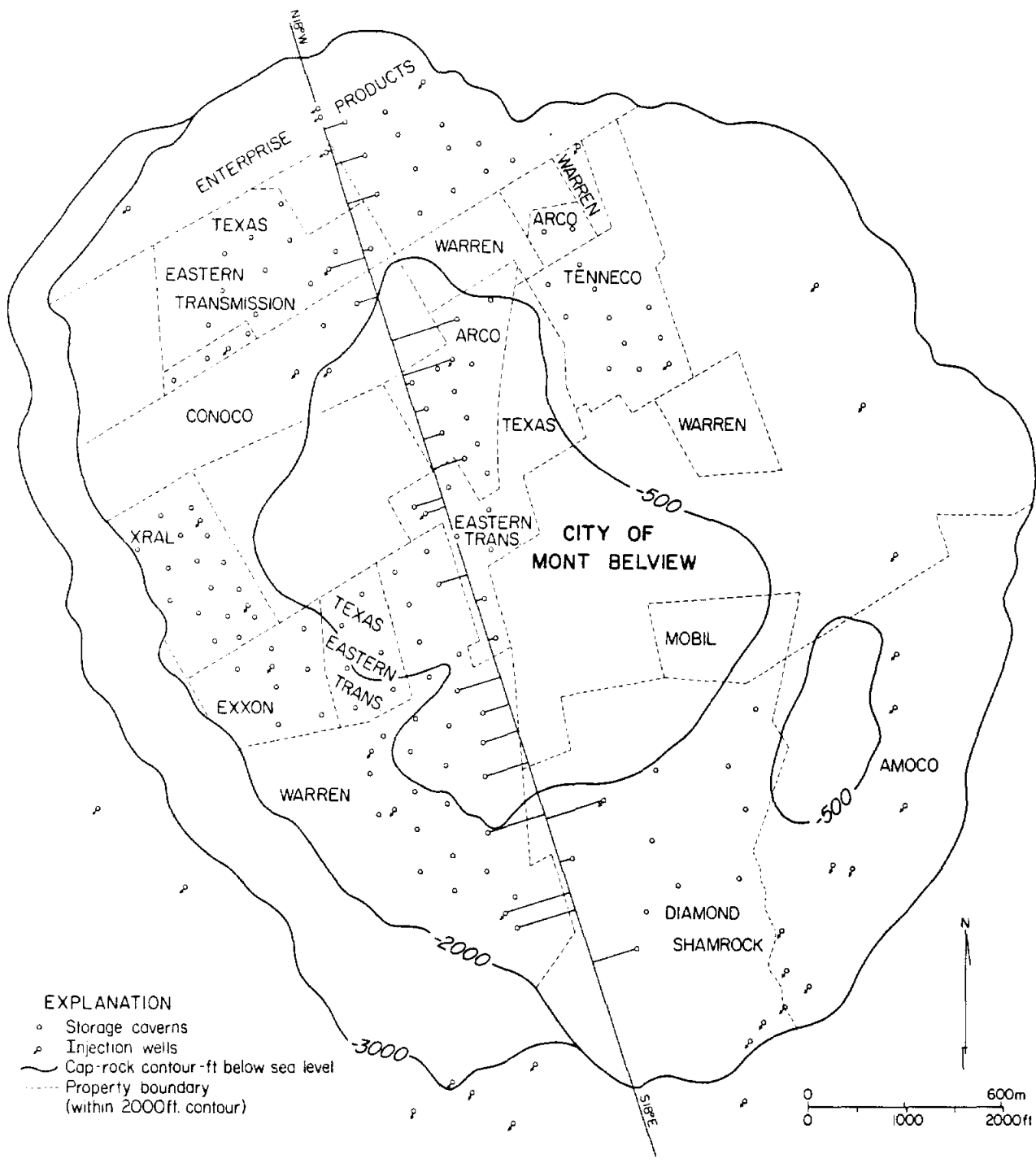


Figure 31. Cross section, Barbers Hill dome, and cap rock showing lost-circulation zones and stylized cavern geometries. Map shows location of caverns in relation to line of section and boundary of salt stock. Appendix 1C lists cavern and injection well names.



(continued)

The brine is injected either by design or by accident into the upper cap-rock zones over the central part of the dome and is injected into progressively deeper middle and lower cap-rock zones over the peripheral areas of the dome. The influence of this injection scheme on cap-rock hydrogeology and salt dissolution is unknown and unstudied.

Discussion

Cap rocks sheath the upper parts of salt stocks and commonly project into shallow zones where the ground water is circulating most rapidly. Cap rocks are mineralogically complex, and many are faulted, brecciated, highly porous, and permeable. Cap rocks by virtue of their location are the focus of a diversity of geologic processes of which those associated with ground water are of the greatest concern.

Research to date on Texas cap rocks has shown that many Gulf Coast salt dome cap rocks (for example, Barbers Hill and Boling salt domes) are characterized by highly porous and permeable lost-circulation zones, whereas some East Texas cap rocks (for example, Oakwood salt dome) do not have such zones substantiated by a drilling record. Clearly, site-specific data on cap rocks of candidate domes are needed to answer questions on whether cap-rock processes could affect negatively toxic-waste disposal in salt caverns. Such questions include (1) geometry, orientation, and activity of cap-rock faults and (2) the nature and origin of porosity and permeability within cap rocks and within cap-rock lost-circulation zones. Hydrogeologic aspects of cap rocks are clearly one of the highest concerns for toxic-waste disposal. Within cap rocks, potentiometric surface levels, direction of ground-water flow, and interconnection of porous zones are necessary concerns; such data are easily compiled and computed from a series of water level measurements and tests which are in the planning stage.

ACKNOWLEDGMENTS

Funding for this research was provided by the Texas Department of Water Resources under Interagency Contract No. (84-85)-1019. Drs. E. G. Wermund and M. P. A. Jackson critically reviewed the manuscript; their comments are gratefully acknowledged. Thanks are extended to Texas Railroad Commission personnel Mark Browning (Central Records) and J. W. Mullican (Underground Injection Control), who provided easy access to records and files. Discussions with the following industry representatives were very helpful: Kermit Allen, Jose Machado, and Edward Voorhees (Fenix and Scisson, Inc.), Neils Van Fossan (Texas Brine Company), Noe Sonnier and Ferris Samuelson (Texas Gulf Sulfur), Carl Brassow (United Resource Recovery, Inc.), Jack Piskura (Pakhoed, Inc.), and Bill Ehni and Mark Katterjohn (Geotronics Corporation). Word processing was done by Ginger Zeikus, under the supervision of Lucille C. Harrell. Mark Bentley, Tom Byrd, Jeff Horowitz, Jamie McClelland, and Richard Platt drafted the figures, under the supervision of Dick Dillon.

REFERENCES

- Aufricht, W. F., and Howard, K. C., 1961, Salt characteristics as they affect storage of hydrocarbons: *Journal of Petroleum Technology*, v. 13, no. 8, p. 733-738.
- Baar, C. A., 1971, Creep measured in deep potash mines vs. theoretical predictions: 7th Canadian Rock Mechanics Symposium, University of Alberta, Edmonton, Canada, p. 23-77.
- _____ 1977, Applied salt-rock mechanics I, the in situ behavior of salt rocks: *Developments in Geotechnical Engineering*, v. 16A, 294 p.
- Bild, R. W., 1980, Chemistry and mineralogy of samples from the Strategic Petroleum Reserve: Sandia National Laboratories, SAND-80-1258, 51 p.
- Bodenlos, A. J., 1970, Cap-rock development and salt-stock movement, *in* Kupfar, D. H., ed., *Geology and technology of Gulf Coast salt domes*: School of Geosciences, Louisiana State University, Baton Rouge, Louisiana, p. 73-86C.
- Burke, P. M., 1968, High temperature creep of polycrystalline sodium chloride: Ph.D. dissertation, Stanford University, Stanford, California, 112 p.
- Carter, N. L., and Hansen, F. D., 1983, Creep of rock salt: *Tectonophysics*, v. 92, p. 275-333.
- Dawson, P. R., 1979, Constitutive models applied in the analysis of creep of rock salt: Sandia Laboratories, SAND-79-0137, 47 p.

- Dix, O. R., and Jackson, M. P. A., 1982, Lithology, microstructures, fluid inclusions, and geochemistry of rock salt and of the cap-rock contact in Oakwood Dome, East Texas: significance for nuclear waste storage: The University of Texas at Austin, Bureau of Economic Geology Report of Investigations No. 120, 59 p.
- Dreyer, W., 1972, The science of rock mechanics, Vol. 1: Tran. Tech. Publications, p. 29-164.
- Empson, F. M., Bradshaw, R. L., McClain, W. C., and Houser, B. L., 1970, Results of the operation of Project Salt Vault: a demonstration of disposal of high-level radioactive solids in salt: III Symposium on Salt, v. 10, p. 455-462.
- Ewing, M., and Ewing, J. L., 1962, Rate of salt-dome growth: American Association of Petroleum Geologists Bulletin, v. 46, no. 5, p. 708-709.
- Ewing, T. E., 1983, Growth faults and salt tectonics in the Houston diapir province--relative timing and exploration significance: Gulf Coast Association of Geological Societies, v. 33, p. 83-89.
- _____, compiler, in preparation, Tectonic map of Texas: The University of Texas at Austin, Bureau of Economic Geology, scale 1:750,000.
- Fernandez, G. M., and Hendron, A. J., 1984, Interpretation of a long-term in situ borehole test in a deep salt formation: Bulletin of the Association of Engineering Geologists, v. 21, no. 1, p. 23-38.
- Hansen, F. D., and Carter, N. L., 1980, Creep of rocksalt at elevated temperatures: Proceedings of the 21st U.S. Symposium on Rock Mechanics, Rolla, Mississippi, p. 217-226.
- Hansen, F. D., and Carter, N. L., 1980, Mechanical behavior of Avery Island halite: a preliminary analysis: RE/SPEC, Inc., Rapid City, South Dakota, prepared for the Office of Nuclear Waste Isolation, ONWI-100, 37 p.

- Hansen, F. D., and Mellegard, K. D., 1980, Quasi-static strength and deformational characteristics of domal salt from Avery Island, LA: RE/SPEC, Inc., Rapid City, South Dakota, prepared for the Office of Nuclear Waste Isolation, ONWI-116, 86 p.
- Heard, H. C., 1972, Steady-state flow to polycrystalline halite at pressures of 2 kilobars, in Heard, H. C., Borg, I. Y., Carter, N. L., and Raleigh, C. B., editors, Flow and fracture of rocks: American Geophysical Union Monograph Series, v. 16, p. 191-210.
- Herrmann, W., and Lauson, H. S., 1981a, Review and comparison of transient creep laws used for natural rock salt: Sandia National Laboratories, SAND-81-0738, 62 p.
- _____ 1981b, Analysis of creep data for various rock salts: Sandia National Laboratories, SAND-81-2567, 96 p.
- Herrmann, W., Wawersik, W. R., and Montgomery, S. T., 1982, Review of creep modeling for rock salt: Sandia National Laboratories, SAND-82-2178C, 9 p.
- Hume, H. R., and Shakoor, A., 1981, Mechanical properties, in Gevantman, L. H., ed., Physical properties data for rock salt: U.S. Department of Commerce National Bureau of Standards, Monograph 167, p. 103-203.
- Jackson, M. P. A., 1984, Natural strain in diapiric and glacial salt, with emphasis on Oakwood Dome, East Texas: The University of Texas at Austin, Bureau of Economic Geology Report of Investigations No. 143.
- Jackson, M. P. A., and Dix, O., 1981, Geometric analysis of macroscopic structures in Oakwood salt core, in Kreitler, C. W., and others, Geology and geohydrology of the East Texas Basin: a report on the progress of nuclear waste isolation feasibility studies (1980): The University of Texas at Austin, Bureau of Economic Geology Geological Circular 81-7, p. 177-182.

- Jackson, M. P. A., and Seni, S. J., 1984a, Atlas of salt domes of the East Texas Basin: The University of Texas at Austin, Bureau of Economic Geology Report of Investigations No. 140, 102 p.
- _____ 1984b, Suitability of salt domes in the East Texas Basin for nuclear-waste isolation: final summary of geologic and hydrogeologic research (1978-1983): The University of Texas at Austin, Bureau of Economic Geology Geological Circular 84-1, 129 p.
- Le Comte, P., 1965, Creep in rock salt: *Journal of Geology*, v. 73, p. 469-484.
- Martinez, J. D., and others, 1978, An investigation of the utility of Gulf Coast salt domes for the storage or disposal of radioactive wastes, Volume I: Louisiana State University, Institute for Environmental Studies, Contract Report EW-78-C-05-5941/53, 390 p.
- McVetty, P. G., 1934, Working stresses for high temperature service: *Mechanical Engineering*, v. 56, p. 149.
- Mellegard, K. D., Senseny, P. E., and Hansen, F. D., 1983, Quasi-strength and creep characteristics of 100 mm-diameter specimens of salt from Avery Island, Louisiana: Prepared for U.S. Department of Energy, Office of Nuclear Waste Isolation, Battelle Memorial Institute, Columbus, OH, ONWI-250, 210 p.
- Munson, D. E., 1979, Preliminary deformation-mechanism map for salt: Sandia National Laboratories, SAND-79-0076, 37 p.
- Obert, L., 1964, Deformational behavior of model pillars made from salt, trona, and potash ore: *Proceedings of the VI Symposium on Rock Mechanics*, Rolla, Missouri, p. 539-560.
- Odé, H., 1968, Review of mechanical properties of salt relating to salt dome genesis: *Geological Society of America Special Publication 88*, p. 543-595.

- Paterson, M. S., 1978, Experimental rock deformation--the brittle field:
New York, Springer-Verlag, 254 p.
- Preece, D. S., and Stone, C. M., 1982, Verification of finite element methods
used to predict creep response of leached salt caverns: 23rd U.S. Rock
Mechanics Symposium, University of California, Berkeley, California,
p. 655-663.
- Price, P. E., Kyle, J. R., and Wessel, G. R., 1983, Salt-dome related zinc-lead
deposits, in Kisvarsanyi, G., and others, eds., Proceedings, International
Conference on Mississippi Valley-type lead-zinc deposits: University of
Missouri, Rolla, p. 558-571.
- Price, R. H., Wawersik, W. R., Hannum, D. W., and Zirzow, J. A., 1981: Sandia
National Laboratories, SAND-81-2521, 46 p.
- Reynolds, T. D., and Gloyna, E. F., 1961, Creep measurements in salt mines, in
Mining Engineering Series--Proceedings of the 4th Symposium on rock
mechanics, 1961: Pennsylvania State University Mineral Industries
Experimental Station Bulletin, v. 76, p. 11-17.
- Sannemann, D., 1968, Salt stock families in northwestern Germany: American
Association of Petroleum Geologists Memoir 8, p. 261-270.
- Seni, S. J., Hamlin, H. S., and Mullican, W. F., III, 1984, Texas salt domes:
natural resources, storage caverns, and extraction technology: The
University of Texas at Austin, Bureau of Economic Geology, report prepared
for Texas Department of Water Resources under interagency contract no. IAC
(84-85)-1019, 161 p.
- Seni, S. J., and Jackson, M. P. A., 1983a, Evolution of salt structures, East
Texas diapir province, Part I: Sedimentary record of halokinesis:
American Association of Petroleum Geologists Bulletin, v. 67, no. 8,
p. 1219-1244.

- Seni, S. J., and Jackson, M. P. ., 1983b, Evolution of salt structures, East Texas diapir province, Part II: Patterns and rates of halokinesis: American Association of Petroleum Geologists Bulletin, v. 67, no. 8, p. 1245-1274.
- _____ 1984, Sedimentary record of Cretaceous and Tertiary salt movement, East Texas Basin: times, rates, and volumes of salt flow and their implications for nuclear-waste isolation and petroleum exploration: The University of Texas at Austin, Bureau of Economic Geology Report of Investigations No. 139, 89 p.
- Seni, S. J., Mullican, W. F., III, and Hamlin, H. S., 1984a, Texas salt domes: natural resources, storage caverns, and extraction technology: The University of Texas at Austin, Bureau of Economic Geology, report prepared for Texas Department of Water Resources under interagency contract no. IAC (84-85)-1019, 161 p.
- Seni, S. J., Mullican, W. F., III, and Ozment, R. W., 1984, Computerized inventory of data on Texas salt domes: The University of Texas at Austin, Bureau of Economic Geology, report prepared for Texas Department of Water Resources under interagency contract no. IAC (84-85)-1019, 34 p.
- Senseny, P. E., 1983, Review of constitutive laws used to describe the creep of salt: RE/SPEC, Inc., Rapid City, South Dakota, prepared for the Office of Nuclear Waste Isolation, ONWI-295, 59 p.
- Serata, S., and Gloyna, E. F., 1959, Development of design principle for disposal of reactor fuel waste into underground salt cavities: University of Texas, Austin, Reactor Fuel Waste Disposal Project.
- Spiers, C. J., Urai, J. L., Lister, G. S., and Zwart, H. J., 1984, Water weakening and dynamic recrystallization in salt (abs.): Geological Society of America, 97th Annual Meeting, v. 16, no. 6, p. 665.

- Talbot, C. J., and Jarvis, R. J., in press, Dynamics, budget, and age of an active salt extrusion in Iran: *Journal of Structural Geology*.
- Talbot, C. J., and Rogers, E. Q., 1980, Seasonal movements in a salt glacier in Iran: *Science*, v. 208, no. 4442, p. 395-397.
- Thoms, R. L., Mogharrebi, M., and Gehle, R. M., 1982, Geomechanics of borehole closure in salt domes: Gas Processors Association, Proceedings of 61st Annual Convention, Dallas, Texas, p. 228-230.
- Verral, R. A., Fields, R. J., and Ashby, M. F., 1977, Deformation mechanism maps for LiF and NaCl: *Journal of The American Ceramic Society*, v. 60, no. 5-6, p. 211-216.
- Wagner, R. A., Mellegard, K. D., and Senseny, P. E., 1982, Influence of creep law form on predicted deformations in salt: 23rd U.S. Rock Mechanics Symposium, University of California, Berkeley, California, p. 684-691.
- Wawersik, W. R., Holcomb, D. J., Hannum, D. W., and Lauson, H. B., 1980, Quasi-static and creep data for dome salt from Bryan Mound, Texas: Sandia National Laboratories, SAND-80-1434, 37 p.
- Wenkert, D. D., 1979, The flow of salt glaciers: *Geophysical Research Letters*, v. 6, no. 6, p. 523-526.
- Weertman, J., 1968, Dislocation climb theory of steady-state creep: *ASM Transactions Quarterly*, v. 61, p. 681.
- Weertman, J., and Weertman, J. R., 1970, Mechanical properties, strongly temperature-dependent, in Cahn, R. W., ed., *Physical metallurgy*: Amsterdam, North-Holland, p. 983-1010.

Appendix 1A. Well Information for Maps

Well Number	Operator	Fee	Field
Brazoria County			
1	Sun Co.	#5 Wisch-Saint Unit	Pledger
2	Sun Co.	#6 Wisch-Saint Unit	Pledger
3	Exxon Co. U.S.A.	#2 Pledger Gas Unit 3	Pledger
4	Pennzoil Prod. Co.	#5 McFarland	Pledger
5	Pennzoil Prod. Co.	#3 McFarland	Pledger
6	Pennzoil Prod. Co.	#4 McFarland	Pledger
7	Southwest Gas Prod. Co.	#1 McDonald	West Columbia
8	Humble Oil and Refining Co.	#1 Pledger Gas Unit 7	Pledger
9	Humble Oil and Refining Co.	#1 L. Carter	Pledger
10	Stanolind Oil and Gas Co.	#1 W. T. Robertson	West Columbia
11	Southern Prod. Co. Inc.	#30 Pledger Gas Field Unit Well	Pledger
12	Gulf Oil Corp.	#1 Link Fee	Damon Mound
13	Rowan Drilling Co.	#1 Krause	West Columbia
14	Pan American Prod. Co.	#1 N. W. Hopkins	Damon Mound
15	John F. Merrick	#3 Bryan Estate	Damon Mound
16	Delin Taylor Oil Do.	#1 L. Becker	West Columbia
17	Caroline Hunt Trust Est.	#1 M. T. Pratt	West Columbia
18	Texas Gulf Sulphur Co.	#1 M. T. Pratt	West Columbia
Chambers County			
2	M. T. Halbouty	#1 Gilbert	Barbers Hill
3	H. S. Cole Jr. and Harrell Drlg. Co.	#1 K. Williams	West Columbia
4	The Texas Co.	#3 Kirby Oil and Gas	Barbers Hill
5	The Texas Co.	#1 Whaley	Barbers Hill
6	General Crude Oil Co.	#1 Nash Fee	West Columbia
7	British Texas Oil Co.	#1 Barber	Barbers Hill
8	Gas Producers Enterprises Inc.	#1 P. C. Ulrich	West Columbia
9	The Superior Oil Co.	#1 O. Z. Smith	Barbers Hill
10	Humble Oil and Refining Co.	#B-1 B. Dutton	West Columbia
11	The Texas Co.	#1 A. A. Davis	Barbers Hill
12	The Texas Co.	#1 Kirby Petroleum Co. NCT	West Columbia
13	M. T. Halbouty	#1 E. Wilburn	West Columbia
14	Kirby Petroleum Co.	#1 Kirby Pet. Co. Fee Tr. 8	West Columbia
15	The Texas Co.	#1 K. Fitzgerald	Barbers Hill
16	The Texas Co.	#2 Kirby Oil and Gas	Barbers Hill
17	Sunray Oil Co.	#C-2 F. W. Harper	Barbers Hill
18	Stanolind Oil and Gas Co.	#33 Chambers County	Barbers Hill
19	Stanolind Oil and Gas Co.	#19 Chambers County	Barbers Hill
20	Marine Contractors Supply Co.	#1 Collier Heirs	Barbers Hill
21	Mills Bennett Estate	#17 E. E. Barrow	Barbers Hill
22	C. L. Chambers	#1 Schilling-Lillie	Barbers Hill

Appendix 1A. (cont.)

Well Name	Operator	Fee	Field
(Chambers County-continued)			
24	Texas Eastern Transmission Co.	#7 M. Belview Storage Well	Barbers Hill
25	Humble Oil and Refining Co.	#5 L.P.G. Storage Well	Barbers Hill
26	Texas Eastern Transmission Co.	#5-10 Storage Well	Barbers Hill
27	The Texas Co.	#1 Kirby Oil and Gas Co.	Barbers Hill
28	Sierra	#1 Trichel	Barbers Hill
29	Sunray-Mid Continent Oil Co.	#A-8 Barber	Barbers Hill
30	The Texas Co.	#1 J. M. Fitzgerald Est.	Barbers Hill
31	Harrison and Gilger	#2 A. E. Barber	Barbers Hill
32	Otis Russel	#1 Blaffer-Farrish	Barbers Hill
35	Kirby Petroleum Co.	#1 Wilburn	West Columbia
37	Warren Petroleum Co.	#13 M. Belview Storage	M. Belview Term.
38	Sun Oil Co.	#23 J. Wilburn	Barbers Hill
39	Warren Petroleum Co.	#3 Caprock Disposal	Barbers Hill
40	Warren Petroleum Co.	#11 Mt. Belview	Barbers Hill
41	Sunray-DX Oil Co.	#D-5 E. W. Barber	Barbers Hill
42	Texas Gulf Prod. Co.	#3-5 L. E. Fitzberald	Barbers Hill
43	Texas Butadiene Co.	#1 Texas Butadiene	Barbers Hill
44	Humble Oil and Refining Co.	#1 M. Belview Storage Facility	Barbers Hill
45	Houston Oil and Minerals Corp.	#12 Chambers County Agricultural Co.	Barbers Hill
46	Sun Oil Co.	#A-1 Higgins	Barbers Hill
47	Humble Oil and Refining Co.	#B-9 Kirby Petroleum Co. Fee	Barbers Hill
48	Texas Eastern Transmission Co.	#11 Storage Well NT	Barbers Hill
49	Humble Oil and Refining Co.	#11 Kirby Fee	Barbers Hill
50	Humble Oil and Refining Co.	#B-14 Kirby	Barbers Hill
51	Texas Gulf Producing Co.	#15 Kirby "A"	Barbers Hill
52	Texas Gulf Producing Co.	#A-11 A. E. Barber	Barbers Hill
53	Pan American Petroleum Co.	#37 Chambers County Agriculture Co.	Barbers Hill
54	R. A. Welch	#2 Barrow Fee	Barbers Hill
55	Mills Bennett Estate	#16 Barrow	Barrows Fee
56	M. T. Halbouty & Hurt Oil Co.	#1 Kirby Oil & Gas	Barbers Hill
57	Lloyd H. Smith Inc.	#1 Claude Williams	Barbers Hill
58	Admiral Drilling Co.	#1 Williams	West Columbia
59	John W. Mecom	#3-B Mayes	West Columbia
Fort Bend County			
20	John B. Coffee	#4 Texas Gulf Sulphur	Boling
21	Coastal Minerals Inc.	#C-37 J. R. Farmer	Boling
22	Coastal Minerals Inc.	#C-35 J. R. Farmer	Boling
23	Coastal Minerals Inc.	#1 J. Byrne	Boling
24	Grover J. Geiselman	#1 Richter-Warncke Gas Unit	Needville
25	Grover J. Geiselman	#1 Leissner	Needville
26	Acoma Oil Corp.	#1-B Farmer	Boling
27	Callery and Hurt	#1 Kasparek	Boling
28	Allied Minerals	#1 E. C. Farmer	Boling
29	Callery and Hurt	#3 Kasparek	Boling

Appendix 1A. (cont.)

Well Name	Operator	Fee	Field
(Fort Bend County-continued)			
30	Callery and Hurt	#2 Kasperek	Boling
31	Callery and Hurt	#2 Texas Gulf Sulphur	West Columbia
32	Caddo Oil Co.	#1 Gaidosik	West Columbia
33	Grover J. Geiselman	#1 Steffek Gas Unit	Needville
34	Grover J. Geiselman	#1 Schwettmann	West Columbia
35	Grover J. Geiselman	#1 Hardin-Roesler Gas Unit	Needville
36	H. M. Amsler	#1 Dance	Needville
37	Exxon Co. U.S.A.	#87 Lockwood and Sharp "A"	Thompson
38	Grover J. Geiselman & General Crude Oil Co.	#1 P. Kueck	West Columbia
39	Powers Prod. Co. & T. T. Drlg. Co.	#1 J. R. Farmer	Needville
40	Fort Bend Oil Co.	#1 J. M. Moore Est.	West Columbia
41	Scurlock Oil Co. & M. T. Halbouty	#1 D. Krause	Beasley
42	Bilbo-Redding Drlg. Co.	#1 G. B. Leaman et al.	West Columbia
43	General Crude Oil Co.	#1 Stavinoma	West Columbia
44	Grover J. Geiselman	#1 Schendel Gas Unit	Needville
45	Slade Oil and Gas Inc.	#1 S. B. Kennelly	West Columbia
46	Houston Oil and Minerals	#1 J. M. Moore	West Columbia
47	The Oil and Gas Company	#1 Byrne	West Columbia
Harris County			
34	The Texas Co.	#1 Mrs. E. K. Busch Est.	West Columbia
60	Pan American Petroleum Corp.	#1 A. Schoeps Oil Unit 1	West Columbia
Liberty County			
1	M. T. Halbouty	#E-1 Kirby Petroleum Co.	West Columbia
33	General Crude Oil Co.	#B-3 Colby	West Columbia
36	General Crude Oil Co.	#D-1 Moores Bluff	West Columbia
Matagorda County			
1	Rowan Drlg. Co. & Texas Gulf Prod. Co.	#1 C. Mason	West Columbia
2	So Belle and So Belle	#1 Le Tulle	West Columbia
3	J. M. Huber Corp. & M. S. Cole, Jr. & Son	#1 S. V. Le Tulle	West Columbia
4	M. T. Williams	#1 C. B. Fisher et al.	West Columbia
5	Placid	#1 Le Tulle	West Columbia
6	Bright and Schiff	#1 Camp	West Columbia
7	Texas Gulf Sulphur Co. and Goodell Pet. Co.	#1 W. D. Cornelieus Est.	Markham
8	Shannon Oil and Gas, Inc.	#1 Kountze-Couch	Markham

Appendix 1A. (cont.)

Well Number	Operator	Fee	Field
(Matagorda County-continued)			
9	Seadrift Pipeline Corp.	#2 Fee	Markham
10	Petroleum Ventures of Texas	#2 Sun Fee	Markham
11	Hamill and Hamill	#1 Sisk and Trull	Markham
12	Shannon Oil and Gas, Inc.	#1 Sun Fee	Markham
13	Holly Energy, Inc.	#1 Hurlbutt	West Columbia
14	The Texas Co.	#1 E. M. Hurlbutt NCT	West Columbia
15	Kennedy and Mitchell, Inc.	#4-207 Buckeye	West Columbia
16	G. P. Johnson and Co.	#1 M. Doman et al.	West Columbia
17	Woodward and Co.	#1 Pierce Ranch	West Columbia
18	The Texas Co.	#1 Hiltpold	West Columbia
19	Robinson Oil and Gas Co.	#1 Anderson	West Columbia
20	Continental Oil Co.	#1 W. W. Fondren, Jr. et al.	West Columbia
21	Michael T. Halbouty	#1 M. E. Crouch	West Columbia
22	Bradco Oil and Gas Co.	#1 E. Burkhardt et al.	West Columbia
23	Geier-Jackson et al.	#1 C. C. Sherill	West Columbia
24	Stanolind Oil and Gas Co.	#1 Hawes-Vineyard	West Columbia
25	Falcon Seaboard Drlg. Co.	#1 F. C. Cornelius	West Columbia
26	Lenoir M. Josey Inc. & J. B. Coffee	#1 G. S. Reifslager	West Columbia
27	Sun Oil Co.	#2 St. Louis	West Columbia
28	Lario Oil and Gas Co. and Felmont Oil Corp.	#1 Lewis	West Columbia
29	Natomas North America, Inc.	#1 Cornelius	West Columbia
30	Union Oil	#1 Grady	West Columbia
31	Barron Kidd	#1 E. Krenek	West Columbia
32	J. M. Huber Corp.	#1 A. Copecet	West Columbia
33	Julian Evans	#1 Stasta	West Columbia
34	Davis Oil Co.	#1 Hickl Gas Unit	West Columbia
35	W. M. Harrison	#1 S. Le Tulle Rugeley	West Columbia
36	La Gorce Oil Co.	#1 H. D. Madsen	West Columbia
37	Rowan Drlg. Co. and Texas Gulf Co.	#1 Stovall	West Columbia
38	Goodale, Bertman and Co., Inc.	#1 Northern Ranch	West Columbia
39	Mid-Century Oil and Gas Co.	#1 F. W. Howard "A"	West Columbia
40	Z. W. Falcone and Bay City Drlg. Co.	#1 Kountze and Couch	Arch
41	Phillips Petroleum Co.	#1 Matagorda	West Columbia
42	Ada Oil Co.	#1 G. F. Stovall	West Columbia
43	J. Ray McDermott	#1 H. L. Brown	West Columbia
44	Sun Oil Co.	#4 First National Bank	Midfield
45	Superior Oil Co.	#1 D. K. Poole	El Maton
46	Sun Oil Co.	#1 C. Jumeck	West Columbia
47	Coastal States Gas Prod. Co.	#1 H. R. Ferguson	West Columbia
48	Monsanto Chemical Co.	#1 Newmont	El Maton
49	Monsanto Chemical Co.	#2 Fee	El Maton
50	Roy R. Gardner	#1 B. W. Trull	West Columbia
51	Coastal States Gas Prod. Co.	#1 Cornelius	Tidehaven
52	Coastal States Gas Prod. Co.	#2 Cornelius	Tidehaven
53	Humble Oil and Refining Co.	#B-1 J. C. Lewis	Duncan Slough

Appendix 1A. (cont.)

Well Number	Operator	Fee	Field
(Matagorda County-continued)			
54	The Texas Co.	#1 Denman-Kountze NCT-1	Markham
55	Hamill and Hamill	#20 C. M. Hudson	Markham
56	Claude B. Hamill and C. B. Hamill Trust	#27 Howard Smith	Markham
57	Lenoir M. Josey Inc.	#1 Pierce Ranch	West Columbia
58	Jack W. Frazier and J. B. Ferguson	#1 Pierce Est.	West Codlumbia
Wharton County			
1	Texas Gulf Sulphur Co.	#41 Abendroth	Boling
2	Texas Gulf Sulphur Co.	#32 O. W. Abendroth	Boling Dome
3	Texas Gulf Sulphur Co.	#33 O. W. Abendroth	Boling Dome
4	Texas Gulf Sulphur Co.	#30 O. W. Abendroth	Boling Dome
5	Texas Gulf Sulphur Co.	#39 Abendroth	Boling
6	Texas Gulf Sulphur Co.	#23 Banker Jr.	Boling Dome
7	Texas Gulf Sulphur Co.	#17-O.W. W. Banker, Jr.	Boling Dome
8	Texas Gulf Sulphur Co.	#18-O.W. W. Banker, Jr.	Boling Dome
9	Texas Gulf Sulphur Co.	#19-O.W. W. Banker, Jr.	Boling Dome
10	Danciger Oil Co.	#3 Mullins	Boling
11	Texas Gulf, Inc.	#18 W. Banker, Jr. "A"	Boling
12	Claude Knight	#2 Fojtik	Boling
13	Otis Russell	#1 M. B. Cloud	Boling
14	Texas Gulf, Inc.	#17-O.W. Chase Trust	Boling
15	Texas Gulf, Inc.	#18 Chase Trust	Boling
16	Texas Gulf, Inc.	#20 Chase Trust	Boling
17	Texas Gulf Sulphur Co.	#16-O.W. Banker Jr. "A"	Boling Dome
18	Texas Gulf Sulphur Co.	#15 O.W. McCarson	Boling Dome
19	Boling Prod. Co., Inc.	#18 A. A. Mullins	Boling
20	Cockburn Oil Corp.	#8 Cockburn Oil Corp.	West Columbia
21	Smith and Smith	#7 Cockburn Oil Corp.	Lane City
22	Goldking Petroleum	#1 M. J. Dupuy	Lane City
23	Prarie Prod. Co.	#5 Blue Creek Ranch	West Columbia
24	Moore and Ahem	#1 Johnson	West Columbia
25	The Atlantic Refg. Co.	#1 Pendergrass	Prasifka
26	Smith and Smith	#1 J. Ziober et ux.	Prasifka
27	Smith and Smith	#1 J. Ziober et ux.	Prasifka
28	Sue-Ann Operating Co.	#1 Vineyard "C"	West Columbia
29	Century Petroleum, Ltd.	#1 Vineyard	West Columbia
30	Chapman Oil Co.	#1 A. M. Brockman	Arrington
31	TexasGulf, Inc.	#20 W. Banker Jr.	Boling
32	Wellco Oil Co.	#3-W F. Sitta	Boling
33	Boling Prod. Co.	#4 M. D. Taylor Est.	Boling
34	Sparta Oil Co. and Mikton Oil Co.	#3 M. D. Taylor	Boling
35	Lyle Cashion Co.	#10 A. A. Mullins	Boling
36	Lyle Cashion Co.	#12 A. A. Mullins	Boling

Appendix 1A. (cont.)

Well Name	Operator	Fee	Field
(Wharton County-continued)			
37	Lyle Cashion Co.	#11 A. A. Mullins	Boling
38	Boling Prod. Co.	#8 A. A. Mullins	Boling
39	Texaco Inc.	#3 G. W. Duffy "B"	Blue Basin
40	Danciger Oil and Refining	#1 Mullins	Boling
41	Texas Oil and Gas Corp.	#1 A. Hlavinka "B"	Duffy
42	Texaco Inc.	#4 C. Barton, Jr.	Duffy, South
43	Danciger Oil and Refining Co.	#5 A. A. Mullins	Boling
44	Danciger Oil and Refining Co.	#7 A. A. Mullins	Boling
45	Danciger Oil and Refining Co.	#4 A. A. Mullins	Boling
46	Danciger Oil and Refining Co.	#2 A. A. Mullins	Boling
47	Sparta Oil Co. and Mikton Oil Co.	#2 Taylor	Boling
48	Texas Gulf Sulphur Co.	#11 G. McC Carson	Boling
49	Texas Gulf Sulphur Co.	#10 G. McC Carson	Boling
50	The Greenbriar Corp.	#4-B J. B. Gary Est.	South Boling
51	The Greenbriar Corp.	#5-B J. B. Gary Est.	South Boling
52	Texas Gulf Sulphur Co.	#A-7 Keller	Boling
53	The Greenbriar Corp.	#3-B J. B. Gary Est.	Boling Dome
54	The Greenbriar Corp.	#1 J. B. Gary Est.	Boling
55	Sisco Oil Co.	#1 E. Hawes	West Columbia
56	Humble Oil and Refining Co.	#8-3 J. B. Gary	Boling
57	W. M. Keck, Jr.	#1 Leissner	West Columbia
58	Brazos Oil and Gas Co. & M. T. Halbouty	#2 Blue Creek Ranch	West Columbia
59	John B. Coffee	#1 G. M. Rauscher	West Columbia
60	Smith and Smith	#D-1 Cockburn Miocene Gas Unit	Magnet-Withers
61	Soloco	#5 Hortman	El Campo North
62	Floyd L. Karsten	#1-B Myatt	Blue Basin
63	Anadarko Prod. Co.	#1 Mangum "A"	West Columbia
64	Humble Oil and Refining Co.	#77 H. C. Cockburn	Magnet-Withers
65	Kilroy Co. of Texas, Inc.	#1 W. H. Banker	West Columbia
66	M. Thompson	#1 J. F. Turner	Boling Dome
67	McKenzie Bros. Oil and Gas Co.	#1 C. Riggs	Boling
68	Gulf Coast Leaseholds, Inc.	#3 Taylor	Iago
69	Layne-Texas Co., Inc.	#1 Trull and Herlin	Water Well
70	Corley and Rice	#1 Gary	West Columbia
71	Mac Drilling Co. and John Mayo	#1 Gary Est.	West Columbia
72	Smith and Smith	#2 Duncan	West Columbia
73	Claude Knight	#1 Fojtik	Boling
74	Neaves Pet. Development Co.	#10 B. M. Floyd	Boling
75	Union Oil Co. of California	#8 C. Riggs	Boling
76	Kirby Petroleum Co.	#1 Dagley	West Columbia
77	Kirby Petroleum Co.	#2 Dagley	West Columbia
78	Roy R. Gardner	#2 R. G. Hawes	Boling
79	J. E. Bishop	#1 E. P. Hawes	Boling
80	Texas Gulf Sulphur Co.	#1 Bassett	Boling
81	The Texas Co.	#1 J. F. D. Moore	West Columbia
82	Davidor and Davidor, Inc.	#1 Moore	West Columbia
83	Standard Oil of Texas	#1 W. M. Meriwether	West Columbia

Appendix 1A. (cont.)

Well Name	Operator	Fee	Field
(Wharton County-continued)			
84	Getty Oil Co.	#1 Esther Beard	West Columbia
85	Curtis Hankamer	#1 Hobbs and Le Fort	West Columbia
86	The Superior Oil Co.	#1 E. Hawes	West Columbia
87	Sinclair Prairie Oil Co.	#1 Hawes Est.	West Columbia
88	Texas Gulf Sulphur Co.	#2 W. T. Taylor	Boling
89	Cerro De Pasco	#1 Gary Est.	West Columbia
90	Miller and Ritter	#1 C. M. Allen	Boling
91	F. S. Pratt	#1 Fleer	West Columbia
92	Texaco, Inc.	#C-143 Pierce Est.	Magnet-Withers
93	Texaco, Inc.	#C-129 Pierce Est.	Magnet-Withers
94	Humble Oil and Refining Co.	#1 Rogers	Lane City
95	Texas Republic Petroleum Co.	#1 G. R. Hawes	West Columbia
96	R. B. Mitchell	#1 H. C. Cockburn	West Columbia
97	Mac Drilling Co. and John Mayo	#1 Gary Est.	West Columbia

Appendix 1B. Well Information for Cross Sections

<u>Well No.</u>	<u>Operator</u>	<u>Fee</u>	<u>County</u>
Barbers Hill Dome			
A - A ¹			
36			Liberty
1			Liberty
7	British Texas Oil Co.	#1 Barber	Chambers
16	The Texas Co.	#2 Kirby Oil and Gas	Chambers
29	Sunray-Mid Continent Oil Co.	A-8 Barber	Chambers
24	Texas Eastern Transmission Co.	#7 Mt. Belview Storage Well S-B	Chambers
40	Warren Petroleum Co.	#11 Mt. Belview	Chambers
45	Houston Oil and Minerals Corp.	#12 Chambers County Agricultural Co.	Chambers
28	Sierra	#1 Trichel	Chambers
10	Humble Oil and Refining Co.	# B-1 B. Dutton	Chambers
B - B ¹			
60	Te		Harris
6	General Crude Oil Co.	#1 Barber	Chambers
51	Texas Gulf Producing Co.	#15 Kirby "A"	Chambers
24	Texas Eastern Transmission Co.	#7 Mt. Belview Storage Well S-B	Chambers
30	The Texas Co.	#1 J. M. Fitzgerald Estate	Chambers
13	M. T. Halbouty	#1 E. Wilburn	Chambers
59	J. W. Mecon	#3-B Mayes	Chambers
Markham Dome			
42	Texaco Inc.	#4 C. Barton Jr.	Wharton
39	Texaco Inc.	#3 G. A. Duffy "B"	Wharton
19	Robinson Oil and Gas Co.	#1 Anderson	Matagorda
18	The Texas Co.	#1 Hiltpold	Matagorda
11	Hamill and Hamill	#1 Sisk and Trull	Matagorda
9	Seadrift Pipeline Corp.	#2 Fee	Matagorda
56	C. B. Hamill and C. B. Hamill Trust	#27 H. Smith	Matagorda
55	Hamill and Hamill	#20 C. M. Hudson	Matagorda

Appendix 1B. (continued)

<u>Well No.</u>	<u>Operator</u>	<u>Fee</u>	<u>County</u>
Markham Dome (continued)			
30	Union Oil Co.	#1 Grady	Matagorda
5	Placid	#1 LeTulle	Matagorda
4	M. T. Williams	#1 C. B. Fisher et al.	Matagorda
Boling Dome			
41	Scurlock Oil Co. and M. T. Halbouty	#1 D. Krause	Fort Bend
40	Fort Bend Oil Co.	#1 J. M. Moore Est.	Fort Bend
82	Davidor and Davidor, Inc.	#1 Moore	Wharton
81	The Texas Co.	#1 J. F. D. Moore	Wharton
79	J. E. Bishop	#1 E. P. Hawes	Wharton
80	Texas Gulf Sulphur Co.	#1 Bassett	Wharton
39	Mid-Century Oil and Gas Co.	#1 F. W. Howard "A"	Matagorda
24	Stanolind Oil and Gas Co.	#1 Hawes-Vineyard	Matagorda

Appendix 1C. Well Information for Caverns and
Salt-Water Disposal Wells at Barbers Hill Salt Dome

<u>Well No.</u>	<u>Operator</u>	<u>Well Name</u>
1	Enterprise Products	Salt-water disposal Well No. 1
2	Enterprise Products	Salt-water disposal Well No. 2
3	Enterprise Products	Cavern Well No. 9
4	Houston Oil and Minerals	Salt-water disposal Well No. 1
5	Enterprise Products	Cavern Well No. 7
6	Enterprise Products	Cavern Well No. 4
7	Texas Eastern Transmission	Cavern Well No. NT-10 LPG
8	Texas Eastern Transmission	Salt-water disposal Well No. 2
9	Conoco	Cavern Well No. 1 UGSW
10	Arco	Cavern Well No. 8 LPG
11	Arco	Salt-water disposal Well No. 1B
12	Arco	Cavern Well No. 3 LPG
13	Arco	Cavern Well No. 4 LPG
14	Arco	Cavern Well No. 6 LPG
15	Arco	Cavern Well No. 11 LPG
16	Texas Eastern Transmission	Cavern Well No. S-8 LPG
17	Texas Eastern Transmission	Salt-water disposal Well No. 1
18	Texas Eastern Transmission	Cavern Well No. S-4 LPG
19	Warren	Cavern Well No. 25 LPG
20	Texas Eastern Transmission	Cavern Well No. S-3 LPG
21	Texas Eastern Transmission	Cavern Well No. S-2 LPG
22	Warren	Cavern Well No. 17 LPG
23	Warren	Cavern Well No. 2 LPG
24	Warren	Cavern Well No. 1 LPG
25	Warren	Cavern Well No. 5 LPG
26	Warren	Cavern Well No. 7 LPG
27	Diamond Shamrock	Salt-water disposal Well No. D-1
28	Diamond Shamrock	Cavern Well No. 2
29	Warren	Salt-water disposal Well No. 3
30	Warren	Cavern Well No. 22 LPG
31	Diamond Shamrock	Cavern Well No. 12

Appendix 2. Conversion tables for stress units, length units (Paterson, 1978), and time.

Example: 1 bar = 14 503 pounds per square inch

	Bars	Kilobars (kbar)	Dynes per square centimeter (dyn/cm ²)	Atmospheres (atm)	Kilograms per square centimeter (kg/cm ²)	Pounds per square inch (lb./in. ²)	Pascals (Pa)	Megapascals (MPa)	Gigapascals (GPa)
Bars	1.0	10 ⁻³	10 ⁸	0.9869	1.0197	14 503	10 ⁵	10 ⁻¹	10 ⁻⁴
Kilobars	10 ³	1.0	10 ⁹	0.9869 x 10 ³	1.0197 x 10 ³	14 503 x 10 ³	10 ⁸	10 ²	10 ⁻¹
Dynes per square centimeter	10 ⁻⁶	10 ⁻⁹	1.0	0.9869 x 10 ⁻⁶	1.0197 x 10 ⁻⁶	14 503 x 10 ⁻⁶	10 ⁻¹	10 ⁻⁷	10 ⁻¹⁰
Atmospheres	1.0133	1.0133 x 10 ⁻³	1.0133 x 10 ⁶	1.0	1.0333	14 695	1.0133 x 10 ⁵	0.1013	1.0133 x 10 ⁻⁴
Kilograms per square centimeter	0.9807	0.9807 x 10 ⁻³	0.9807 x 10 ⁶	0.9678	1.0	14 223	0.9807 x 10 ⁵	0.9807 x 10 ⁻¹	9.807 x 10 ⁻⁵
Pounds per square inch	6.895 x 10 ⁻²	6.895 x 10 ⁻⁵	6.895 x 10 ⁴	6.805 x 10 ⁻²	7.031 x 10 ⁻²	1.0	6.895 x 10 ³	6.895 x 10 ⁻³	6.895 x 10 ⁻⁶
Pascals	10 ⁻⁵	10 ⁻⁸	10	0.9869 x 10 ⁻⁵	1.0197 x 10 ⁻⁵	14 503 x 10 ⁻⁵	1.0	10 ⁻⁶	10 ⁻⁹
Megapascals	10	10 ⁻²	10 ⁷	9.869	10.197	145.03	10 ⁶	1.0	10 ⁻³
Gigapascals	10 ⁴	10	10 ¹⁰	0.9869 x 10 ⁴	1.0197 x 10 ⁴	14 503 x 10 ⁴	10 ⁹	10 ³	1.0

92

Conversion table for length units

Example: 1 meter = 3.281 feet.

	Centimeters	Inches	Feet	Meters	Kilometers	Miles
Centimeters	1.0	0.3937	0.0328	0.01	10 ⁻⁵	6.215 x 10 ⁻⁶
Inches	2.540	1.0	0.0833	0.0254	2.54 x 10 ⁻⁵	1.578 x 10 ⁻⁵
Feet	30.48	12.0	1.0	0.3048	3.048 x 10 ⁻⁴	1.894 x 10 ⁻⁴
Meters	100.0	39.37	3.281	1.0	10 ⁻³	6.215 x 10 ⁻⁴
Kilometers	10 ⁵	3.937 x 10 ⁴	3281	10 ³	1.0	0.6215
Miles	1.609 x 10 ⁵	63360	5280	1609	1.609	1.0

Conversion table for time units

	Seconds (s)	Minutes	Hours	Days	Months	Years
seconds	1 x 10 ⁰	6.0 x 10 ¹	3.6 x 10 ³	8.64 x 10 ⁴	2.63 x 10 ⁶	3.16 x 10 ⁷

Appendix 3. Cap-rock injection data for domes in Texas.

<u>Dome</u>	<u>Operator/Well No./Lease</u>	<u>Injection Interval</u>	<u>RRC Permit Date</u>
Day	International Underground Storage, 3 G.P. Day	2450 - 2550	1964
	International Underground Storage, 1 LPG Pure Oil	2400 - 2500	1964
Fannett	Warren, 15 I.R. Bordages, et al. "A"	2115 - 2145	1971
	Gulf, 3 SWD I.R. Bordages, et al. "A"	unknown	
	TX Gulf Sulphur, 1 SWD I.R. Bordages, et al. "A"	unknown	
	TX Gulf Sulphur, 2 SWD I.R. Bordages, et al. "A"	unknown	
Hull	Magnolia, 2 SWD Hull Underground Storage	700 - unknown	1956
	Magnolia, 3 SWD Hull Underground Storage	702 - unknown	1956
	Sinclair, 5-A SWD Dolbear Fee	700 - 800	1962
	J.W. Mecom, 1 Elsie Taylor	1150 - 1181	1967
	Texaco, 2-F H.G. Camp Fee	700 - 860	1969
	R.V. Ratts, 1 Jim Best	800 - 820	1974
	T. True, 1 Fuel Oil Manufacturing Plant	400 - 700	1974
	Gulf, 2 SWD J.W. Canter "A" Fee	700 - 710	1975
Markham	Texas, 7 SWD H. Smith Fee	1594 - 1736	1959
	Texaco, 9 N.N. Meyers "E"	2209 - 2334	1959
	Texaco, 24 SWD N.R. Meyers "C"	1950 - 3060	1960
	Texaco, 9 SWD N.R. Meyers "B"	1500 - 2070	1960
	Seadrift, 2 Fee	1400 - 1510	1961
	Seadrift, A-3 Fee	2874 - 3110	1962
	Seadrift, A-3 Fee	1590 - 1930	1976
	Seadrift, A-3 Fee	1590 - 2575	1979
	Seadrift, 1 SWD Fee	1280 - 3300	1977
Moss Bluff	Moss Bluff Storage Venture, 1 SWD Fee	1320 - 3040	1980
	Moss Bluff Storage Venture, 2 SWD Fee	1320 - 3040	1980
	Moss Bluff Storage Venture, 4 SWD Fee	1320 - 3040	1980
Nash	Humble, 2 Mary Svocek	1470 - 1505	1953
	Humble, 1 SWD P. Meier	1900 - 3850	1955
	(2 post-1975 permits, unknown)		
North Dayton	Texaco, 12 J.A. Deering, Jr. "N"	2590 - 2970	1962
	Texaco, 3 J.A. Deering, Jr. "N"	2300 - 2735	1963
	(1 post-1975 permit, unknown)		
Pierce Junction	J.S. Abercrombie, II J. Ritter	1376 - 1378	1951
	Wanda, 2-B Settegast	860 - 1000	1971
	Sparta, 1 J.C. Calvert	1020 - 1060	1972
	Martin, 6 White Head	2890 - 3300	1975
	Coastal States, 1 Almeda Underground Storage	801 - 1000	1983
Orchard	Gulf, 2 J.M. Moore, et al. (2 post-1975 permits, unknown)	478 - 510	1959
Damon Mound may have cap rock injection, but wells, locations, intervals unknown.			

Appendix 3. (cont.)

<u>Dome</u>	<u>Operator/Well No./Lease</u>	<u>Injection Interval</u> (feet)	<u>RRC Permit Date</u>
Barbers Hill	Texas Butadiene (Arco), 1-A Fee	750 - 752	1956
	Texas Butadiene (Arco), 1-A Fee	775 - 779	1956
	Tenneco, 1 SWD Mt. Belvieu Storage Terminal	745 - 820	1956
	Tenneco, 1 SWD Mt. Belvieu Storage Terminal	820 - 823	1962
	Houston O & M, 1 SWD Kirby Pet. "B"	1348 - 3776	1964
	Pyndus, 4 Kirby	700 - 740	1964
	Sinclair, 4 J.F. Wilburn	935 - 1326	1967
	Sinclair, 13 Kirby Pet. "A"	1900 - 2120	1967
	Sinclair, 10 Kirby Pet. "B"	995 - 1396	1967
	Sunray DX, 1 E. W. Barber "B"	1379 - 1389	1967
	Mills Bennett Est., 1 SWD Kirby Pet.	850 - 1370	1967
	TX Ntnl. Bank of Comm. Houston, 17 J.F. Wilburn	800 - 1379	1967
	Sun, 1 SWD Higgins	1190 - 1367	1967
	Mills Bennett Est., 1 SWD Gulf Fee Fisher	1100 - 1520	1968
	Universal Pet., 1 Gulf Fee Lee Brothers	1344 - 1375	1969
	Arco, 10 J. F. Wilburn	1300 - 1370	1971
	Sun, 15 SWD Higgins	1270 - 1320	1972
	Sun, 15 SWD Higgins	912 - 1270	1972
	TX Eastern Transmission, 1 SWD L.P.G. Storage	500 - 1200	1973,1975
	TX Eastern Transmission, 1 SWD Fee	650 - 810	1972
	Exxon Pipeline, 1 SWD Fee	1125 - 1300	1974,1975
	Warren, 3-A SWD Fee	800 - 1550	1974
	Conoco, 1 SWD Fee	600 - 1300	1975
	XRAL, 1 SWD Fee	1020 - 1300	1975
	TX Eastern Transmission, 2 SWD Fee	720 - 950	1976
	Warren, 4 SWD Fee	800 - 1550	1976
	Arco, 1-B Fee	750 - 1185	1977
	Warren, 5 SWD Fee	800 - 1500	1977
	XRAL, 2 SWD Fee	1350 - 1380	1978
	Enterprise Products, 1 SWD Mt. Belvieu	1120 - 1400	1978
	Enterprise Products, 2 SWD Mt. Belvieu	1120 - 1400	1978
	Conoco, 2 SWD Fee	575 - 1150	1978
	Mills Bennett Est., 1 SWD J.F. Wilburn "C"	900 - 1300	1979
Diamond Shamrock, D-1 Fee	1000 - 1200	1979	
Amoco, 50 Chambers County Ag.	1400 - 1900	1979	
Big Hill	Pure, 1 Fee	830 - 845	1956
	Goodale, Bertman, & Co., 7 TX Exploration	1070 - 1475	1965
	Pan Am, 19 TX Exploration	1460 - 3300	1968
	(2 post-1975 permits, unknown)		
Blue Ridge	L.D. French, II Robinson-Bashare	2435 - 2700	1969
	Ramco, I Wist & Schenck	1980 - 2090	1972
Boling	Cecil Hagen, 6 A.C. Mich (4 post-1975 permits, unlocated & unknown)	2052 - 2085	1950

PHASE I Report

July 1984

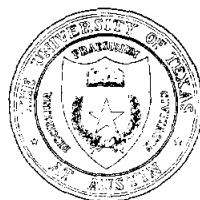
ROBERT L. BLUNTZER

BUREAU OF ECONOMIC GEOLOGY

THE UNIVERSITY OF TEXAS

AT AUSTIN

W. L. FISHER, DIRECTOR



TEXAS SALT DOMES:
Natural Resources, Storage Caverns, and
Extraction Technology

Steven J. Seni, William F. Mullican III, and H. Scott Hamlin

Contract Report for Texas Department of Water Resources
under Interagency Contract No. IAC (84-85)-1019

Bureau of Economic Geology
W. L. Fisher, Director
The University of Texas at Austin
University Station, P.O. Box X
Austin, Texas 78713-7508

CONTENTS

INTRODUCTION	1
TEXAS SALT DOMES.	2
SOLUTION-MINED CAVERNS	7
Public information	8
CAVERN CONSTRUCTION	9
Casing program	10
Salt-dissolution process	12
Blanket material and function	13
Sump	13
CAVERN GEOMETRY	15
Direct circulation	15
Reverse circulation	16
Modified circulation.	16
CAVERN FAILURES	20
Mechanisms of cavern failure	27
SALT-DOME RESOURCES	28
Salt-dome storage	29
Salt resources	39
Rock-salt mine	42
Solution-brine well	42
Petroleum resources.	45
Shallow salt-dome oil fields	45
Cap-rock reservoirs	47
Salt-dome flank reservoir	52
Deep-seated dome crest reservoir	54
Petroleum resources of salt domes in the Rio Grande and East Texas Basins	56
Sulfur resources	57
History and technology	57
Characteristics of cap-rock sulfur deposits	60
Cap-rock resources	60
Crushed stone	66
Other resources	66
ACKNOWLEDGMENTS	68
REFERENCES.	69
APPENDIX 1. Structure-contour map of Texas salt domes constructed on a topographic base.	74
APPENDIX 2. Railroad Commission of Texas Authority Numbers for storage-well permits.	159

APPENDIX 3. Railroad Commission of Texas Rule 74 procedures and requirements for storage-well operations 160

Figures

1. Salt basins and diapir provinces in the United States. 3

2. Location map for Texas salt domes. 4-5

3. Typical casing string detail for solution-mined cavern in salt. 11

4. Casing configuration for direct circulation. 14

5. Phased expansion of solution cavern with direct circulation. 17

6. Casing configuration for reverse circulation. 18

7. Evolution of brine and storage caverns, Pierce Junction salt dome. 19

8. Cross section of Blue Ridge salt dome showing geometry of salt mine and storage cavern that failed. 25

9. Histogram of 1983 storage capacity in Texas salt domes and proposed Strategic Petroleum Reserve caverns. 30

10. Map of salt domes showing active, abandoned, and pending storage facilities. 32-33

11. Cross section of Bryan Mound salt dome (north-south) showing geometry of present Strategic Petroleum Reserve caverns. 34

12. Cross section of Bryan Mound salt dome (east-west) showing geometry of present and proposed Strategic Petroleum Reserve caverns. 35

13. Cross section of Big Hill salt dome (north-south) showing geometry of proposed Strategic Petroleum Reserve caverns and Union Oil Co. storage cavern. 36

14. Cross section of Big Hill salt dome (east-west) showing geometry of proposed Strategic Petroleum Reserve caverns. 37

15. Map of Boling salt dome showing locations of oil fields, sulfur production, Valero Gas Co. gas-storage caverns, and United Resource Recovery, Inc., lease area. 40

16. Cross section of Boling salt dome (east-west) showing location of sulfur production, geometry of Valero Gas Co. gas-storage caverns, and proposed location and geometry of United Resource Recovery, Inc. waste-storage caverns. 41

17. Map of salt domes showing active rock-salt mines and solution-brine wells. 43

18. Yearly oil production from Spindletop salt-dome oil field. 46

19. Map of piercement salt domes showing oil fields that have produced more than 10 million barrels of oil.	48
20. Graph showing depth to the crest of Texas salt domes and their cumulative oil production through 1975.	49
21. Map of Boling salt dome showing locations of oil fields.	50
22. Cross section of (Moore's) Orchard salt dome showing upturned strata on the flank of the dome and the crest of the dome truncated by erosion.	53
23. Map of Yegua and Frio reservoirs over the crest of deep-seated salt domes.	55
24. Casing string detail for cap-rock sulfur-production well.	58
25. Graph showing the chronology of sulfur mining in Texas salt domes.	61
26. Map of salt domes showing active and abandoned sulfur mining.	62-63
27. Cross section of Boling salt dome showing cap rock and zone of sulfur mineralization.	64
28. Map of Texas salt domes showing area of sulfur mineralization.	65

Tables

1. List of salt domes with cavern failures, mechanisms, and consequences.	21
2. List of salt domes with storage, operating company, Railroad Commission of Texas applicant, number of caverns, capacity, and product stored.. . . .	38
3. List of salt domes with salt production, method, status, company, and history.	44
4. List of salt domes with large oil fields and production status.	51
5. List of salt domes with sulfide mineral occurrences and documentation.	67

INTRODUCTION

This report reviews natural resources associated with salt domes in Texas. Salt domes provide a broad spectrum of the nation's industrial needs including fuel, minerals, chemical feedstock, and efficient storage space. This report focuses on the development, technology, uses, and problems associated with solution-mined caverns in salt domes. One proposed new use for salt domes is the permanent isolation of toxic chemical waste in solution-mined caverns. As the Texas Department of Water Resources (TDWR) is the State authority responsible for issuing permits for waste disposal in Texas, TDWR funded this report to judge better the technical merits of toxic waste disposal in domes and to gain a review of the state of the art of applicable technology.

Salt domes are among the most interesting and intensively studied structural-stratigraphic geologic features. Individual domes may be the largest autochthonous structures on earth. Yet many aspects of salt-dome genesis and evolution, geometry, internal structure, and stratigraphy are problematic. Details of both external and internal geometry of salt stocks and their cap rocks are vague, and information is restricted to the shallow parts of the structure. These facts are all the more surprising considering that salt diapirs dominate the fabric of the Gulf Coastal Province, which is one of the most explored and best known geologic regions on earth.

This report includes information on present and past uses of Texas salt domes, their production histories, and extractive technologies (see also Halbouty, 1979; Hawkins and Jirik, 1966; and Jirik and Weaver, 1976). Natural resources associated with salt domes are dominated by petroleum that is trapped in cap rocks and in strata flanking and overlying salt structures. Sulfur occurs in the cap rock of many domes. Some cap rocks also host potentially valuable Mississippi Valley-type sulfide and silver deposits. Salt is produced both by underground mining of rock salt and by solution brining.

The caverns created in salt by solution mining also represent a natural resource. The relative stability, economics, location, and size of these caverns makes them valuable storage vessels for various petroleum products and chemical feedstocks.

TEXAS SALT DOMES

Texas salt structures are clustered in the Gulf Coast, Rio Grande, and East Texas Salt Basins. Shallow piercement salt domes form diapir provinces within the larger salt basins (fig. 1). A regional map shows the distribution of salt domes in the three salt basins (fig. 2). Structure-contour maps (sea-level datum) of individual domes were prepared and plotted on a map with surface topographic contours (appendix 1).

Physically, salt domes are composed of three elements--the salt stock, the cap rock, and the host strata. The central core of the salt dome is a subcylindrical to elongate salt stock. Typically, the cap rock immediately overlies the crest of the salt stock and normally drapes down the uppermost flanks of the stock. An aureole of sediments surrounds the salt stock. Drag zones, gouge zones, and diapiric material transported with the salt stock are included in the aureole.

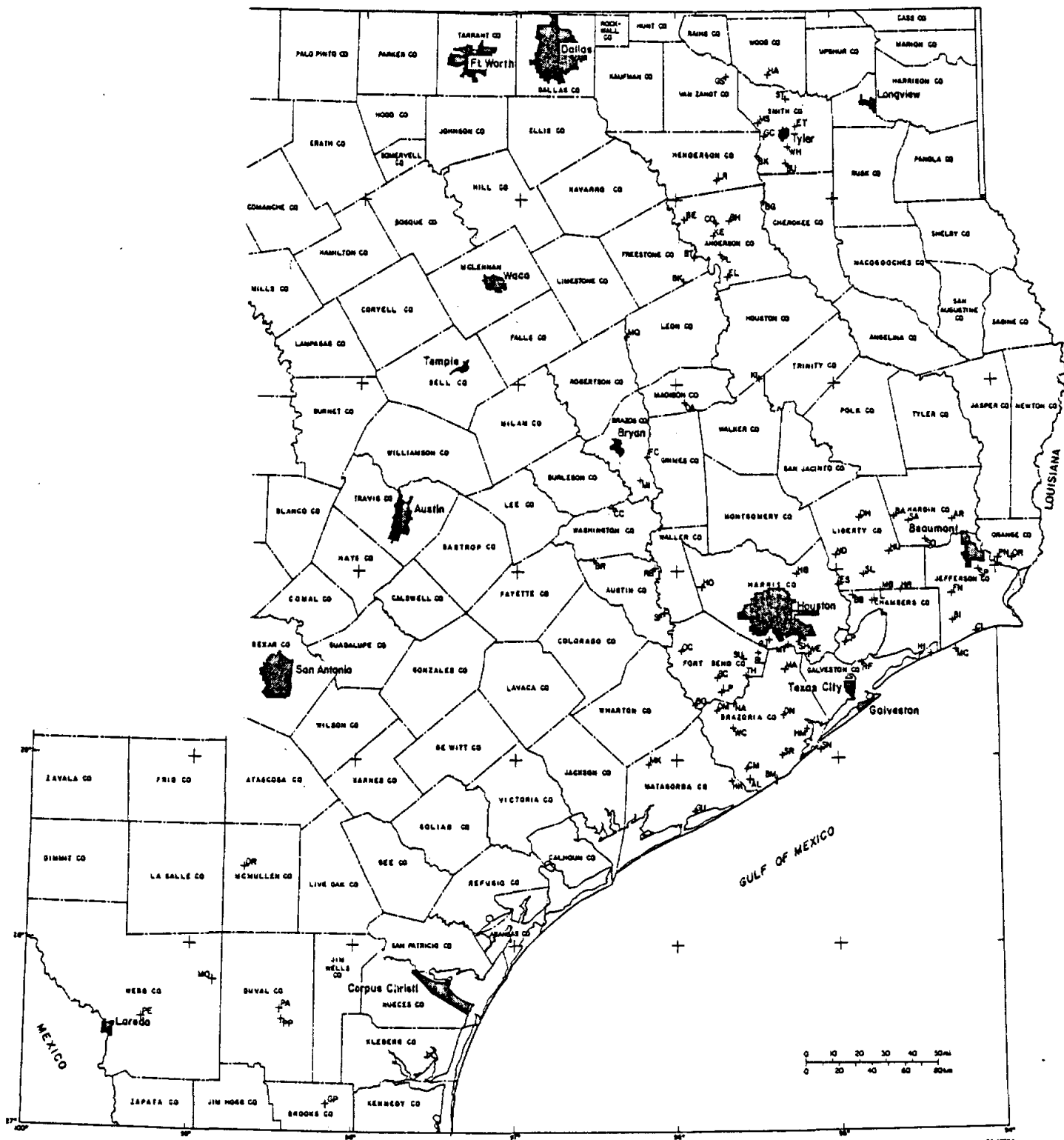
Salt diapirs are the mature end members of an evolutionary continuum of salt structures. Diapirs begin as low-relief salt pillows that are concordant with surrounding strata. The flanks of the salt pillow steepen with continued growth, and overlying strata are stretched and faulted. Salt becomes diapiric when the relation of salt and surrounding strata becomes discordant. At that point, the salt structure may be intrusive with respect to surrounding strata or it may be extruding at the surface. The phase of active diapirism is typically accompanied by rapid rates of sedimentation. Subsequent to active diapirism, dome evolution enters a slower phase of growth characterized by slow rates of upward movement or by crest attrition owing to salt dissolution in excess of growth.

Dome-growth history is an important aspect in understanding the many problems associated with dome stability (Jackson and Seni, 1983). A complete understanding of dome



OA 2194

Figure 1. Salt basins and diapir provinces in the United States (modified from Smith and others, 1973).



TEXAS SALT DOMES

Figure 2. Location map for Texas salt domes.

(continued)

Figure 2 (cont.).

Code	Dome Name	County			
AL	Allen	Brazoria	HB	Humble	Harris
AR	Arriola	Hardin	KE	Keechi	Anderson
BB	Barbers Hill	Chambers	KI	Kittrell	Houston/Walker
BA	Batson	Hardin	LR	La Rue	Henderson
BE	Bethel	Anderson	LP	Long Point	Fort Bend
BC	Big Creek	Fort Bend	LL	Lost Lake	Chambers
BI	Big Hill	Jefferson	MA	Manvel	Brazoria
BL	Blue Ridge	Fort Bend	MK	Markham	Matagorda
BG	Boggy Creek	Anderson/Cherokee	MQ	Marquez	Leon
BO	Boling	Wharton/Fort Bend	MC	McFaddin Beach	State waters
BR	Brenham	Austin/Washington	MI	Millican	Brazos
BK	Brooks	Smith	MO	Moca	Webb
BH	Brushy Creek	Anderson	MB	Moss Bluff	Chambers/Liberty
BM	Bryan Mound	Brazoria	MS	Mount Sylvan	Smith
BU	Bullard	Smith	MY	Mykawa	Harris
BT	Butler	Freestone	NA	Nash	Brazoria/Fort Bend
CP	Cedar Point	Chambers	ND	North Dayton	Liberty
CL	Clam Lake	Jefferson	OK	Oakwood	Freestone/Leon
CC	Clay Creek	Washington	OR	Orange	Orange
CM	Clemens	Brazoria	OC	Orchard	Fort Bend
CO	Concord	Anderson	PA	Palangana	Duval
DM	Damon Mound	Brazoria	PL	Palestine	Anderson
DN	Danbury	Brazoria	PE	Pescadito	Webb
DH	Davis Hill	Liberty	PP	Piedras Pintas	Duval
DA	Day	Madison	PJ	Pierce Junction	Harris
DR	Dilworth Ranch	McMullen	PN	Port Neches	Orange
ET	East Tyler	Smith	RB	Raccoon Bend	Austin
EL	Elkhart	Anderson	RF	Red Fish Reef	State waters
ES	Esperson	Harris/Liberty	SF	San Felipe	Austin
FN	Fannett	Jefferson	SN	San Luis Pass	State waters
FC	Ferguson Crossing	Brazos/Grimes	SA	Saratoga	Hardin
GC	Girlie Caldwell	Smith	SO	Sour Lake	Hardin
GS	Grand Saline	Van Zandt	SH	South Houston	Harris
GU	Gulf	Matagorda	SL	South Liberty	Liberty
GP	Gyp Hill	Brooks	SP	Spindletop	Jefferson
HA	Hainesville	Wood	ST	Steen	Smith
HR	Hankamer	Chambers/Liberty	SR	Stratton Ridge	Brazoria
HK	Hawkinsville	Matagorda	SU	Sugarland	Fort Bend
HI	High Island	Galveston	TH	Thompson	Fort Bend
HO	Hockley	Harris	WE	Webster	Harris
HM	Hoskins Mound	Brazoria	WC	West Columbia	Brazoria
HU	Hull	Liberty	WH	Whitehouse	Smith

growth requires detailed knowledge of dome geometry, stratigraphy, and structure and stratigraphy of surrounding strata, geohydrology (both past and present), and surficial strata. Such detailed studies have been completed for salt domes in the East Texas Basin (Jackson and Seni, 1984; Seni and Jackson, 1983a, b). Currently, the required data base for understanding growth history of the domes in the Houston Salt Basin is only partly assembled. Public data on the geometry of the salt stock have been collected. Much work remains to understand the geology of cap rocks and surrounding strata.

The influence of dome growth on the topography of the modern surface over the crests of salt structures is one aspect of dome-growth history that is available for domes in both the Houston and the East Texas Salt Basins. The topography of the modern surface over the crests of diapirs is readily influenced by diapir growth or dissolution. Positive topographic relief (in excess of regional trends) over the dome crest is linked to uplift or to active diapir growth. In contrast, subsidence of the topographic surface over the dome crest is linked to attrition or dissolution of the dome crest. Comparison of the topographic relief over domes in the salt basins indicates the relative importance of growth or dissolution processes. For salt domes in the Houston Salt Basin with crests shallower than 4,000 ft, 63 percent of the domes show evidence of positive topographic relief over their crests, whereas only 8 percent of these domes show evidence of subsidence at the depositional surface. In contrast, in the East Texas Salt Basin, 81 percent of the shallow domes (those with crests shallower than 4,000 ft) show evidence of subsidence over the crest, whereas no domes in the East Texas Salt Basin express evidence of uplift. Clearly, strata over the crests of domes in the East Texas Salt Basin have responded differently to processes at the diapir crest than have domes in the Houston Salt Basin. Supradomal topography over domes in the East Texas Basin reflects the dominance of dissolution and crest attrition processes, whereas the dominance of uplift is shown over domes in the Houston Salt Basin.

SOLUTION-MINED CAVERNS

Salt caverns were originally an unrecognized resource formed when salt was removed by dissolution to produce brine principally as a chemical feedstock. Along the Texas coast, a large petrochemical industry evolved because abundant petroleum reserves were associated with Texas coastal salt domes. This close association between salt domes and the petroleum industry in turn promoted both brine and storage industries near the domes. Texas domes are now being considered as chemical waste repositories. The petroleum-refining industry would be the source of much of that chemical waste.

Natural resources from Texas salt domes have been efficiently exploited with a multiple-use philosophy. Permanent disposal of toxic-chemical waste in solution-mined caverns may remove a given region of the dome from resource development forever. Multiple use of domes in the future would then be restricted.

Brining and solution mining are two different operations that form two types of caverns. Brining is used here to describe operations in which the primary economic product is the Na^+ and Cl^- in the brine. Caverns that form around brine wells are incidental to the production of brine. The cavern is just the space from which salt was dissolved during brine production. Solution mining is used here to describe the process of forming an underground cavern specifically for product storage. In this case the brine is typically discarded either into the cap rock or the saline aquifers.

Both brining and solution mining operate on a large scale in Texas. Of 13 domes with a history of brining operations, 7 are active. Similarly, of 18 domes with a history of storage, 16 are active. Two additional domes have proposed storage operations approved by the Texas Railroad Commission (RRC). According to Griswold (1981), approximately 900 cavities have been solutioned in the United States (circa 1981). Statistics from the Gas Processors Association (GPA) reveal that in 1983, 47 percent of the national storage capacity of light hydrocarbons was in Texas salt domes (GPA, 1983).

The primary objectives differ for brine operations and solution mining for storage. Currently, many former brine caverns serve as storage caverns. Simultaneous product storage and brining began in Texas at Pierce Junction salt dome (Minihan and Querio, 1973). The difference between salt dissolution to produce brine and creating space for storage may be subtle but variations in operating parameters often produce vastly different salt-cavern geometries. The primary objective in brining is lessening pumping costs and increasing brine production. Solution mining for storage is primarily directed toward a controlled cavern shape yielding maximum cavern stability. The mechanisms by which differences in operating parameters affect cavern shape and stability will be described in sections titled Cavern Geometry, Cavern Failures, and Mechanisms of Cavern Failure.

As with many fledgling industries, initial solution-mining operations were originally seat-of-the-pants. Experience was gained from the early operations, and many new techniques were employed to complete successfully and set casing in problem holes, to control and monitor cavern development, and to predict eventual cavern shapes and stabilities. Some predicted conditions later proved wrong, however. Despite industry safeguards, a total of 10 brine and storage caverns have failed in Texas.

Both long-term and short-term cavern stability is a critical issue for the storage industry and especially for the permanent disposal of chemical waste. Despite concerted research effort in this area, even industry leaders admit "no universally accepted technique to predict cavern closure (or stability) has been developed" (Fenix and Scisson, Inc., 1976a).

Public Information

At this point a caveat is warranted. The total number and capacities of solution-mined caverns in Texas is unknown. Most individual companies treat information on cavern capacities as classified data. Much research time and effort were spent at the RRC examining original documents requesting storage permits. Railroad Commission of Texas authority numbers are included in appendix 2 to aid future research efforts. Early regulatory practices of the RRC

were laissez-faire. The original permit specifically allowed any and all improvements including the creation of additional storage caverns and space as desired. Other caverns that received permit approval were never completed. Some caverns have been abandoned as a result of technological or economic problems. Thus although a comprehensive list of caverns approved by the RRC was obtained, its exact equivalence with currently active caverns and their present use is not assured. Capacities of storage for Texas salt domes are from the Gas Processors Association (1983), which lists present storage capacities for light hydrocarbons. Storage of natural gas and crude oil was not listed by the Gas Processors Association. Much additional storage capacity primarily resulting from brining is undocumented.

The RRC created the Underground Injection Control Section and strengthened application procedures and reporting requirements for constructing underground hydrocarbon storage facilities after a storage cavern failed at Barbers Hill salt dome. Beginning April 1, 1982, all storage wells must be tested for mechanical integrity at least once every 5 years. Rule 74 is the document that details State requirements for underground hydrocarbon storage. It is reproduced in appendix 3.

CAVERN CONSTRUCTION

A salt cavern is solution mined by drilling a hole to expose salt, circulating fresh or low-salinity water to dissolve salt, and then displacing the resulting brine. With time, the hole enlarges and becomes the cavern. Constructing a solution-mined cavern in salt requires thick salt, a supply of fresh or low-salinity water, and a means of disposing or using the brine (Fenix and Scisson, 1976a). With some exceptions, solution-mined wells are drilled and cemented with what is generally the same technology as that is used in completing oil-, water-, and brine-disposal wells. The unique set of conditions generated during cavern dissolution requires some specialized procedures. Hole straightness is critical because this affects cavern geometry and location. Massive drill collars are used to reduce the "walk-of-the-bit," or the tendency of the

bit to trace a helicoidal path during drilling. Drilling in salt also requires special salt-saturated drilling muds for preventing hole enlargement by unwanted salt dissolution.

The casing program is the single most important aspect for successfully drilling and completing a well for solution mining. Industry experts agree that most cavern failures and all reported instances of catastrophic product loss resulted from some form of casing failure (Fenix and Scisson, 1976a; Van Fossan, 1979).

Casing Program

Casing programs for solution-mined wells are designed to (1) prevent contamination of surrounding formations by drilling fluids, (2) prevent sloughing of surrounding formations into the drillhole, (3) anchor the casing, tubing, and braden-head assembly firmly into the salt, and (4) prevent loss of storage products. Casing programs have become more complex with time. A typical casing program is shown in figure 3. Early casing programs in brine wells used two or three casing strings and one production tubing. Modern casing programs use up to seven casing strings and up to three production tubing strings.

Conductor pipe is the first and largest diameter (30 to 42 inch) casing. Conductor pipe is commonly used in the Gulf Coast area where it is simply driven 50 to 300 ft into the ground until rejection. After drilling through fresh-water aquifers in the upper section, surface casing is set and cement is circulated to the surface up the annulus between the surface casing on one side and exposed formations and conductor casing on the other. Typically the surface casing is set at the top or slightly into the cap rock. Intermediate casing is set through the cap rock and from 100 to 500 ft into the top of the salt. Intermediate casing is used to isolate lost-circulation zones that commonly occur in the cap rock. Two intermediate casing strings may be cemented through the cap rock where lost-circulation zones cause severe problems. The intermediate casing is set at a depth in salt sufficient to ensure a good cement-formation bond. Salt-saturated muds are used when drilling into salt. Similarly, intermediate casing is cemented

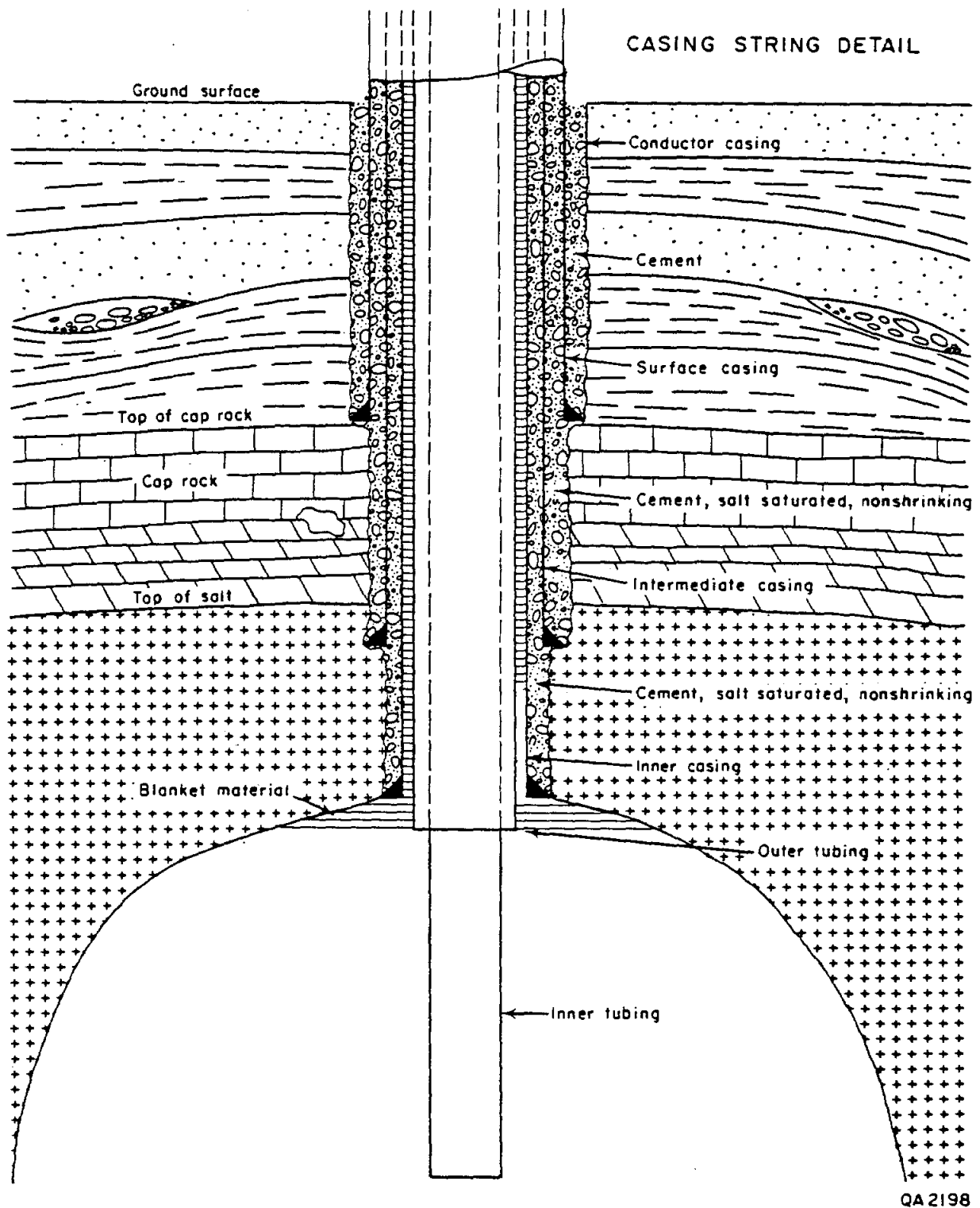


Figure 3. Typical casing string detail for solution-mined cavern in salt (after Fenix and Scisson, 1976a).

with specialized salt-saturated and nonshrinking cements. Clearly, a secure cement-formation bond is critical for cavern integrity. Cement is circulated to the surface.

Inner or Product casing is set if the depth of the top of the cavern is significantly deeper than the bottom of the intermediate casing. Again, salt-saturated, nonshrinking cements are circulated at least to the intermediate casing and preferably to the surface.

Salt-Dissolution Process

Two processes--diffusion and circulation--cause salt to dissolve. Diffusion is the ionic movement of Na^+ and Cl^- ions away from the salt face toward regions of lower ionic pressure in the water. This process is very slow and is not considered the primary mechanism of cavern formation (Bays, 1963). In contrast, circulation implies mass movement of unsaturated fluid to the salt face. The saturation can then be increased as circulation brings additional unsaturated fluid to the salt face. Low-pressure jetting techniques (Van Fossan and Prosser, 1949) are used to create a predictable circulation pattern.

Temperature, gravity, and pressure all influence the circulation process. Thermal convection of the brine within the cavern is due to temperature differences between cold, dense injection water and hotter, stabilized cavity water. Thermal convection is actually a gravity phenomenon of short duration. Temperature and circulation equilibria are achieved within 24 to 72 hours in a stable cavern (Bays, 1963). Gravity is the most important factor controlling fluid movement within a cavern. Injected fresh waters are lighter than brines that are saturated. Thus, injected waters will rise through the brines. Fluids at the base of the cavern are nearly saturated, and fluids at the top of a cavity are rarely more than 10 to 15 percent saturated and may be essentially fresh. Pressure gradients imposed by brine-lift pumps also cause circulation within a cavern. However, as cavern size increases, the circulation effects of pressure differentials become insignificant (Bays, 1963).

Blanket Material and Function

The blanket is inert material at the top of the cavern. The main function of the blanket is preventing unwanted salt dissolution at the top of the cavern around the casing seat. The blanket also prevents corrosion of the product casing. Many materials have been used as blankets including air, diesel oil, crude oil, butane, propane, and natural gas. The blanket must be lighter than water and must not dissolve salt. The blanket material is injected in the annulus between the last or innermost casing string and the outermost wash or blanket tubing. Thus brine is prevented from contacting the casing seat.

Raising or lowering the blanket tubing controls the position of the blanket. The location of the blanket can locally produce a desired cavern shape by dictating where dissolution is allowed to take place. This technique is typically used at the beginning and end of cavern construction, first to wash the sump and finally to dome the cavern roof. A sump is produced at the bottom of the borehole by using a long blanket tubing to depress leaching to the base of the hole. Once the cavern has been leached, blanket control can shape the cavern roof into a dome or arch for added stability. By periodically withdrawing the blanket tubing and raising the level of the blanket during a wash cycle, a flat roof is progressively shaped into a domed or arched roof.

Sump

A sump or local depression is mined at the bottom of solution caverns to collect the relatively insoluble constituents of salt domes that remain after the salt is dissolved and removed (fig. 4). A typical Gulf Coast salt dome contains from 1 to 10 percent anhydrite, which is the chief insoluble mineral. Country rock, sandstone, and shale are insoluble constituents that may be encountered in the salt stock. These insoluble materials generally become more abundant as the periphery of the salt stock is approached. The volume of the

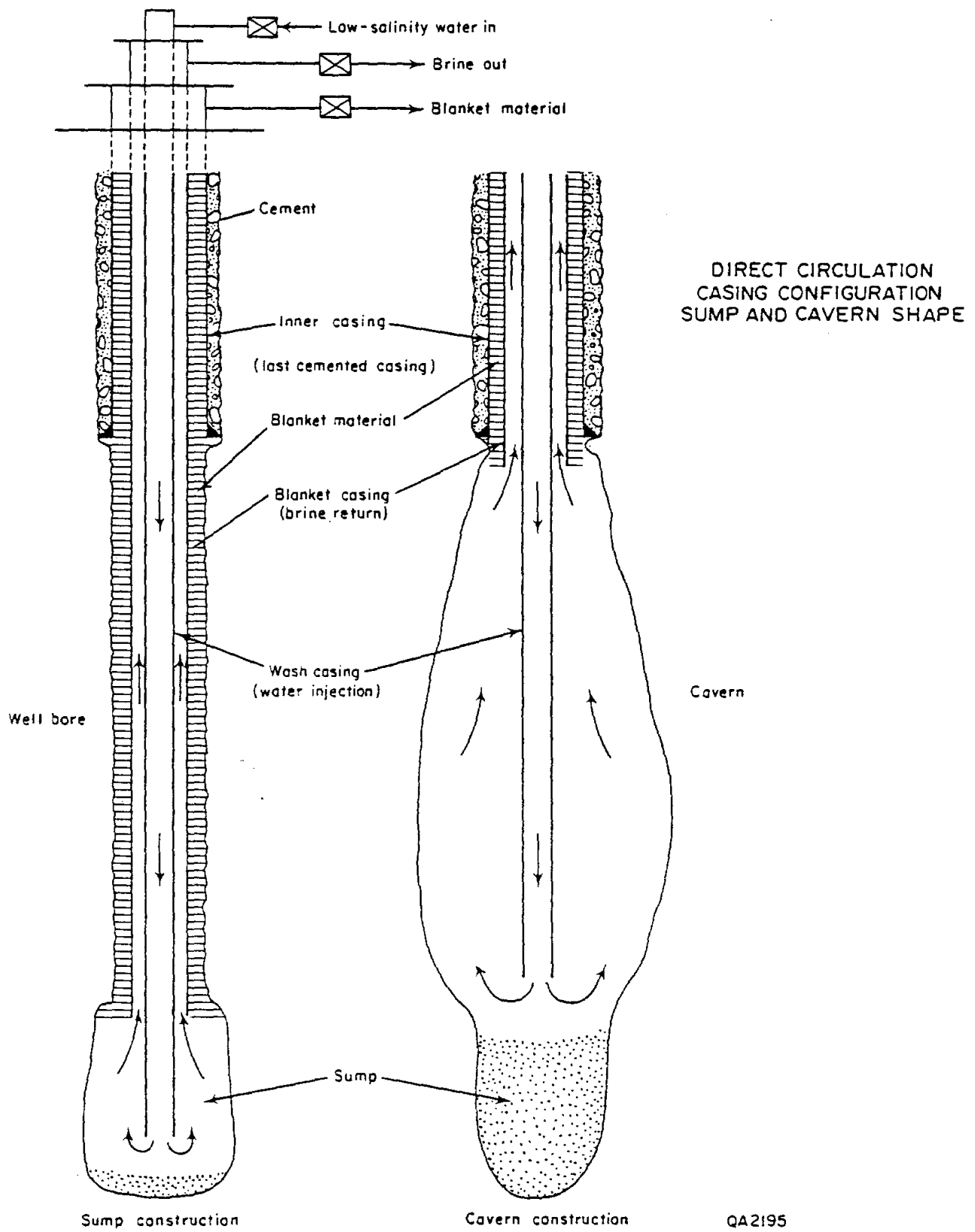


Figure 4. Casing configuration for direct circulation (after Fenix and Scisson, 1976a).

sump is dictated by the volume of the cavern and by the insoluble percentage. A core of the salt mass is normally used to determine percentage of insoluble constituents.

CAVERN GEOMETRY

The two basic techniques to control the shape of the caverns are direct circulation and reverse circulation. The techniques are differentiated by the location of the fresh-water injection and brine-return tubing within the cavern. Additionally the thickness and location of the blanket controls cavern shape during the initial and final stages of cavern mining. Final cavern shape is also influenced by variables that cannot be controlled. Such variables include salt-stock inhomogeneities, percentage and distribution of insoluble constituents, salt solubility, and space limitations with respect to the edge of the salt stock, property lines, or adjacent caverns.

Caverns that were solution mined for storage are typically leached with direct circulation, whereas brining operations typically use reverse circulation. The leaching technique for a single cavern may vary with time to adjust to changing uses or to modify original cavern shapes. The leaching technique is an important factor in cavern stability because each technique produces a "typical" shape. Clearly cavern stability is, in part, a function of cavern shape (Fossum, 1976).

Direct Circulation

A cavern is leached by direct circulation when fresh or low-salinity water is injected down the wash tubing and exits near the base of the cavern (fig. 4). Brine is returned up the annulus between the wash tubing and blanket casing located near the top of the cavern. The freshest water enters the system near the base of the cavern; thus, most of the dissolution is concentrated there. A pressure differential between the injection and brine return helps drive the progressively more saline water upward toward the brine return point. Characteristically

with direct circulation, the discharged brine is less saturated with Na^+ and Cl^- than is the brine discharged during reverse circulation.

A cavern formed by direct circulation is typically tear-drop shaped because fresh water is injected at the base of the cavern and the brine is returned at the top. Cavern geometries after phased expansion using direct circulation are shown in figure 5.

Reverse Circulation

A cavern is leached by reverse circulation when fresh water is injected down the annulus between the blanket casing and the wash tubing. The fresh-water injection point is at the top of the cavern. The brine returns up the wash tubing for which the opening is located near the base of the cavern (fig. 6). The typical geometry of a cavern leached by reverse circulation is "flower pot" with a characteristically broad and flat roof. Density differences between fresh water at the top and brine at the base allow brine to sink toward the base of the cavern. The lighter fresh injection water is forced to circulate near the top of the cavern, thus forming the broad cavern roof. With increasing dissolution, the fresh water becomes denser and sinks toward the base of the cavern.

Brining operations favor leaching by reverse circulation because operating costs are lessened as only the densest brines are produced at the base of the cavern. Less wash water is required per volume of produced brine than for direct circulation, which typically produces brines that are less dense. Careful blanket control is often used to shape the flat roof into the arch. This process adds stability and lessens the probability of roof caving.

Modified Circulation

Caverns may also be mined with modified circulation in which leach conditions are modified during the formation of the cavern. For instance, a sump may be formed by direct circulation; then the rest of the cavern is formed by reverse circulation by raising the wash casing and reversing the position of the fresh-water injection and brine return. Similarly,

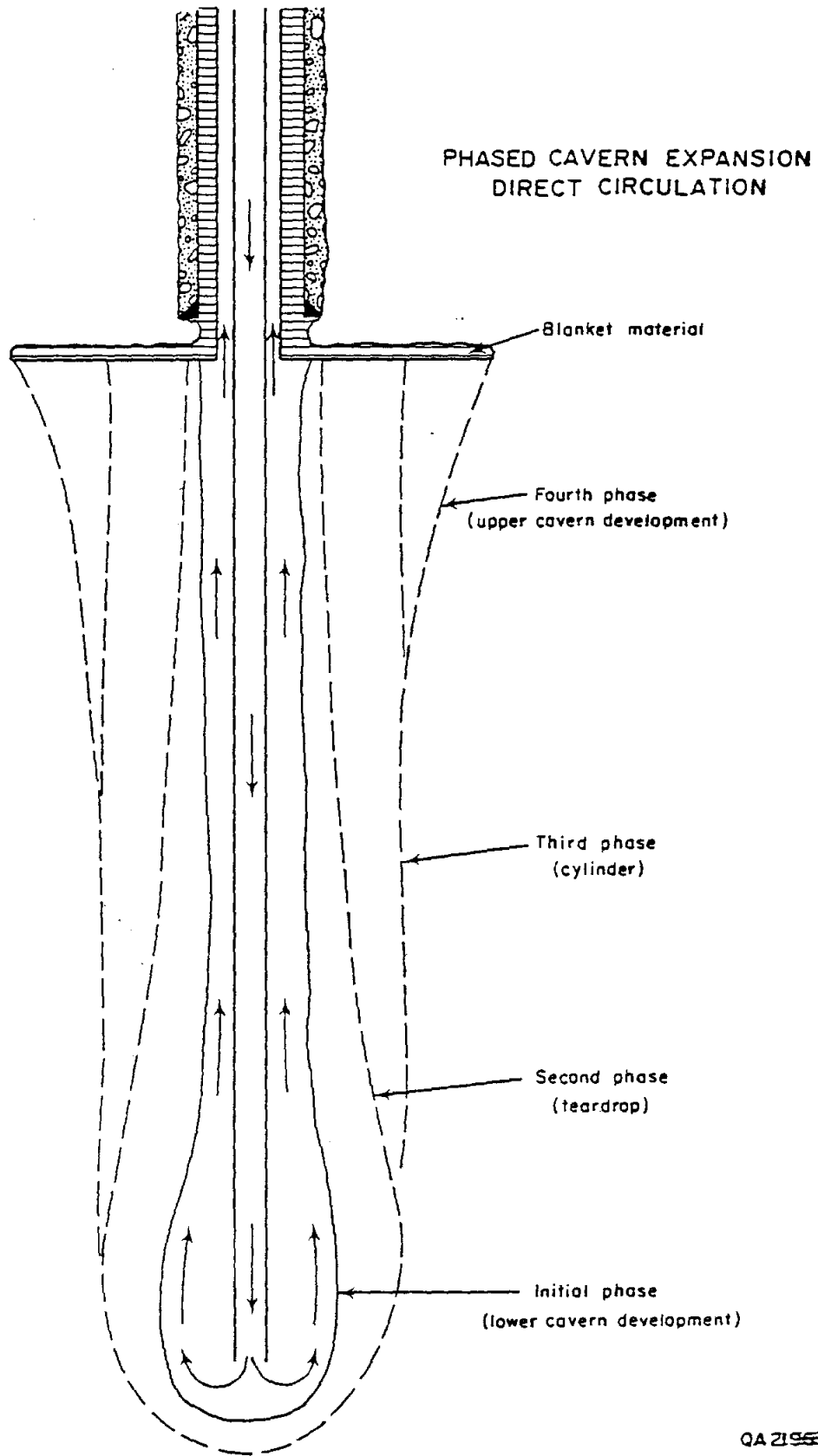
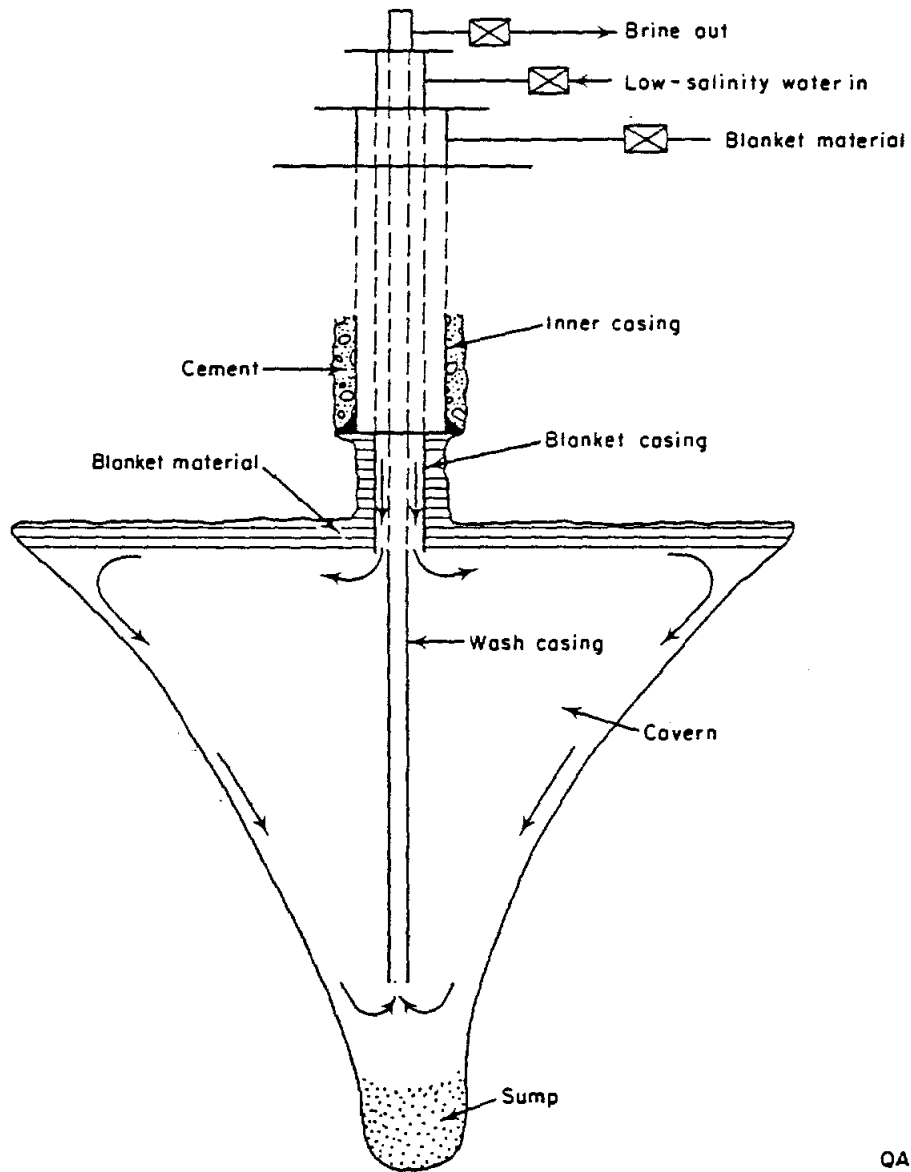


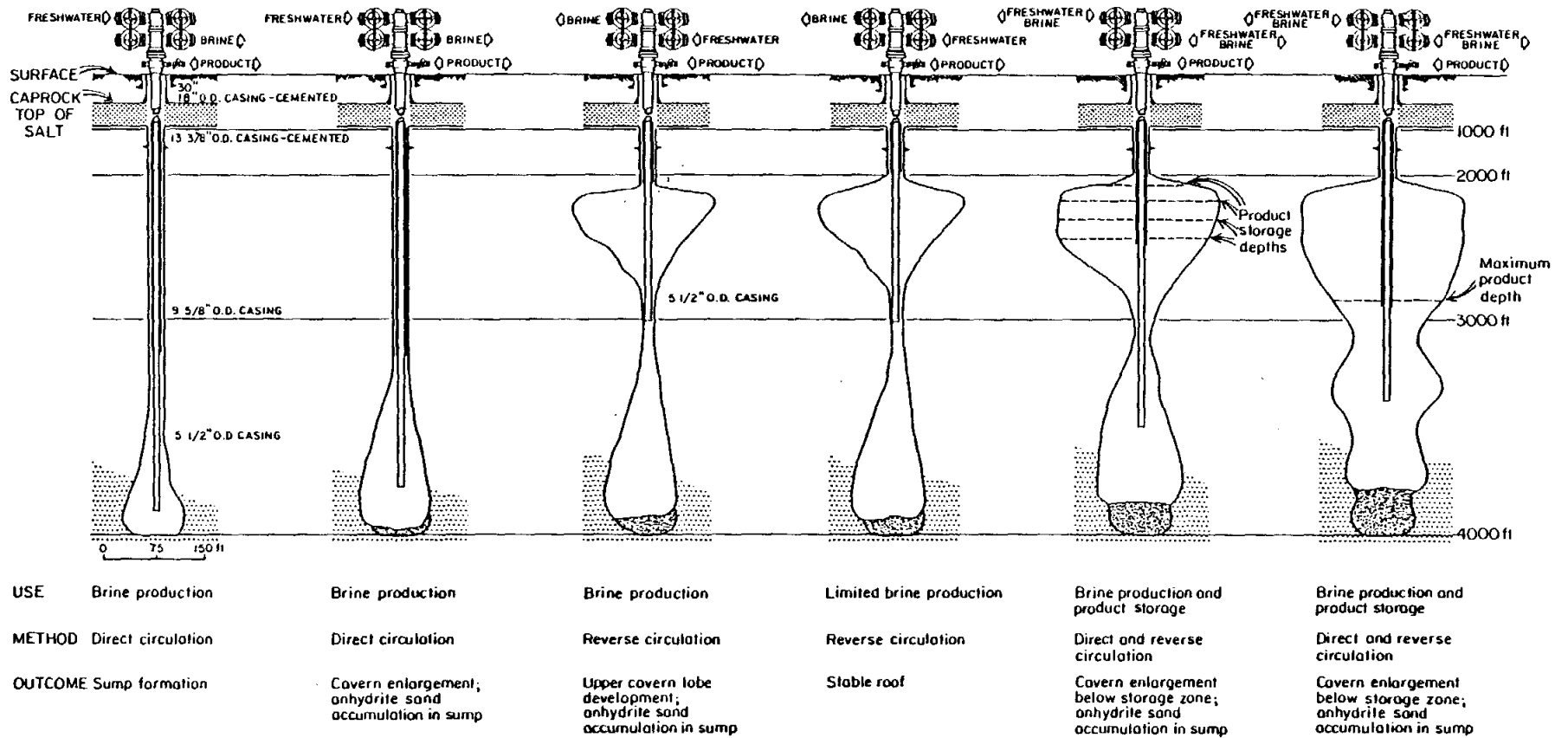
Figure 5. Phased expansion of solution cavern with direct circulation (after Fenix and Scisson, 1976a).

REVERSE CIRCULATION
CASING CONFIGURATION AND
CAVERN SHAPE



QA 2197

Figure 6. Casing configuration for reverse circulation (after Fenix and Scisson, 1976a).



QA-2215

Figure 7. Evolution of brine and storage caverns, Pierce Junction salt dome (after Minihan and Querio, 1973).

changes in the use of a cavern may dictate modifications in the leach technique. Figure 7 shows a cavern that initially was a brine cavern and then was used simultaneously for brine production and product storage (Minihan and Querio, 1973). Clearly, by varying the positions of the blanket strings and wash tubing and switching injection and return points, new cavern geometries were created that facilitated new uses of the dome.

CAVERN FAILURES

At least 10 solution caverns in Texas salt domes have failed. Failure is here defined as the loss of integrity of an individual cavern. Storage caverns (in contrast to brine caverns) have also failed in salt domes in Louisiana and Mississippi (Science Applications, Inc., 1977). The consequences of failure of a storage cavern are much greater than failure of a brine production cavern because of the value of the product that is lost and the cost of abatement procedures. Brine caverns show a much greater failure rate than do storage caverns. However, many brine caverns have been converted to storage caverns. Thus, any consideration of the stability of storage caverns must include brine caverns as well.

Three types of known cavern failures in Texas include (1) loss of stored products, (2) surface collapse, and (3) cavern coalescence. Table 1 lists cavern failures, possible mechanisms, and consequences.

There are approximately 254 caverns in Texas salt domes. On the basis of failure of 10 modern caverns (post-1946), the probability (p) of failure of a given cavern is approximately 4 percent ($p=0.039$). Statistics based on the years of cavern operation also yield indications of the useful life of a cavern. Railroad Commission of Texas permits indicate that the 254 Texas caverns have a cumulative operational history of 4,717 cavern-years. With 10 failures, the average operational life of an individual cavern is 472 years.

Two cavern failures in Texas salt domes resulted in catastrophic loss of liquid petroleum gas (LPG) at Barbers Hill salt dome in 1980 and at Blue Ridge salt dome in 1974. The failure of a storage cavern at Barbers Hill salt dome released LPG into subsurface formations below the

Table 1. List of salt domes with cavern failures, mechanisms, and consequences.

Failure mechanism	Dome	Storage cavern	Brine-well cavern	Rock-salt mine	Comments
Closure	Eminence salt dome, Mississippi	Natural gas storage cavern			Eminence salt dome--very deep cavern, depth 5,700 to 6,700 ft; cavern closure up to 40 percent in first year; cavern bottom rose 120 ft; closure related to rapid pressure declines used to produce natural gas (i.e., cavern is operated "dry" without brine).
				No data--creep closure probably common	
					Minor problem with creep-related closure and creep rupture of walls and roof
Loss of integrity	Barbers Hill salt dome, Texas	LPG storage cavern			Barbers Hill salt dome--catastrophic loss of LPG in 1980; LPG lost to subsurface formations, and at surface over dome; town of Mount Belvieu evacuated; problem inferred to be casing seat failure.
	Blue Ridge salt dome, Texas	LPG storage cavern			Blue Ridge salt dome--catastrophic loss of LPG in 1974; LPG lost to subsurface formations and at surface over dome; minor flash fire--explosion injured 4 workmen during utility construction; RRC ordered cavern plugged and abandoned.
			Common		
				Not applicable	

Table 1. List of salt domes with cavern failures, mechanisms, and consequences (cont.).

Coalescence	Pierce Junction salt dome, Texas	5 LPG storage caverns comprise 2 multicavern systems		Pierce Junction salt dome--timing of coalescence is not known; caverns previously were brine producers; caverns currently used for LPG storage.
	Bayou Choctaw salt dome, Louisiana		3 brine caverns coalesced	Caverns abandoned.
	Sulfur Mines salt dome, Louisiana		3 brine caverns coalesced	Caverns abandoned.
Not applicable				
Surface collapse	Palestine salt dome, Texas		16 collapse structures at surface over dome	Historic brine-well operations from 1904-1937 resulted in very common surface collapse over old brine wells; 3 collapse structures formed since 1937.
	Grand Saline salt dome, Texas		1 collapse structure	Collapse occurred in 1976 over probable brine well.
	Blue Ridge salt dome, Texas		1 collapse structure	Collapse occurred in 1949 at brine well that formerly was a rock-salt mine.
	Bayou Choctaw salt dome, Louisiana		1 collapse structure	Collapse occurred in 1954 over brine well; water-filled sinkhole.
	Jefferson Island salt dome, Louisiana			Major disaster--mine flooded and abandoned Oil-drilling rig probably breached mine opening; Lake Peigneur flooded into mine; disaster occurred 1980.

Table 1. List of salt domes with cavern failures, mechanisms, and consequences (cont.).

	Belle Island salt dome, Louisiana	Major disaster-- mine flooded and abandoned	Water leak around mine shaft resulted in surface collapse in 1973.
Other	Winnfield salt dome, Louisiana	Major disaster-- mine flooded and abandoned	Water leak issuing from mine wall flooded mine in 1965; water sand at cap-rock-salt- stock interface is inferred source of water.

city of Mount Belvieu (Underground Resource Management, 1982), causing evacuation of the residents. The Warren Petroleum Co. assumed financial responsibility for the abatement and monitoring program. Over 400 shallow relief wells were drilled to vent the escaped LPG (Underground Resource Management, 1982). Although the Warren Petroleum Co. has not made public the cause of the leak, a failure in the casing seat is suspected. The defective cavern has since been returned to service after remedial work on the casing resulted in a successful integrity test.

Failure of a storage cavern at Blue Ridge salt dome also resulted in the escape of LPG. Four workmen installing a utility conduit were injured in an explosion and flash fire suspected to have been caused by leaking LPG. At that time, the cavern was owned by Amoco and used by Coastal States to store LPG. In 1975 the Railroad Commission of Texas issued special order 03-64,673, rescinding the authority to store LPG in that cavern (RRC Authority Number 03-34,658). That cavern is now abandoned. Figure 8 is a cross section of the upper part of Blue Ridge salt dome showing dome shape and the location and geometry of the salt mine and cavern.

Failure of brine caverns at Grand Saline, Blue Ridge, and Palestine salt domes have caused localized surface collapse. Sixteen collapse structures mar the surface above Palestine salt dome and are attributed to historic brine production (Fogg and Kreitler, 1980). The brine caverns that collapsed at Palestine salt dome have not been included in the statistics of cavern failures because those caverns were constructed with no regard for their stability, and construction techniques pre-date modern practices beginning in the late 1940's and 1950's.

From 1904 to 1937, Palestine Salt and Coal Company used brine wells to produce salt from Palestine salt dome. The collapse structures form circular water-filled depressions with diameters of 27 to 105 ft and depths of 2 to 15 ft (Fogg and Kreitler, 1980). Each collapse structure is assumed to mark the location of a former brine well. Powers (1926) described the brine operation as follows: Wells were drilled 100 to 250 ft into salt. Water from the "water sand" between the cap rock and the salt stock flowed into the well, dissolved the salt, and brine

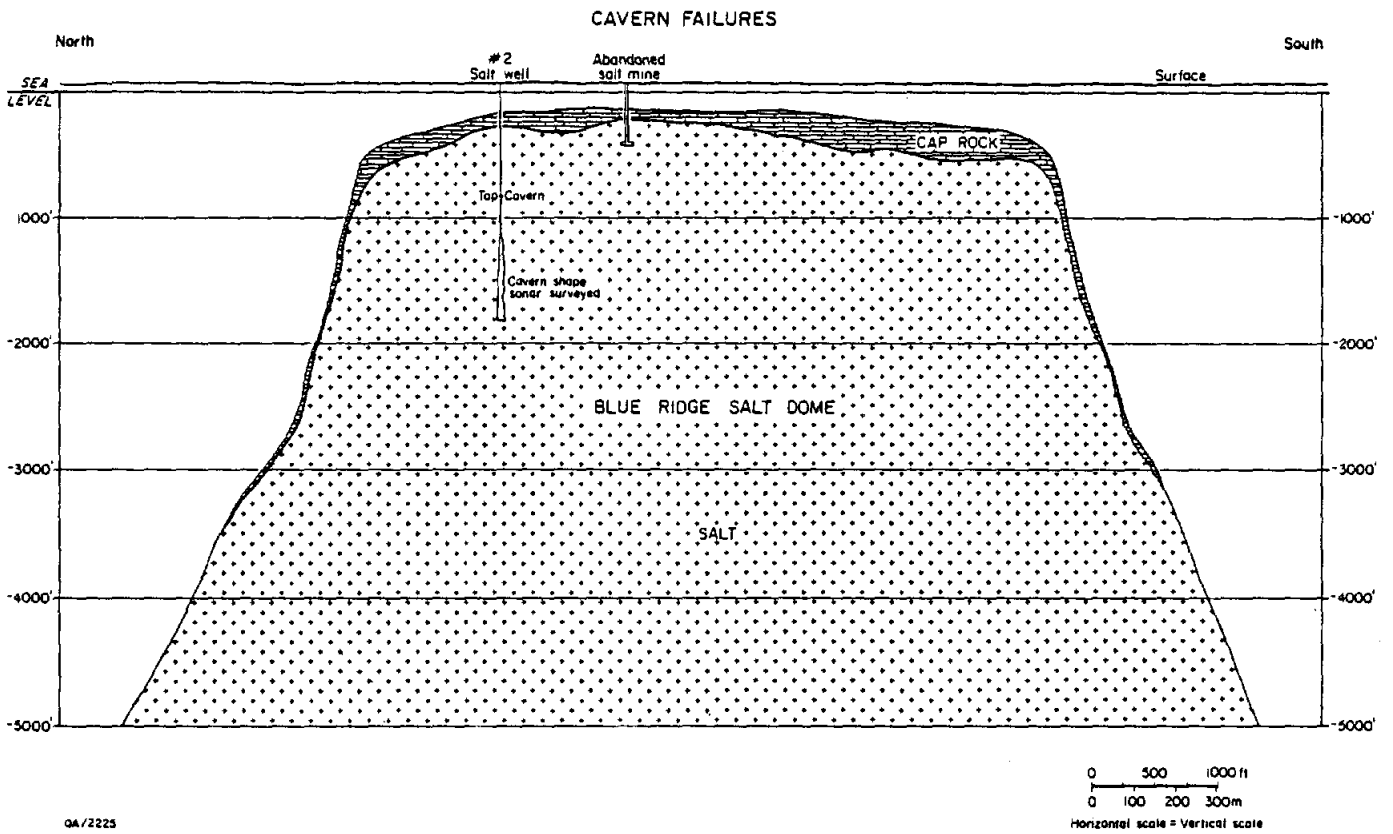


Figure 8. Cross section of Blue Ridge salt dome showing geometry of salt mine and storage cavern that failed.

was then displaced by compressed air. The cap rock was undermined by the large brine cavern below it. The cap rock eventually collapsed forming a large sinkhole (Hopkins, 1917). A new brine well was simply offset a safe distance. Although brining operations ceased in 1937, three collapsed structures have formed since 1978 (Fogg and Kreitler, 1980).

In 1975, a circular collapse structure formed at Grand Saline, Texas. Although the exact origin is unknown, the collapse structure is inferred to overlie an old brine production well (Martinez and others, 1976; Science Applications, Inc., 1977). In 1949, a spectacular collapse occurred at Blue Ridge salt dome (Science Applications, Inc., 1977). An old rock-salt mine operated by Gulf Salt Co. had been converted into a brine production well. Without warning, the main building and well assembly collapsed around the original mine shaft and well bore. The brine cavern is inferred to have dissolved to the cap rock. A "water sand" composed of loose anhydrite grains at the cap-rock - salt-stock interface may have contributed water to help undermine the cap rock. The cap rock and overlying strata then collapsed into the brine cavity after removal of too much underlying support.

Railroad Commission of Texas records (Authority Number 03-60,093) indicate that five former brine caverns at Pierce Junction salt dome have coalesced to form two independent caverns. These caverns currently are used as storage caverns. When the caverns coalesced is unknown. Although five individual caverns have coalesced, integrity within each of the two multicavern systems has been maintained.

Conspicuous examples of cavern failures and surface collapses have been reported in Louisiana and Mississippi (Science Applications, Inc., 1977; Griswold, 1981; Fenix and Scisson, 1976b). One brine cavern has collapsed and formed a water-filled sinkhole at the surface over Bayou Choctaw salt dome (Science Applications, Inc., 1977). Two other caverns at Bayou Choctaw are abandoned because the caverns have dissolved to the cap rock. Three additional caverns, separated by at least 200 ft of pillar salt in plan, are now hydraulically connected (Griswold, 1981; Fenix and Scisson, 1976b). Rock-salt mines have also failed by flooding at Winnfield, Avery Island, and Jefferson Island salt domes. A jet of water issuing from a mine

wall caused the flooding and abandonment of Winnfield mine in 1965 (Martinez and others, 1976).

The Jefferson Island disaster of 1980 is an instructive example of the consequences of possible inadvertent breach into a mined opening in salt (Autin, 1984). Diamond Salt Company was operating a rock salt mine at Jefferson Island salt dome when a Texaco oil exploration rig (spudded from a barge in Lake Peigneur) was searching for flank oil production in sandstone pinch-outs near the salt stock. The chain of events that led to the draining of Lake Peigneur into the salt mine is paraphrased here on the basis of a description of the event by Autin (1984).

During the morning of the disaster, the Texaco drill bit became stuck in the hole at a depth of 1,245 ft, and mud circulation was lost. Efforts to free the bit and reestablish mud circulation failed. The drill rig began to tilt and rapidly overturned. Within 3 hours the drill rig, the support barge, and Lake Peigneur all disappeared down into a rapidly developing sinkhole. At approximately the same time, the 1,300-ft-level of the mine was flooded. All mine personnel were evacuated safely.

Mechanisms of Cavern Failure

Most cavern failures result from integrity loss at the casing seat. Cavern coalescence is another common mode of cavern failure, especially with brine caverns. The casing system is vulnerable at zones of lost circulation during cavern construction and during product cycling. Clearly, the cemented zone, production tubing, and casing strings are the weak link in any cavern system because many problems that begin there can quickly evolve into severe problems, including eventual cavern collapse.

Blanket control protects salt from being dissolved behind the casing seat. This dissolution, if left unchecked, can lead to loss of the casing seat, loss of tubing, and eventual cavern collapse.

Another point of attack on the integrity of a cavern system is within the cap rock. The cap rocks of many salt domes are characterized by lost-circulation zones. These zones compose vuggy areas with open caverns up to tens of feet in vertical extent. The vuggy zones are concentrated in the transition and anhydrite zones of the cap rock. Many cap rocks also contain

a zone of loose anhydrite sand at the cap-rock - salt-stock interface. Presence of this zone at the cap-rock - salt-stock interface is critical because it indicates active salt dissolution with the accumulation of loose anhydrite sand as a residuum and the presence of an active brine-circulation system.

Lost-circulation zones weaken the integrity of any cavern system in two ways. During drilling, the difficulty of maintaining mud circulation forces the use of many circulation-control measures. Drilling may continue "blind," that is without mud returns, until salt is encountered. Then a temporary liner is set through the lost-circulation zone. Alternatively, cement may be pumped down the tubing to plug the lost-circulation zone. The cement is then drilled out, and if circulation is lost again the process is repeated until circulation is reestablished.

Even with modern drilling techniques, lost-circulation zones can cause problems severe enough to force hole abandonment. In 1974, a hole was lost while drilling a gas-storage well at Bethel salt dome (RRC Authority Number 06-05,840). Circulation was lost within the cap rock and was not reestablished even though 1,300 sacks and 80 yd³ of cement were added. Ground subsidence then caused the rig to tilt, and the hole was abandoned.

Vuggy zones in cap rock are areas of natural cap-rock and salt dissolution. Therefore cement-formation bonds are vulnerable to attack by natural dissolution. The natural brine-circulation system also may attack the cement itself and reduce its useful life. The brine is very corrosive, and its long-term effects on cements and casings are inadequately known.

Van Fossan (1979) has listed various mechanisms whereby product loss may occur through loss of cavern integrity.

SALT-DOME RESOURCES

Valuable natural resources are associated with the salt stock, cap rock, and favorable geological structures and reservoirs associated with the growth and emplacement of the dome. Dome salt is an important chemical feedstock. Salt is extracted both by underground mines and by solution-brine wells. Storage space, available in cavities formed by brining operations, was

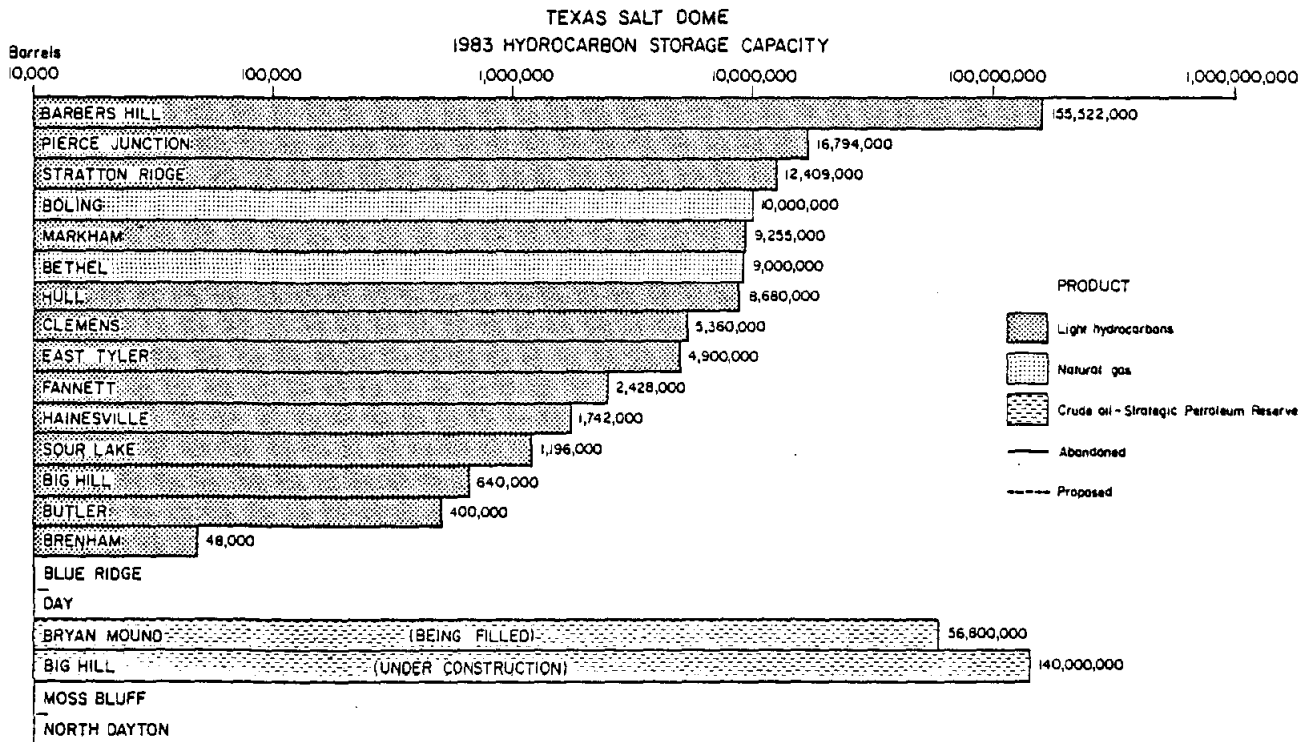
initially an unrecognized resource, but now many cavities in domes are created exclusively for storage space and the brine is discarded. The cap rock is quarried as a source of road metal, and cap-rock sulfur is mined by the Frasch process. Petroleum in salt-dome-related traps is by far the most valuable salt-dome-related resource.

The long-term trends for petroleum and sulfur production are in decline owing to depleted reserves and few new discoveries. Salt production is stable to slightly growing, but production is constrained by demand. Demand for storage space is growing rapidly especially with the requirements of the Strategic Petroleum Reserve (Fenix and Scisson, 1976b, c, d; U.S. Federal Energy Administration, 1977a, b, c; Hart and others, 1981). Conceivably, the storage space within a dome may be the most valuable salt-dome-related resource.

Salt-Dome Storage

Texas is the national leader in storage capacity for hydrocarbons in salt domes. In 1983, Texas salt domes housed 47 percent of the nation's total stored light hydrocarbons (liquified petroleum gas, or LPG). Texas salt domes are also becoming a major repository for the Strategic Petroleum Reserve (SPR) (fig. 9). Crude oil for the SPR is currently being stored at Bryan Mound salt dome, and additional storage capacity is under construction at Big Hill salt dome (Hart and others, 1981). Storage of toxic-chemical waste in solution-mined caverns is also being considered at Boling salt dome (United Resource Recovery, 1983).

The most common hydrocarbons stored in Texas salt domes are light hydrocarbons, natural gas, and crude oil. Rarely fuel oil may be stored near a plant to generate power during a gas curtailment. Light hydrocarbons, such as ethane, propane, butane, and isobutane, comprise the bulk of stored products. They are gases under atmospheric pressure and room temperature, but are liquids under the slight confining pressure. Light hydrocarbons were the first products stored in salt-dome caverns because the demand for the products was strongly cyclical with the seasons. In 1983, approximately 219,464,000 barrels of light hydrocarbons were stored in Texas



GA/2218

Figure 9. Histogram of 1983 storage capacity in Texas salt domes and proposed Strategic Petroleum Reserve caverns.

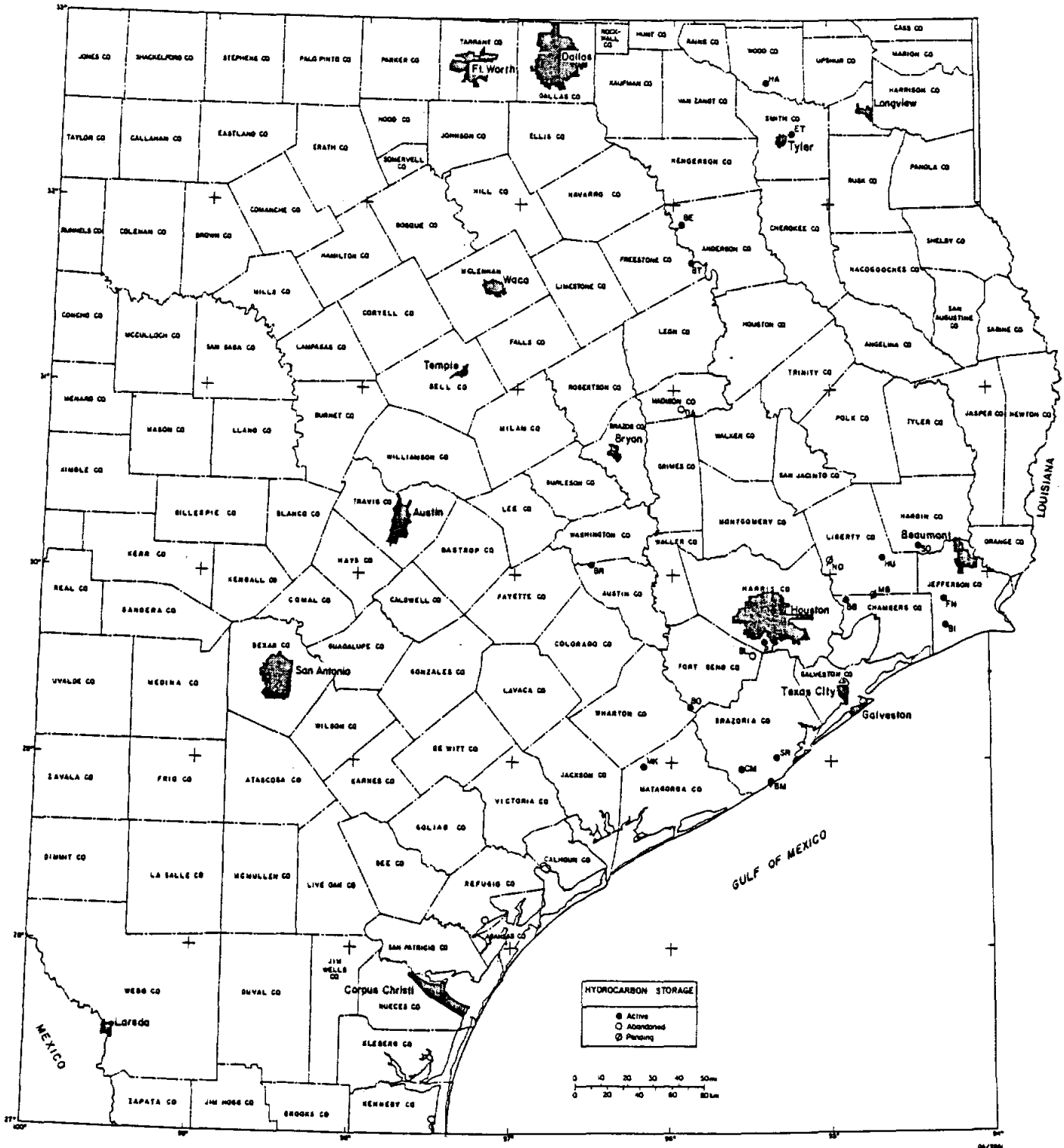
salt domes (Gas Processors Association, 1983). Of hydrocarbons, 77 percent is in salt domes, and the r

Whether a dome is a good candidate for storage near industrial suppliers and pipelines. Geologic criteria primarily to obtain site information for casing dome size and cap-rock-lost-circulation zones were dealt with and not as site selection criteria. For and pending storage facilities. Table 2 is a list history of hydrocarbon storage.

Barbers Hill salt dome houses the greatest concentration of storage facilities in the world. Nine separate companies store light hydrocarbons in the dome. The 1983 capacity for light hydrocarbons storage at Barbers Hill salt dome was 155,522,000 barrels (Gas Processors Association, 1983). There are approximately 137 caverns in Barbers Hill salt dome.

Congress in 1975 passed the Energy Policy and Conservation Act, which established the Strategic Petroleum Reserve to protect the nation against future oil supply interruptions. The size of the reserve was expanded to 1 billion barrels by President Carter's National Energy Plan. Crude oil for the SPR is currently being stored in preexisting brine caverns at Bryan Mound salt dome, and new caverns are being constructed at Big Hill salt dome.

Present capacity at Bryan Mound salt dome is 56.8 million barrels in four caverns originally mined for brine. Figures 11 and 12 are cross sections of the dome showing the geometries and locations of the caverns. Their irregular shape is typical of caverns originally mined for brine. Projections include construction of an additional 120 million barrels of storage space at Bryan Mound salt dome. Cavern construction for the SPR is underway at Big Hill salt dome. Fourteen caverns will be constructed, each with a capacity of 10 million barrels. Figures 13 and 14 are cross sections showing the proposed geometries and locations of the SPR caverns at Big Hill salt dome and the location and geometry of a storage cavern used by Union Oil Co. to store light hydrocarbons.



HYDROCARBON STORAGE IN SALT DOMES OF TEXAS

Figure 10. Map of salt domes showing active, abandoned, and pending storage facilities.

(continued)

Figure 10 (cont.).

Code	Dome Name	County
BB	Barbers Hill	Chambers
BE	Bethel	Anderson
BI	Big Hill	Jefferson
BL	Blue Ridge	Fort Bend
BO	Boling	Wharton/Fort Bend
BR	Brenham	Austin/Washington
BM	Bryan Mound	Brazoria
BT	Butler	Freestone
CM	Clemens	Brazoria
DA	Day	Madison
ET	East Tyler	Smith
FN	Fannett	Jefferson
HA	Hainesville	Wood
HU	Hull	Liberty
MK	Markham	Matagorda
MB	Moss Bluff	Chambers/Liberty
ND	North Dayton	Liberty
PJ	Pierce Junction	Harris
SO	Sour Lake	Hardin
SR	Stratton Ridge	Brazoria

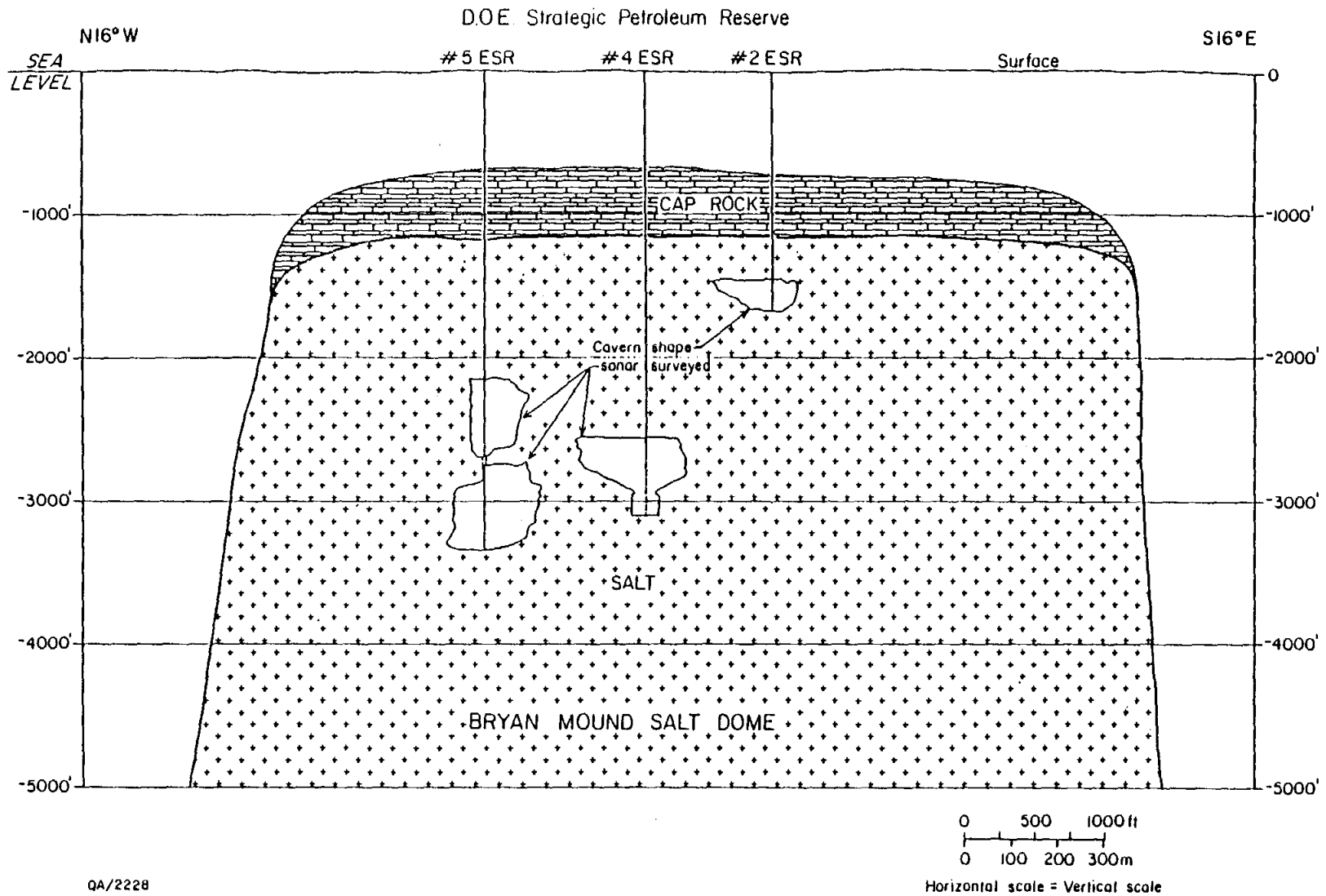


Figure 11. Cross section of Bryan Mound salt dome (north-south) showing geometry of present Strategic Petroleum Reserve caverns.

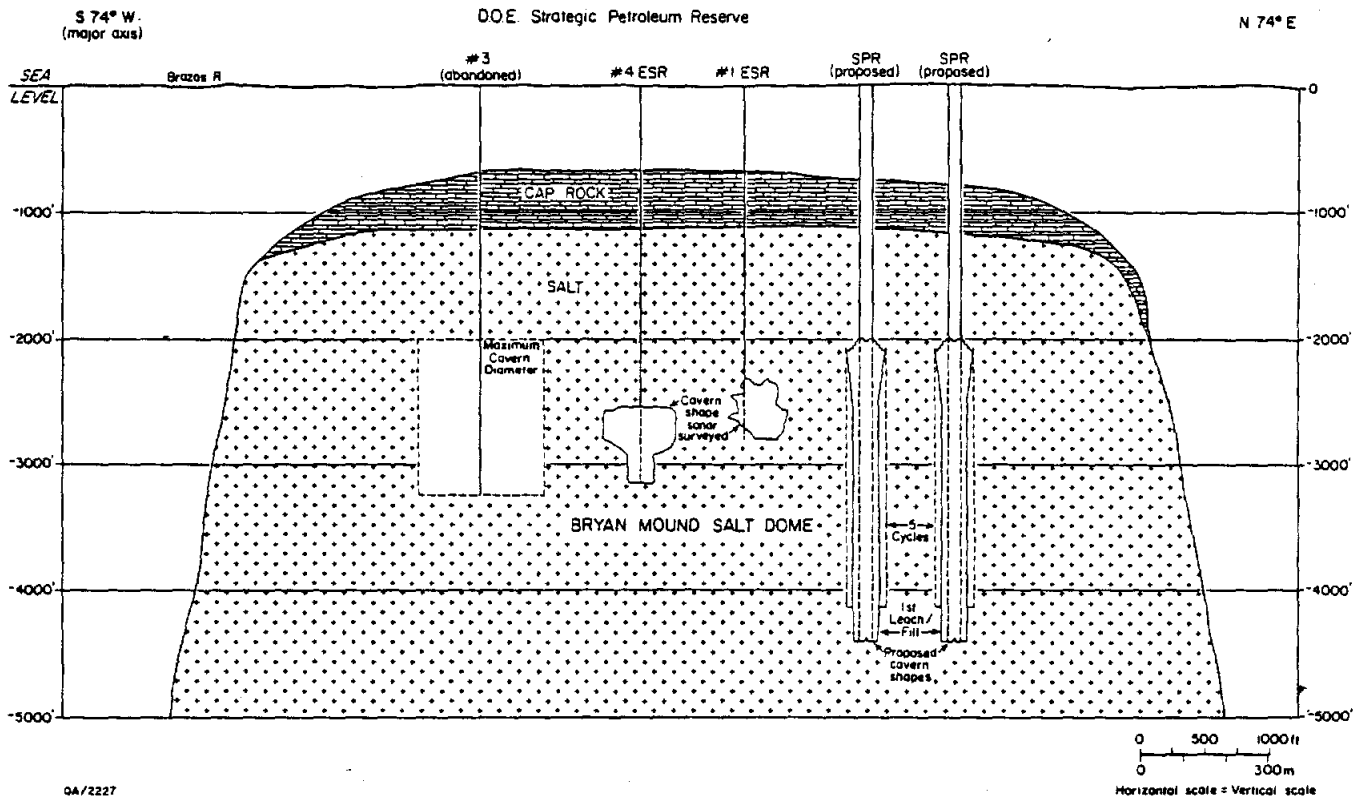


Figure 12. Cross section of Bryan Mound salt dome (east-west) showing geometry of present and proposed Strategic Petroleum Reserve caverns.

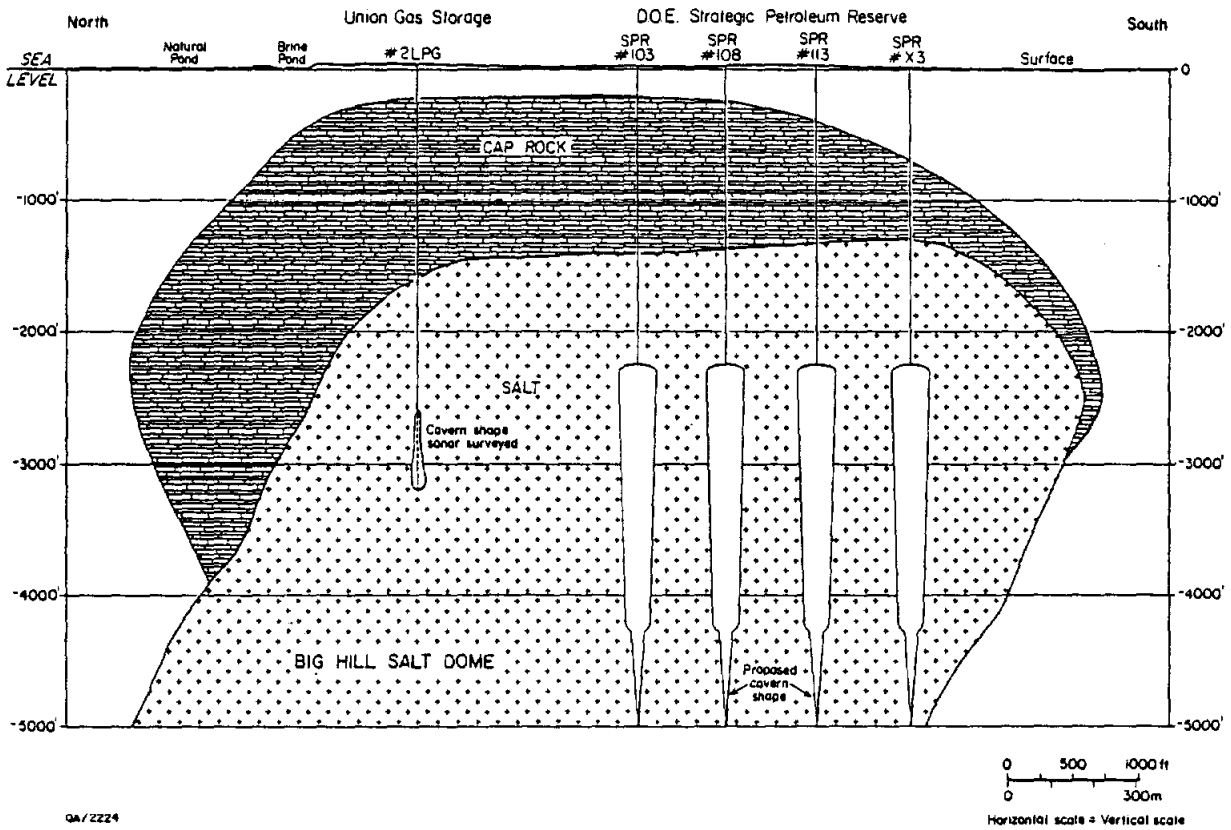


Figure 13. Cross section of Big Hill salt dome (north-south) showing geometry of proposed Strategic Petroleum Reserve caverns and Union Oil Co. storage cavern

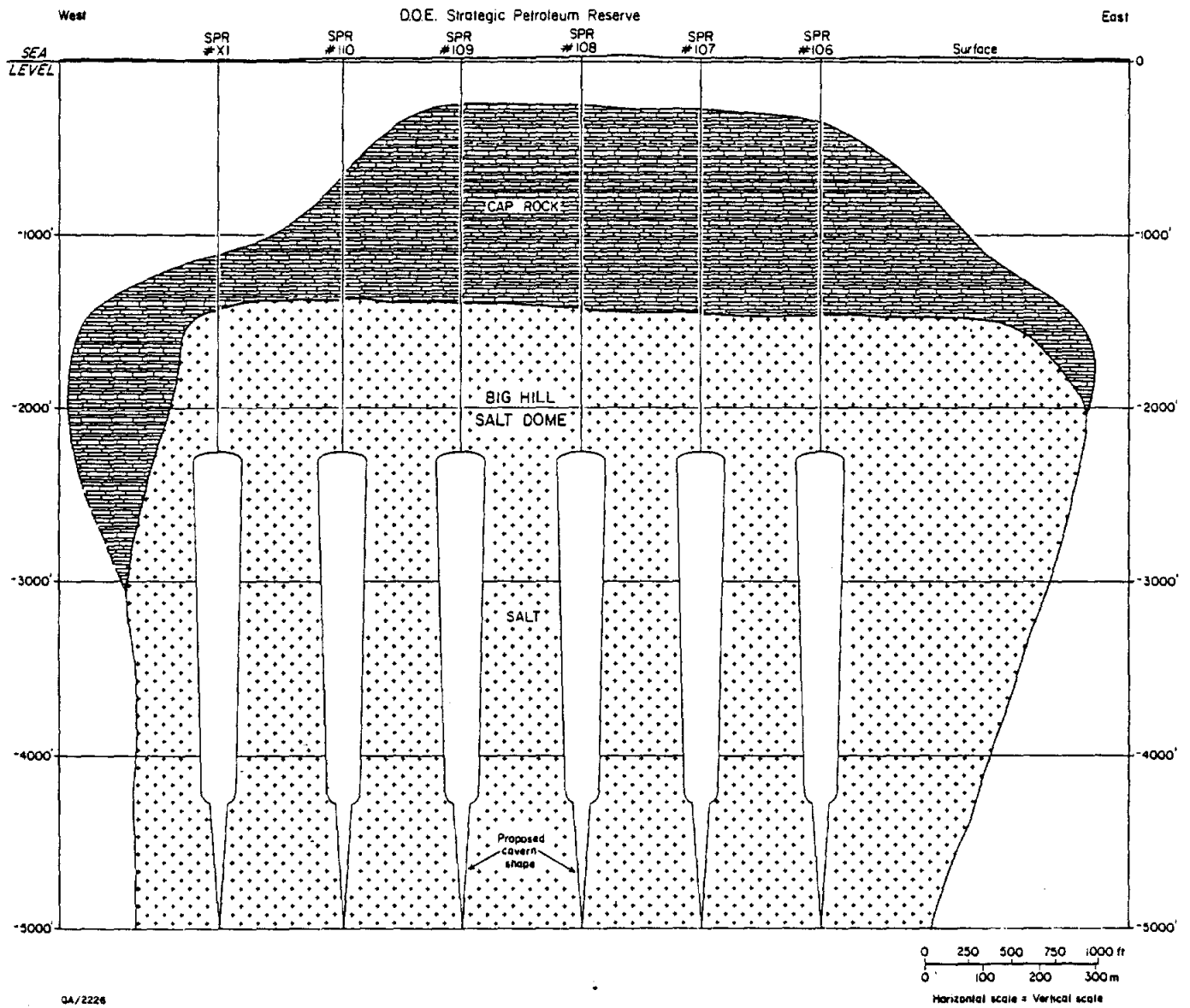


Figure 14. Cross section of Big Hill salt dome (east-west) showing geometry of proposed Strategic Petroleum Reserve caverns.

Table 2. List of salt domes with storage, operating company, Railroad Commission of Texas applicant, number of caverns, capacity, and product stored.

NAME OF SALT DOME	CURRENT OPERATOR OF STORAGE FACILITIES	ORIGINAL APPLICANT	NUMBER OF CAVERNS	STORAGE CAPACITY IN BARRELS	PRODUCT STORED

* BARBERS HILL	TEXAS EASTERN	TEXAS NATURAL GASOLINE	27	30978000	LIGHT HYDROCARBONS
* BARBERS HILL	DIAMOND SHAMROCK	DIAMOND SHAMROCK	10	34700000	LIGHT HYDROCARBONS
* BARBERS HILL	WARREN	WARREN	29	45032000	LIGHT HYDROCARBONS
* BARBERS HILL	X-RAL	X-RAL	16	22065000	LIGHT HYDROCARBONS
* BARBERS HILL	TENNECO	TENNESSEE GAS TRANSMISSION	18	9823000	LIGHT HYDROCARBONS
* BARBERS HILL	EXXON	HUMBLE OIL AND REFINING	7	5710000	LIGHT HYDROCARBONS
* BARBERS HILL	ENTERPRISE	ENTERPRISE	12	13300000	LIGHT HYDROCARBONS
* BARBERS HILL	CONOCO	CONOCO	3	1200000	LIGHT HYDROCARBONS
* BARBERS HILL	ARCO	TEXAS BUTADIENE AND CHEMICAL CORP.	14	4914000	LIGHT HYDROCARBONS
* BETHEL DOME	BI-STONE FUEL	BI-STONE FUEL	3	9000000	NATURAL GAS
* BIG HILL	UNION	PURE OIL CO.	2	640000	LIGHT HYDROCARBONS
* BIG HILL	DEPARTMENT OF ENERGY	DEPARTMENT OF ENERGY	14	0	CRUDE OIL
* BLUE RIDGE	ABANDONED	TULONA-AMOCO	3	0	LIGHT HYDROCARBONS
* BOLING	VALERO	LO-YACA GATHERING CO.	4	10000000	NATURAL GAS
* BRENNHAM	SEMINOLE PIPELINE CO.	SEMINOLE PIPELINE CO.	1	48000	LIGHT HYDROCARBONS
* BRYAN MOUND	DEPARTMENT OF ENERGY	DOW CHEMICAL	4	56300000	CRUDE OIL
* BRYAN MOUND	DEPARTMENT OF ENERGY	DEPARTMENT OF ENERGY	12	0	CRUDE OIL
* BUTLER DOME	U.P.G.	FREESTONE UNDERGROUND STOR.	3	490000	LIGHT HYDROCARBONS
* CLEMENS	PHILLIPS PETROLEUM	PHILLIPS PETROLEUM	17	5360000	LIGHT HYDROCARBONS
* DAY	ABANDONED	PURE OIL	1	0	LIGHT HYDROCARBONS
* EAST TYLER	TEXAS EASTMAN	WARREN PETROLEUM	10	4900000	LIGHT HYDROCARBONS
* FANNETT	WARREN PETROLEUM	GULF OIL	5	2428000	LIGHT HYDROCARBONS
* HAINESVILLE	BUTANE SUPPLIES	ENTERPRISE PETROLEUM GAS CORP.	3	1742000	LIGHT HYDROCARBONS
* HULL	MOBIL	MAGNOLIA PETROLEUM CORP.	11	3630000	LIGHT HYDROCARBONS
* MARKHAM	TEXAS BRINE	TEXAS BRINE	9	1800000	LIGHT HYDROCARBONS
* MARKHAM	SEADRIFT PIPELINE	SEADRIFT PIPELINE	6	7455000	LIGHT HYDROCARBONS
* MOSS BLUFF	MOSS BLUFF STORAGE VENTURE	MOSS BLUFF STORAGE VENTURE	5	0	LIGHT HYDROCARBONS
* NORTH DAYTON	ENERGY STORAGE TERMINAL INC.	ENERGY STORAGE TERMINAL INC.	2	0	LIGHT HYDROCARBONS
* PIERCE JUNCTION	ENTERPRISE	WYNDY PETROLEUM AND ELLIS TRANSPORT	10	4060000	LIGHT HYDROCARBONS
* PIERCE JUNCTION	COASTAL STATES CRUDE GATHERING	COASTAL STATES CRUDE GATHERING	7	12734000	LIGHT HYDROCARBONS
* SOUR LAKE	TEXACO	THE TEXAS CO.	3	1196000	LIGHT HYDROCARBONS
* STRATTON RIDGE	SEMINOLE PIPELINE	SEMINOLE PIPELINE	4	152000	LIGHT HYDROCARBONS
* STRATTON RIDGE	AMOCO	FENIX AND SCISSON	7	5257000	LIGHT HYDROCARBONS
* STRATTON RIDGE	DOW	DOW	22	7000000	LIGHT HYDROCARBONS

LIST/TITLE L(18)NAME OF SALT DOME,B(1),R(30)CURRENT OPERATOR OF STORAGE FACILITIES +
 LIST/TITLE L(18)NAME OF SALT DOME,B(1),R(30)CURRENT OPERATOR OF STORAGE FACILITIES +

STORAGE FACILITIES ,B(1),R(36)ORIGINAL APPLICANT ,B(1),
 STORAGE FACILITIES ,B(1),R(36)ORIGINAL APPLICANT ,B(1),

R(7)NUMBER +OF +CAVERNS,B(1),R(10)STORAGE +CAPACITY +IN BARRELS,B(3),
 R(7)NUMBER +OF +CAVERNS,B(1),R(10)STORAGE +CAPACITY +IN BARRELS,B(3),

R(18)PRODUCT STORED /C1,C226,C227,C228,C229,C236,08 LOW CI WH C226 EXISTS:
 R(18)PRODUCT STORED /C1,C226,C227,C228,C229,C236,08 LOW CI WH C226 EXISTS:

Two domes in Texas--Bethel and Boling salt domes--store natural gas. Natural gas is significantly different from other products stored in salt domes because of its high pressures during storage and rapid pressure declines during production. At Bethel salt dome, natural gas is stored in caverns under a cavern-storage pressure of 3,500 pounds per square inch gauged (psig). The depth of the cavern is between 4,300 and 4,800 ft.

Boling salt dome is a good example of a salt dome with multiple use of the available resources (fig. 15). Oil is produced from oil fields over the cap rock, within the cap rock, and from flank reservoirs. Boling salt dome has been the world's largest single source of sulfur. Valero Gas Co. has recently expanded its natural-gas storage facility at Boling to four caverns.

A cross section of Boling salt dome shows the geometry of the upper part of the salt dome illustrating cap rock, sulfur production, the location and size of two Valero storage caverns, and the proposed locations of a field of toxic-chemical waste caverns by United Resource Recovery, Inc. (fig. 16). Several aspects are important. The Valero caverns are located about 10,000 ft from the Texas Gulf Sulfur producing zone. Despite the 10,000 ft of separation, however, during construction of the Valero storage cavern no. 3, problems occurred that apparently are directly related to sulfur production. The well encountered, within the cap rock, a zone bearing high-pressure "mine waters" that caused the well to "kick." Texas Gulf Sulfur personnel were needed to cap the well. Although there is a large separation between the sulfur-mining operations and the active and proposed storage operations, the impact of the sulfur-mining operation extends far across the salt dome. Additionally, the proposed toxic-waste caverns are located near the periphery of the dome. Characteristically the internal constituents of salt domes--anhydrite and other country rock--increase toward the margins of salt stocks.

Salt Resources

Texas salt domes constitute an immense reservoir of salt that has risen through gravity deformation from great depths to lie within man's reach. Salt is a major industrial commodity that is used as a chemical feedstock, for road deicing, and for human and animal consumption.

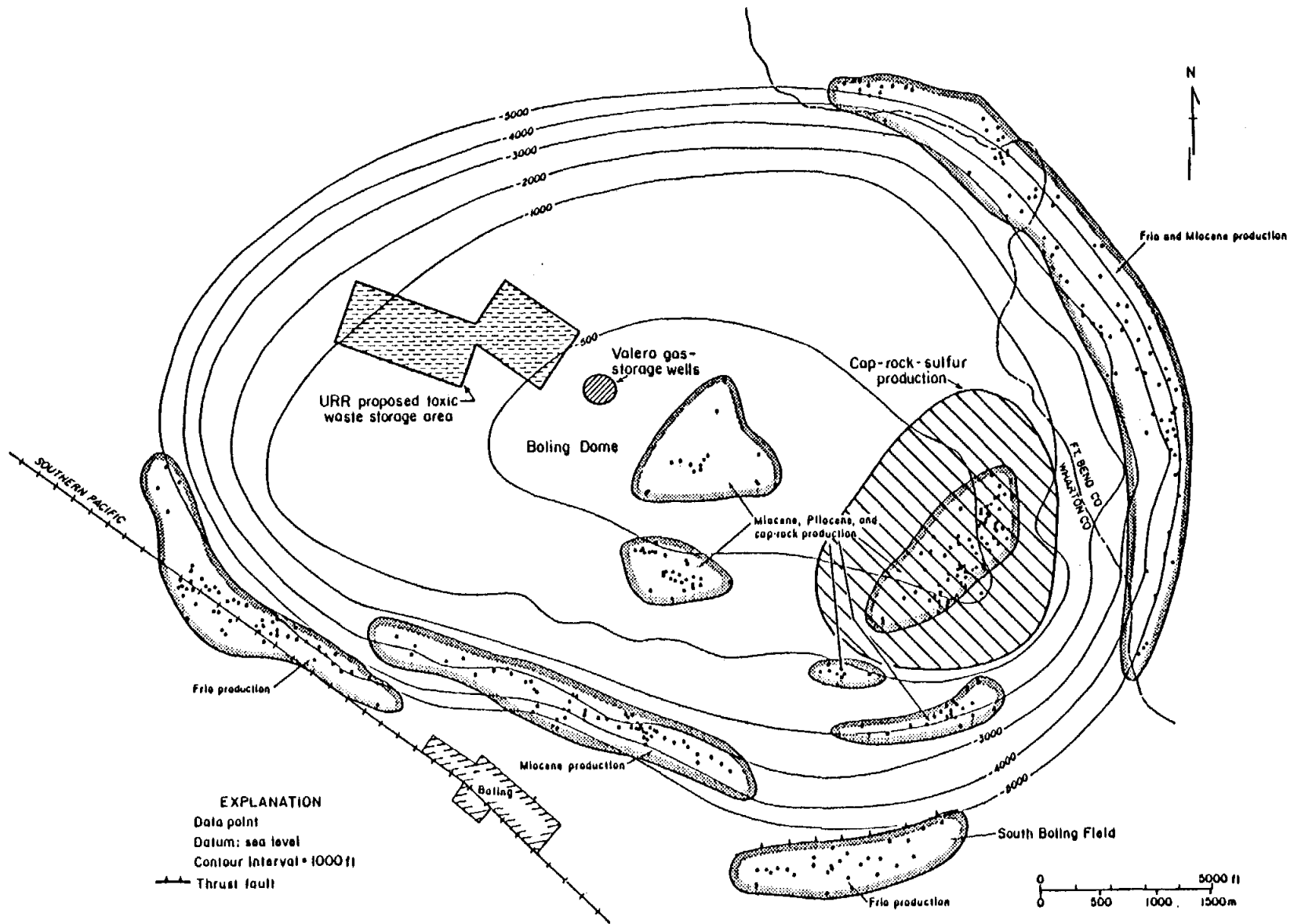


Figure 15. Map of Boling salt dome showing locations of oil fields, sulfur production, Valero Gas Co. gas-storage caverns, and United Resource Recovery, Inc., lease area (modified from Galloway and others, 1983).

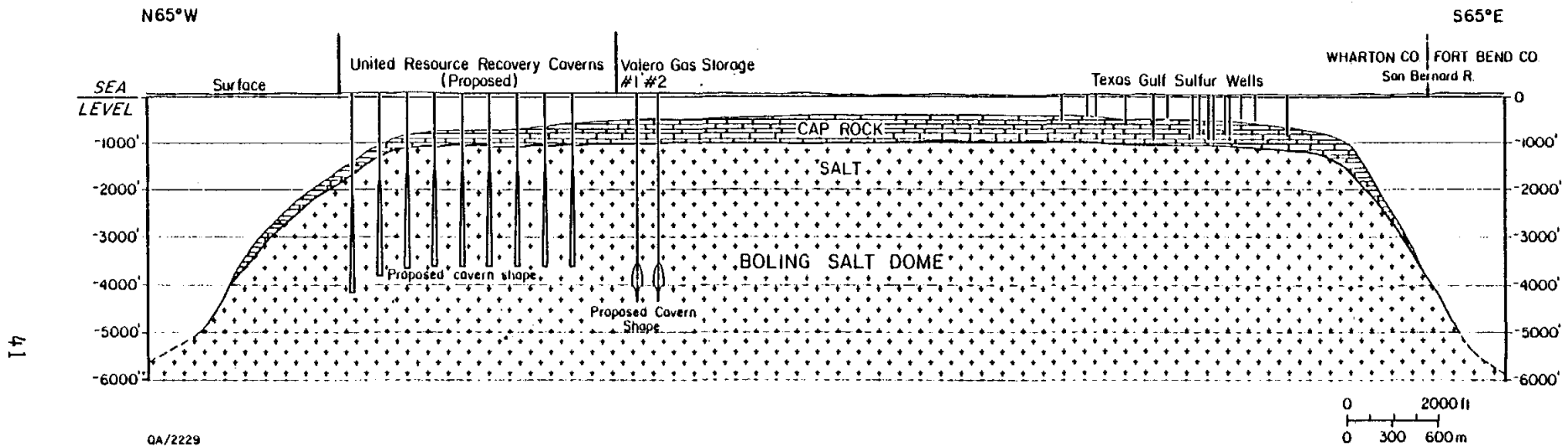


Figure 16. Cross section of Boling salt dome (east-west) showing location of sulfur production, geometry of Valero Gas Co. gas storage caverns, and proposed location and geometry of United Resource Recovery, Inc., waste-storage caverns.

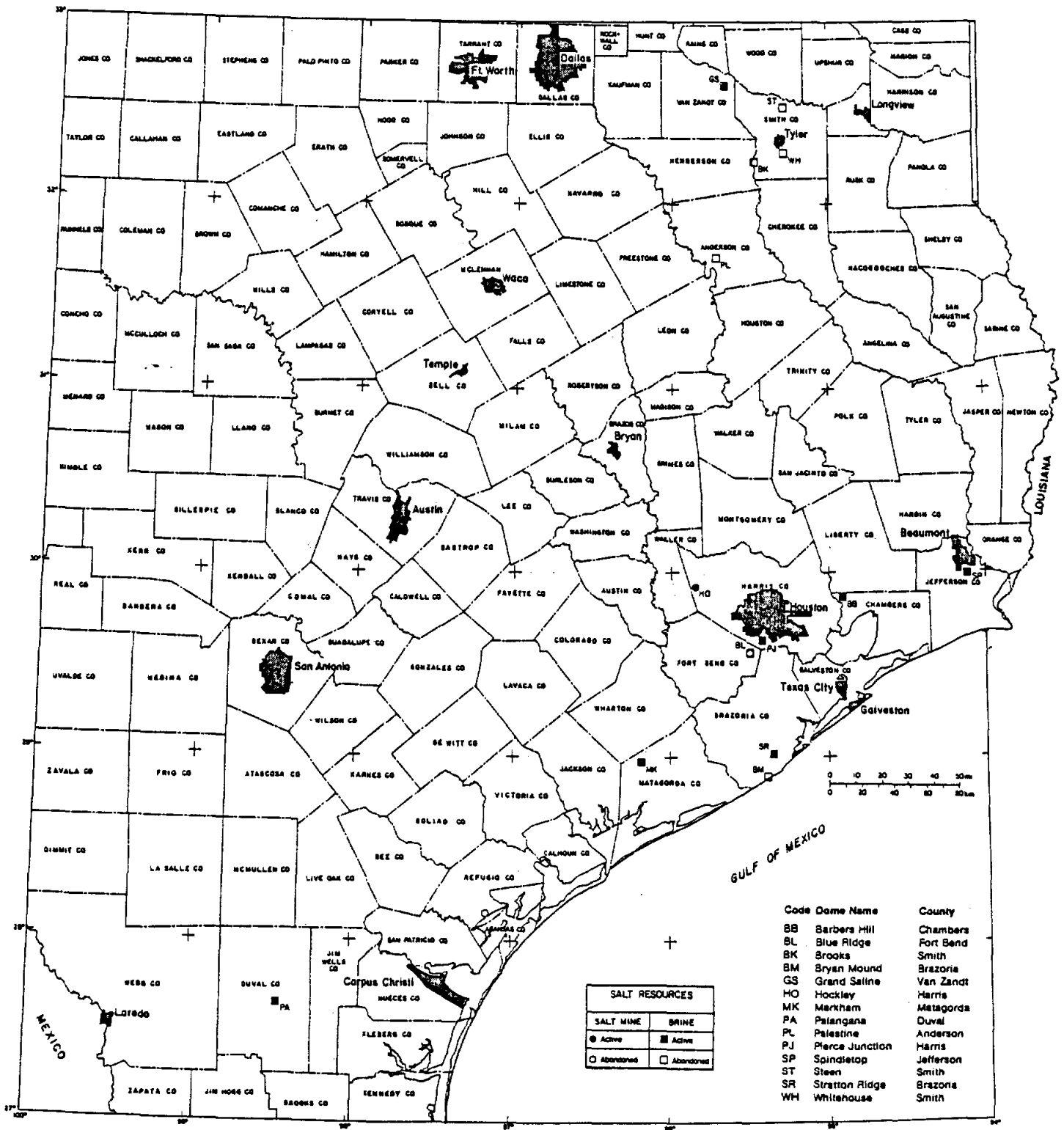
Salt is produced from Texas salt domes by conventional underground mining and by solution-brine wells. Estimates indicate that salt reserves will be adequate for 381 years (Griswold, 1981) to 26,000 (Hawkins and Jirik, 1966). The smaller figure is more reasonable on the basis of less recoverable salt at shallower depth, growth in salt demand, and preemption of some domes by storage requirements. Figure 17 shows those domes with active rock-salt mines and brine operations. Table 3 lists pertinent information on the operations at those domes.

Rock-Salt Mine

Currently, two active underground salt mines exist in Texas salt domes, the Kleer mine at Grand Saline salt dome and the United Salt mine at Hockley salt dome. According to Science Applications, Inc. (1977), Blue Ridge salt dome also housed a rock-salt mine that was later converted to a solution-brine mine. The well and mine opening collapsed in 1949. Both the Hockley and the Grand Saline salt mines are relatively small, and the operations are constrained by demand. Production is from one level in each of the mines. The primary use for the mined granulated and compressed rock salt is as a dietary supplement for animals (that is, salt lick).

Solution-Brine Well

Solution-brine wells for the production of chemical feedstock are active at seven salt domes in Texas including Barbers Hill, Blue Ridge, Markham, Palangana, Pierce Junction, Spindletop, and Stratton Ridge salt domes. Historically, the Indians first used natural brines from East Texas salt domes as a source of salt and brine for tanning hides. In the past, salt caverns, which were created as the brine was produced, constituted an unrecognized resource. Many brine caverns have been converted to store light hydrocarbons. Currently, the DOE is using four large storage caverns in Bryan Mound salt dome, created by Dow Chemical Co. during past brining operations, for crude-oil storage in the SPR. The present capacity of the former brine caverns at Bryan Mound is 56.8 million barrels.



SALT RESOURCES FROM SALT DOMES OF TEXAS

Figure 17. Map of salt domes showing active rock-salt mines and solution-brine wells.

Table 3. List of salt domes with salt production, method, status, company, and history.

NAME OF SALT DOME	MINERAL	STATUS OF PRODUCTION	REPORTING ORGANIZATION OR MINING METHOD	NAME OF COMPANY	MINING HISTORY

* BARBERS HILL	BRINE	ACTIVE	BRINE WELLS	DIAMOND SHAMROCK	
* BLUE RIDGE	BRINE	ACTIVE	BRINE WELLS	UNITED SALT	
* BLUE RIDGE	ROCK SALT	ABANDONED	SALT MINE	UNITED SALT	
* BROOKS DOME	BRINE	ABANDONED	L.S.U.-1976	UNKNOWN	1865
* BRYAN MOUND	BRINE	ABANDONED	BRINE WELLS	DOW CHEMICAL	
* GRAND SALINE DOME	ROCK SALT	ACTIVE	SALT MINE	MORTON SALT	
* GRAND SALINE DOME	BRINE	ABANDONED	BRINE WELLS	MORTON SALT	1845
* HOCKLEY	ROCK SALT	ACTIVE	SALT MINE	UNITED SALT	1929-PRESENT
* MARKHAM	BRINE	ACTIVE	BRINE WELLS	TEXAS BRINE CORP.	
* PALMAGANA DOME	BRINE	ACTIVE	BRINE WELLS	P. P. G. IND. INC.	
* PALESTINE DOME	BRINE	ABANDONED	L.S.U.-1976	UNKNOWN	1865
* PIERCE JUNCTION	BRINE	ACTIVE	BRINE WELLS	TEXAS BRINE CORP.	
* SPINDLETOP	BRINE	ACTIVE	BRINE WELLS	TEXAS BRINE CORP.	
* STEEN DOME	BRINE	ABANDONED	L.S.U.-1976	UNKNOWN	1865
* STRATTON RIDGE	BRINE	ACTIVE	BRINE WELLS	DOW CHEMICAL	
* WHITEHOUSE DOME	BRINE	ABANDONED	L.S.U.-1976	UNKNOWN	

LIST/TITLE L(18)NAME OF SALT DOME,B(4),R(9)MINERAL ,B(4),R(10)
 LIST/TITLE L(18)NAME OF SALT DOME,B(4),R(9)MINERAL ,B(4),R(10)

STATUS OF +PRODUCTION,B(4),R(22)REPORTING ORGANIZATION+
 STATUS OF +PRODUCTION,B(4),R(22)REPORTING ORGANIZATION+

OR MINING METHOD ,B(4),R(18)NAME OF COMPANY ,B(4),R(14)MINING HISTORY/
 OR MINING METHOD ,B(4),R(18)NAME OF COMPANY ,B(4),R(14)MINING HISTORY/

C1,C199,C200,C201,C202,C203,08 LOW C1 WH C199 EQ ROCK SALT OR C199 EQ BRINE:
 C1,C199,C200,C201,C202,C203,03 LOW C1 WH C199 EQ ROCK SALT OR C199 EQ BRINE:

Petroleum Resources

Oil discovered in 1901 at Spindletop salt dome gave birth to the modern petrochemical industry. The petroleum production of many Gulf Coast salt domes is truly staggering. Cumulative production from the salt-dome-related oil reservoirs (those greater than 10 million barrels cumulative production) is 3.46 billion barrels (Galloway and others, 1983). Oil is not found in the salt stock but in surrounding strata. Intrusion of the salt diapir can form a wide range of structural and stratigraphic traps for petroleum. Highly productive zones around salt domes include cap rocks, dome flanks, and supradomal crests.

An oil play is an assemblage of geologically similar reservoirs exhibiting similar trapping mechanisms, reservoir rocks, and source rocks (Galloway and others, 1983). Four major oil plays are associated with Gulf Coast salt domes. They include cap rock, Yegua salt-dome flanks, Yegua deep-salt-dome crests, and Frio deep-salt-dome crests.

This discussion of petroleum resources associated with salt domes centers on diapirs in the highly productive Gulf Coast (Houston Salt Basin) of Texas. Shallow piercement oil fields will be discussed generally, and then specific examples of the major oil plays associated with salt domes will be discussed in turn. Much of this discussion is based on two sources: a recent publication by Galloway and others (1983), which has proved to be a valuable guide to oil in Texas, and a book by Halbouty (1979), which is the standard oil-related salt-dome text.

Shallow Salt-Dome Oil Fields

Shallow salt-dome fields were the first oil fields discovered in the Gulf Coast area. Many fields discovered 70 and 80 years ago are still producing. This productive longevity stems in part from diapirism and faulting, which segmented reservoirs thus creating a diverse range of traps at many different stratigraphic levels. The yearly oil production of Spindletop salt dome illustrates that production has been prolonged and periodically increased dramatically by discovery of new types of salt dome traps (fig. 18).

YEARLY SPINDLETOP OIL PRODUCTION

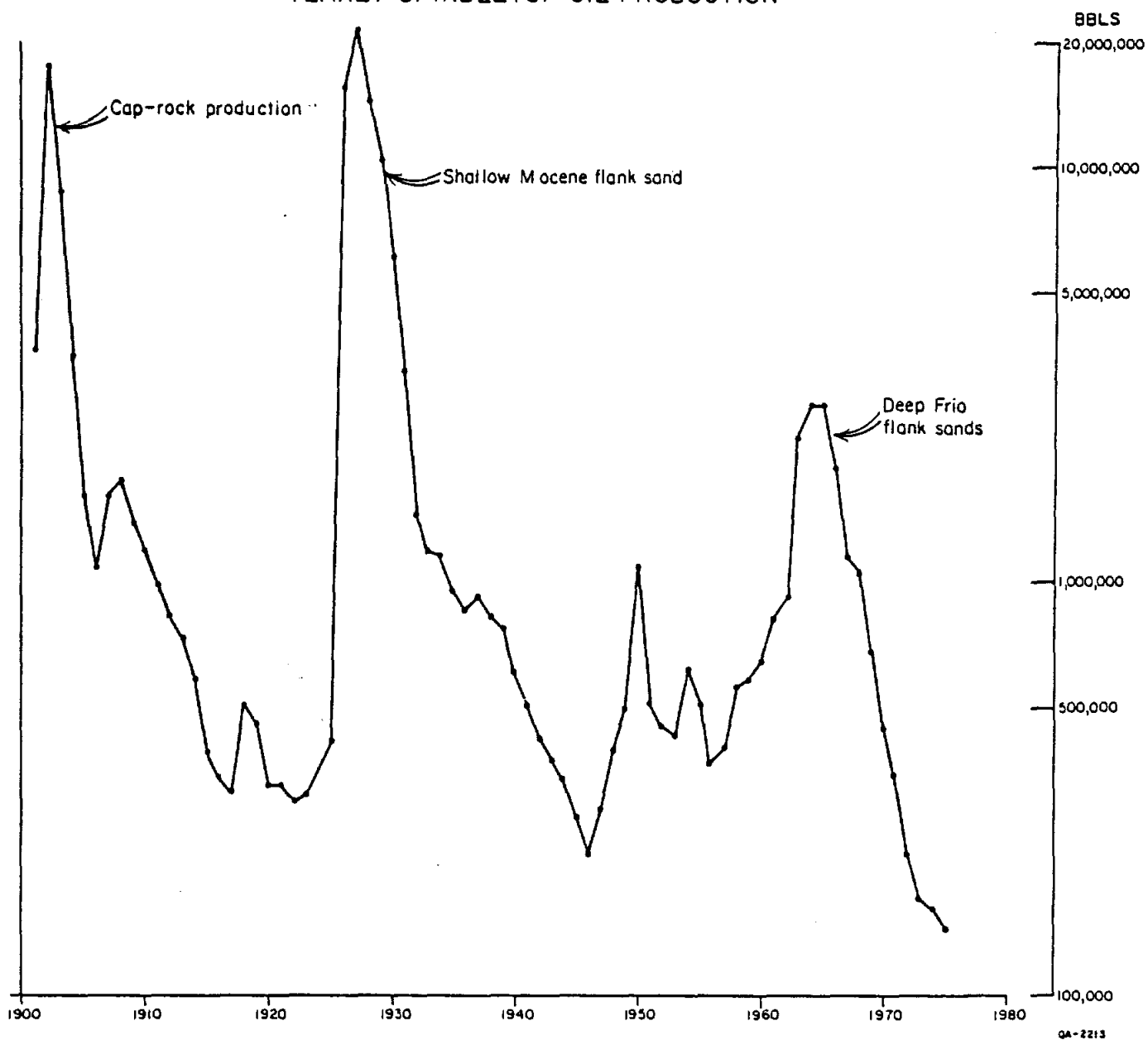


Figure 18. Yearly oil production from Spindletop salt-dome oil field (data from Halbouty, 1978).

Shallow-piercement-salt domes with cumulative oil production greater than 10 million barrels are located on figure 19. These domal fields are listed in table 4 with discovery dates, depth to cap rock and salt, productive area, and production figures (Galloway and others, 1983). Most oil has been produced from traps in cap rock, in strata truncated or pinched out against dome flanks, and in strata arched over dome crests. Although some very shallow diapirs are highly productive, there is a correlation between greater depth of burial of the dome and greater oil production (fig. 20). According to statistics from Halbouty (1979), known salt domes with crests greater than 4,000 ft deep have approximately twice the cumulative production of domes with crests buried less than 4,000 ft (80 million barrels vs. 38 million barrels).

Strata of Eocene through Pliocene age host most of the production associated with Gulf Coast salt domes. The Wilcox Group and the Yegua, Frio, and Fleming Formations compose the host strata. Major reservoirs and trap types discussed below are cap rock, dome flank (Yegua), and deep-salt-dome crest (Yegua and Frio). Boling salt dome is a good example of a shallow piercement dome with a large number of oil fields (fig. 21). Production is from supradomal sands, cap rock, and flank traps in Miocene, Heterostegina Limestone, and Frio reservoirs. Cumulative production through 1981 is 35.7 million barrels.

Cap-Rock Reservoirs

Four of the oldest fields in the Gulf Coast area--Spindletop, Sour Lake, Batson, and Humble--produce oil from calcite cap rock overlying shallow piercement salt domes. A total of eight shallow Gulf Coast diapirs had significant oil production from their cap rock. Most cap rocks have been exploited and their oil exhausted. Minor cap-rock production from Day salt dome in Madison County, however, was initiated in 1981. The location of some cap-rock fields over Boling salt dome is shown in figure 21.

Cap-rock fields typically showed prolific initial production and then rapid production decline (fig. 17). Production is from microscopic to cavernous porosity. Porosity values up to 40 percent are reported (Galloway and others, 1983).

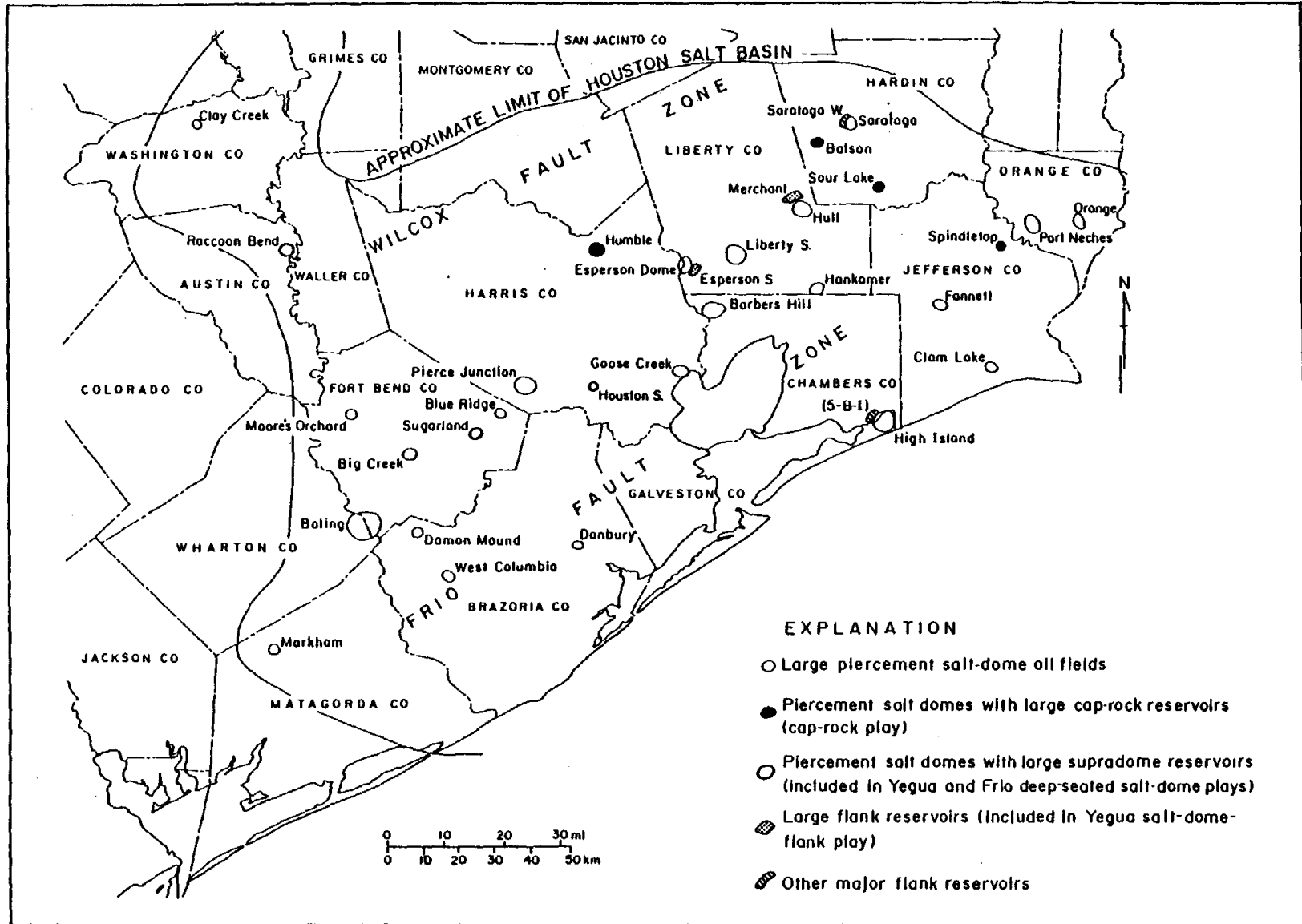


Figure 19. Map of piercement salt domes showing oil fields that have produced more than 10 million barrels of oil (after Galloway and others, 1983).

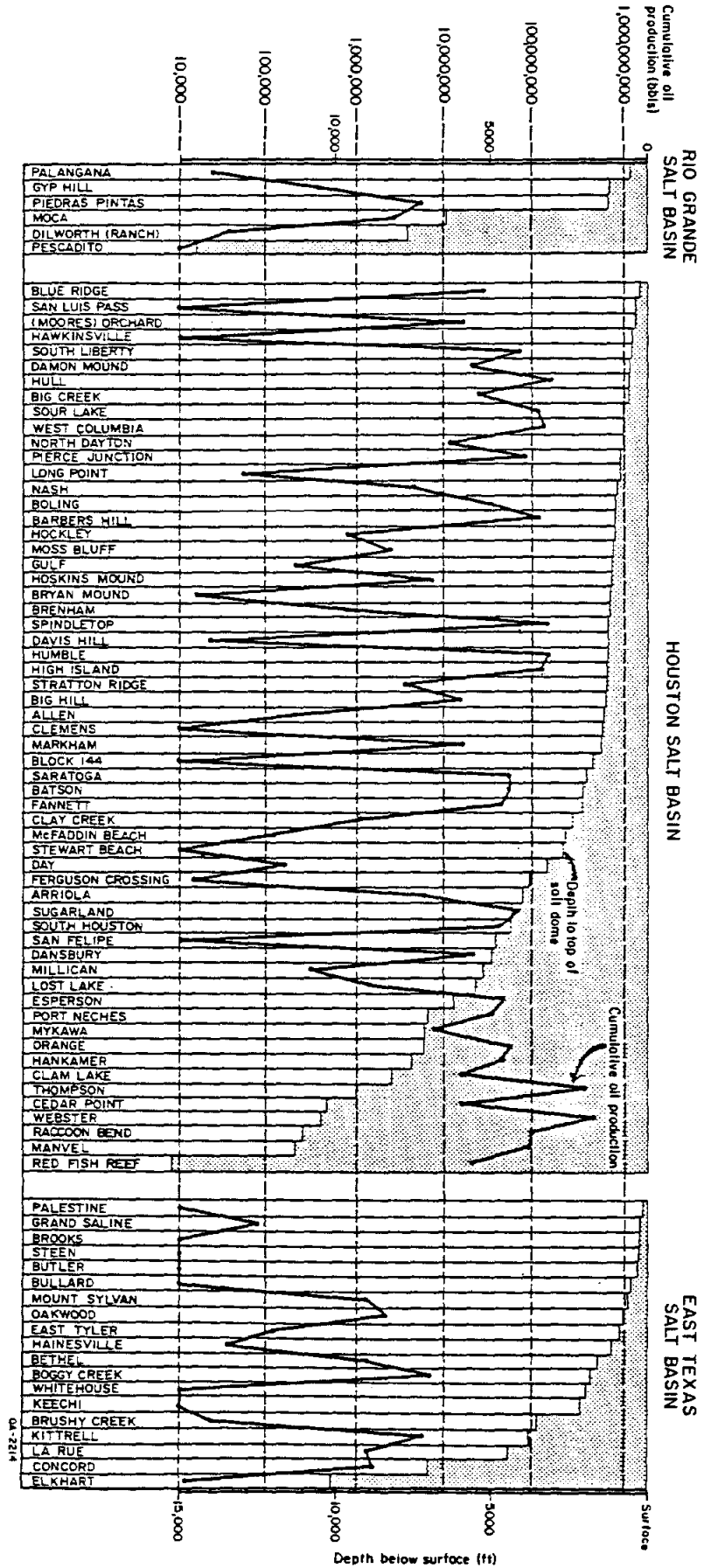


Figure 20. Graph showing depth to the crest of Texas salt domes and their cumulative oil production through 1975 (modified from Halbouty, 1979).

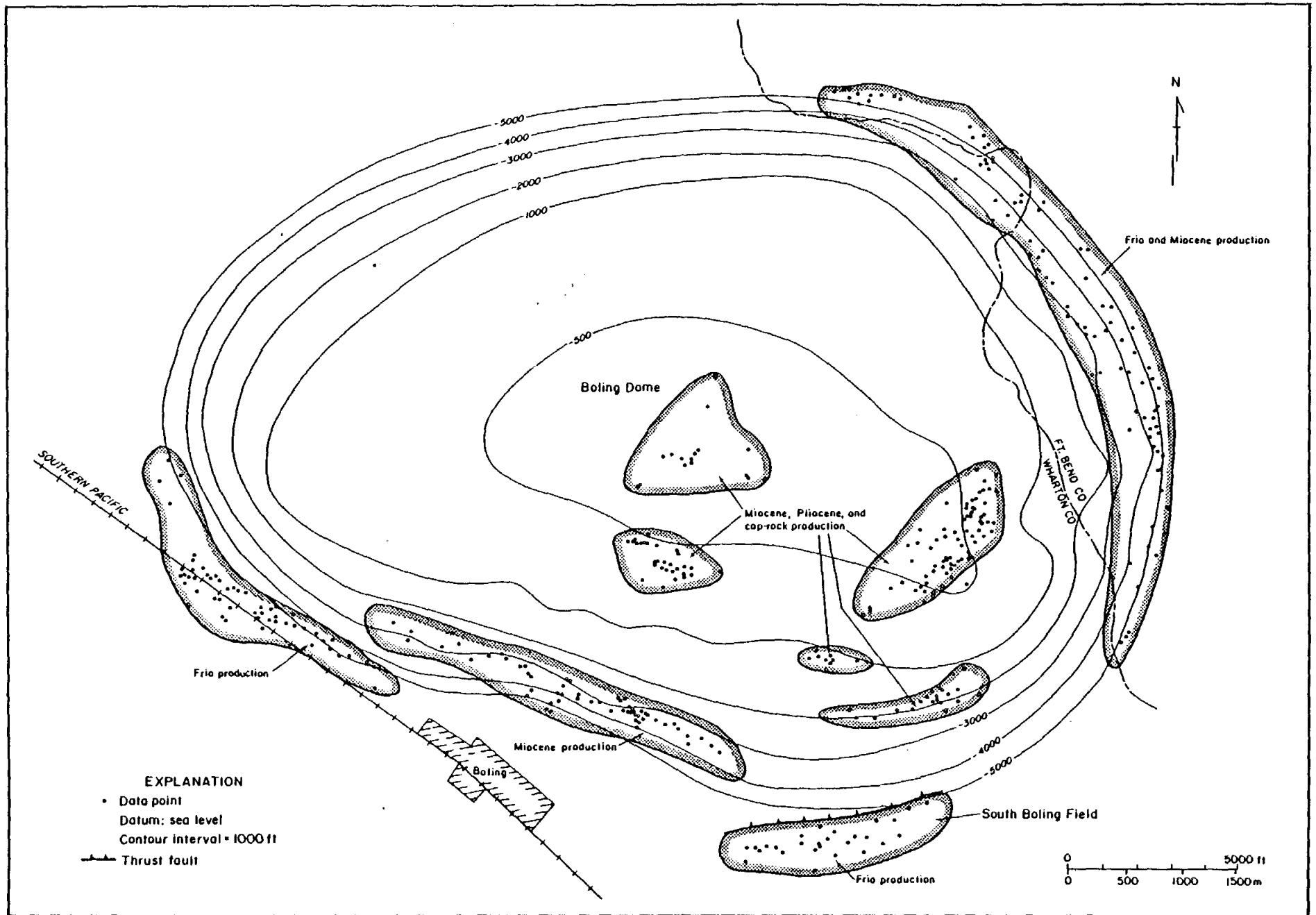


Figure 21. Map of Boling salt dome showing locations of oil fields (after Galloway and others, 1983).

Table 4. List of salt domes with large oil fields and production status.

Field	Discovery date	Top cap (ft)	Top salt (ft)	Production			Cumulative production (million barrels)	Estimated ultimate recovery (million barrels)
				Supradome	Cap	Flank		
Barbers Hill	1916	350	1,000	No	No	Frio, Miocene	128.0	129.3
Baton	1903	1,080	2,050	Miocene	Yes	Miocene, Frio, Yegua	60.6	61.0
Big Creek	1922	450	635	Miocene, Frio	No	Vicksburg	24.6	27.0
Blue Ridge	1919	143	230	No	No	Miocene, Frio, Vicksburg	24.3	24.3
Buling	1925	383	975	Miocene	Yes	Miocene, Frio	35.7	36.2
Clam Lake	1937	none	8,173	Miocene	No	No	18.7	19.4
Clay Creek	1928	1,800	2,400	Wilcox, Sparta and Queen City	No	No	12.8	13.2
Damon Mound	1915	surface	529	No	No	Frio, Miocene	21.6	21.9
Danbury	1930	none	4,948	Miocene	No	Frio	21.6	21.9
Esperson	1929	none	6,170	Miocene, Frio, Vicksburg	No	Yegua	50.5	51.9
Fannett	1927	741	2,080	Miocene	No	Frio	51.0	52.9
Goose Creek	1908	>5,000	?	Frio, Miocene	No	No	134.7	135.2
Hankamer	1929	7,535	7,582	Miocene, Frio	No	No	48.8	51.0
High Island	1922	150	1,228	No	No	Miocene, Frio	132.0	134.2
Hull	1918	260	595	No	Yes	Miocene, Frio, Yegua	183.5	185.9
Humble	1905	700	1,214	Pliocene, Miocene	Yes	Frio, Yegua	168.2	169.5
Liberty South	1925	275	480	No	No	Miocene, Frio, Vicksburg, Yegua	86.1	88.0
Markham	1908	1,380	1,417	Miocene	Yes	Frio	17.6	17.7
Moore's Orchard	1926	285	369	No	No	Miocene, Frio, Yegua	21.8	22.1
Orange	1913	none	7,120	Miocene, Frio	No	Hackberry	61.8	62.8
Pierce Junction	1921	630	860	No	No	Miocene, Frio, Vicksburg, Jackson, Yegua	88.3	88.9
Port Neches	1928	none	6,948	Miocene, Frio	No	Hackberry	31.7	32.4
Saratoga	1901	1,500	1,900	Miocene	No	Yegua	59.2	61.1
Sour Lake	1902	660	719	Miocene	Yes	Frio, Jackson, Yegua	123.8	126.8
Spindletop	1901	700	1,200	Miocene	Yes	Miocene, Frio	153.2	153.9
West Columbia	1904	650	768	No	Yes	Miocene, Frio	162.2	163.6
							1,922.1	1,952.1

The genesis of cap rock is complex. Cap rock typically occurs at the crest of shallow piercement salt domes and may extend for some distance down the dome flanks. Mineralogically, most cap rocks are composed of a basal anhydrite zone, a middle gypsum or transition zone, and an upper calcite zone. The anhydrite is a dissolution residuum that accumulated as ground water dissolved anhydrite-bearing salt at the dome crest and flank. Gypsum then formed by hydration of anhydrite. Calcite is formed by sulfate reduction of gypsum with bacterial reaction with oil. The calcite zone is the typical oil reservoir in the cap rock.

Cap rocks are complex karstic features. They accumulated as a dissolution residuum and may themselves be undergoing dissolution. To this day, cap rocks are exceptionally difficult zones to complete and case a well through. Lost-circulation zones cause major problems involving mud circulation and complete cementation of casing strings. Active circulation of brine in cap-rock pores also provides a geochemical environment that is corrosive to casing and cements.

Some Gulf Coast cap rocks record evidence of erosion over the dome (Hanna, 1939). The cap rock of Orchard salt dome is thin over the dome crest but is up to 1,000 ft thick (stratigraphically) on the dome flanks (fig. 19). Pleistocene sands and gravels truncate Miocene strata around the dome periphery and apparently have stripped calcite cap rock from the dome crest.

Salt-Dome Flank Reservoirs

Important oil production from sandstones flanking salt domes was initiated at Spindletop dome in 1925 (Halbouty, 1979) (fig. 18). These flank reservoirs typically are thin sandstones steeply inclined upward toward the diapir flank. The sandstones may be truncated by the dome or pinch out toward the dome (fig. 22). Commonly, radial faults segment the sand bodies into discrete fault blocks.

Delta-front sheet sandstones of the Yegua Formation constitute the most important dome flank reservoir (Galloway and others, 1983). Major Yegua flank sands are reservoirs at Hull,

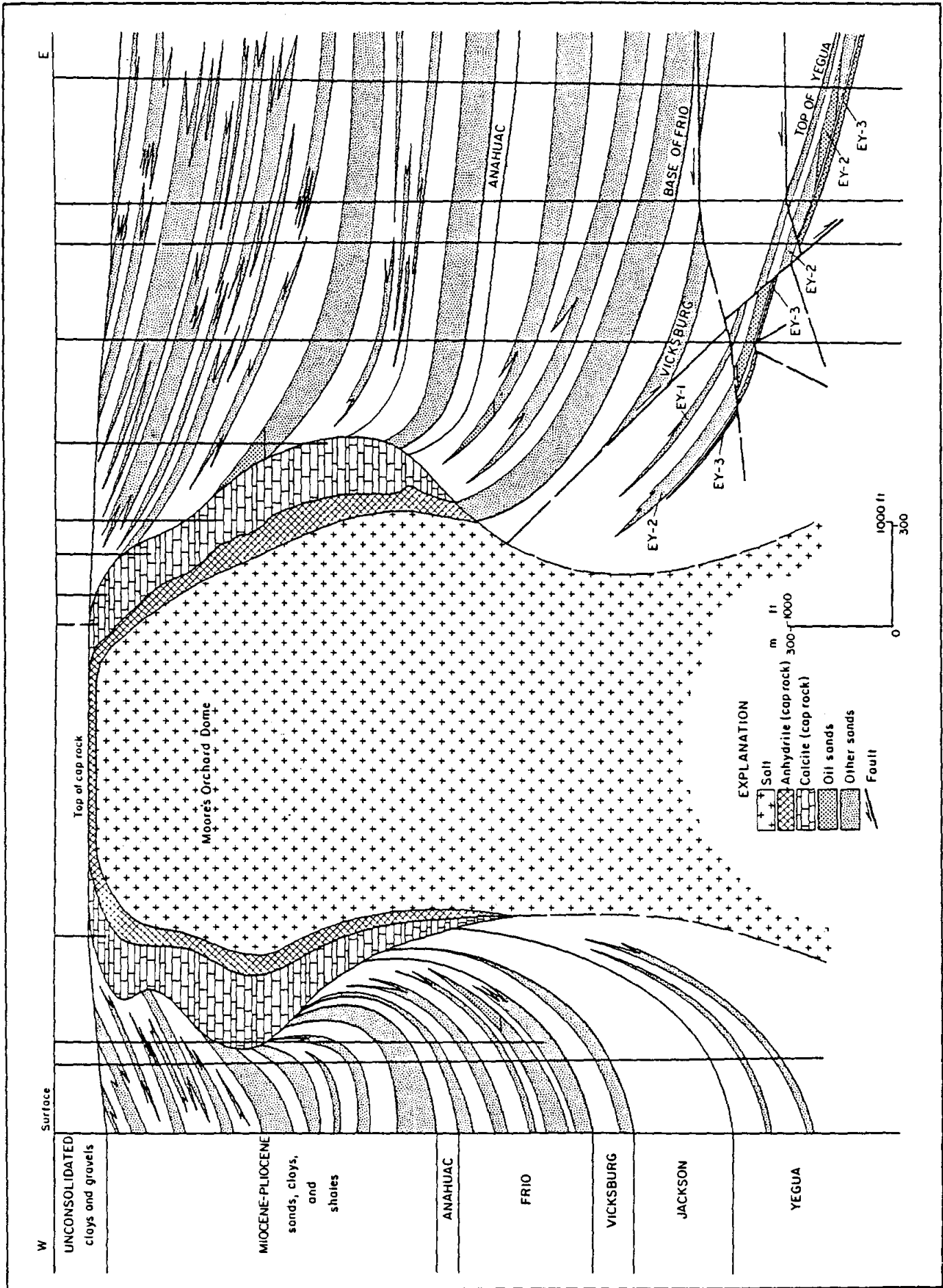


Figure 22. Cross section of (Moore's) Orchard salt dome showing upturned strata on the flank of the dome and the crest of the dome truncated by erosion (after Galloway and others, 1983).

Esperson, and Saratoga salt domes. An example of the geometry of these flank sands and reservoirs is illustrated by Orchard (Moore's Orchard) salt dome (fig. 22). The steep inclination of the flank sands makes them elusive targets, but this inclination also yields thick oil columns, efficient gravity segregation, and efficient water drives for impressive single-well production statistics.

Deep-Seated Dome Crest Reservoirs

Yegua and Frio sandstones arched over the crest of deep-seated salt domes produce the greatest cumulative amount of salt-dome-related oil in the Texas Gulf Coast (Galloway and others, 1983) (fig. 23). Most fields overlie known deep-seated salt domes such as Raccoon Bend (Yegua production) and Thompson, Manvel, Webster, and Cedar Point (Frio production). Other fields such as Katy may overlie non-piercing salt structures (Halbouty, 1979) or turtle-structure sediment-cored anticlines (Winker and others, 1983; Galloway and others, 1983).

Faults play a variable role in oil trapping and compartmentalization of reservoirs. For example, the Frio deep-seated dome crest trend is along the Vicksburg and Frio growth-fault trends. In contrast to the ubiquitous radial faults associated with shallow piercement salt domes, deeply buried salt domes normally have fewer associated faults as at Sugarland salt dome.

The average depth of reservoir rocks in the Yegua trend is approximately 5,000 ft. The reservoir sandstones are a complex of deltaic sand bodies including distal fluvial, distributary-channel-fill, and crevasse-splay facies (Galloway and others, 1983). The average depth of reservoir rocks in the deep Frio trend is approximately 6,000 ft. Reservoir rocks include a wide range of deltaic facies including delta-front, delta-margin, distributary-channel-fill, and destructional barrier facies (Galloway and others, 1983). The reservoir-drive mechanism is an efficient water drive commonly assisted by gas-cap expansion. Most of the larger fields are unitized with reservoir-wide secondary gas injection.

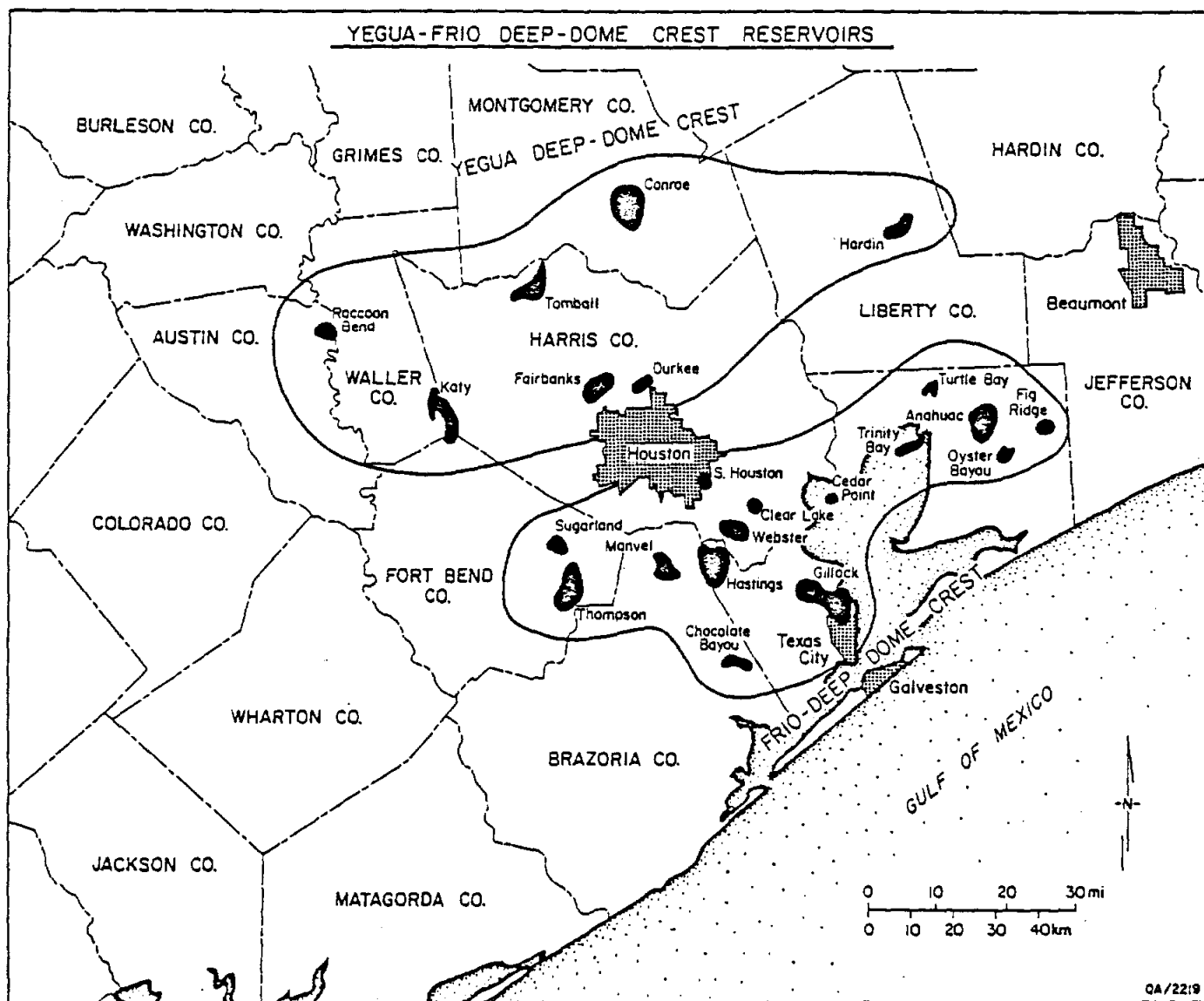


Figure 23. Map of Yegua and Frio reservoirs over the crest of deep-seated salt domes.

Petroleum Resources of Salt Domes in the East Texas and Rio Grande Basins

Oil production from East Texas and Rio Grande salt diapirs is much less than production from diapirs in the Houston Salt Basin (fig. 20). No fields around diapirs in the East Texas or the Rio Grande Basins have produced greater than 10 million barrels of oil. Shallow salt domes (less than 6,000 ft) have produced less than 1 percent of the oil from the central part of the East Texas Basin (Wood and Giles, 1982).

The East Texas Basin on the whole is an extraordinarily oil-rich basin. The East Texas oil field alone has produced 4.68 billion barrels of oil. Deeply buried non-piercing salt structures are highly productive in the East Texas Basin. Hawkins and Van salt structures have produced 734 million and 485 million barrels of oil, respectively. The question remains, why are diapirs in the interior basins so barren in comparison with coastal diapirs?

Several factors have acted to minimize the entrapment of oil in interior salt diapirs. Diapirs in interior basins have greater structural maturity than do coastal diapirs. This structural maturity is characterized by steep flanks of the diapir and a surrounding rim syncline. Most diapirs in the East Texas Basin are surrounded by strata that dip toward the diapir or are flat lying. In contrast, the flanks of many coastal diapirs are less steep, and strata typically are inclined upward toward the dome. The increased maturity of East Texas diapirs results in the structural closure being minimized around the domes.

The domes of the East Texas Basin are also much older than coastal diapirs. Most coastal domes probably became diapirs in the Oligocene or Miocene, 10 to 35 million years ago. In contrast, East Texas domes became diapirs from 80 to more than 112 million years ago (Seni and Jackson, 1983b). Thus, if large amounts of oil had accumulated over the crests of early pillows that later evolved into East Texas diapirs, the hydrocarbons would have had a long period of time to leak during dome uplift, during erosion of previously deposited strata over the dome crest, or both.

Sulfur Resources

Historically, a major proportion of the world supply of sulfur came from Texas salt domes. Sulfur production began in Texas at Bryan Mound salt dome. Sulfur has been produced commercially from the cap rocks of 15 Texas salt domes. Currently, Boling salt dome contains the only active cap-rock-sulfur mine in Texas (fig. 15). Texas cap-rock sulfur mining has declined owing to exhaustion of reserves, lack of new cap-rock discoveries, and price competition from sulfur produced by secondary recovery of sulfur from sour gas and petroleum refining.

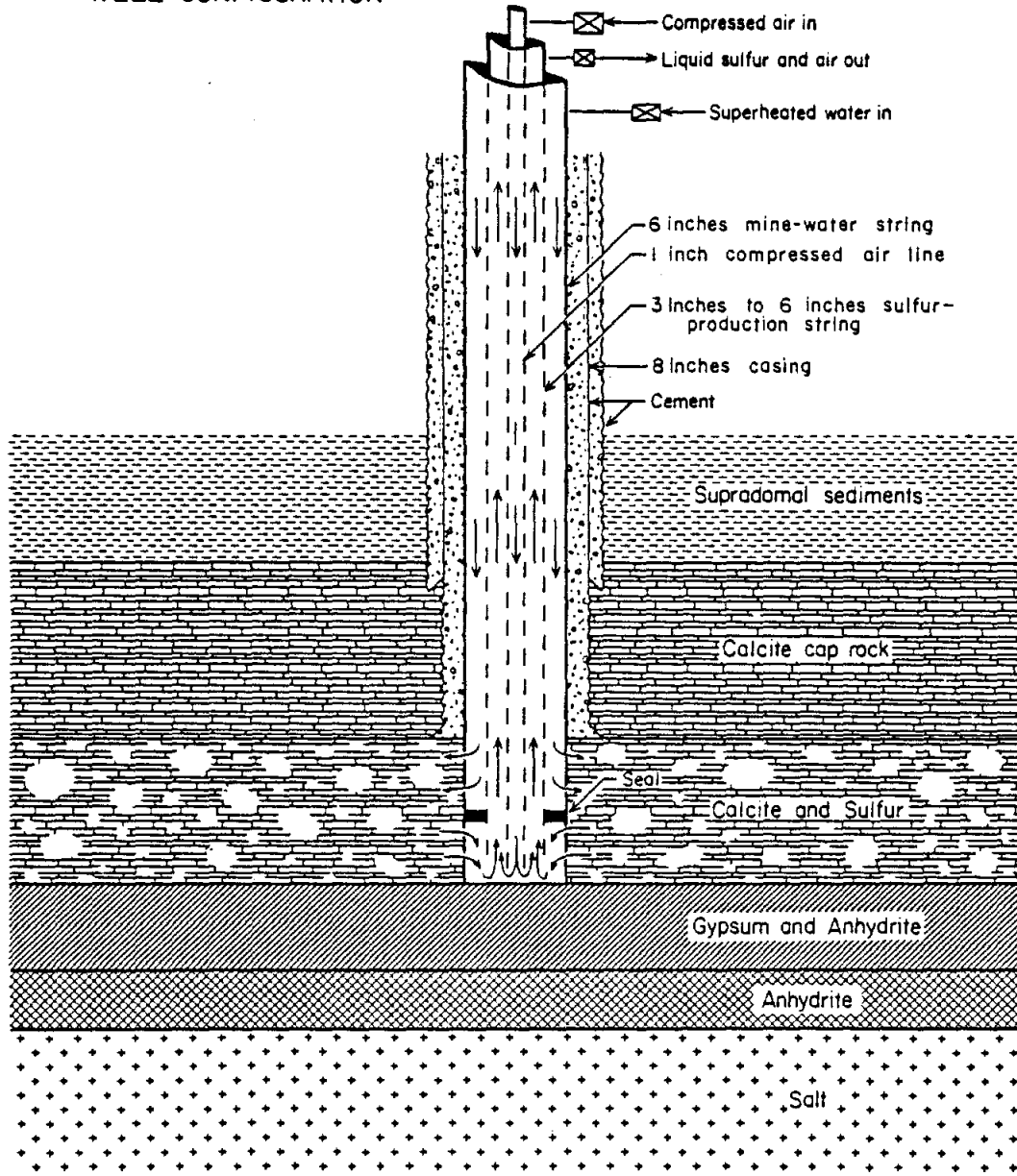
This section will present the history and technology of sulfur mining and the geology of cap-rock sulfur deposits.

History and Technology

Sulfur was first discovered in 1867 in cap rock of coastal salt domes at Sulfur Mines salt dome in Louisiana. Louisiana Petroleum and Coal Oil Co. was searching for oil and instead discovered a thick deposit of native (free elemental) sulfur in cap rock at a depth of 650 ft. For 20 years, a number of ventures designed to mine the sulfur by underground methods failed. H. Frasch patented in 1890 a revolutionary sulfur-mining technology that is still used today with minor modifications. Basically the Frasch process uses hot water to melt the sulfur and compressed air to help lift the sulfur to the surface. Standard oil-field technologies are used to drill a hole to the base of the sulfur-bearing zone. Three stands of pipe are then set concentrically into the hole--the outer casing, the middle sulfur-production string, and the inner compressed-air line (fig. 24).

Casing (usually with diameter of 6 to 8 inches) is cemented into the hole. Two separate sets of perforations are made through the casing at the top and near the bottom of the sulfur-bearing zone. According to Ellison (1971), the upper set of perforations is 8 to 10 ft above the base of the productive zone, and the lower set is 1 to 5 ft above the base. A ring-shaped seal is placed in the annulus between the sulfur-production string and the casing string between the

CAP-ROCK SULFUR
FRASCH SULFUR-MINING
WELL CONFIGURATION



QA/2223

Figure 24. Casing string detail for cap-rock sulfur-production well (after Myers, 1968).

upper and lower sets of perforations. The seal prevents communication between the upper and the lower perforations within the annular space.

Superheated (300° to 325°F) and pressurized (125 to 100 psi) water is injected down the annulus between the casing and the sulfur-production string. The hot water exits through the upper set of perforations. The sulfur melts as the superheated water enters the sulfur-bearing zone. Molten sulfur is heavier than water and therefore sinks to the lower part of the sulfur-bearing zone. Pressure differentials drive the molten sulfur through the lower set of perforations into the casing. The seal forces the sulfur into the sulfur-production string. Compressed air at 500 to 600 psi is injected into the innermost compressed-air string. This helps force the sulfur to the surface by lowering the bulk density of the molten sulfur-air mixture.

Sulfur, having a purity of 99.5 percent, solidifies at the surface in large vats. Some operations directly ship the molten sulfur in insulated vessels.

Two ancillary operations during sulfur production involve recycling of the injected water and mitigating surface subsidence owing to sulfur removal. "Bleed-water" wells are drilled to produce and recycle excess water that was injected to melt the sulfur. Once the water has cooled below the melting point of sulfur, it must be recycled. By drilling "bleed-water" wells beyond the productive area, costs can be lowered and water flow is improved (Hawkins and Jirik, 1966).

Surface subsidence over areas of sulfur production is a problem common to many sulfur-mining areas. The removal of sulfur opens a series of void spaces in the cap rock. The collapse of these voids causes the subsidence over the mining operations. The closing of voids is beneficial in that less water is needed to mine the remaining sulfur. Many sulfur operations now pump special muds into the zone where sulfur has been produced to fill the voids and prevent surface subsidence. A 2 mi² area over Boling salt dome has subsided up to 20 ft. An extensive system of levees protects the area from flooding. In addition to flooding, subsidence may cause damage to well bores, casing, and surface facilities.

Characteristics of Cap-Rock Sulfur Deposits

Native (free) sulfur has been reported in cap rock of 25 Texas salt domes. Fifteen of these domes have undergone commercial sulfur production (figs. 25 and 26). Only Boling salt dome has active sulfur production. Boling salt dome has been continuously active since 1929 (fig. 24) and is the world's largest single sulfur source. A cross section of Boling salt dome, its cap rock, and sulfur zone is shown in figure 27.

Cap rock is a particularly complex area of a salt dome. Cap-rock thickness ranges from a feather edge to more than 1,000 ft. Cap-rock depth ranges from above sea level to depths greater than 4,000 ft. Sulfur typically occupies vugular porosity at the base of the calcite zone. The thickness of the sulfur-bearing zone may exceed 300 ft. Sulfur is typically found on the outer periphery, or shoulder, of shallow piercement salt domes (fig. 28) (Myers, 1968). Some small domes have sulfur deposits across the entire crestal area. Even though the larger domes, such as Boling salt dome, have sulfur over only a portion of their crests, the larger domes have mineralization over a much larger area and generally of greater thicknesses. In the Gulf Coast area, the depth of sulfur mining is typically from 900 to 1,700 ft. Orchard salt dome exhibits the greatest depth of sulfur production at 3,200 ft.

Cap-Rock Resources

The cap rock hosts and also comprises most of the other resources associated with salt domes. The cap rock is an exceedingly complex environment as demonstrated by its variable stratigraphy including calcite, gypsum (transition), and anhydrite zones. In addition to the cap-rock petroleum and sulfur resources already discussed, some cap rocks of Texas domes contain uranium (Palangana salt dome), Mississippi Valley-type sulfide deposits (Hockley salt dome), and silver minerals (Hockley salt dome). The cap rock is a valuable commodity as crushed stone in the rock-poor coastal regions. Just as the caverns in salt domes were an unrecognized resource for a long time, lost-circulation zones have been converted into convenient disposal zones for brine leached from storage cavern projects.

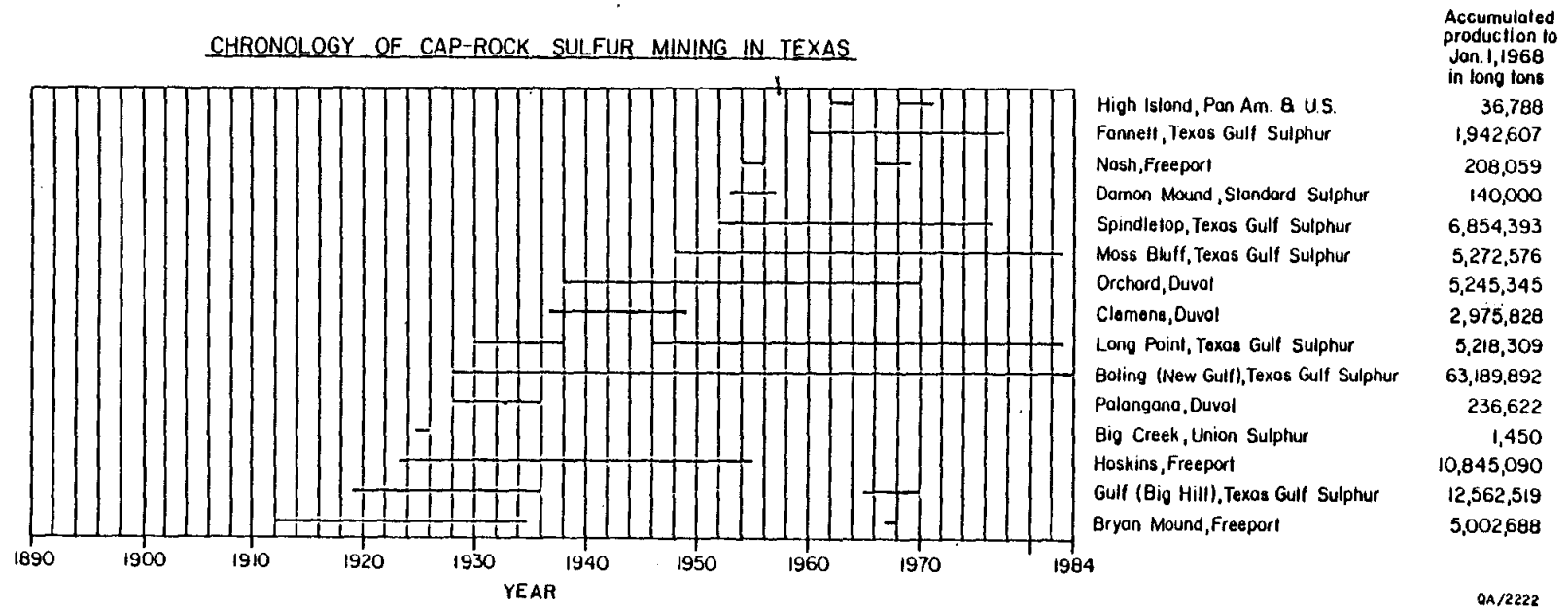
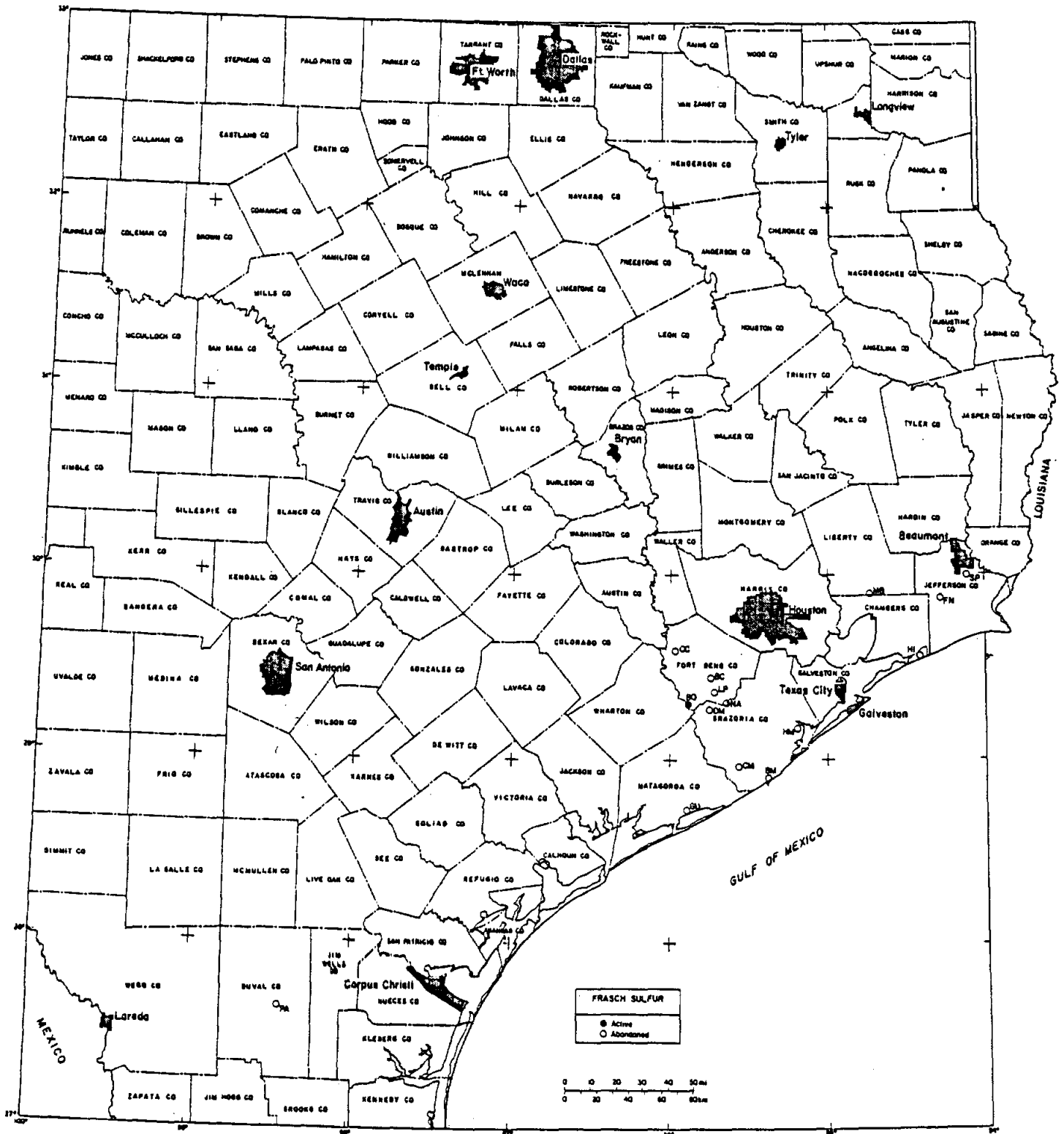


Figure 25. Graph showing the chronology of sulfur mining in Texas salt domes (modified from Ellison, 1971).



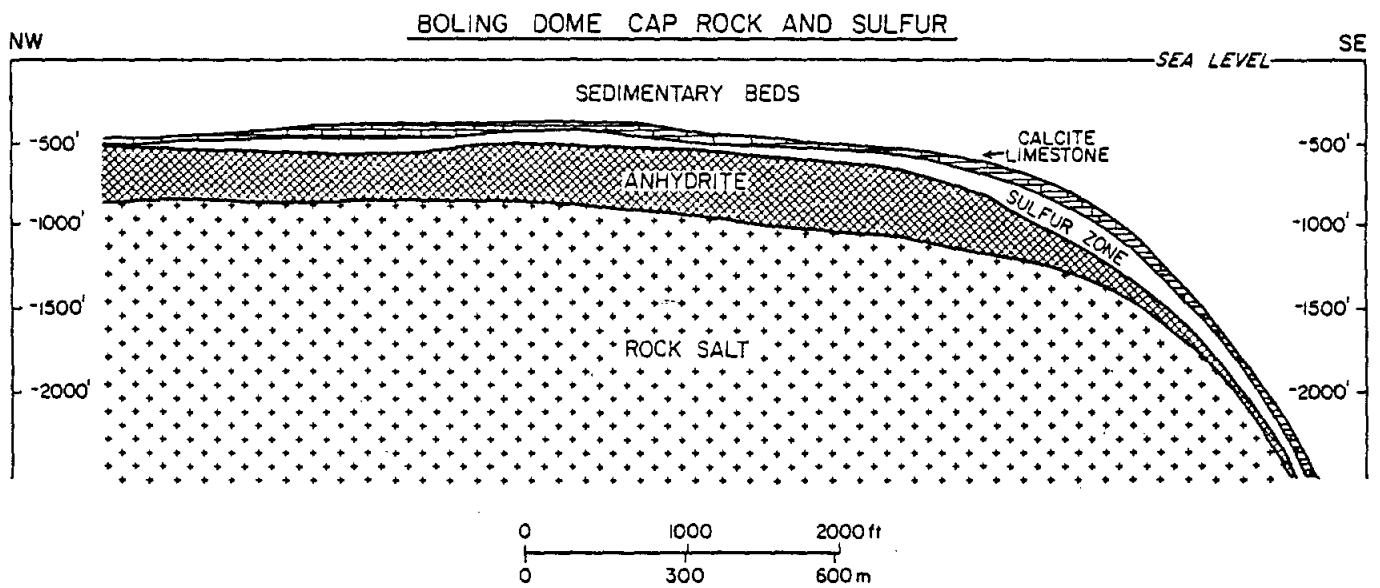
FRASCH SULFUR FROM SALT DOMES OF TEXAS

Figure 26. Map of salt domes showing active and abandoned sulfur mining.

(continued)

Figure 26 (cont.).

Code	Dome Name	County
BC	Big Creek	Fort Bend
BO	Boling	Wharton/Fort Bend
BM	Bryan Mound	Brazoria
CM	Clemens	Brazoria
DM	Damon Mound	Brazoria
FN	Fannett	Jefferson
GU	Gulf	Matagorda
HI	High Island	Galveston
HM	Hoskins Mound	Brazoria
LP	Long Point	Fort Bend
MB	Moss Bluff	Chambers/Liberty
NA	Nash	Brazoria/Fort Bend
OC	Orchard	Fort Bend
PA	Palangana	Duval
SP	Spindletop	Jefferson



QA/2220

Figure 27. Cross section of Boling salt dome showing cap rock and zone of sulfur mineralization (after Myers, 1968).

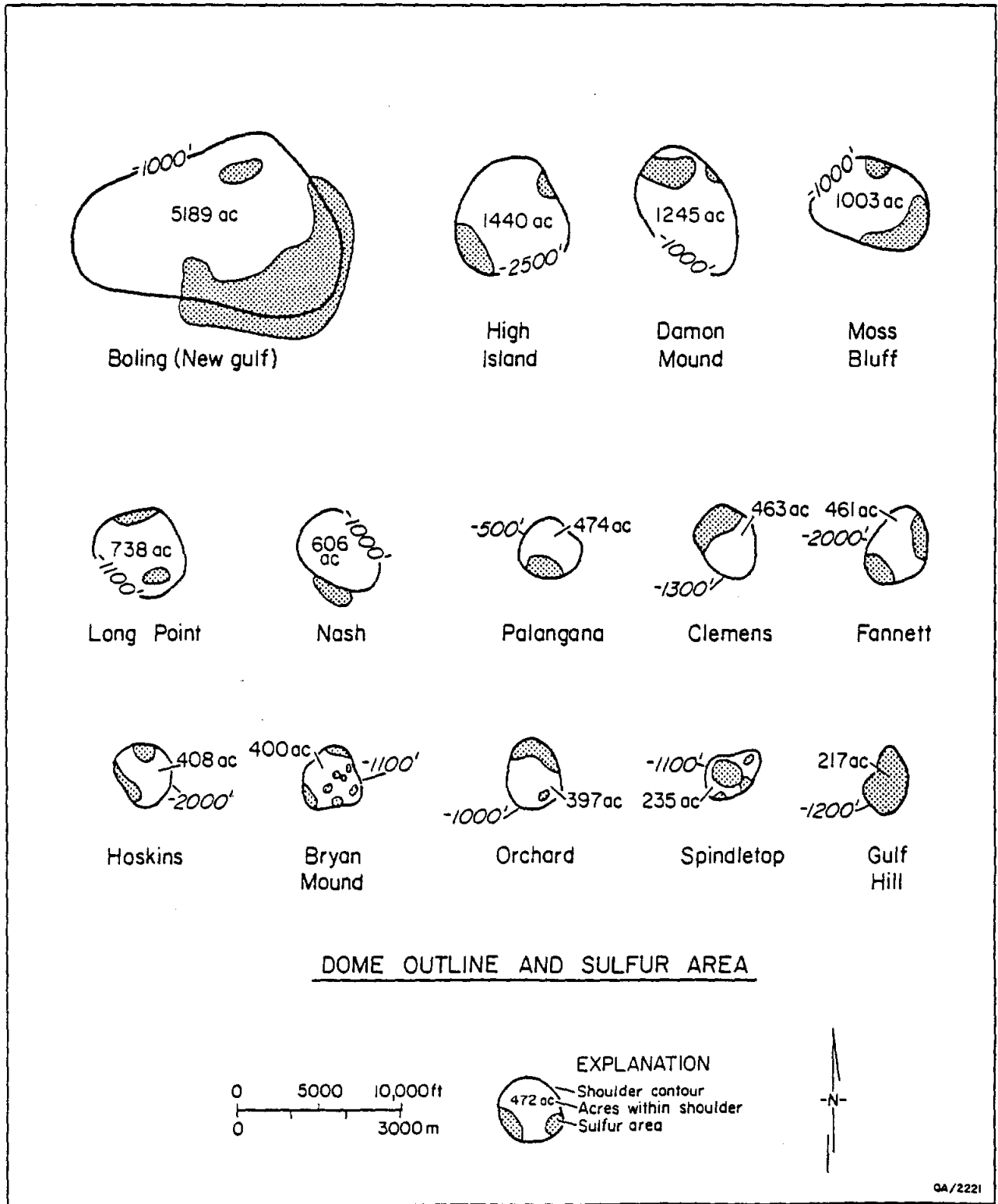


Figure 28. Map of Texas salt domes showing area of sulfur mineralization.

Crushed Stone

Cap rock has been mined from conventional above-ground quarries at Gyp Hill and Damon Mound salt domes. Only the quarry at Damon Mound is currently active. Cap rock has also been exploited on a small scale by underground mining at Hockley salt dome. False-cap-rock, or mineralized supracap, sandstones are now quarried at Butler salt dome. Most of the cap rock is used as road metal and base fill.

Other Resources

Mississippi Valley-type sulfide deposits and uranium have been reported (Smith, 1970a, b) and locally have been explored for in Gulf Coast cap rocks (Price and others, 1983). There has been no commercial production, however. The recent recognition that cap rocks may host Mississippi Valley-type sulfide deposits has generated intense interest in cap-rock genesis and fluid flow around salt domes. Price and others (1983) reported extensive sulfide mineralization and local silver minerals from an annular zone around the periphery of the cap rock. They related the deposition of the sulfide minerals to reduction in the cap rock environment by petroleum and possibly by H_2S , and to periodic expulsion of deep-basin brines that were the mineralizing fluids. Smith (1970a, b) listed 18 Texas coastal domes for which occurrence of sulfide minerals had been reported. Table 5 lists such Texas salt domes, type of sulfide mineral, and documentation.

Table 5. List of salt domes with sulfide mineral occurrences and documentation.

NAME OF SALT DOME	NAME OF SULFIDE	PRODUCTION STATUS	DOCUMENTATION REFERENCE	MINING COMPANY

* BIG HILL	GALENA	OCCURRENCE	SMITH-1970,A,B-	NA
* BLUE RIDGE	PYRITE	OCCURRENCE	SMITH-1970,A,B-	NA
* BOLING	SPHALERITE	OCCURRENCE	SMITH-1970,A,B-	NA
* BOLING	BARITE	OCCURRENCE	SMITH-1970,A,B-	NA
* BOLING	CELESTITE	OCCURRENCE	SMITH-1970,A,B-	NA
* BOLING	GALENA	OCCURRENCE	SMITH-1970,A,B-	NA
* BOLING	HAVERITE	OCCURRENCE	SMITH-1970,A,B-	NA
* BOLING	PYRITE	OCCURRENCE	SMITH-1970,A,B-	NA
* CLEMENS	HAUERITE	OCCURRENCE	SMITH-1970,A,B-	NA
* DAWSON MOUND	MARCASITE	OCCURRENCE	SMITH-1970,A,B-	NA
* DAWSON MOUND	MELANTERITE	OCCURRENCE	SMITH-1970,A,B-	NA
* FANNETT	HAUERITE	OCCURRENCE	SMITH-1970,A,B-	NA
* FANNETT	ALABANDITE	OCCURRENCE	SMITH-1970,A,B-	NA
* FERGUSON CROSSING	GALENA	OCCURRENCE	SMITH-1970,A,B-	NA
* FERGUSON CROSSING	SPHALERITE	OCCURRENCE	SMITH-1970,A,B-	NA
* GULF	GALENA	OCCURRENCE	SMITH-1970,A,B-	NA
* GULF	HAUERITE	OCCURRENCE	SMITH-1970,A,B-	NA
* GULF	PYRITE	OCCURRENCE	SMITH-1970,A,B-	NA
* GULF	SPHALERITE	OCCURRENCE	SMITH-1970,A,B-	NA
* HIGH ISLAND	GALENA	OCCURRENCE	SMITH-1970,A,B-	NA
* HIGH ISLAND	HAUERITE	OCCURRENCE	SMITH-1970,A,B-	NA
* HIGH ISLAND	SPHALERITE	OCCURRENCE	SMITH-1970,A,B-	NA
* HOCKLEY	SPHALERITE	EXPLORATION	CORE-PRICE ET AL-1983	MARATHON MINERALS
* HOCKLEY	GALENA	EXPLORATION	CORE-PRICE ET AL-1983	MARATHON MINERALS
* HOCKLEY	MARCASITE	EXPLORATION	CORE-PRICE ET AL-1983	MARATHON MINERALS
* HOCKLEY	PYRITE	EXPLORATION	CORE-PRICE ET AL-1983	MARATHON MINERALS
* HOSKINS MOUND	GALENA	OCCURRENCE	SMITH-1970,A,B-	NA
* HOSKINS MOUND	HAUERITE	OCCURRENCE	SMITH-1970,A,B-	NA
* HOSKINS MOUND	SPHALERITE	OCCURRENCE	SMITH-1970,A,B-	NA
* HOSKINS MOUND	PYRRHOTITE	OCCURRENCE	SMITH-1970,A,B-	NA
* HUMBLE	GALENA	OCCURRENCE	SMITH-1970,A,B-	NA
* MOSS BLUFF	HAUERITE	OCCURRENCE	SMITH-1970,A,B-	NA
* ORCHARD	SPHALERITE	OCCURRENCE	SMITH-1970,A,B-	NA
* ORCHARD	GALENA	OCCURRENCE	SMITH-1970,A,B-	NA
* PALANGANA DOME	SPHALERITE	OCCURRENCE	SMITH-1970,A,B-	NA
* PALANGANA DOME	GALENA	OCCURRENCE	SMITH-1970,A,B-	NA
* PIERCE JUNCTION	GALENA	OCCURRENCE	SMITH-1970,A,B-	NA
* SOUR LAKE	PYRRHOTITE	OCCURRENCE	SMITH-1970,A,B-	NA
* SOUR LAKE	PYRITE	OCCURRENCE	SMITH-1970,A,B-	NA
* SPINDLETOP	PYRITE	OCCURRENCE	SMITH-1970,A,B-	NA

list/title l(18)name of salt dome,b(3),r(15)name of sulfide,
LIST/TITLE L(18)NAME OF SALT DOME,B(3),R(15)NAME OF SULFIDE,

b(3),r(12)production +status ,b(3),r(25)documentation reference,
B(3),R(12)PRODUCTION +STATUS ,B(3),R(25)DOCUMENTATION REFERENCE,

b(3),r(20)mining company /c1,c199,c200,c201,c202,ob low cl
B(3),R(20)MINING COMPANY /C1,C199,C200,C201,C202,OB LOW C1

wh c200 eq exploration or c200 eq occurrence:
WH C200 EQ EXPLORATION OR C200 EQ OCCURRENCE:

ACKNOWLEDGMENTS

Thanks are extended to Texas Railroad Commission personnel Mark Browning (Central Records) and J. W. Mullican (Underground Injection Control), who provided easy access to records and files. Discussions with the following industry representatives were very helpful: Kermit Allen, Jose Machado, and Edward Voorhees (Fenix and Scisson, Inc.), Neils Van Fossan (Texas Brine Company), Ferris Samuelson (Texas Gulf Sulfur), Carl Brassow (United Resource Recovery, Inc.), Jack Piskura (Pakhoed, Inc.), and Bill Ehni and Mark Katterjohn (Geotronics Corporation). Word processing was done by Joann Haddock, under the supervision of Lucille C. Harrell. Mark Bentley, Tom Byrd, Jeff Horowitz, Jamie McClelland, and Richard Platt drafted the figures, under the supervision of Dick Dillon.

REFERENCES

- Autin, W. J., 1984, Observations and significance of sinkhole development at Jefferson Island: Louisiana Geological Survey Department of Natural Resources Geological Pamphlet No. 7, 75 p.
- Bays, C. A., 1963, Use of salt solution cavities for underground storage: Northern Ohio Geological Society, 1st International Symposium on Salt, Cleveland, Ohio, p. 564-578.
- Ellison, S. P., Jr., 1971, Sulfur in Texas: The University of Texas at Austin, Bureau of Economic Geology, Handbook No. 2, 48 p.
- Fenix and Scisson, Inc., 1976a, Review of applicable technology--solution mining of caverns in salt domes to serve as repositories for radioactive wastes: Prepared for U.S. Energy Research and Development Administration, Office of Nuclear Waste Isolation, Oak Ridge, Tennessee, Y/OWI/SUB-76/92880, 122 p.
- _____ 1976b, Final report, Project 1, investigation of new leached caverns in salt domes, vol. 1: Prepared for U.S. Federal Energy Administration, Washington, D. C.
- _____ 1976c, Final report, Project 1, investigation of new leached caverns in salt domes, vol. 2: Prepared for U.S. Federal Energy Administration, Washington, D.C.
- _____ 1976d, Final report, Project 2, engineering feasibility study of underground storage in existing leached caverns in salt formations: Prepared for U.S. Federal Energy Administration, Washington, D.C.
- Fogg, G. E., and Kreitler, C. W., 1980, Impacts of salt-brining on Palestine Dome: in Kreitler, C. W., and others, Geology and geohydrology of the East Texas Basin: a report on the progress of nuclear waste isolation feasibility studies (1979): The University of Texas at Austin, Bureau of Economic Geology Geological Circular 80-12, p. 46-54.
- Fossum, A. F., 1976, Structural analysis of salt cavities formed by solution mining: I. Method of analysis and preliminary results for spherical cavities: Prepared for U.S. Energy Research

- and Development Administration, Office of Nuclear Waste Isolation, Oak Ridge, Tennessee, ORNL/SUB-4269/19, 26 p.
- Galloway, W. E., Ewing, T. E., Garrett, C. M., Tyler, N., and Bebout, D. G., 1983, Atlas of major Texas oil reservoirs: The University of Texas at Austin, Bureau of Economic Geology Special Publication, 139 p.
- Gas Processors Association, 1983, North American storage capacity for light hydrocarbons and U.S. LP-gas import terminals 1983: Tulsa, Oklahoma, 26 p.
- Griswold, G. B., 1981, Solution mining in salt domes of the Gulf Coast Embayment: Richland, Washington, Pacific Northwest Laboratory, prepared for Office of Nuclear Waste Isolation, PNL-3190.
- Halbouty, M. T., 1979, Salt domes; Gulf region, United States and Mexico, 2d ed.: Houston, Texas, Gulf Publishing, 561 p.
- Hanna, M. A., 1939, Evidence of erosion of salt stock in Gulf Coast salt plug in late Oligocene: American Association of Petroleum Geologists Bulletin, v. 23, no. 4, p. 604-607.
- Hart, R. J., Ortiz, T. S., and Magorian, T. R., 1981, Strategic petroleum reserve (SPR) geological site characterization report, Big Hill salt dome: Sandia National Laboratories, Albuquerque, New Mexico, SAND81-1085.
- Hawkins, M. E., and Jirik, C. J., 1966, Salt domes in Texas, Louisiana, Mississippi, Alabama, and offshore tidelands: a survey: U.S. Bureau of Mines Information Circular 8313, 78 p.
- Hopkins, O. B., 1917, The Palestine salt dome, Anderson County, Texas: U.S. Geological Survey Bulletin 661, contributed to Economic Geology, pt. 2, Mineral Fuels, p. 253-270.
- Jackson, M. P. A., and Seni, S. J., 1983, Suitability of salt domes in the East Texas Basin for nuclear-waste isolation: final summary of geologic and hydrogeologic research: The University of Texas at Austin, Bureau of Economic Geology, milestone contract report for the U.S. Department of Energy under Contract No. DE-AC97-80ET46617, 247 p.
- Jackson, M. P. A., and Seni, S. J., 1984, The domes of East Texas: in Presley, M. W., ed., The Jurassic of East Texas: East Texas Geological Society, p. 163-239.

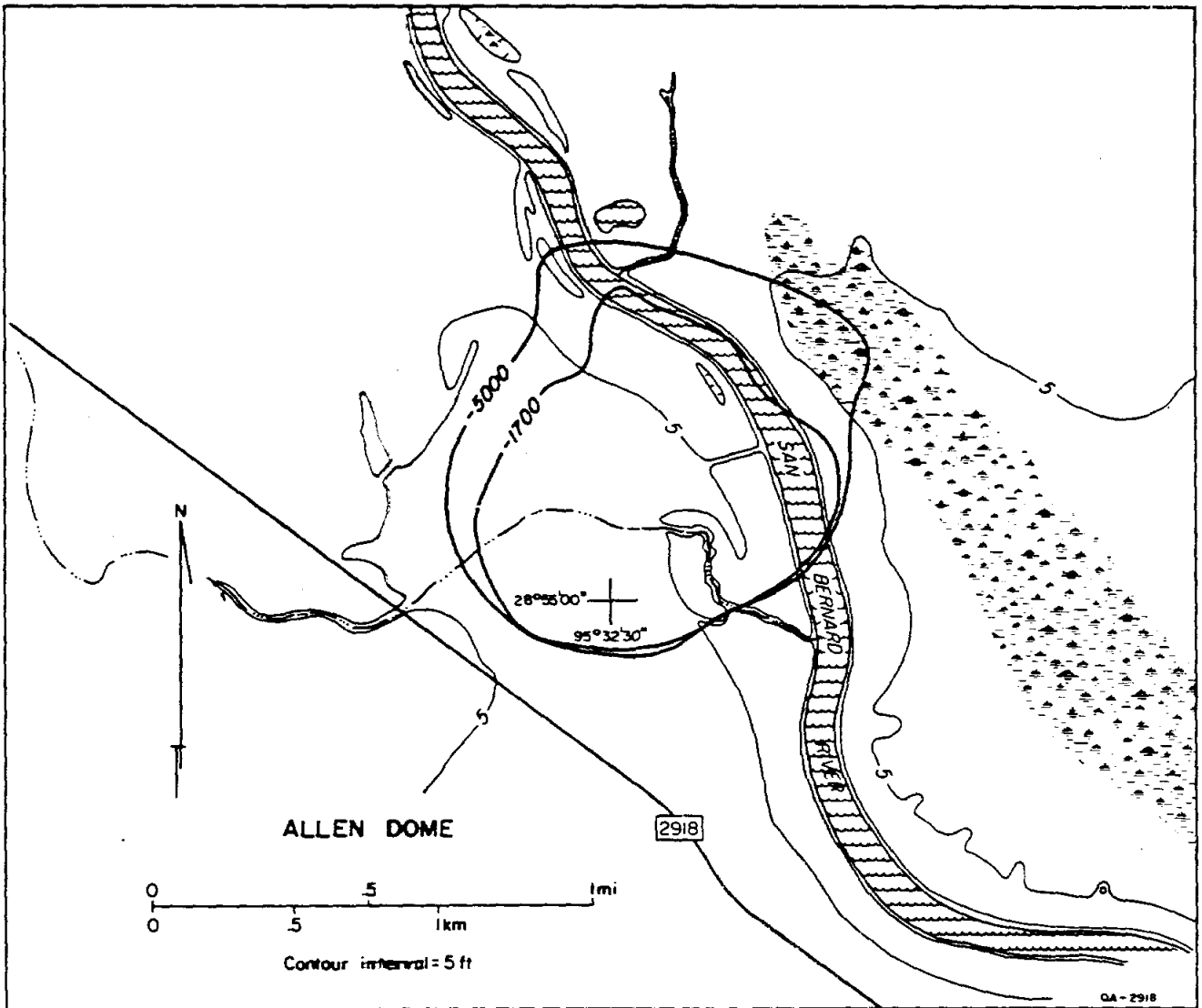
- Jirik, C. J., and Weaver, L. K., 1976, A survey of salt deposits and salt caverns, their relevance to the strategic petroleum reserve: Federal Energy Administration, Report FEA/S-76/310, 64 p.
- Martinez, J. D., Thoms, R. L., Kupfer, D. H., Smith, C. J., Jr., Kolb, C. R., Newchurch, E. J., Wilcox, R. E., Manning, T. A., Jr., Romberg, M., Lewis, A. J., Rovik, J. E., 1976, An investigation of the utility of Gulf Coast salt domes for isolation of nuclear wastes: Louisiana State University Institute for Environmental Studies, Baton Rouge, Report No. ORNL-SUB-4112-25, prepared for U.S. Department of Energy, 329 p.
- Minihan, T. J., and Querio, C. W., 1973, Simultaneous storage of LPG and production of brine, Pierce Junction Dome, Houston, Texas: Northern Ohio Geological Society, 4th Symposium on Salt, Cleveland, Ohio, v. 2, p. 285-290.
- Myers, J. C., 1968, Gulf Coast sulfur resources: in Brown, L. F., Jr., ed., Fourth Forum on Geology of Industrial Minerals: The University of Texas at Austin, Bureau of Economic Geology Special Publication, p. 57-65.
- Powers, S., 1926, Interior salt domes of Texas: American Association of Petroleum Geologists Bulletin, v. 10, no. 1, p. 1-60.
- Price, P. E., Kyle, J. R., and Wessel, G. R., 1983, Salt-dome related zinc-lead deposits: in Kisvarsanyi, G., and others, eds., Proceedings, International Conference on Mississippi Valley-Type Lead-Zinc Deposits: University of Missouri, Rolla, p. 558-571.
- Science Applications, Inc., 1977, The mechanisms and ecological impacts of the collapse of salt dome oil storage caverns: McLean, Virginia, Report No. 5-210-00-567-04.
- Seni, S. J., and Jackson, M. P. A., 1983a, Evolution of salt structures, East Texas diapir province, part 1: sedimentary record of halokinesis: American Association of Petroleum Geologists Bulletin, v. 67, no. 8, p. 1219-1244.
- _____ 1983b, Evolution of salt structures, East Texas diapir province, part 2: patterns and rates of halokinesis: American Association of Petroleum Geologists Bulletin, v. 67, no. 8, p. 1245-1274.

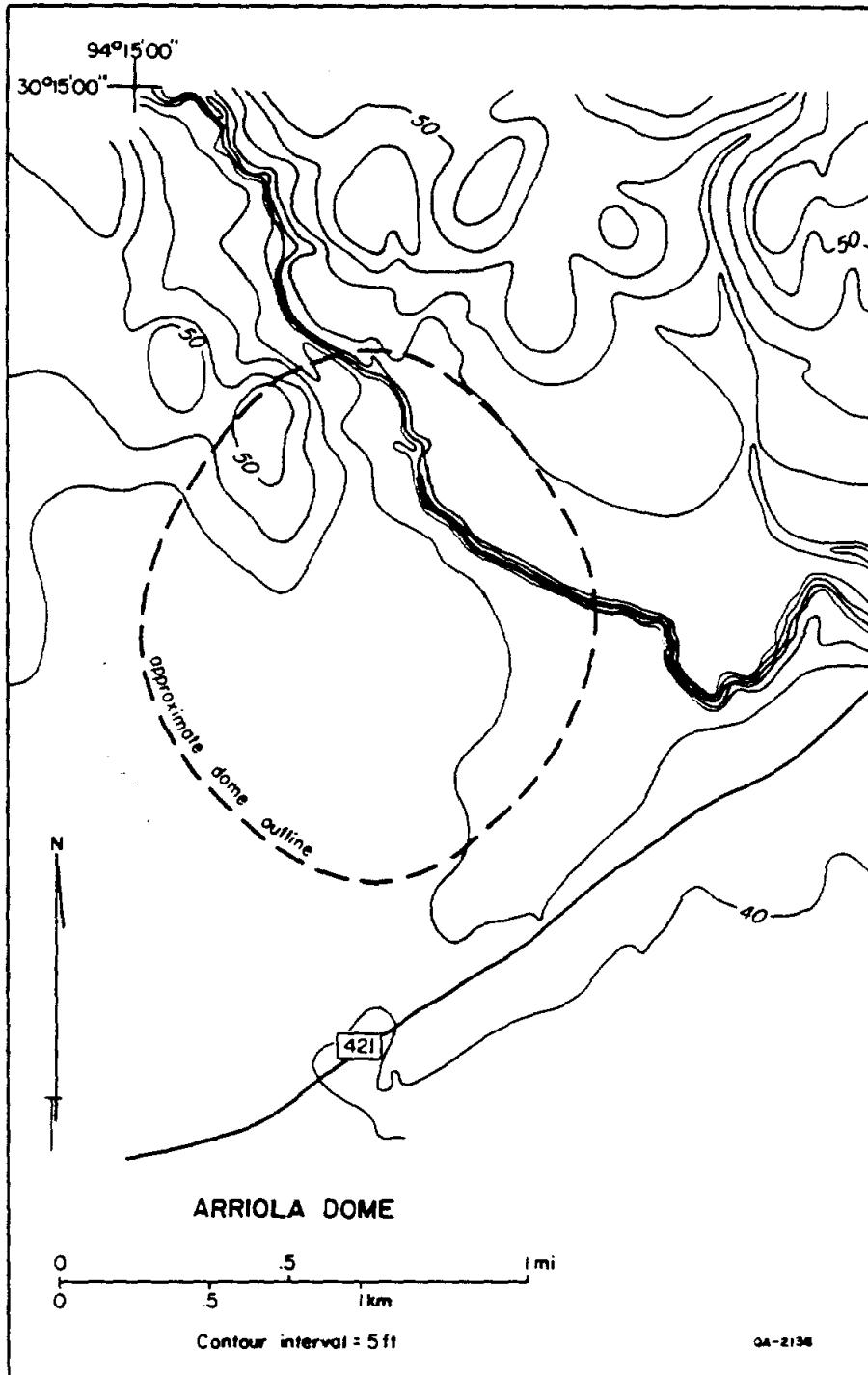
- Smith, A. E., Jr., 1970a, Minerals from Gulf Coast salt domes, part I: rocks and minerals, v. 45, no. 5, p. 299-303.
- Smith, A. E., Jr., 1970b, Minerals from Gulf Coast salt domes, part II: rocks and minerals, v. 45, no. 6, p. 371-380.
- Smith, G. I., Jones, C. L., Culbertson, W. C., Ericksen, G. E., Dyni, J. R., 1973, Evaporites and brines: in Brobst, D. A., and Pratt, W. P., eds., United States Mineral Resources: U.S. Geological Survey Professional Paper 820, p. 197-216.
- U.S. Federal Energy Administration, 1977a, Strategic petroleum reserve, final environmental impact statement for Cote Blanche Mine: FEA/S-77/016, FES 76/77-7.
- _____ 1977b, Strategic petroleum reserve, final environmental impact statement, Bryan Mound salt dome: FEA/S-76/502, FES 76/77-6.
- _____ 1977c, Strategic petroleum reserve, final environmental impact statement (final supplement to FEA FES 76/77-6), Bryan Mound salt dome, Brazoria County, Texas: DOE/EIS-0001.
- Underground Resource Management, 1982, Hydrogeologic investigation in the vicinity of Barbers Hill salt dome: Austin, Texas, Job No. 82-807, 104 p.
- United Resource Recovery, Inc., 1983, Application of United Resource Recovery, Inc., to dispose of waste by well injection at the Boling salt dome: Submitted by Keysmith Corp., Austin, Texas, 121 p.
- Van Fossan, N. E., 1979, Mechanisms of product leakage from solution caverns: Northern Ohio Geological Society, 5th Symposium on Salt, Cleveland, Ohio, v. 2, p. 213-230.
- Van Fossan, H., and Prosser, L. E., 1949, The application of free jets to the mixing of fluids in bulk: London, Institute of Mechanical Engineers Proceedings, v. 160, p. 224-251.
- Winker, C. D., Morton, R. A., Ewing, T. E., and Garcia, D. D., 1983, Depositional setting, structural style, and sandstone distribution in three geopressed geothermal areas, Texas Gulf Coast: The University of Texas at Austin, Bureau of Economic Geology Report of Investigations No. 134, 60 p.

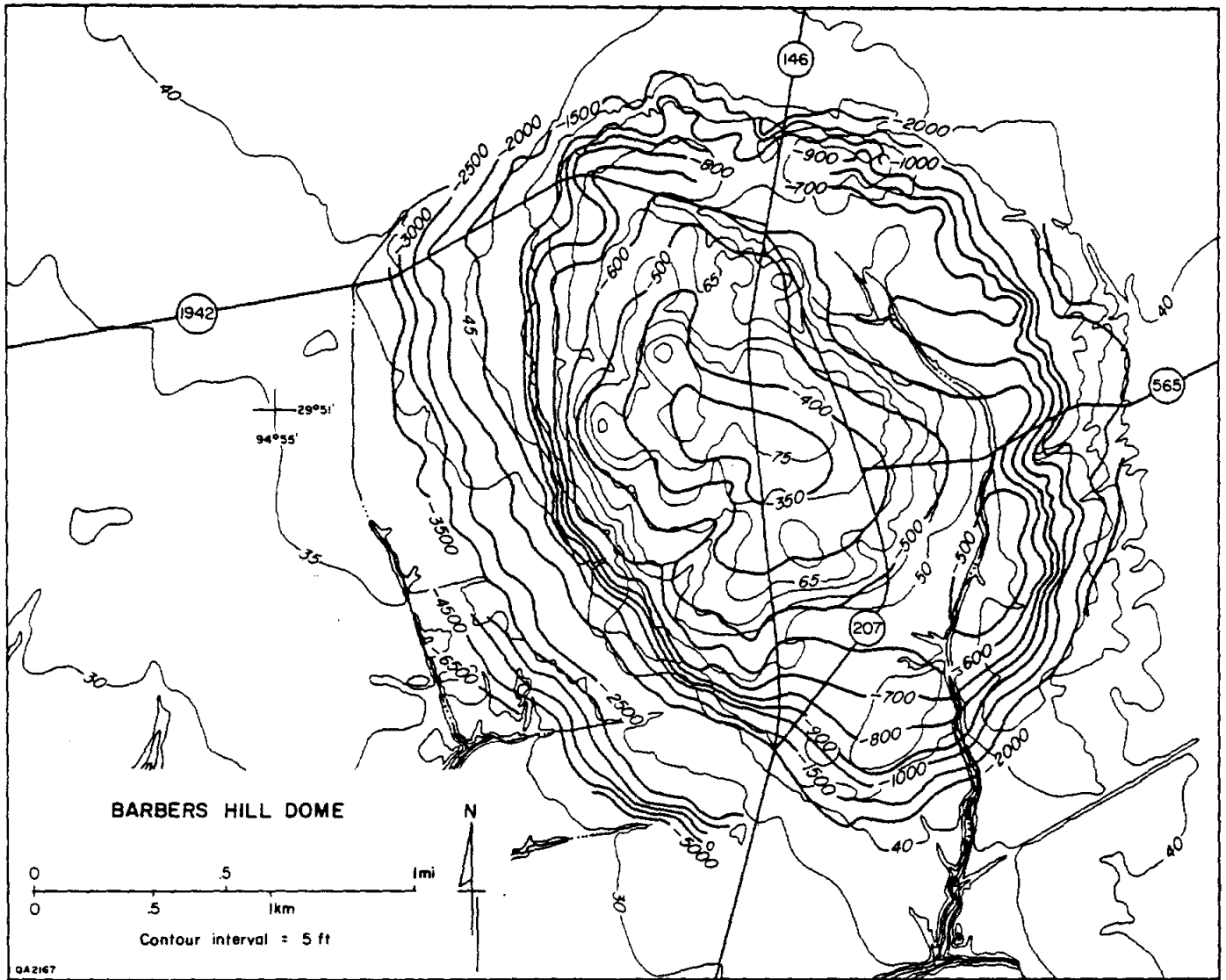
Wood, D. H., and Giles, A. B., 1982, Hydrocarbon accumulation patterns in the East Texas salt dome province: The University of Texas at Austin, Bureau of Economic Geology Geological Circular 82-6, 36 p.

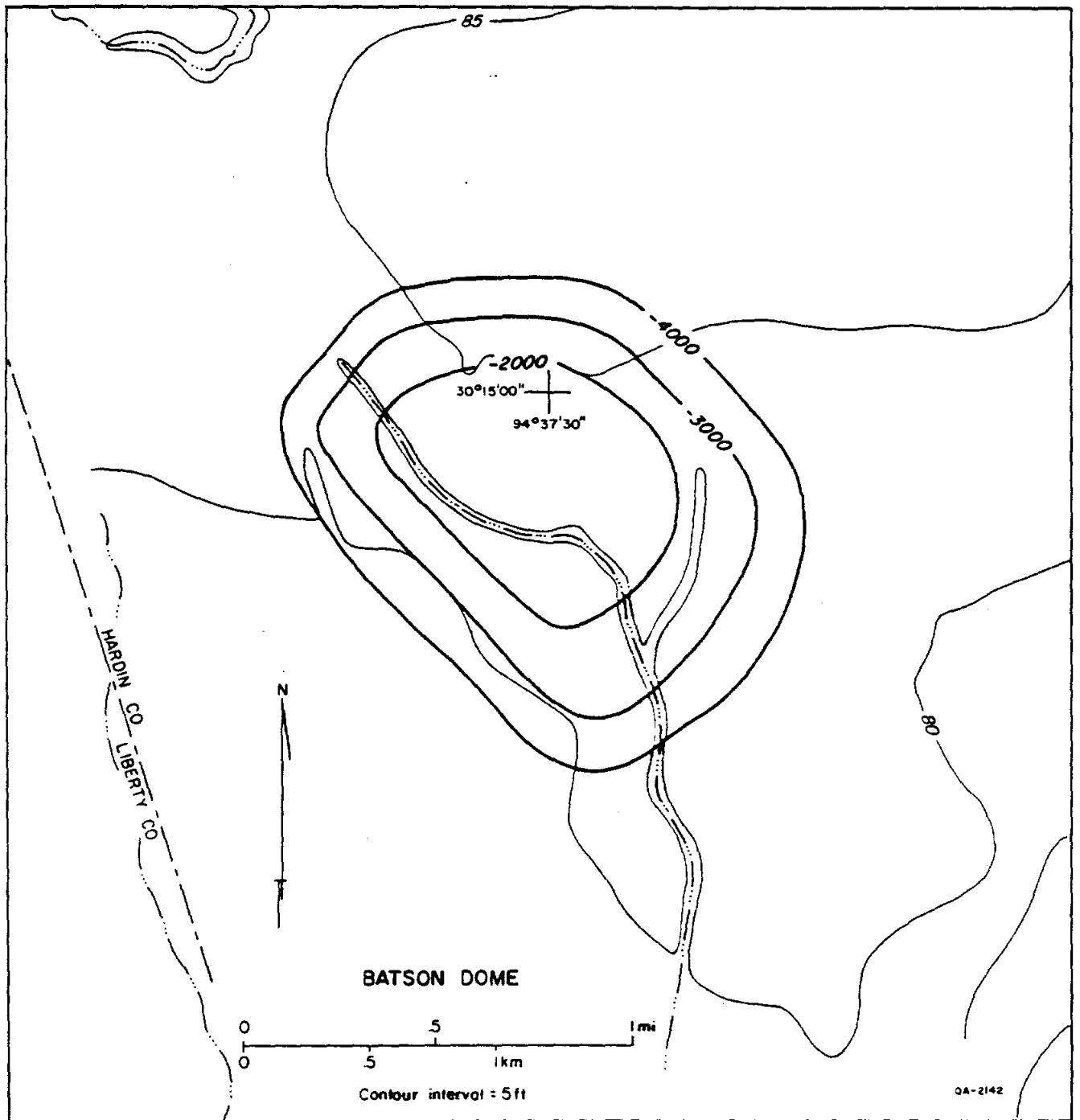
APPENDIX 1: Texas salt domes: natural resources, storage caverns, and extraction technology.

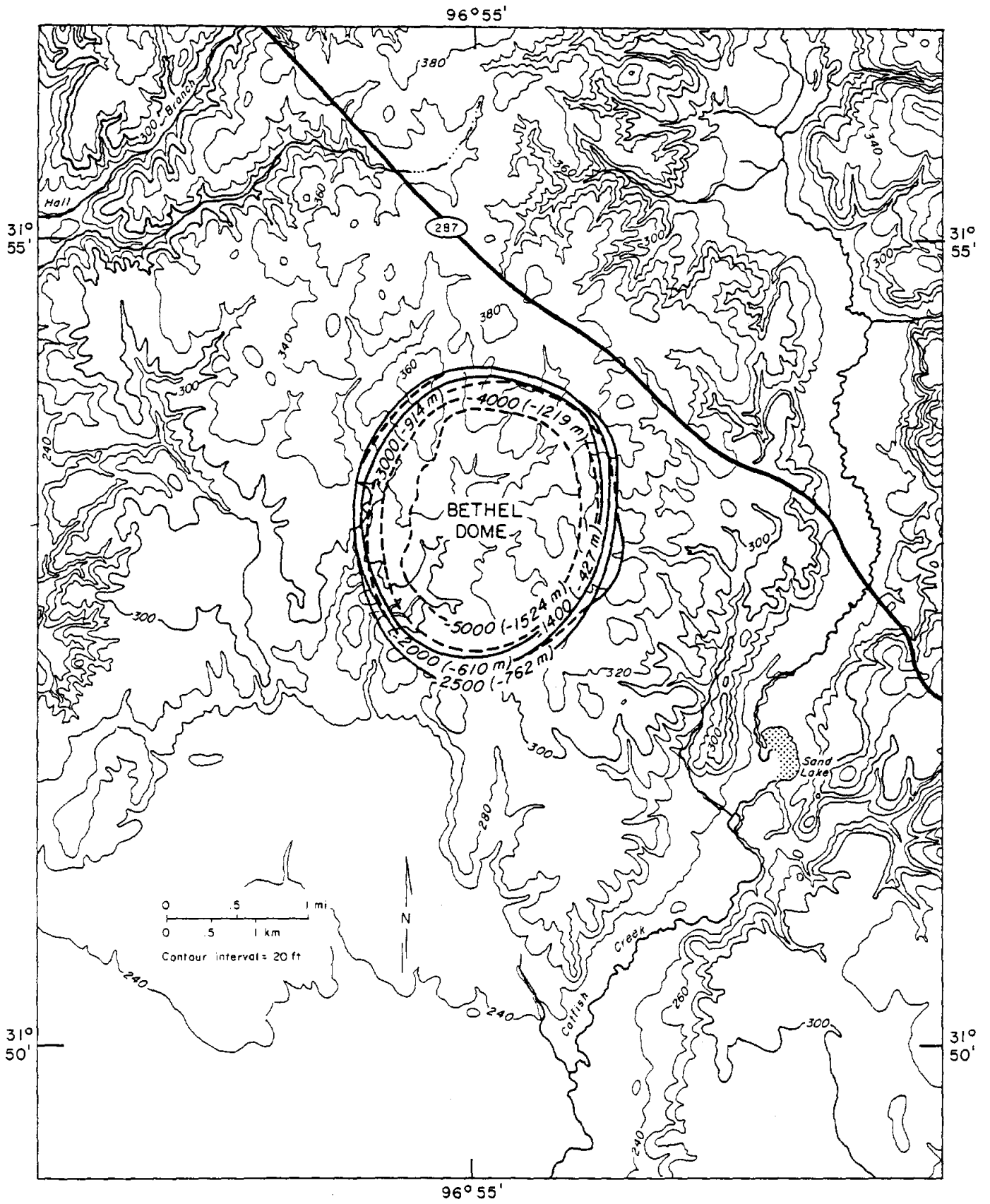
Structure-contour maps of Texas salt domes. Heavy lines are salt structure contours; light lines are surface topographic contours.

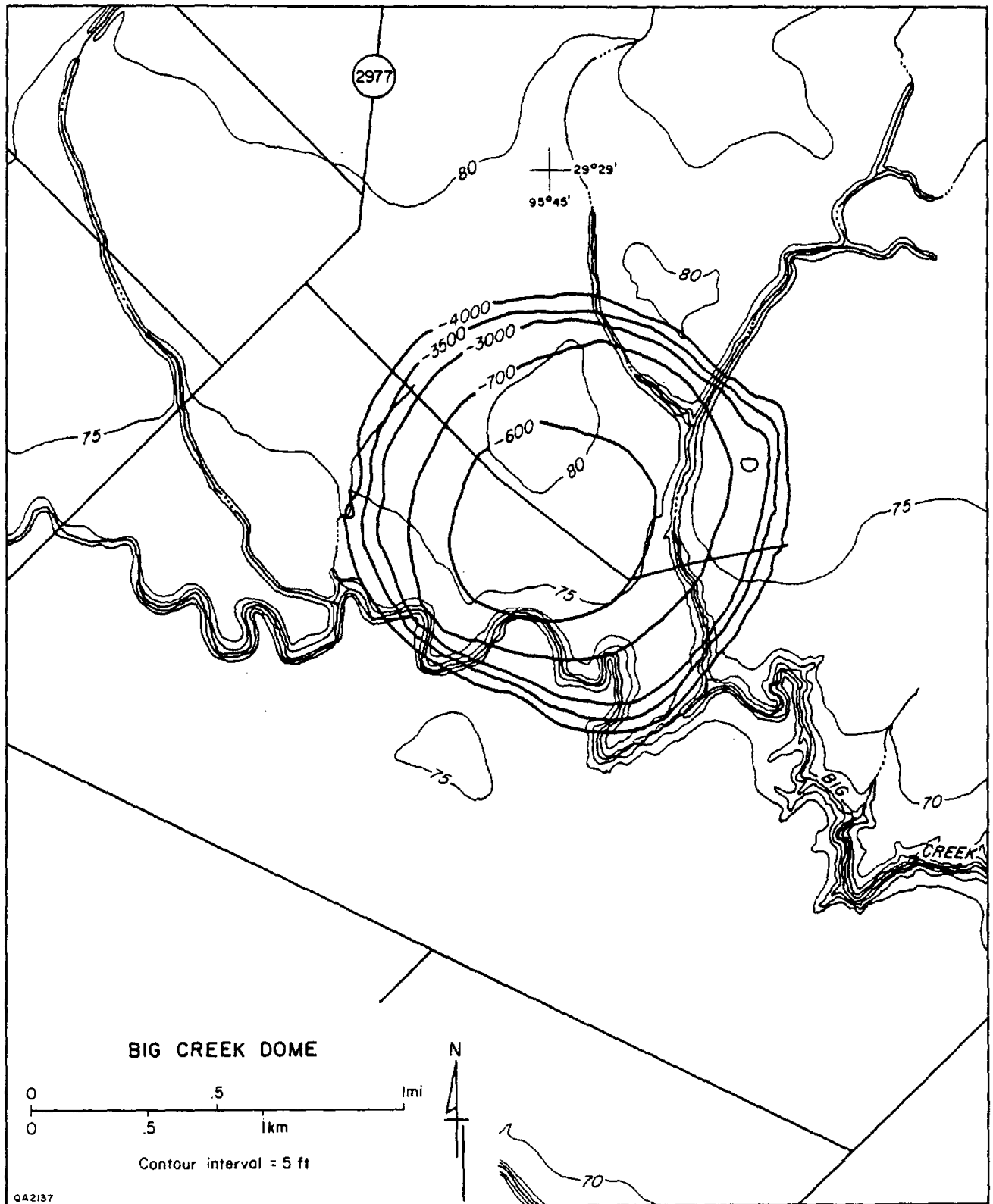




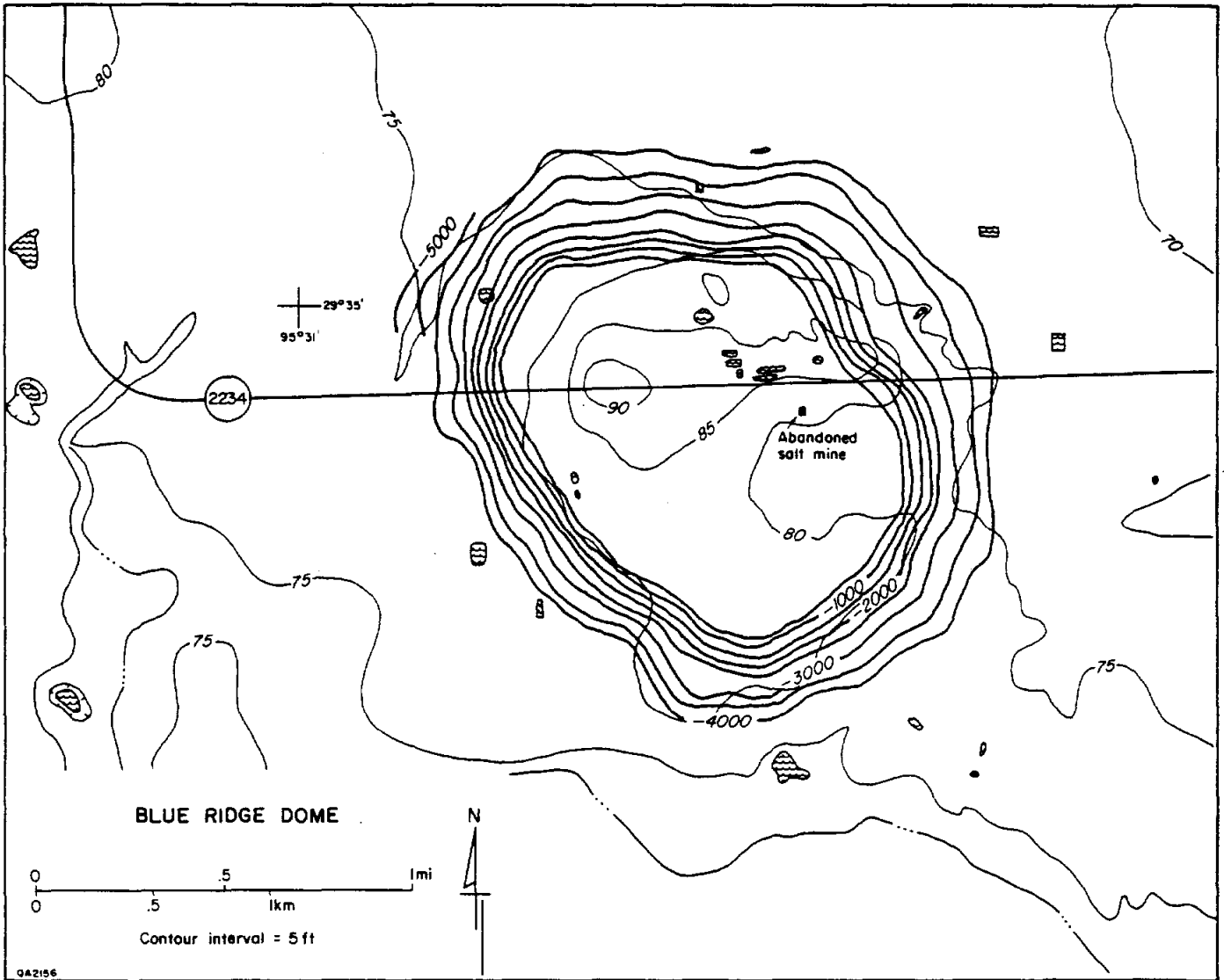




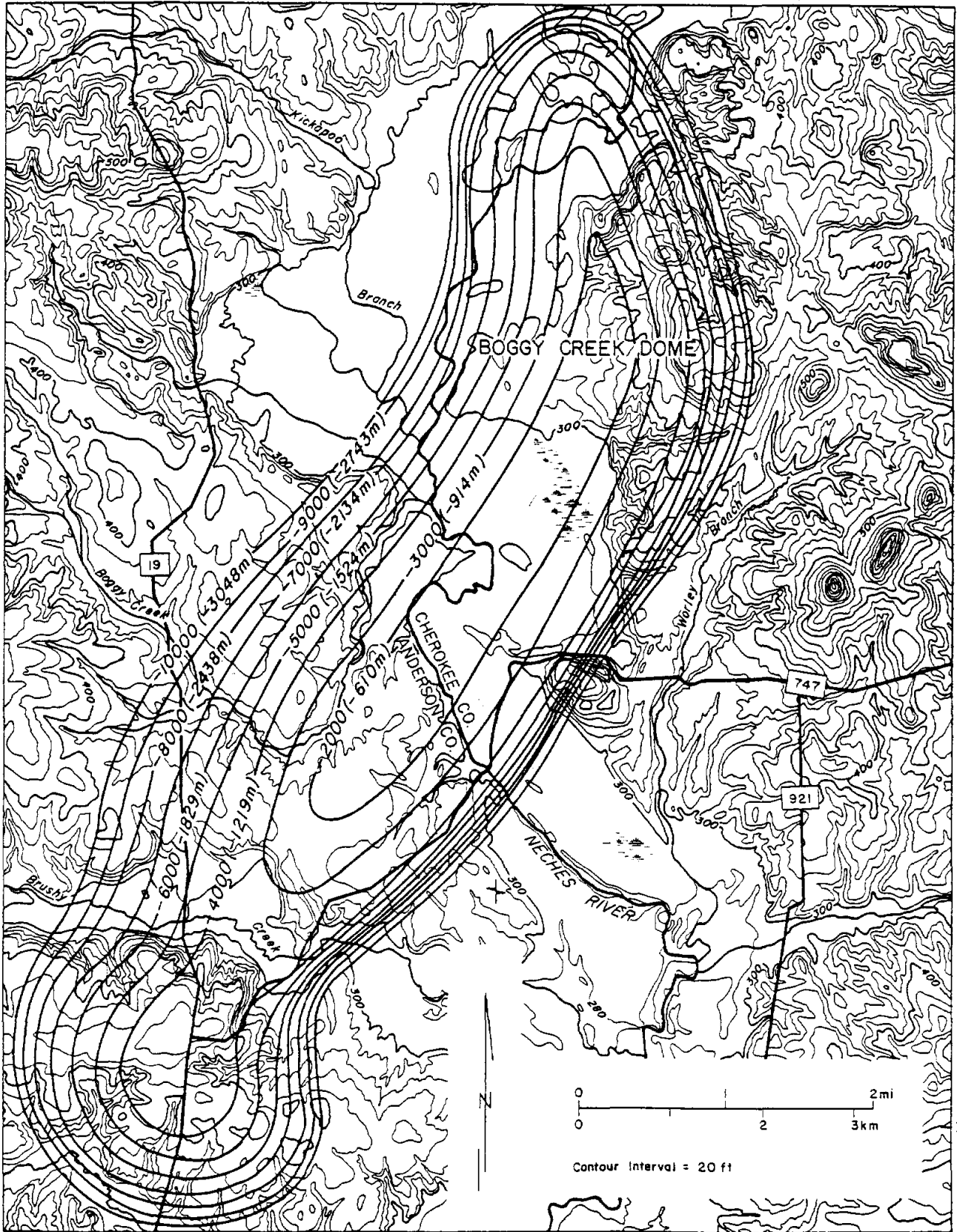








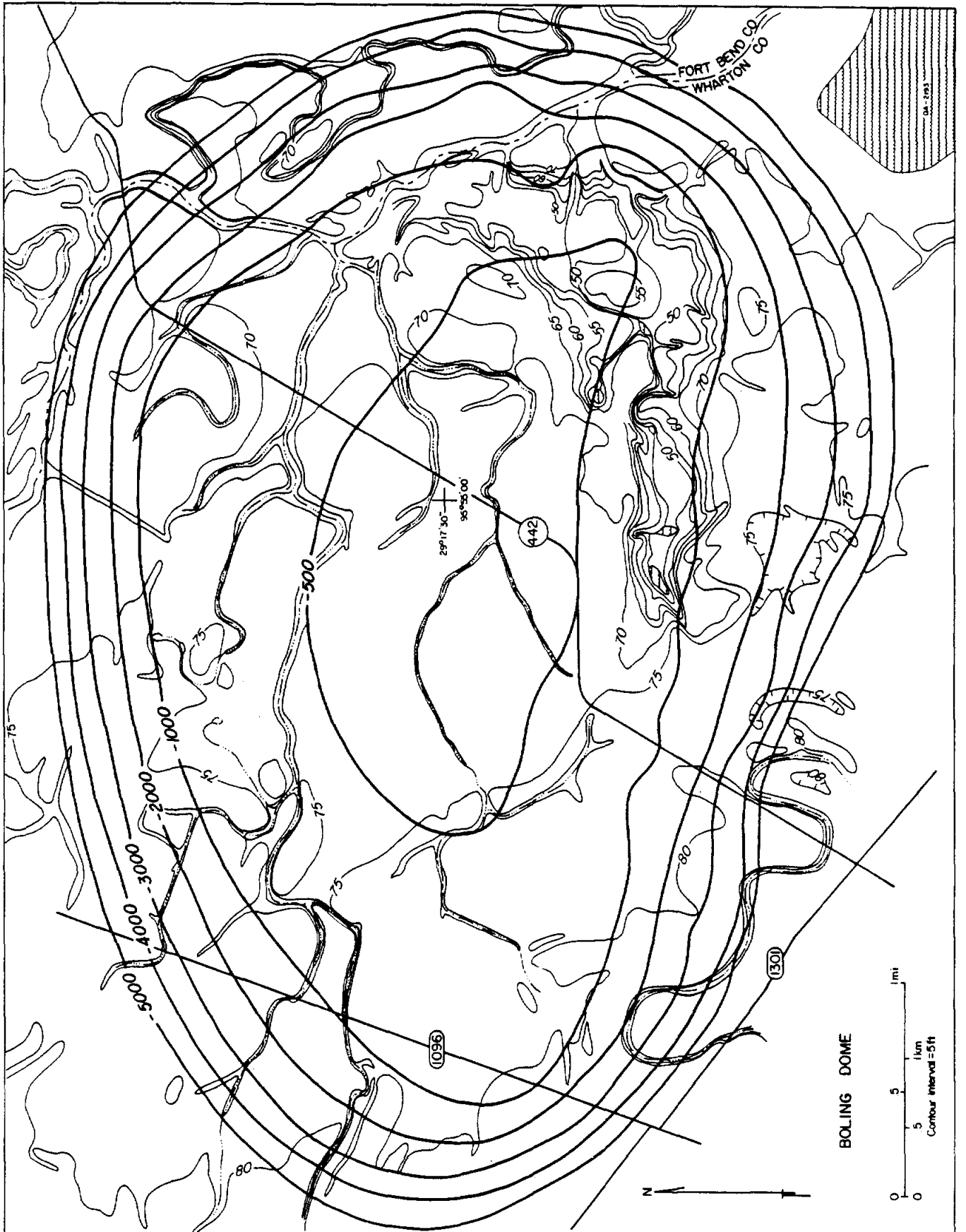
95° 25'

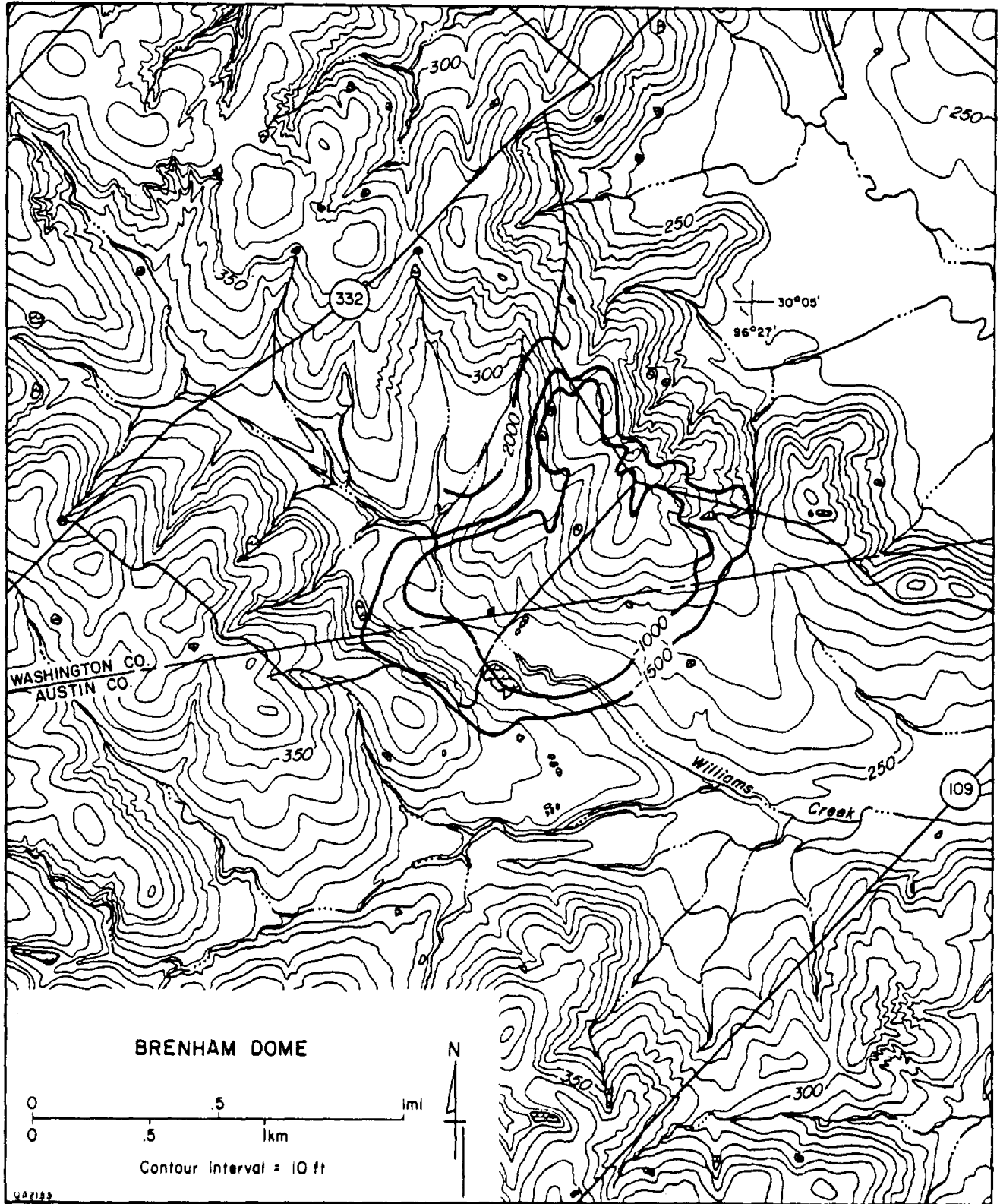


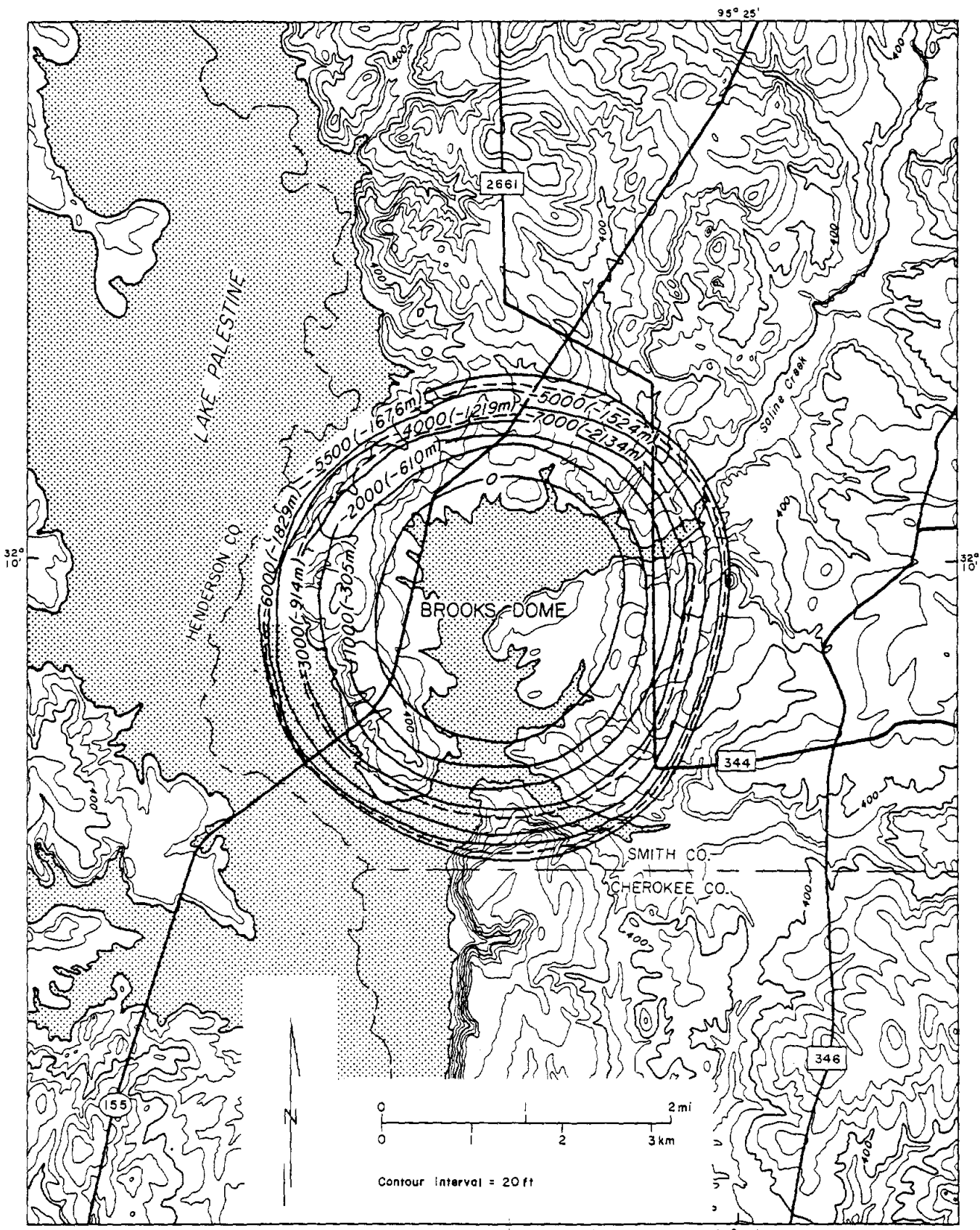
95° 25'

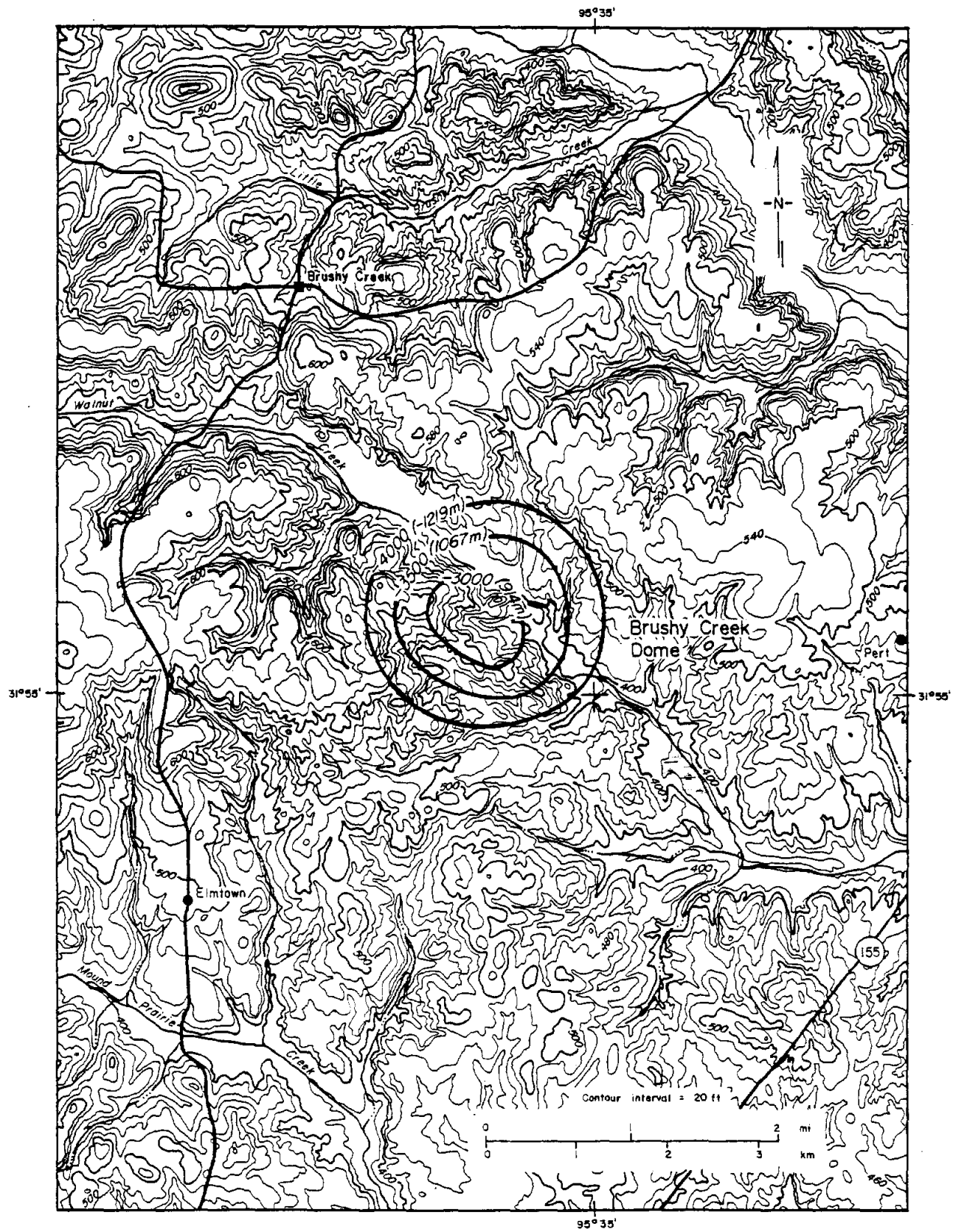
31° 55'

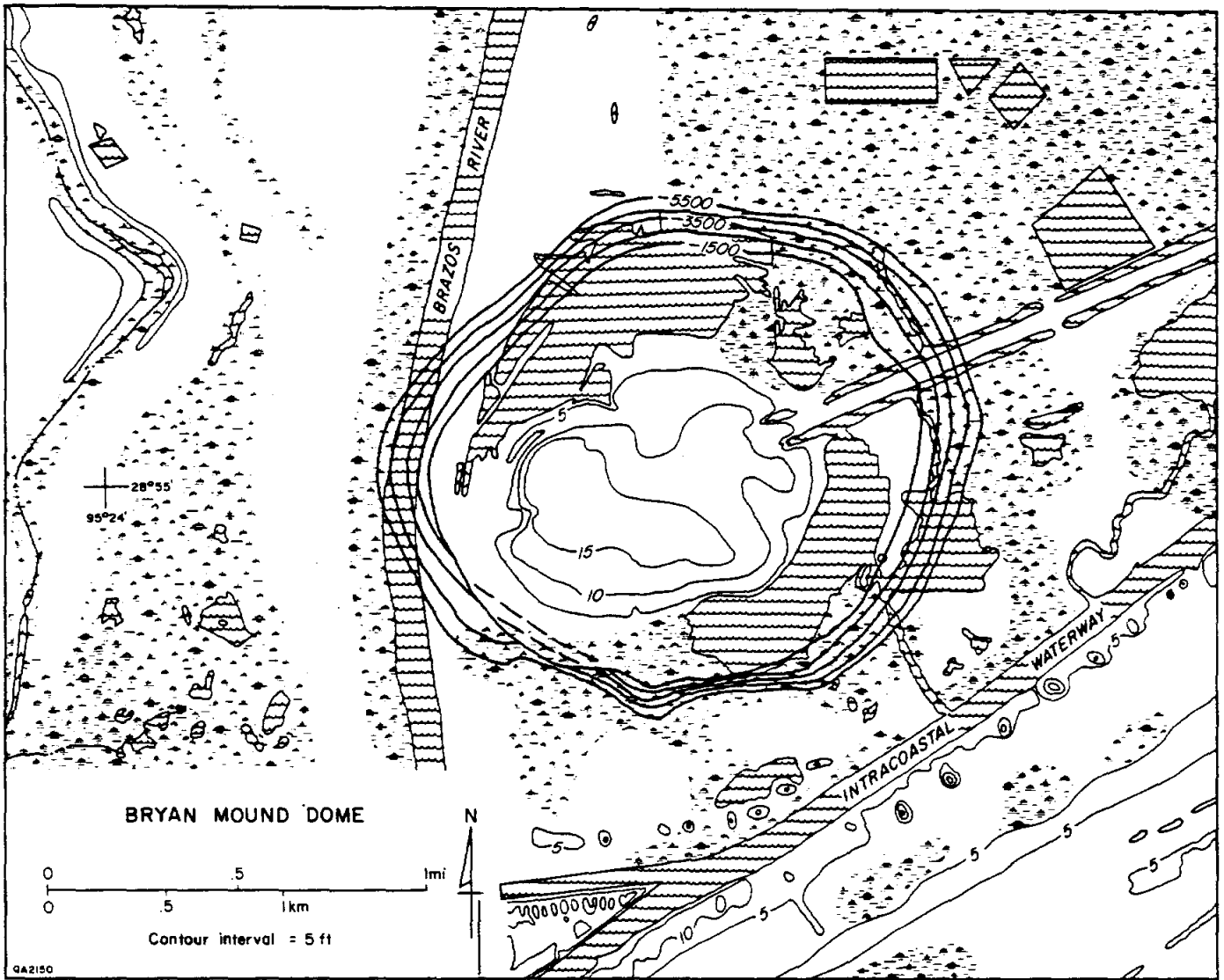
31° 55'

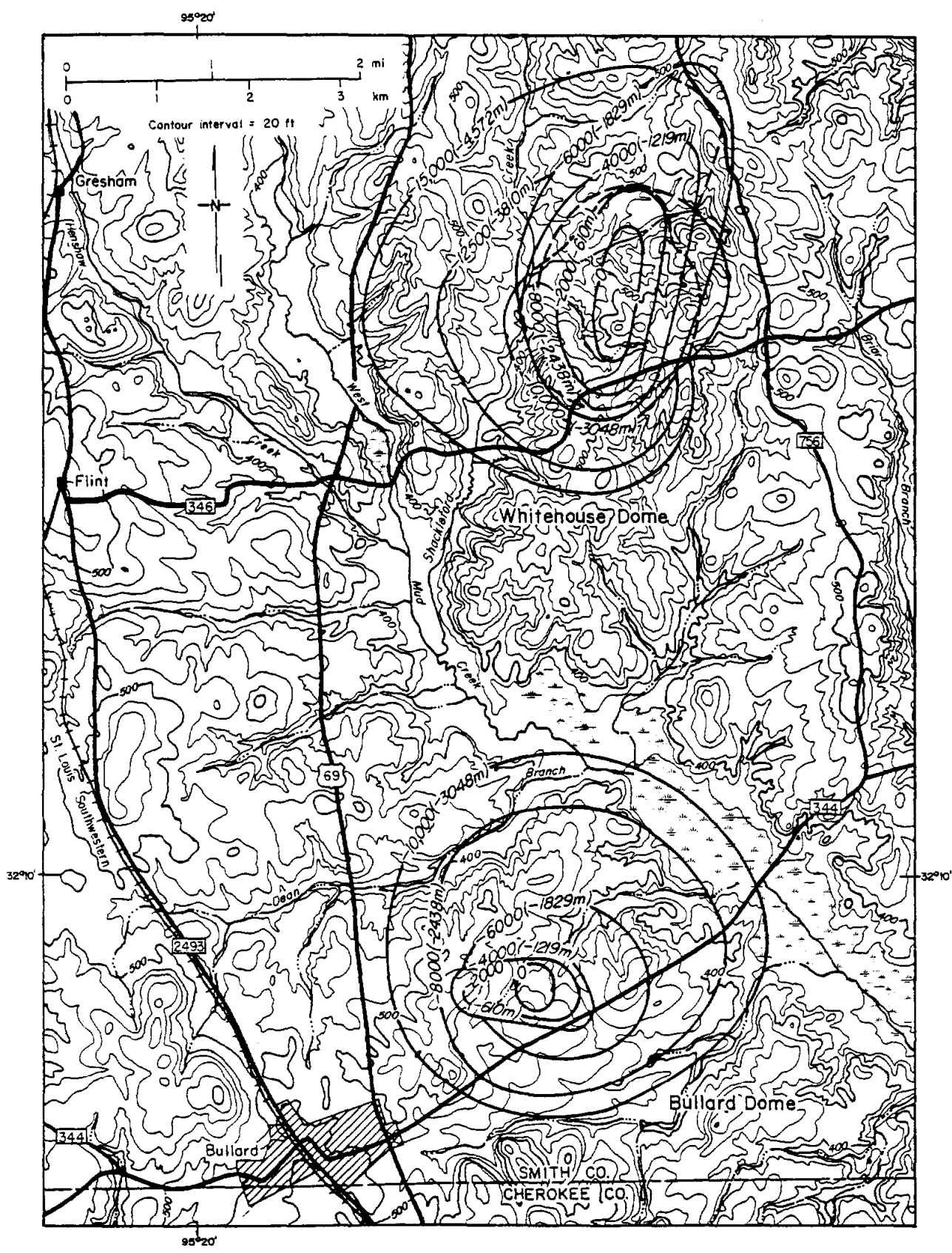


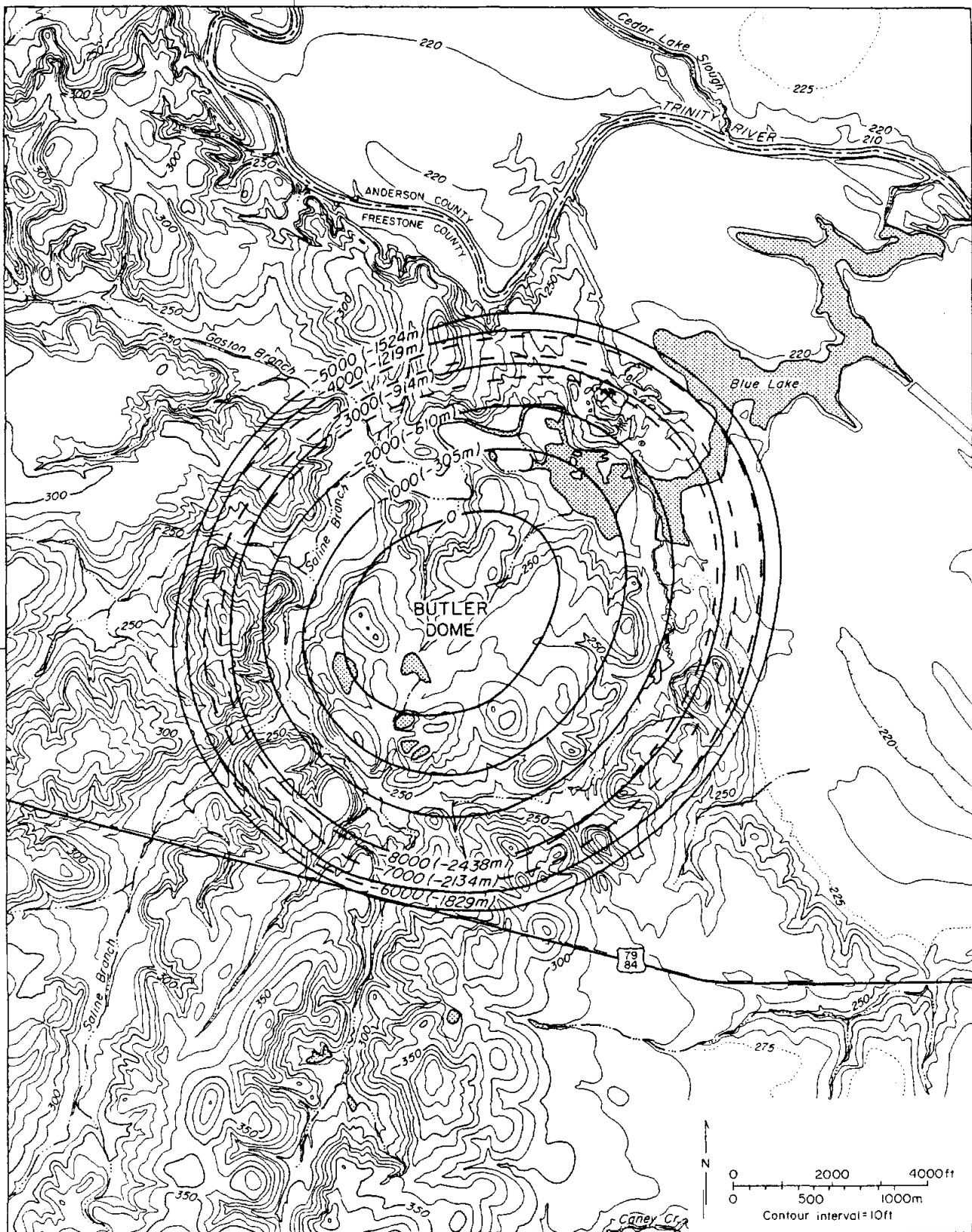


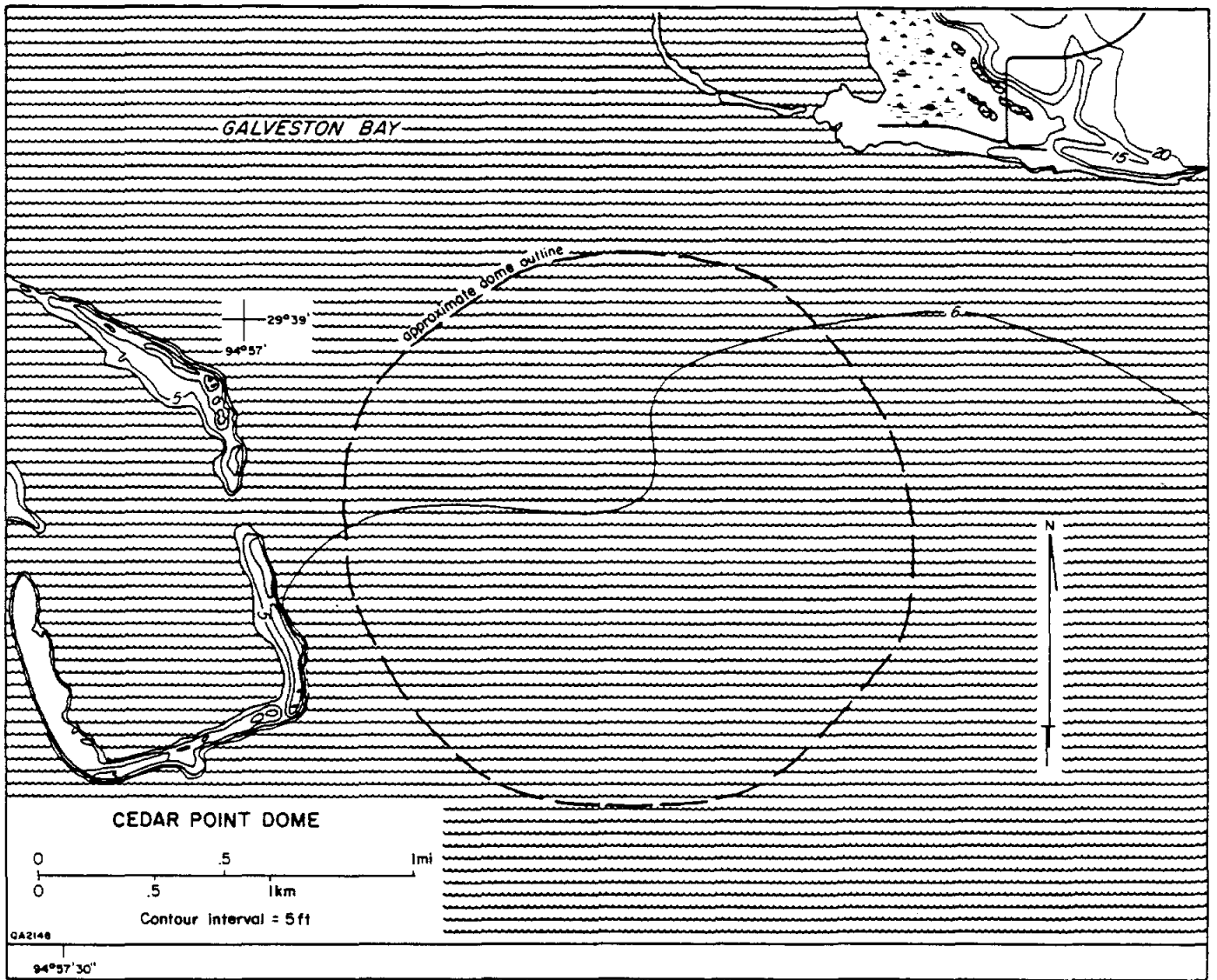




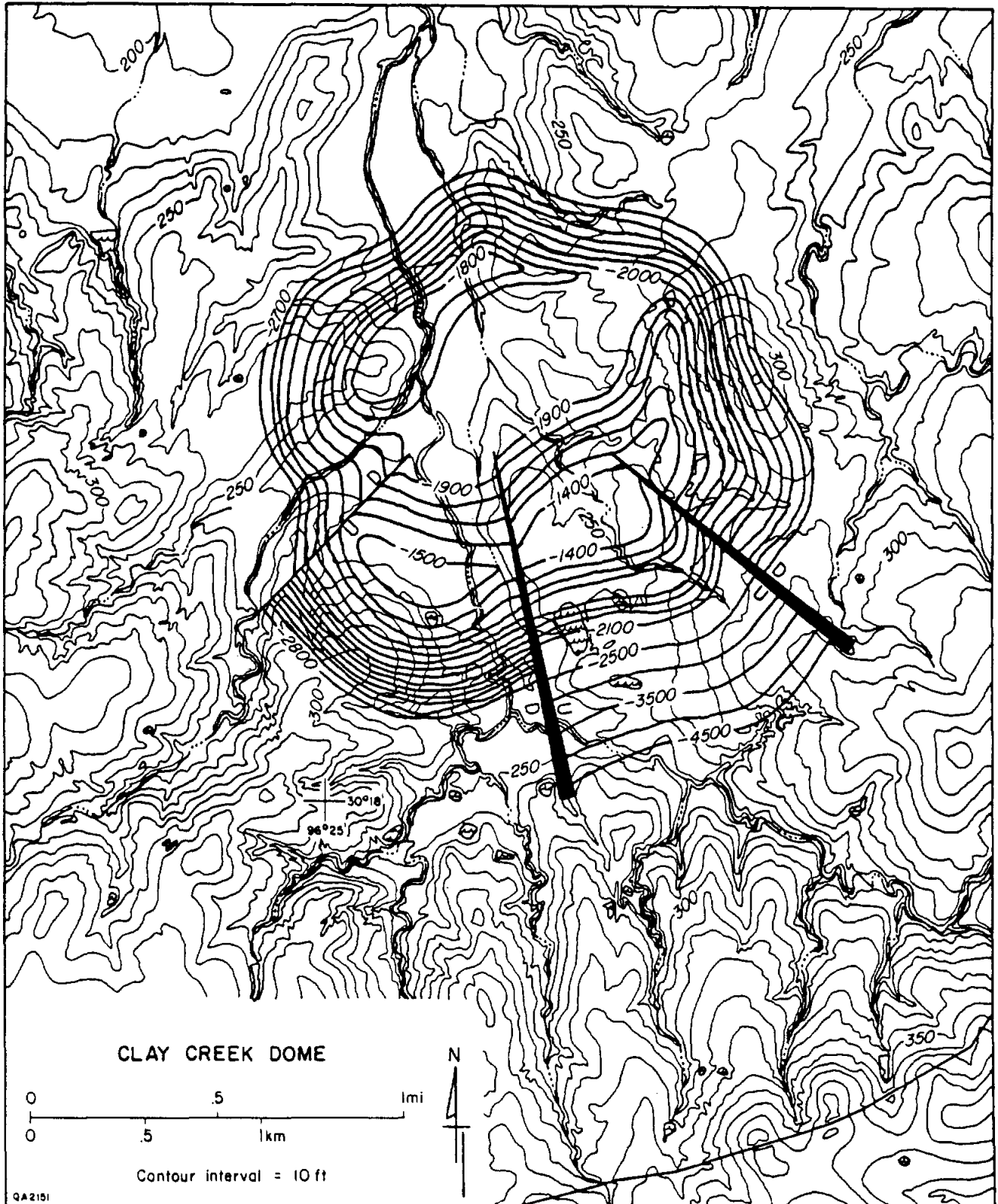


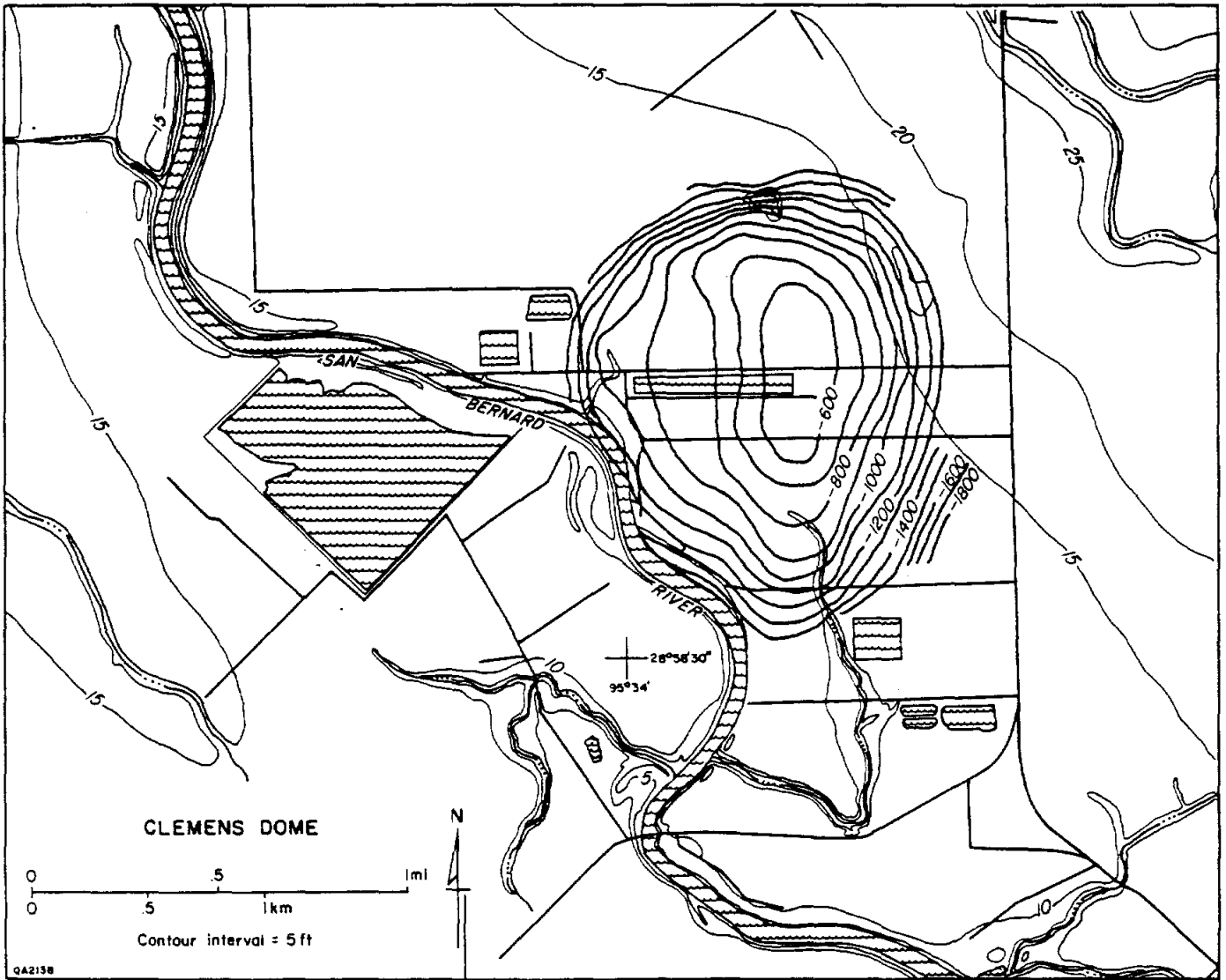


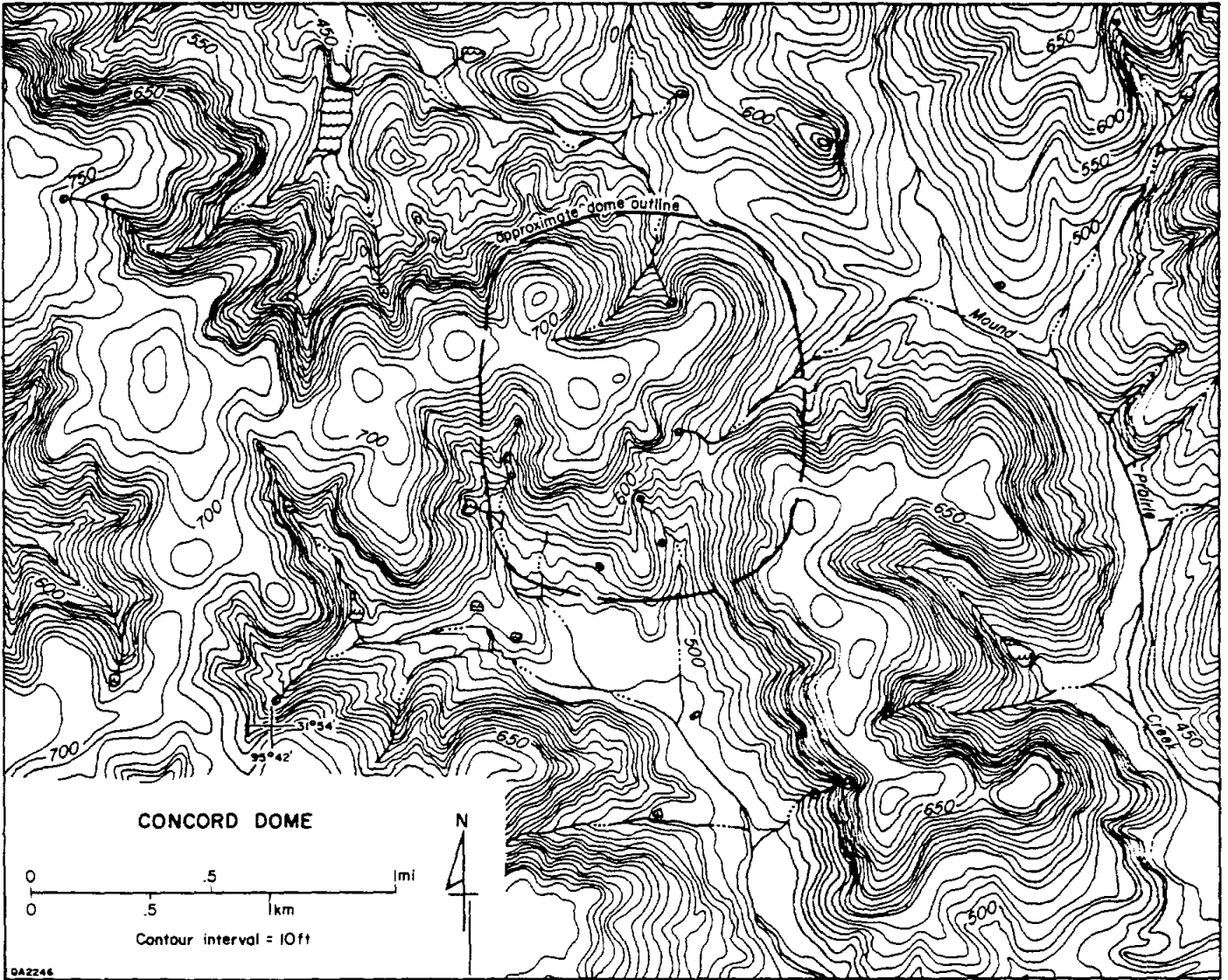


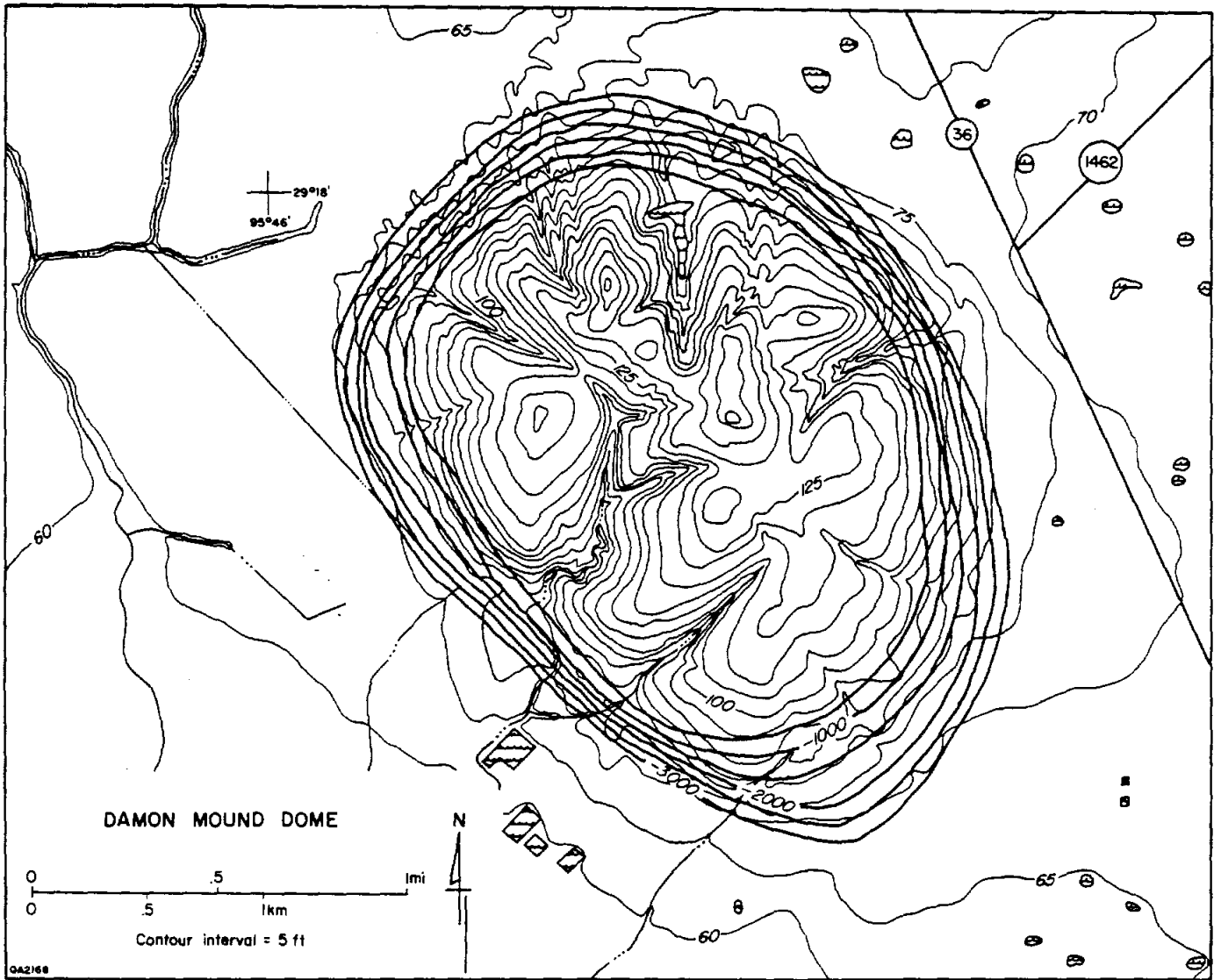


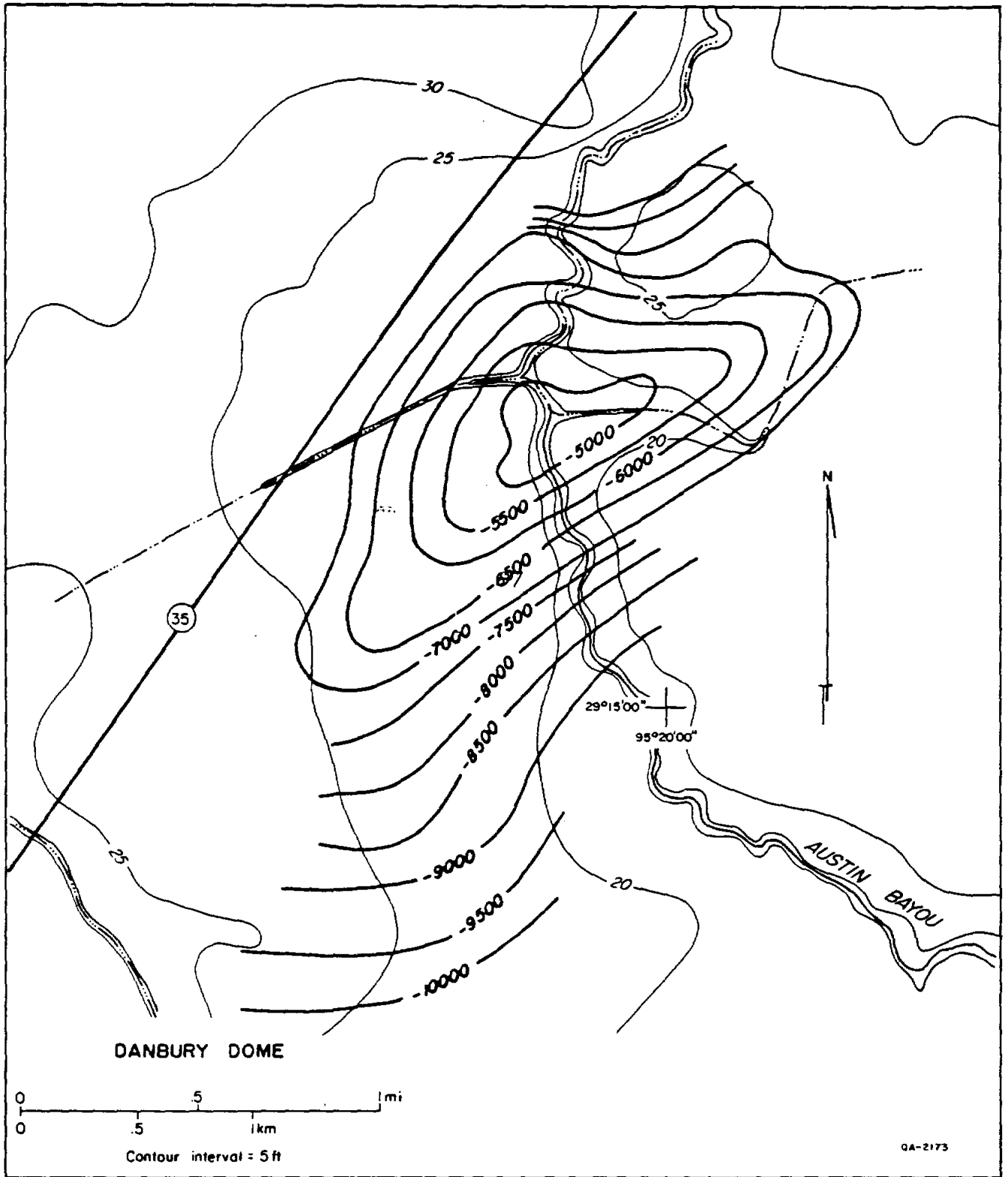


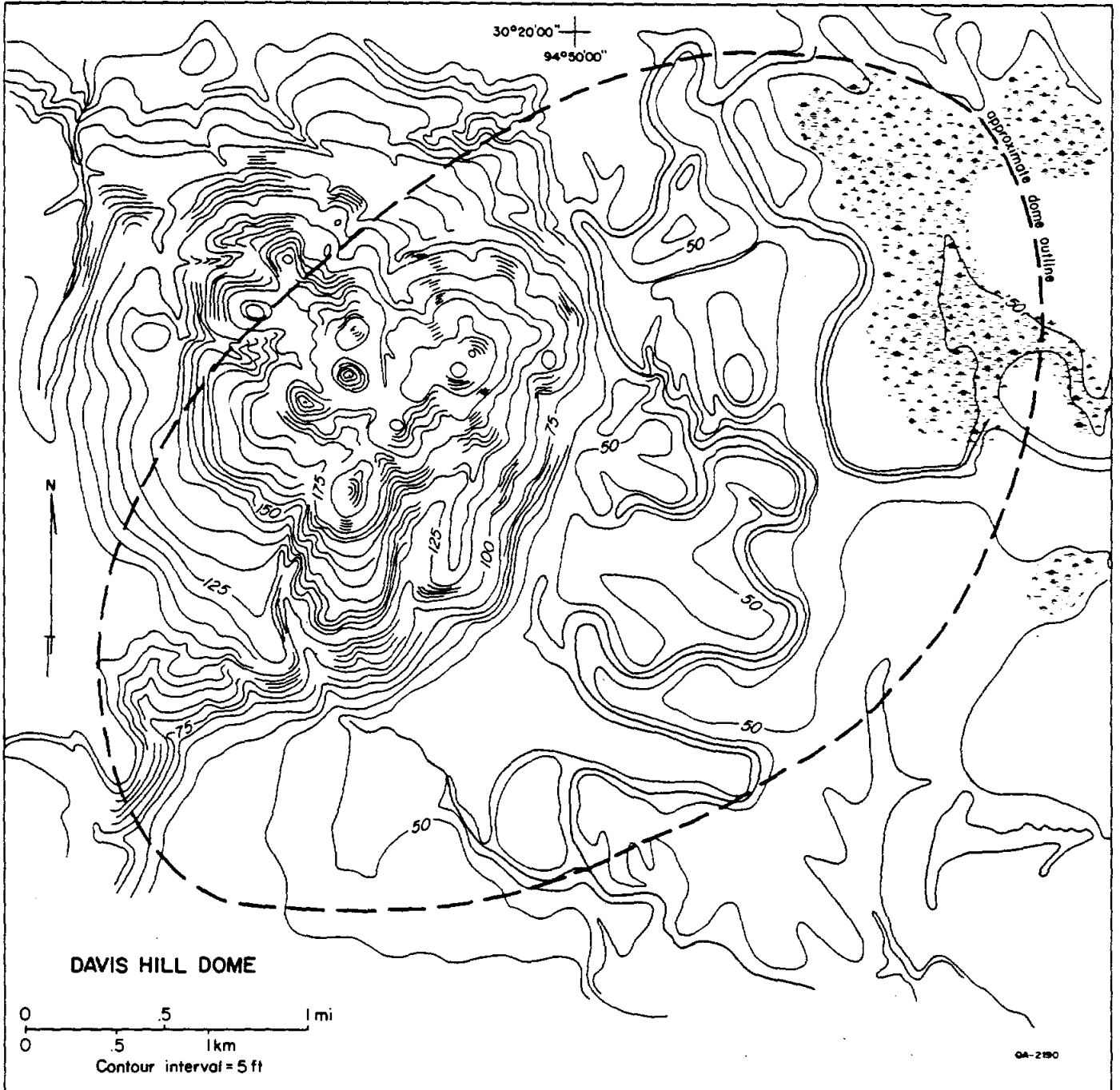


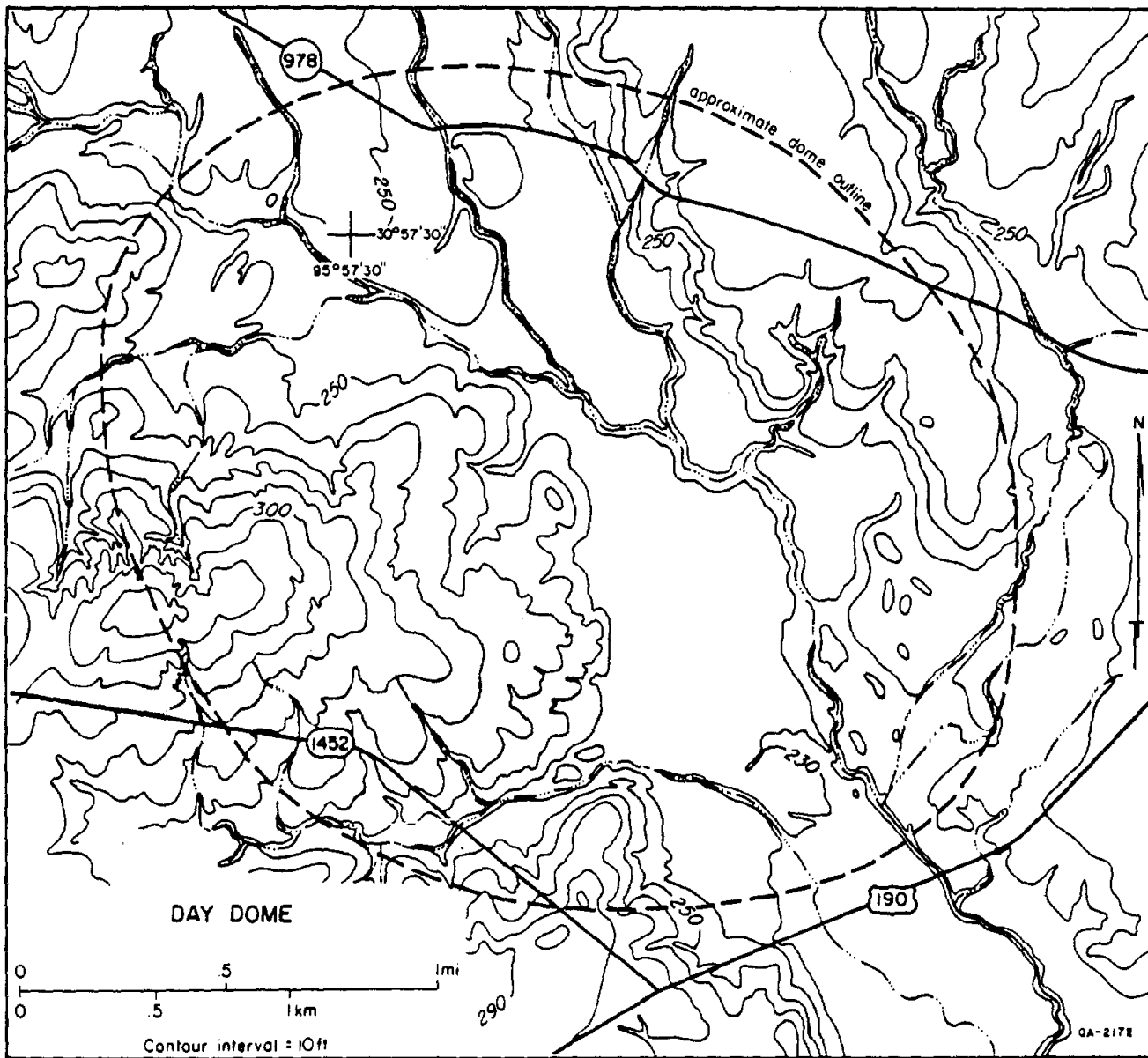


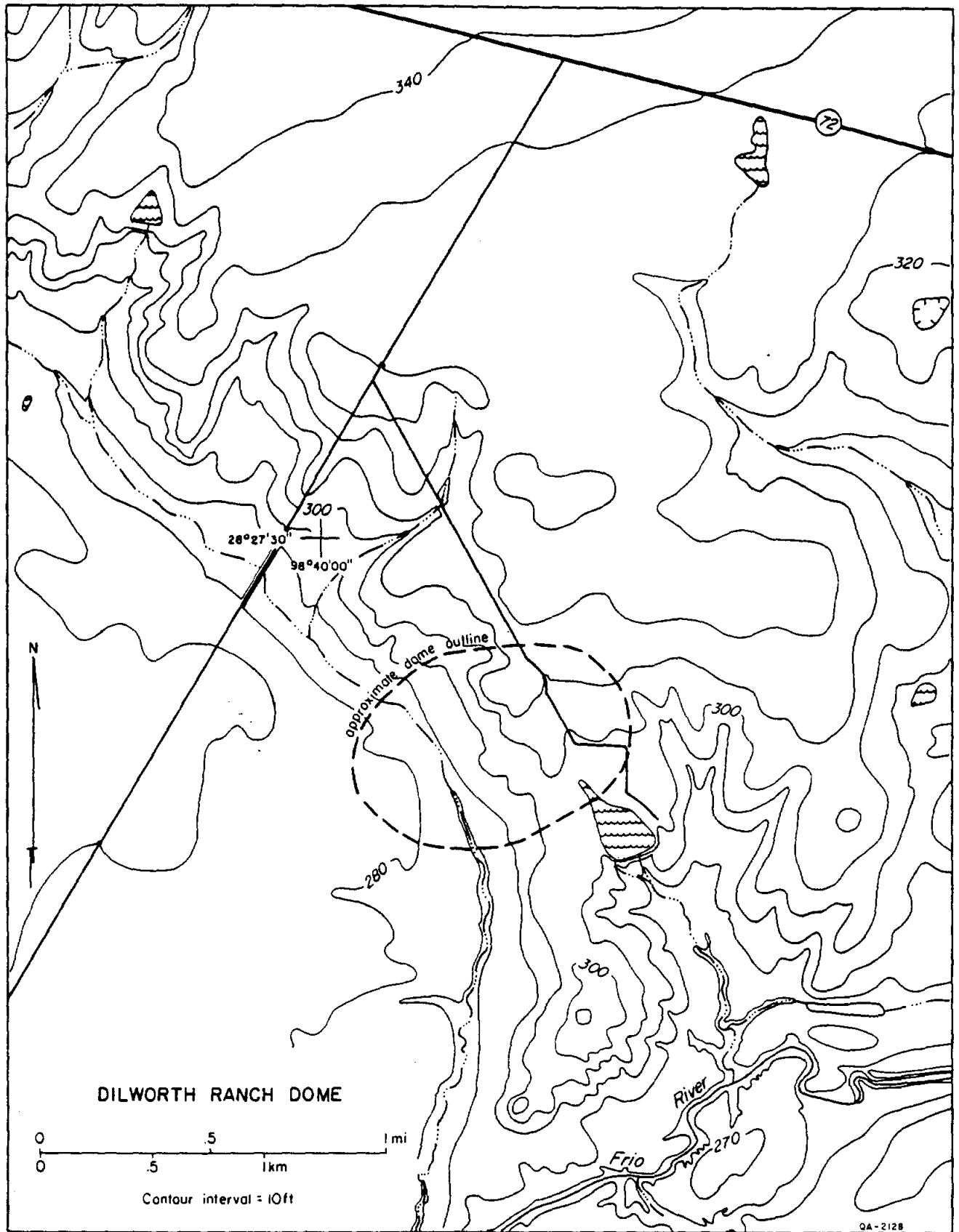


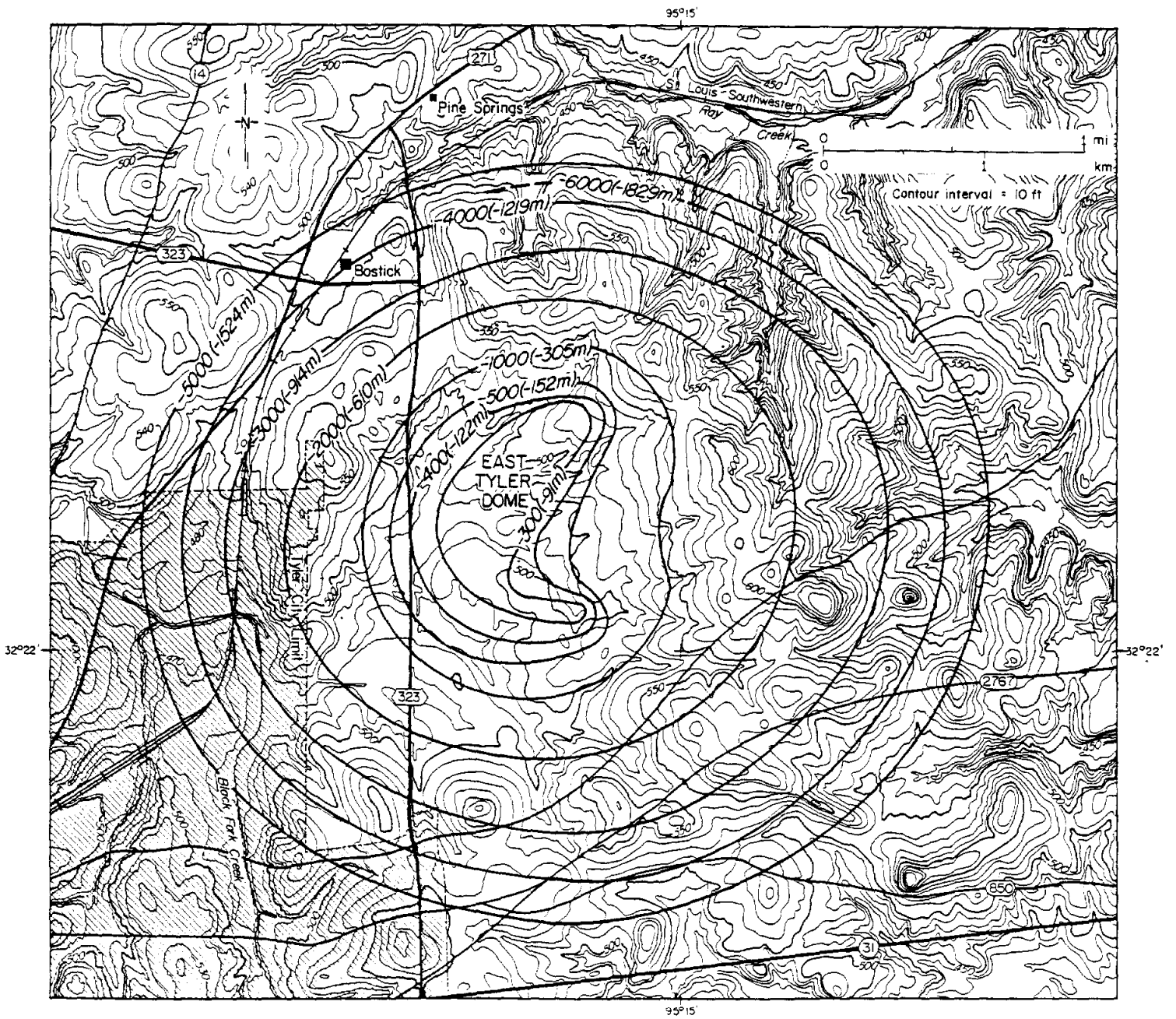


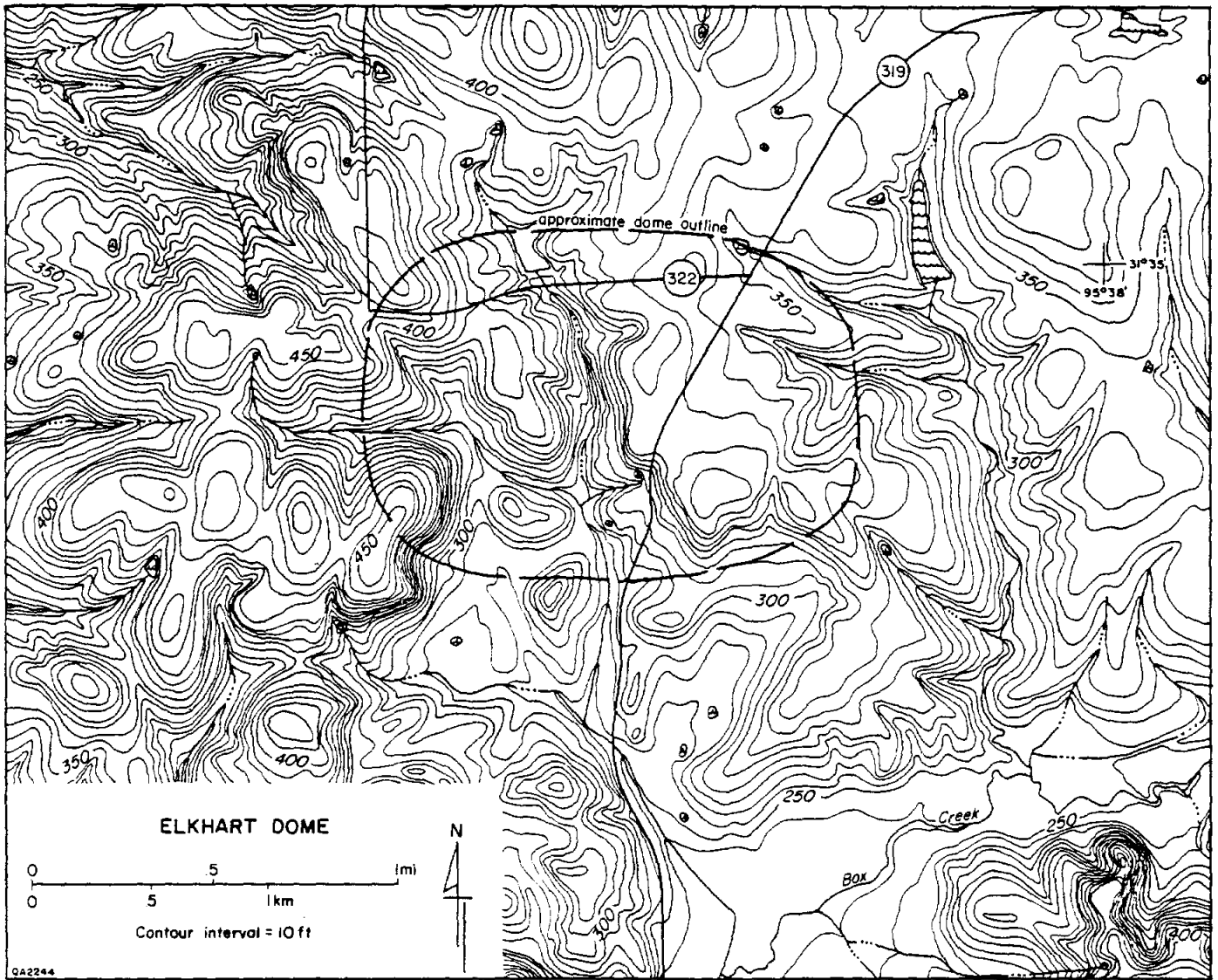


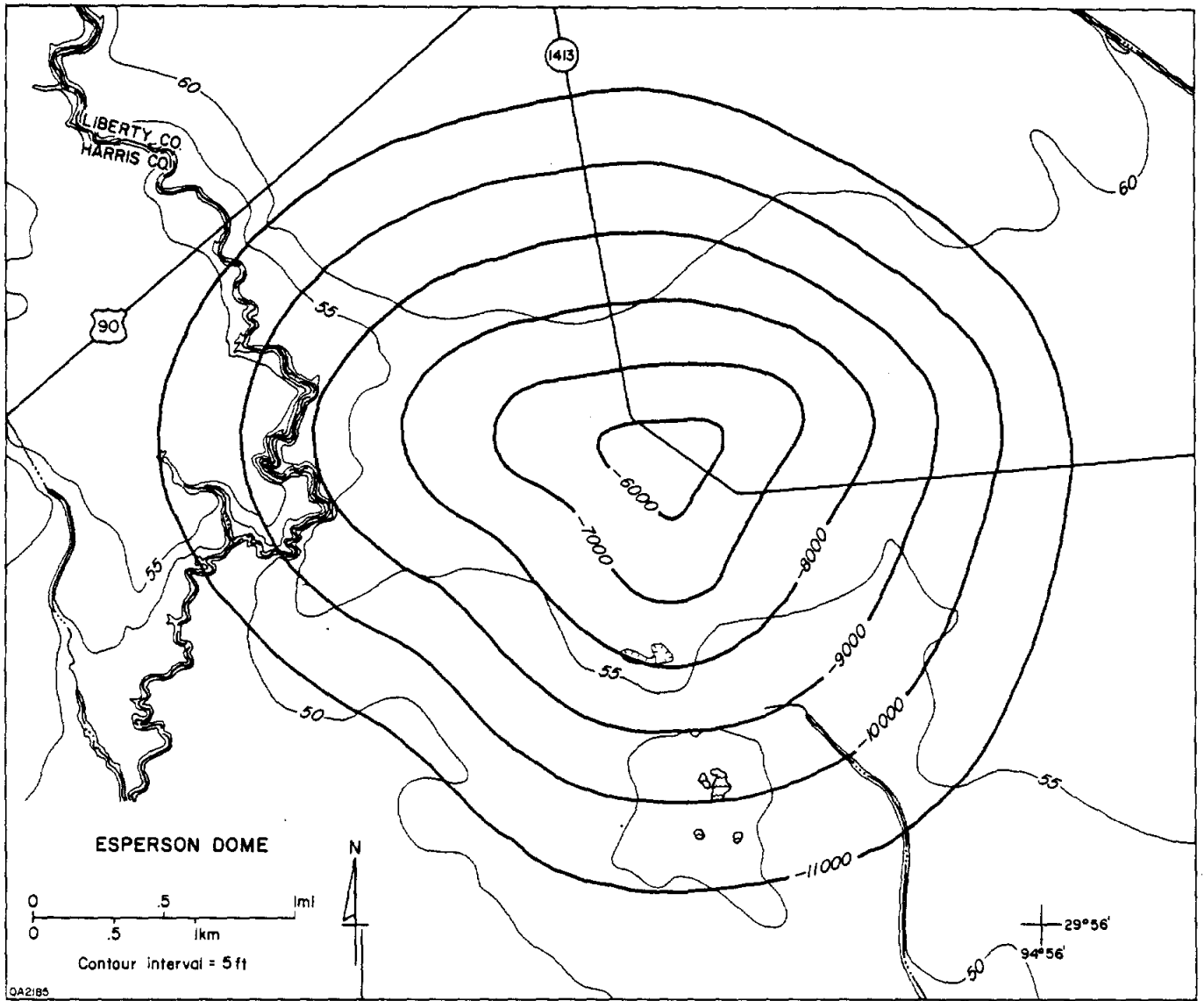


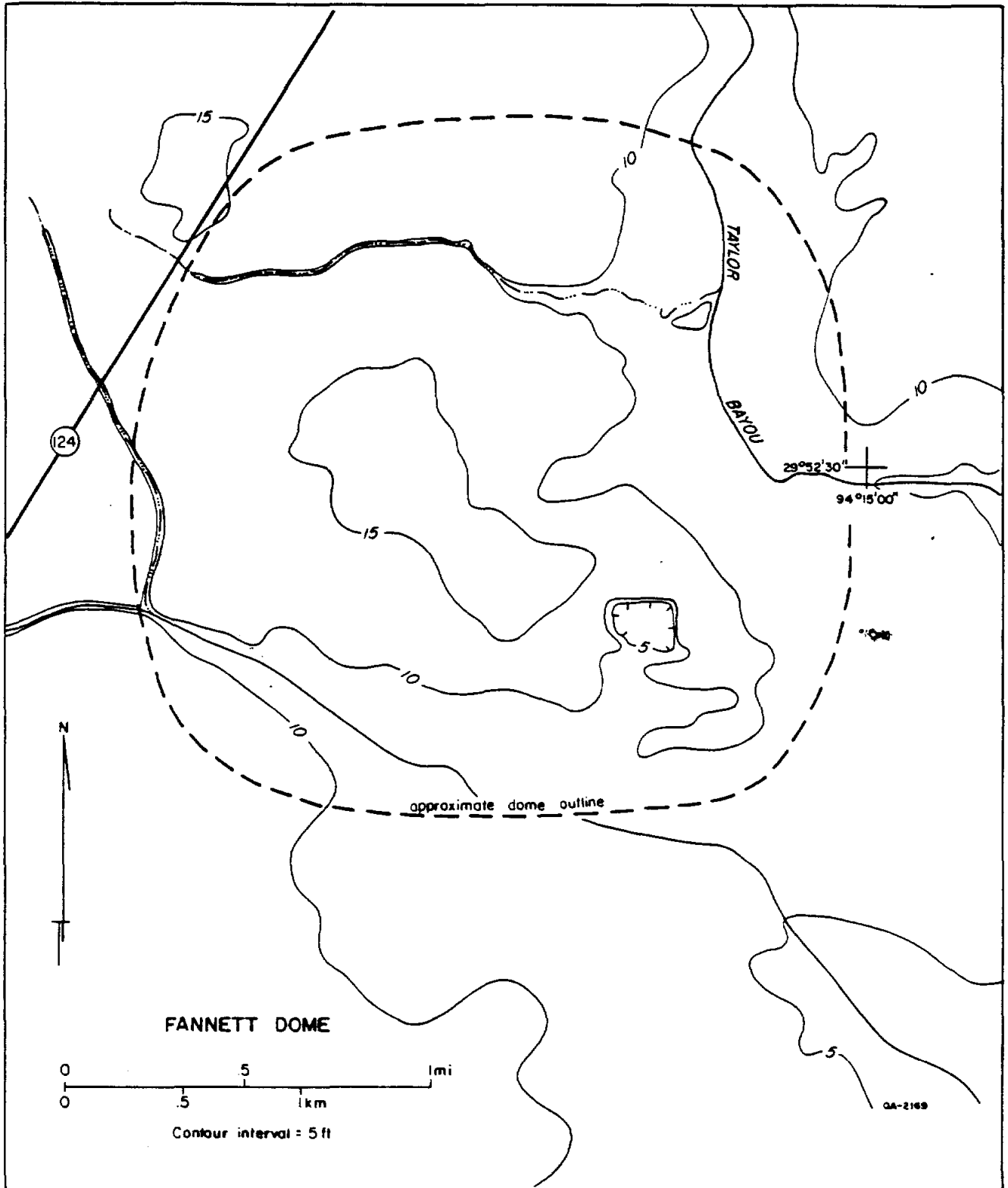


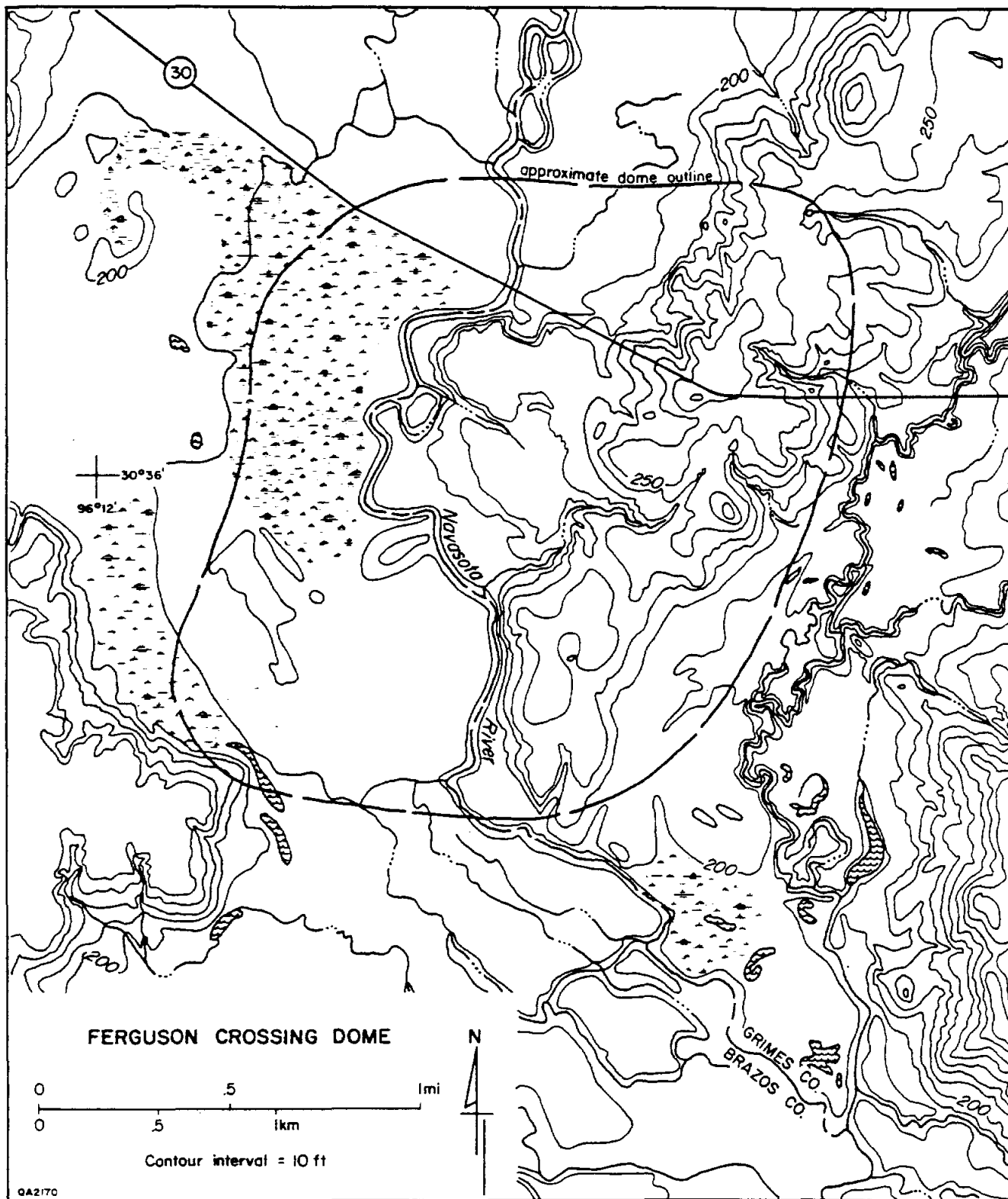


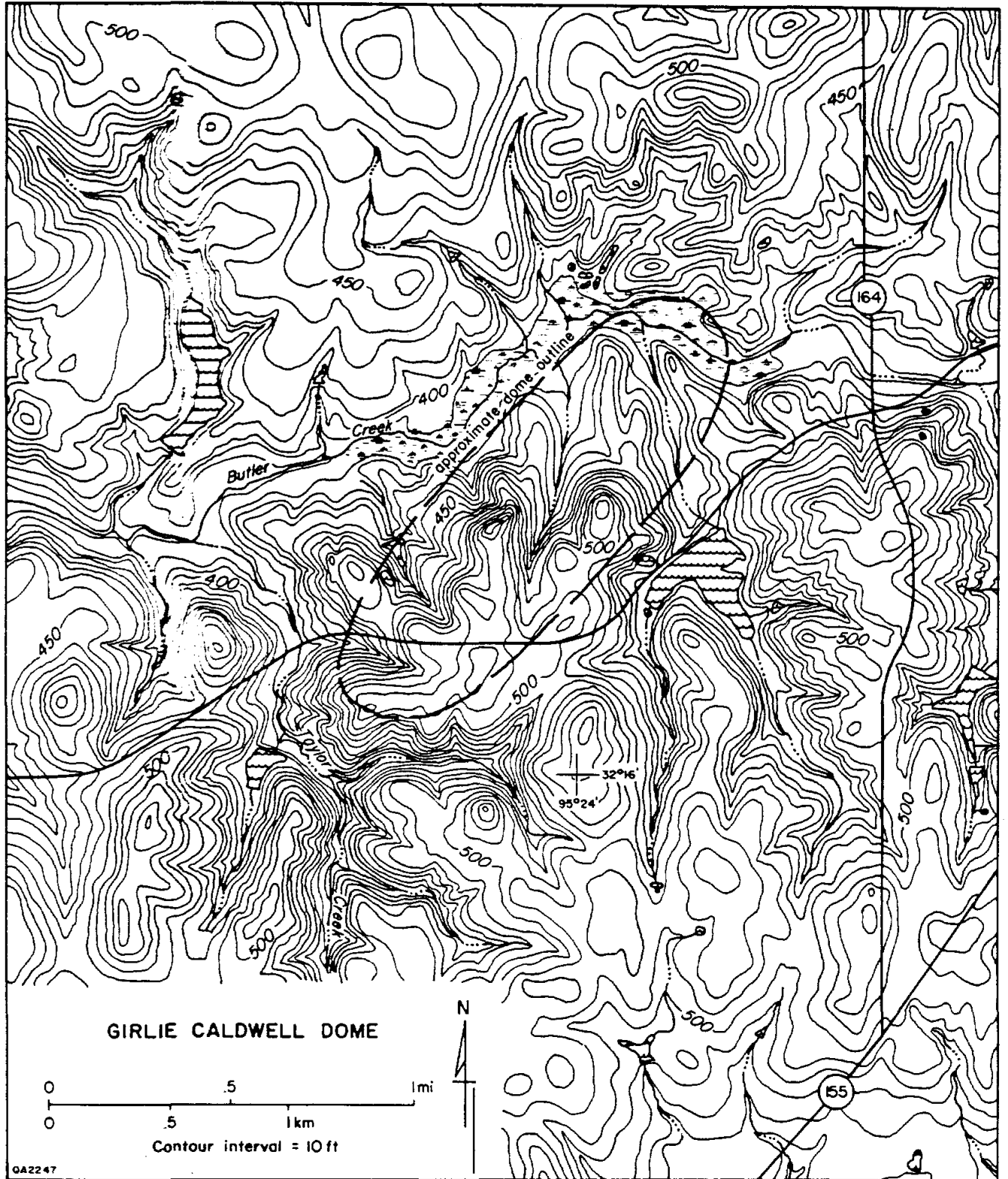






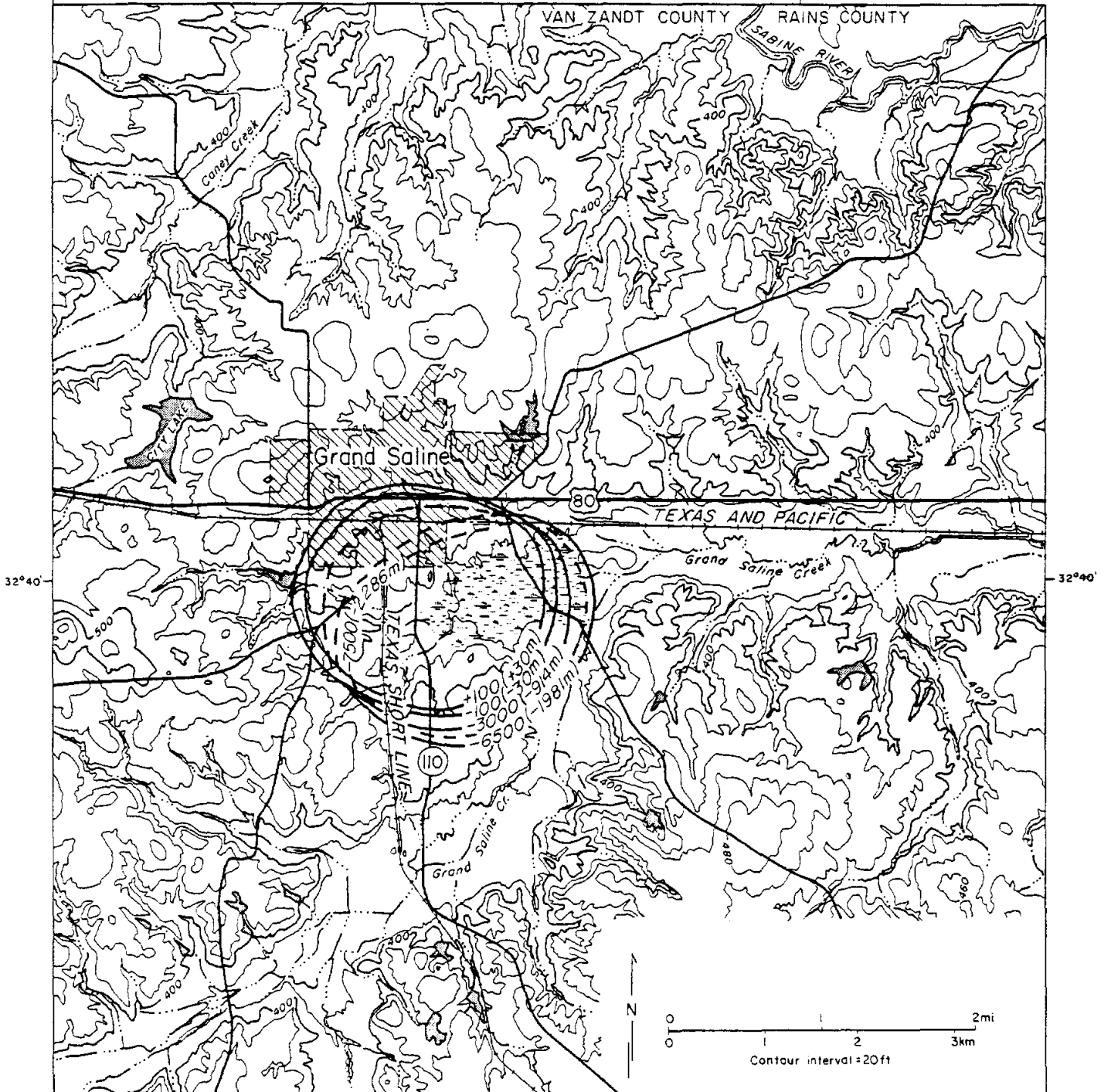


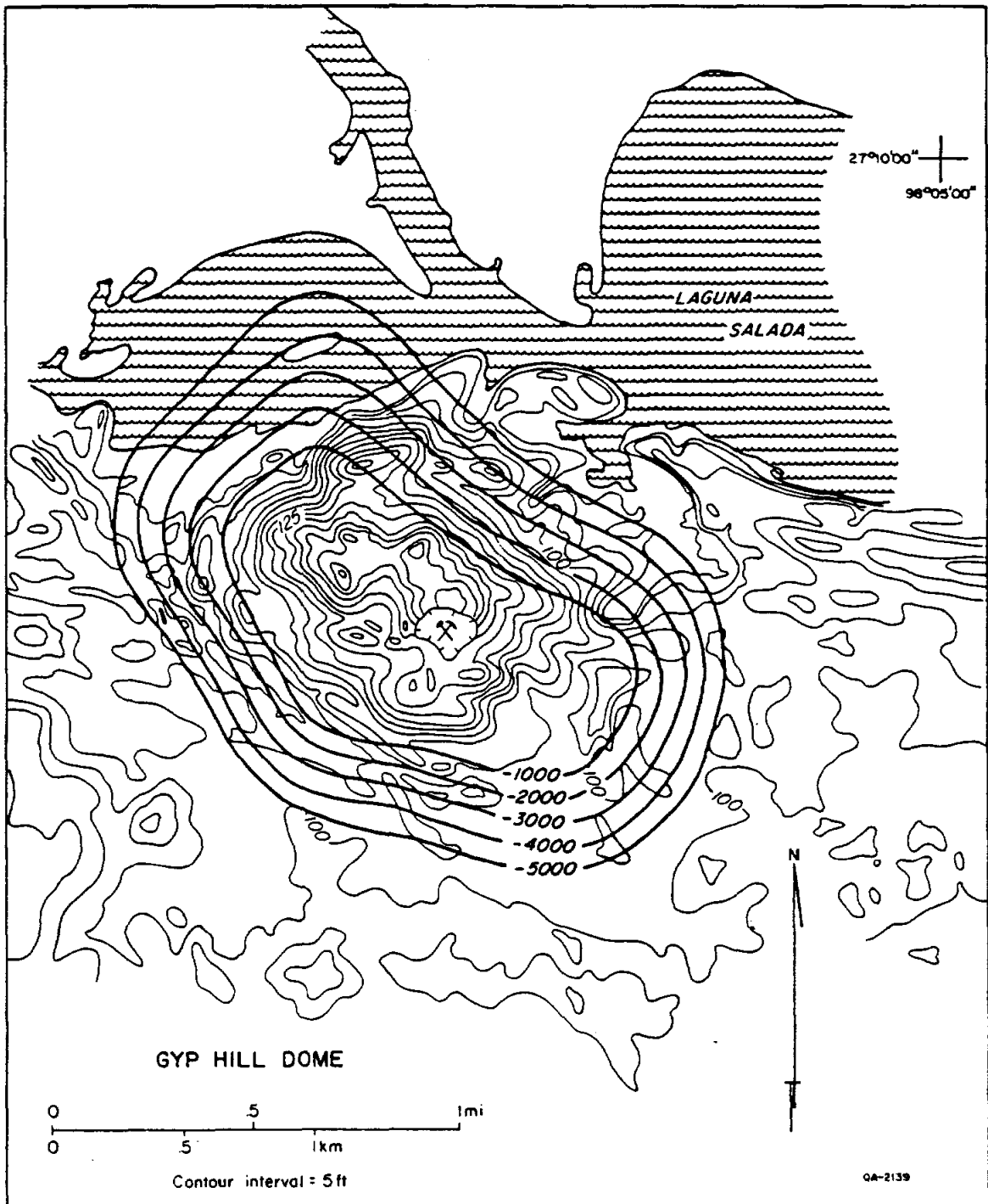


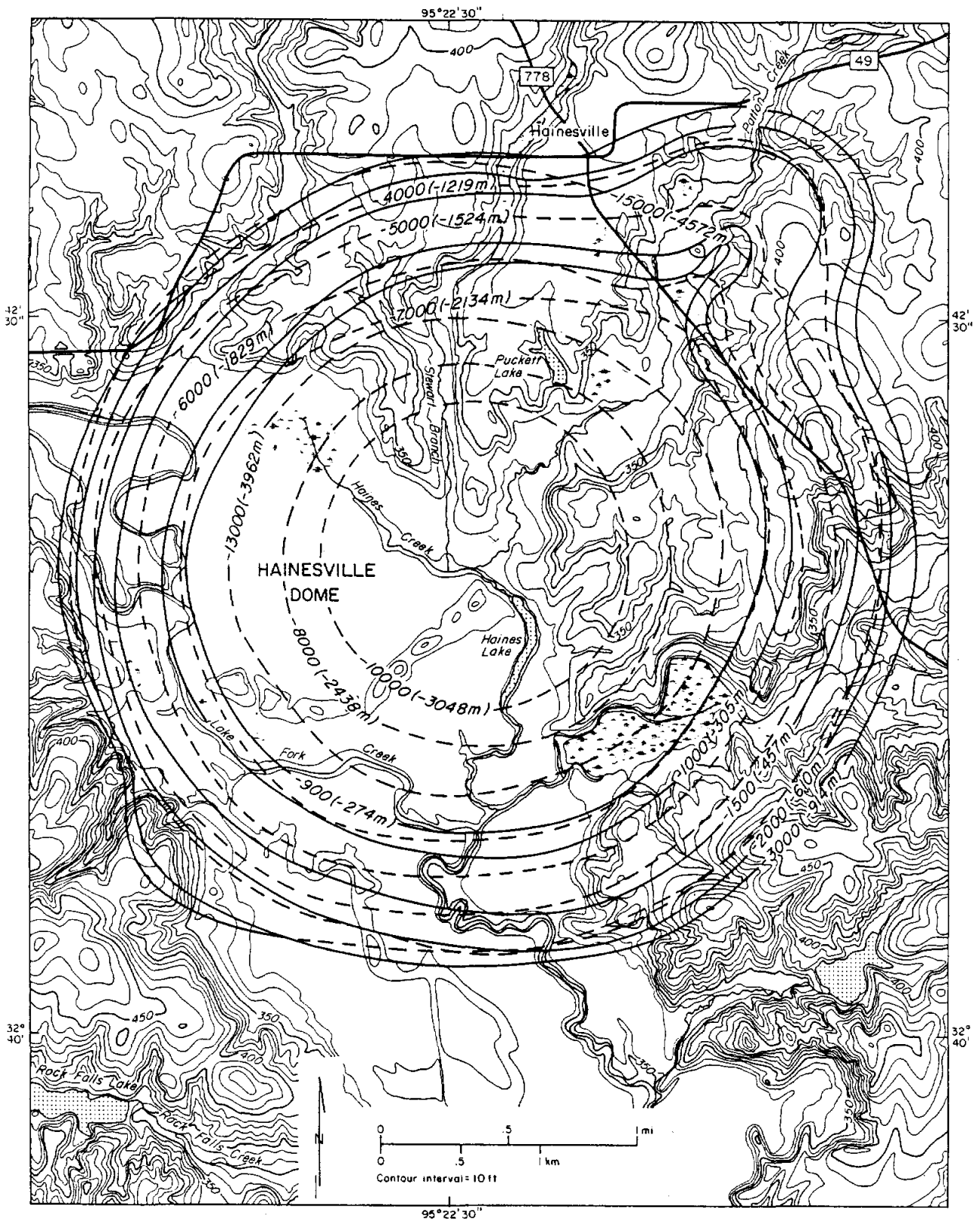


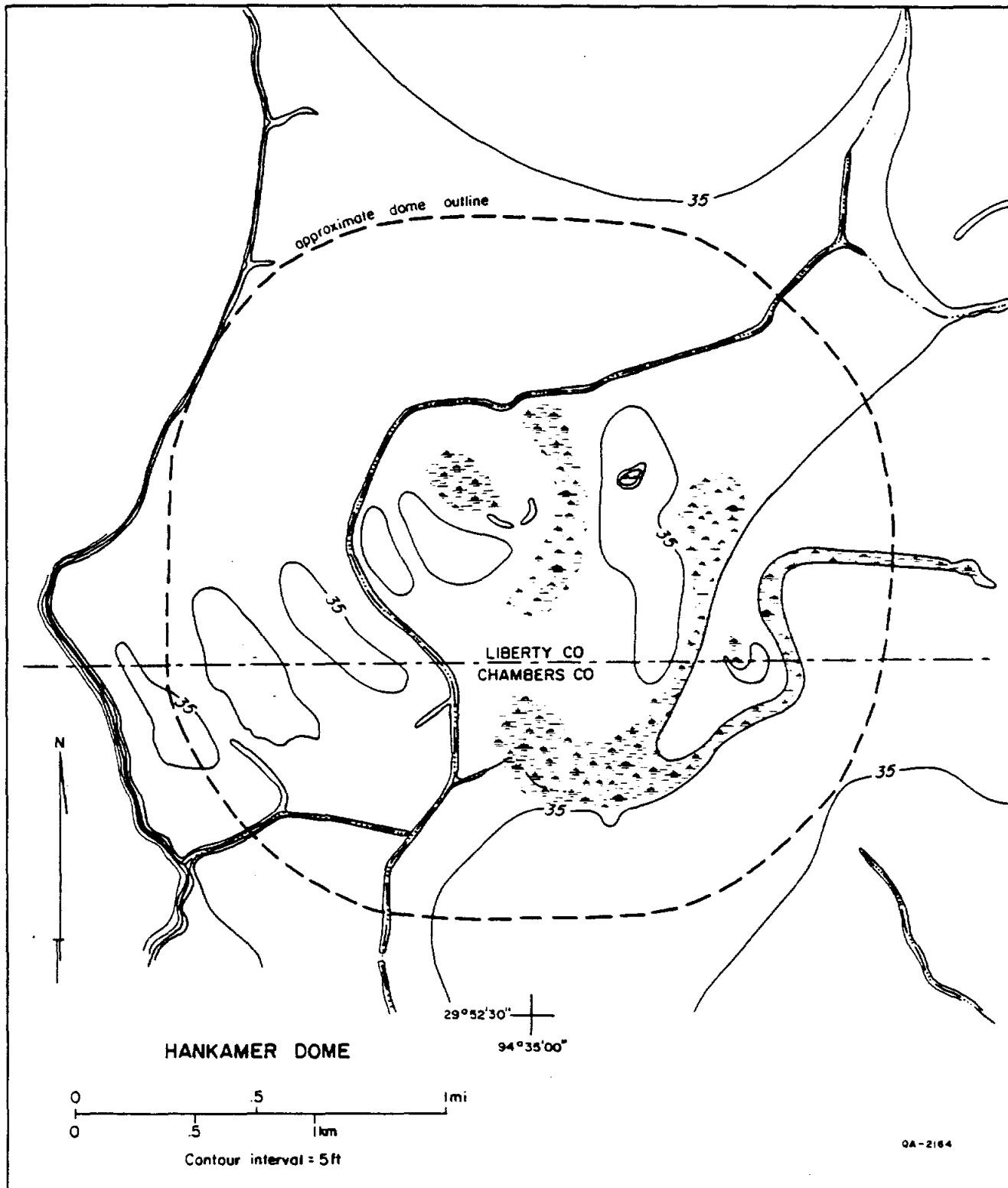
95° 45'

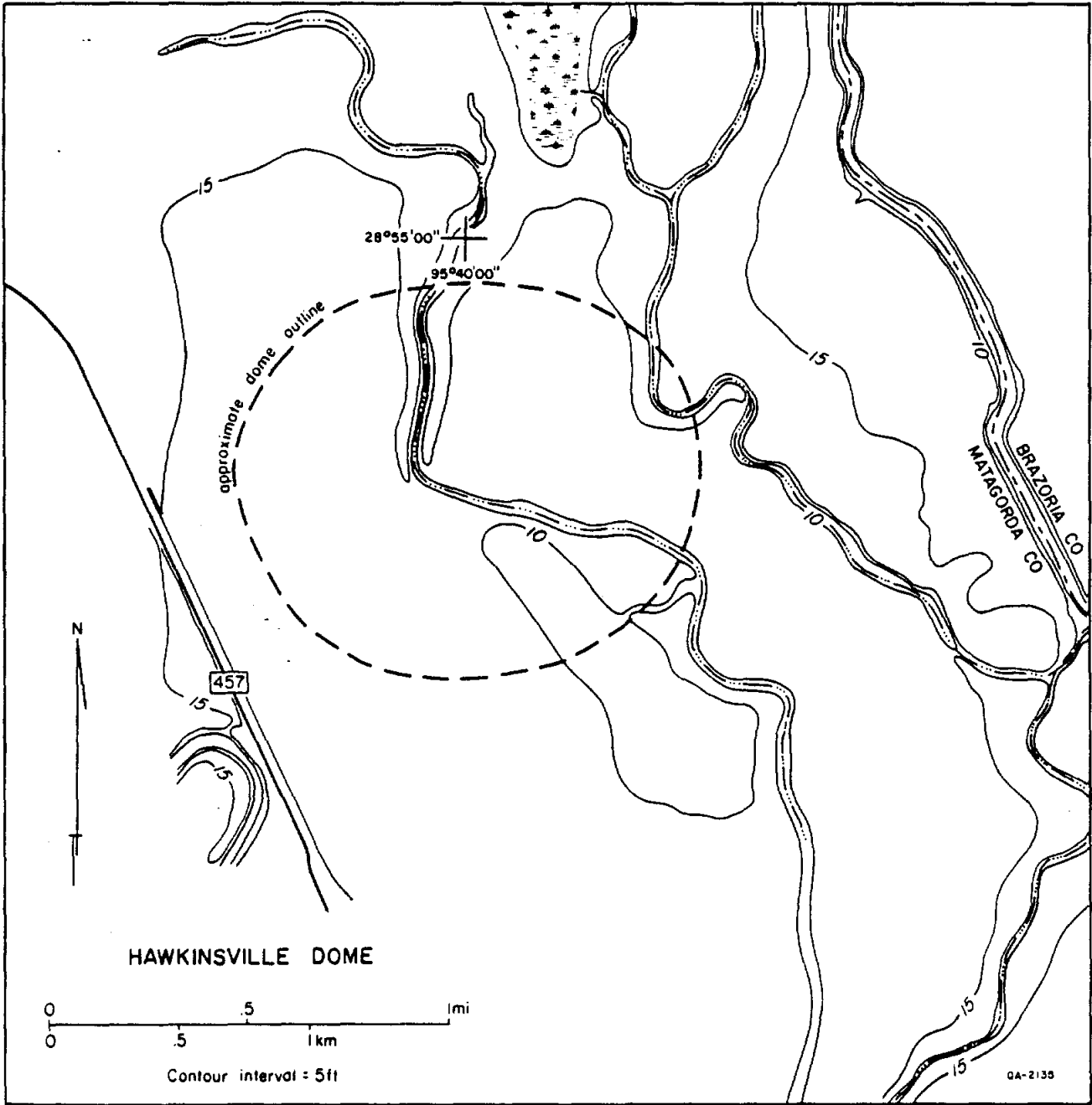
95° 40'

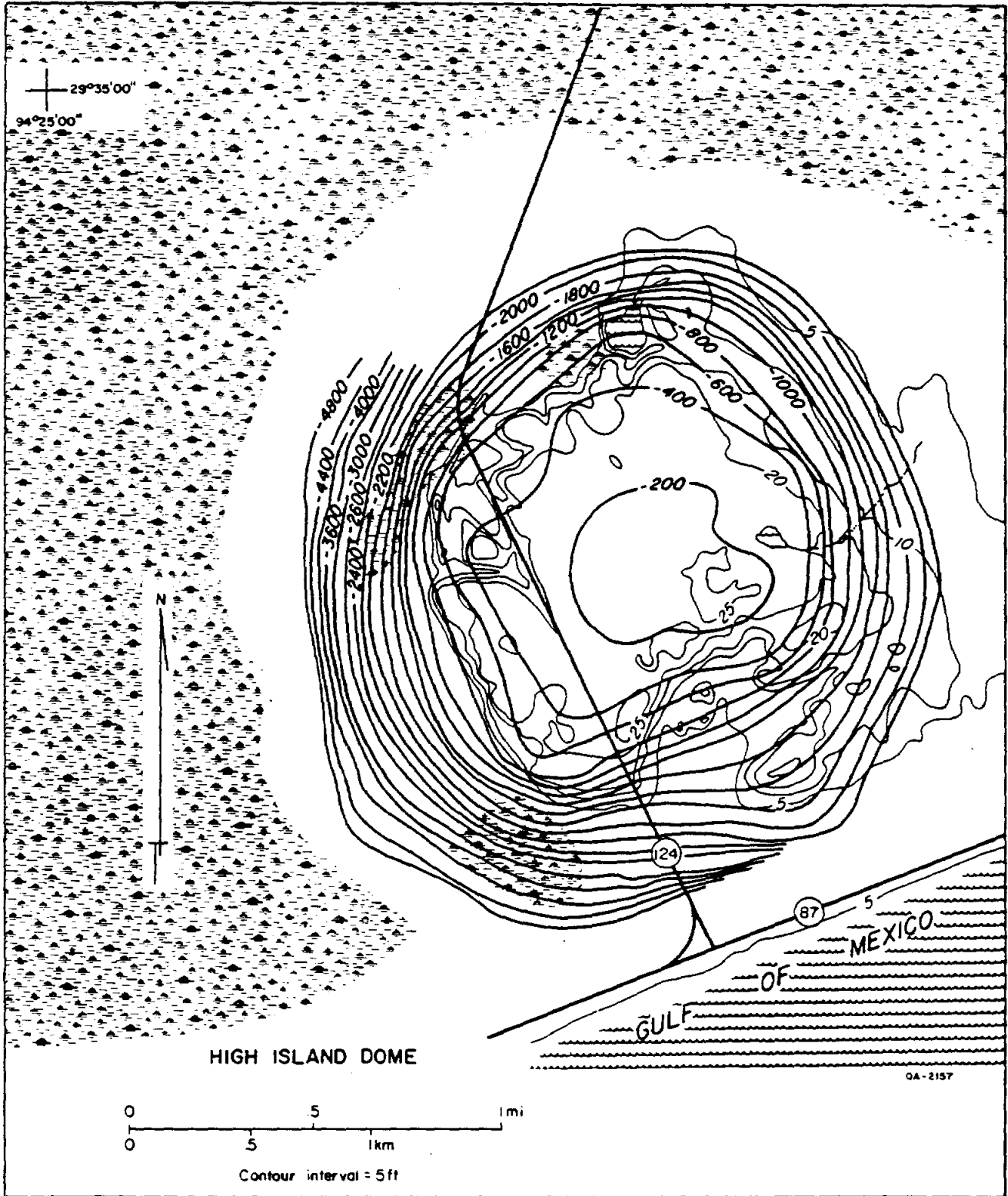


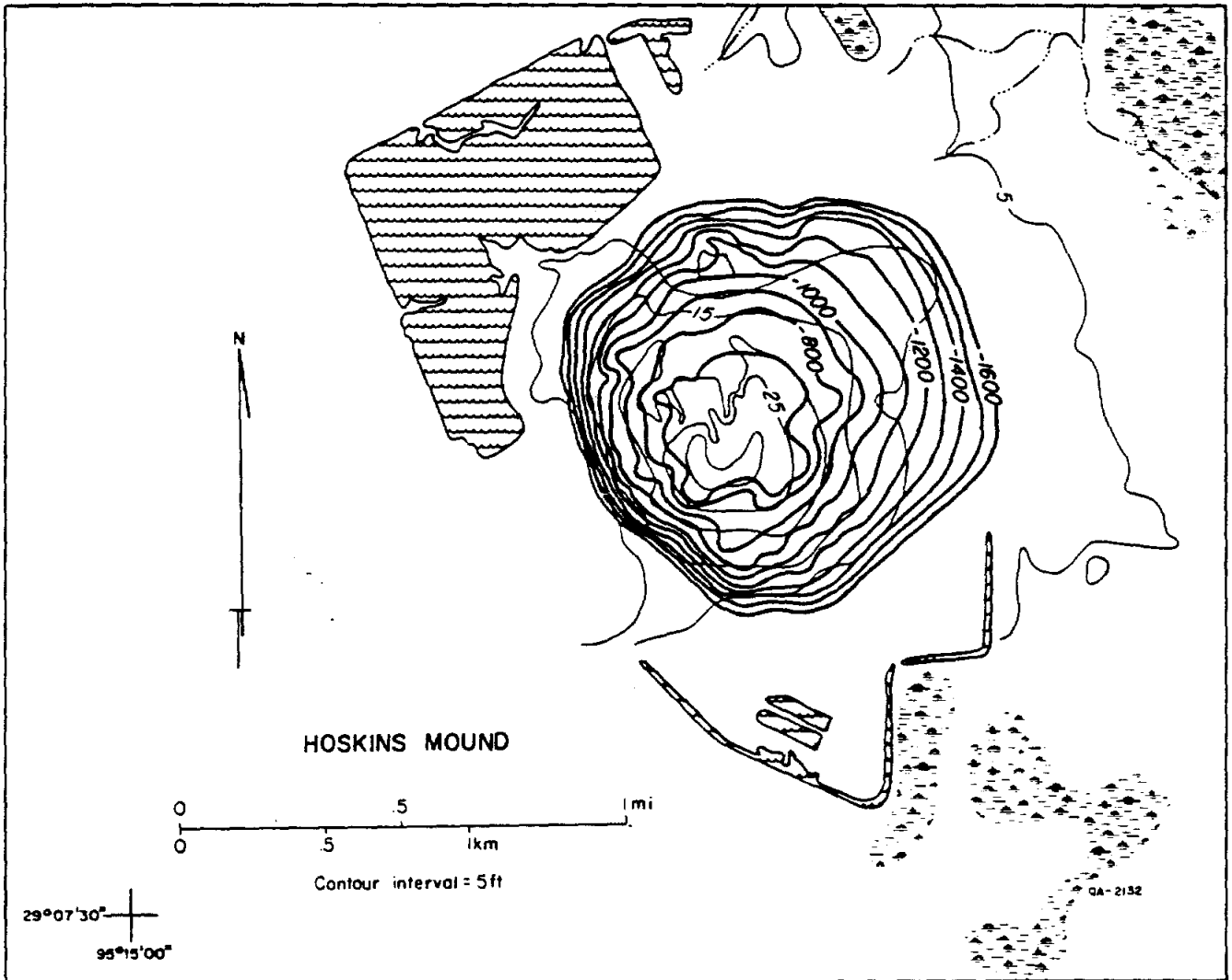


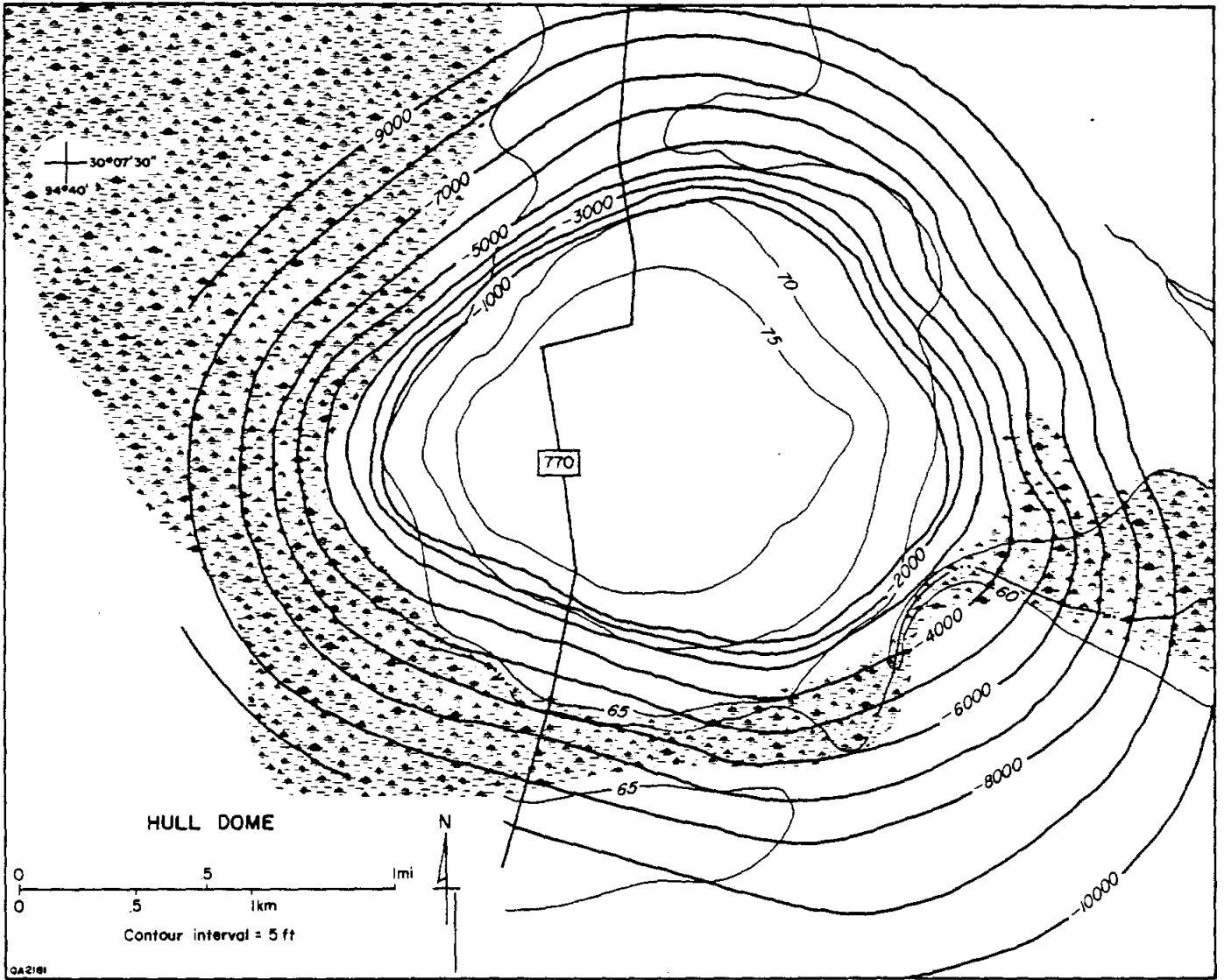


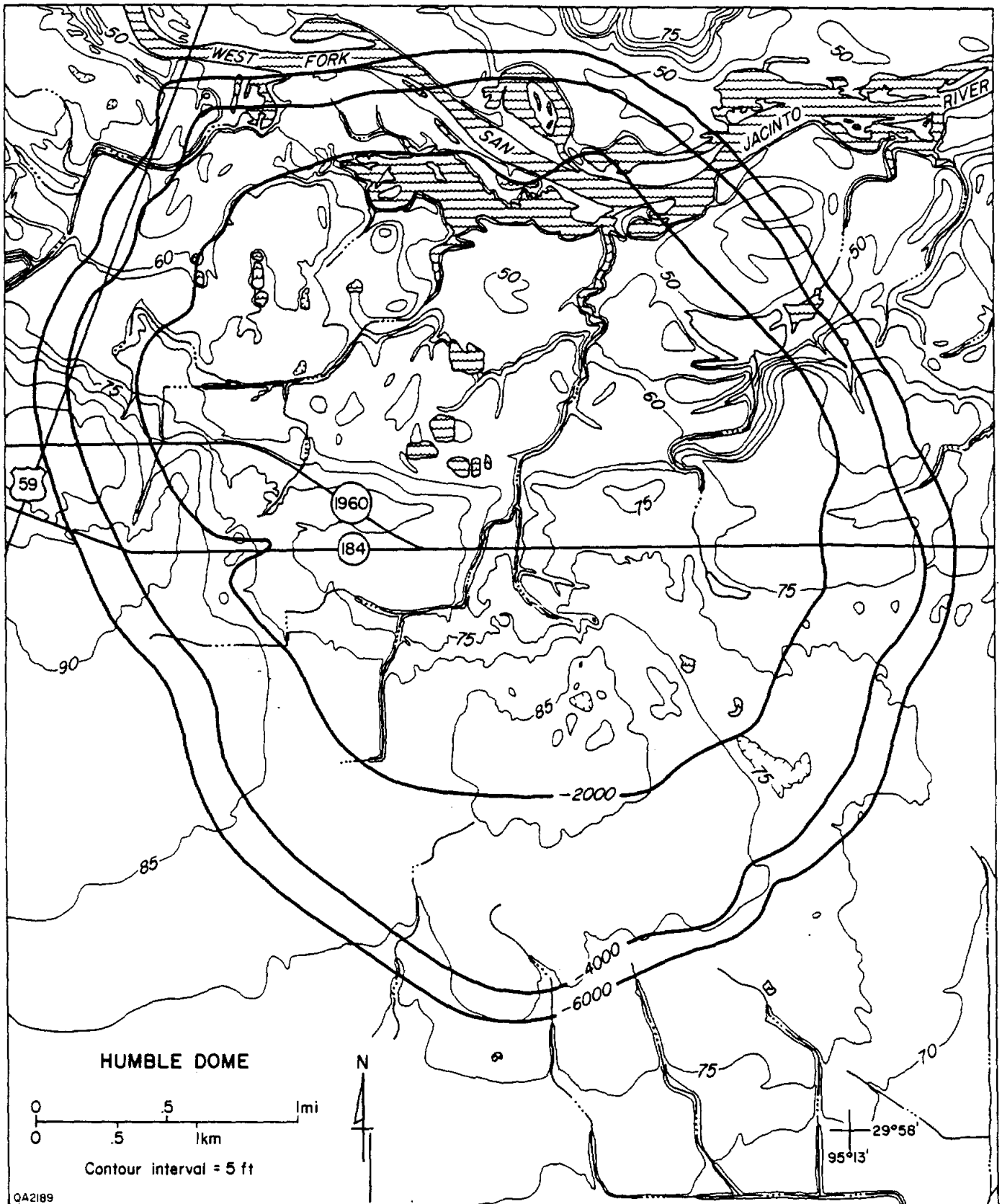


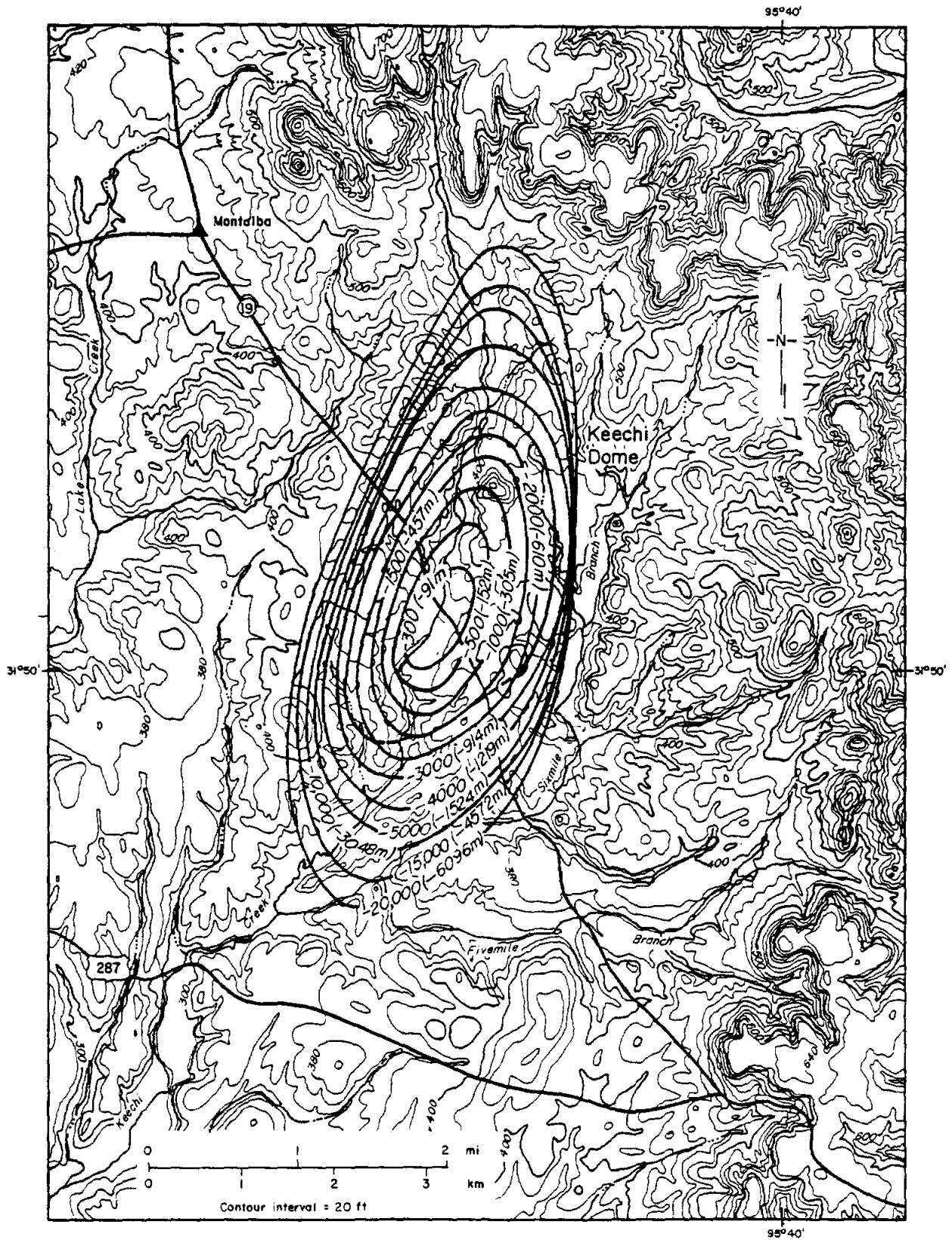


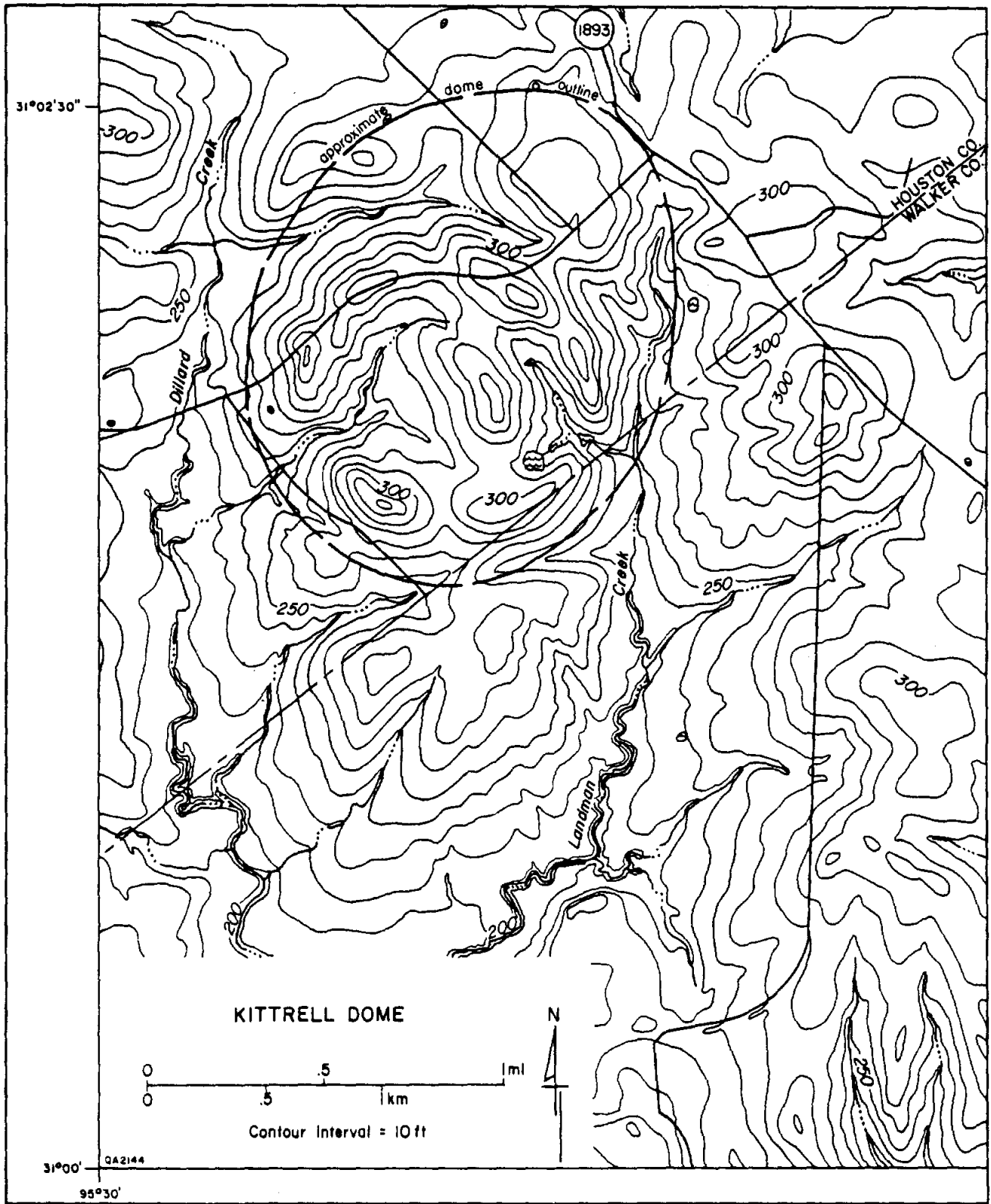


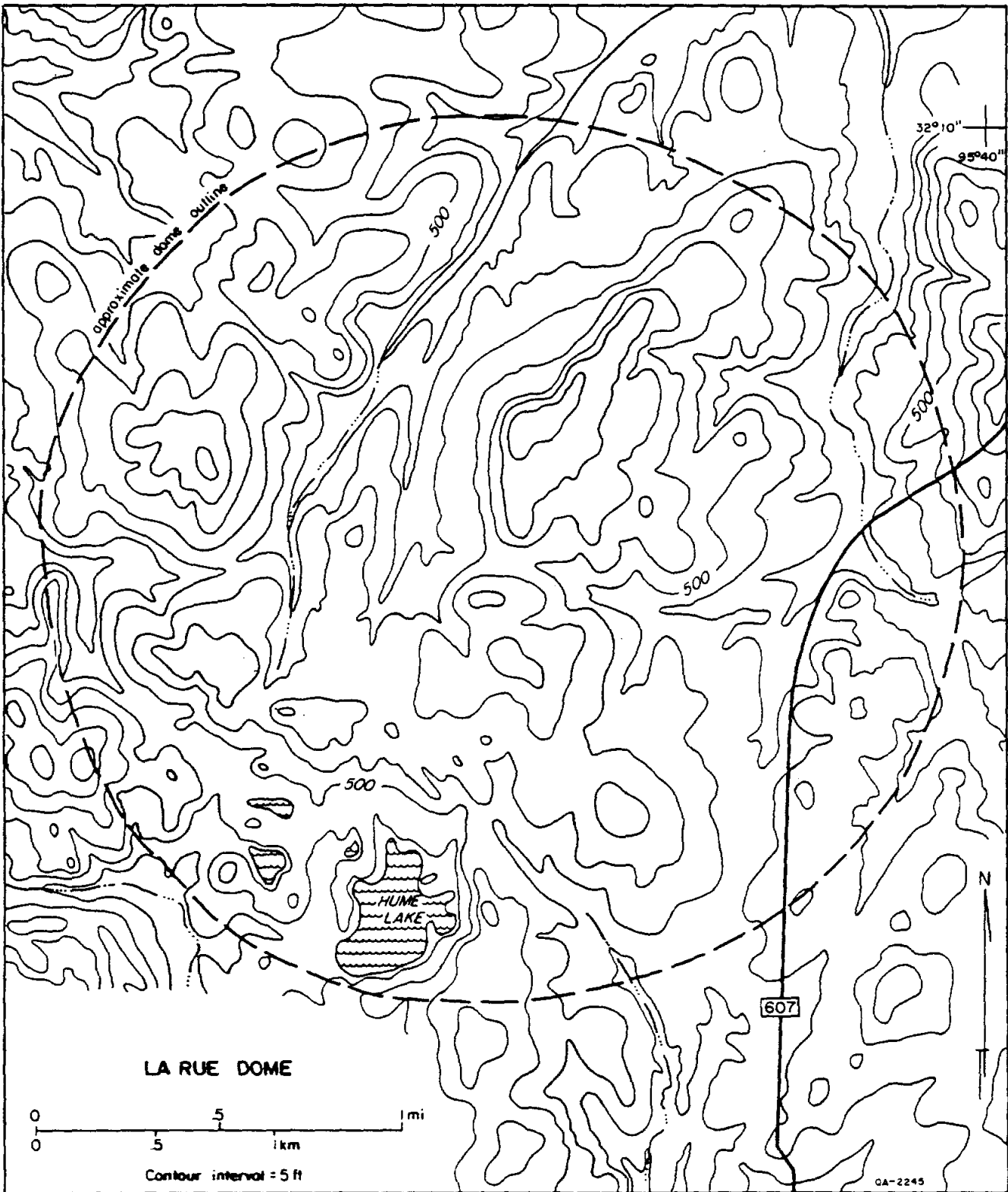


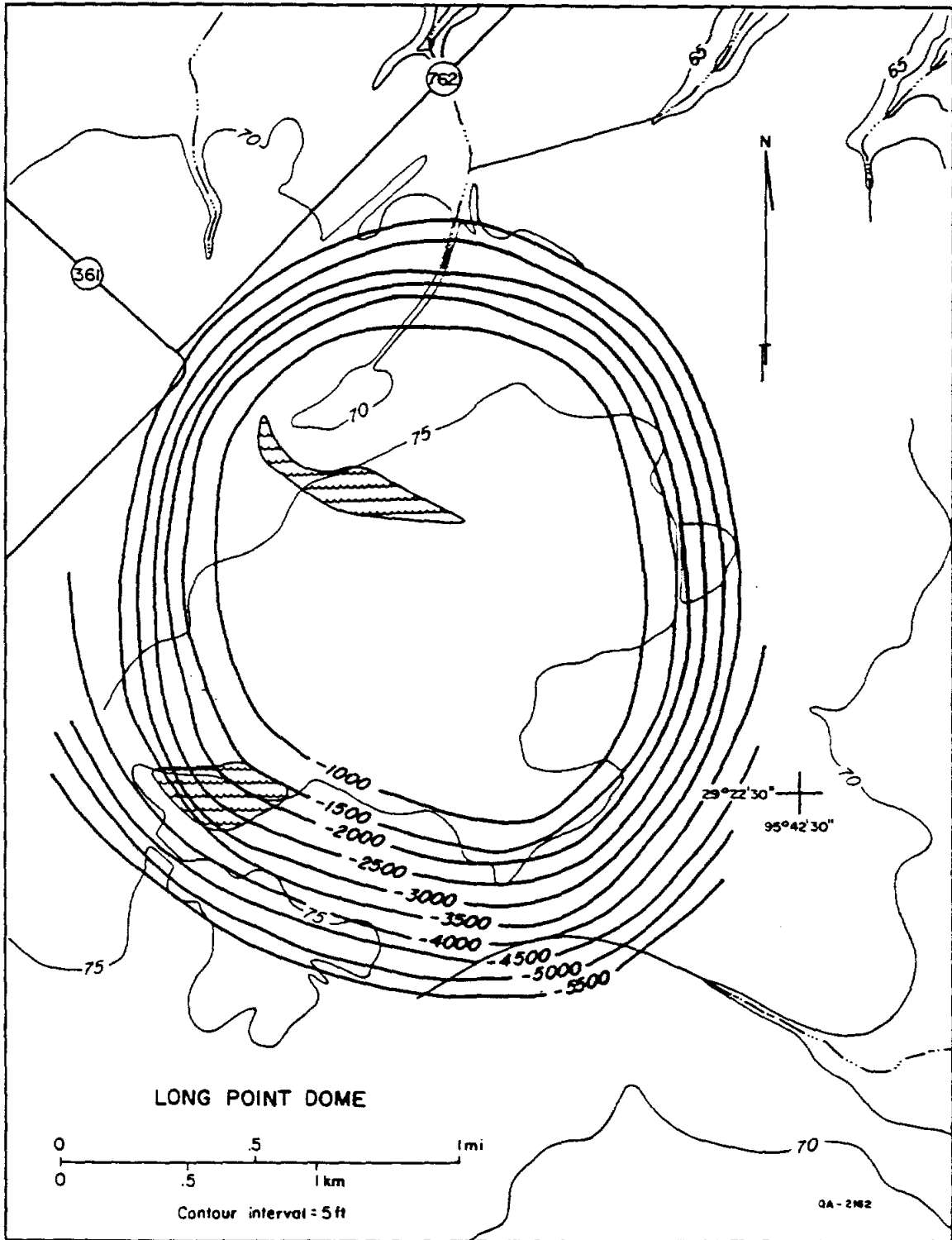


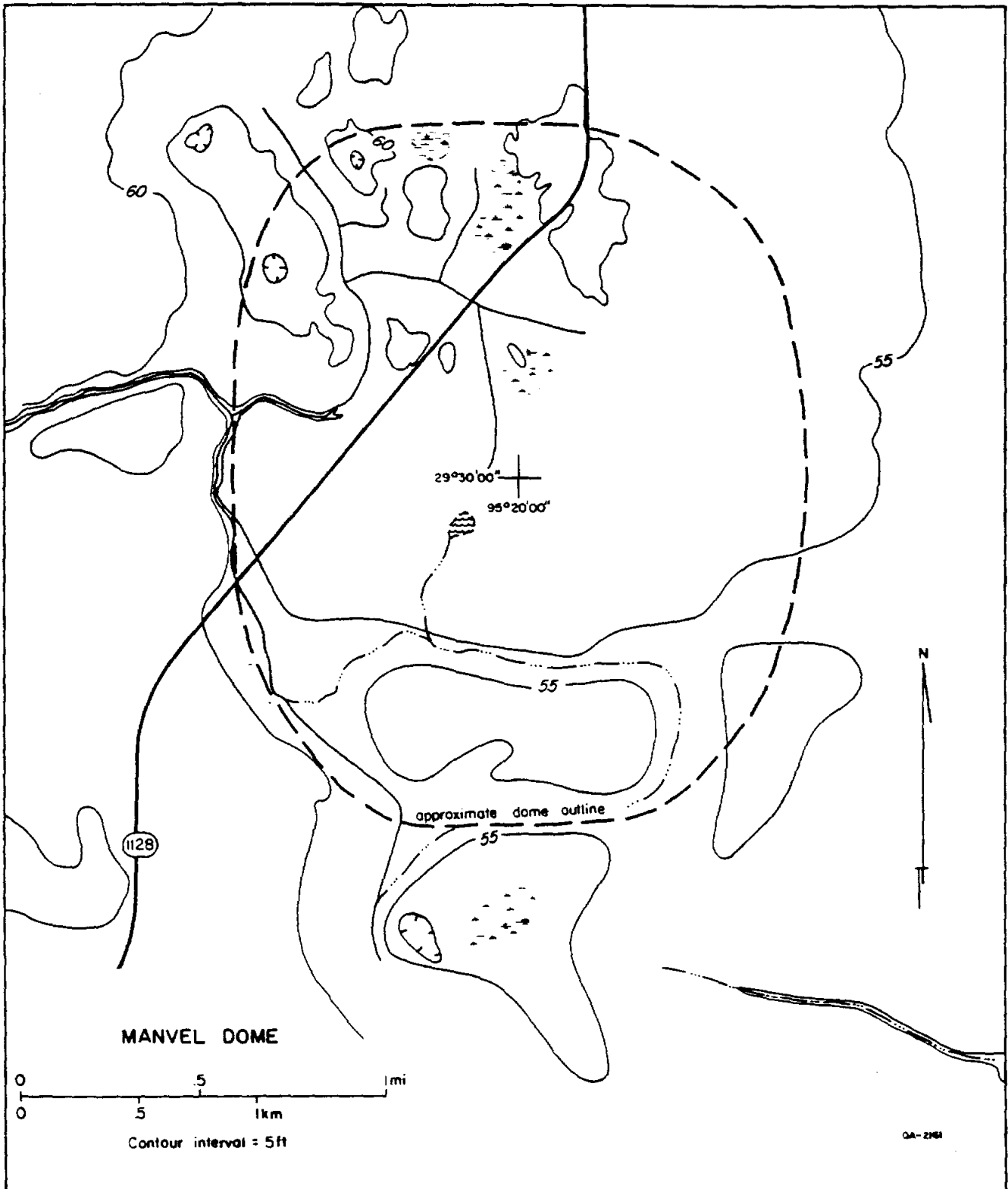


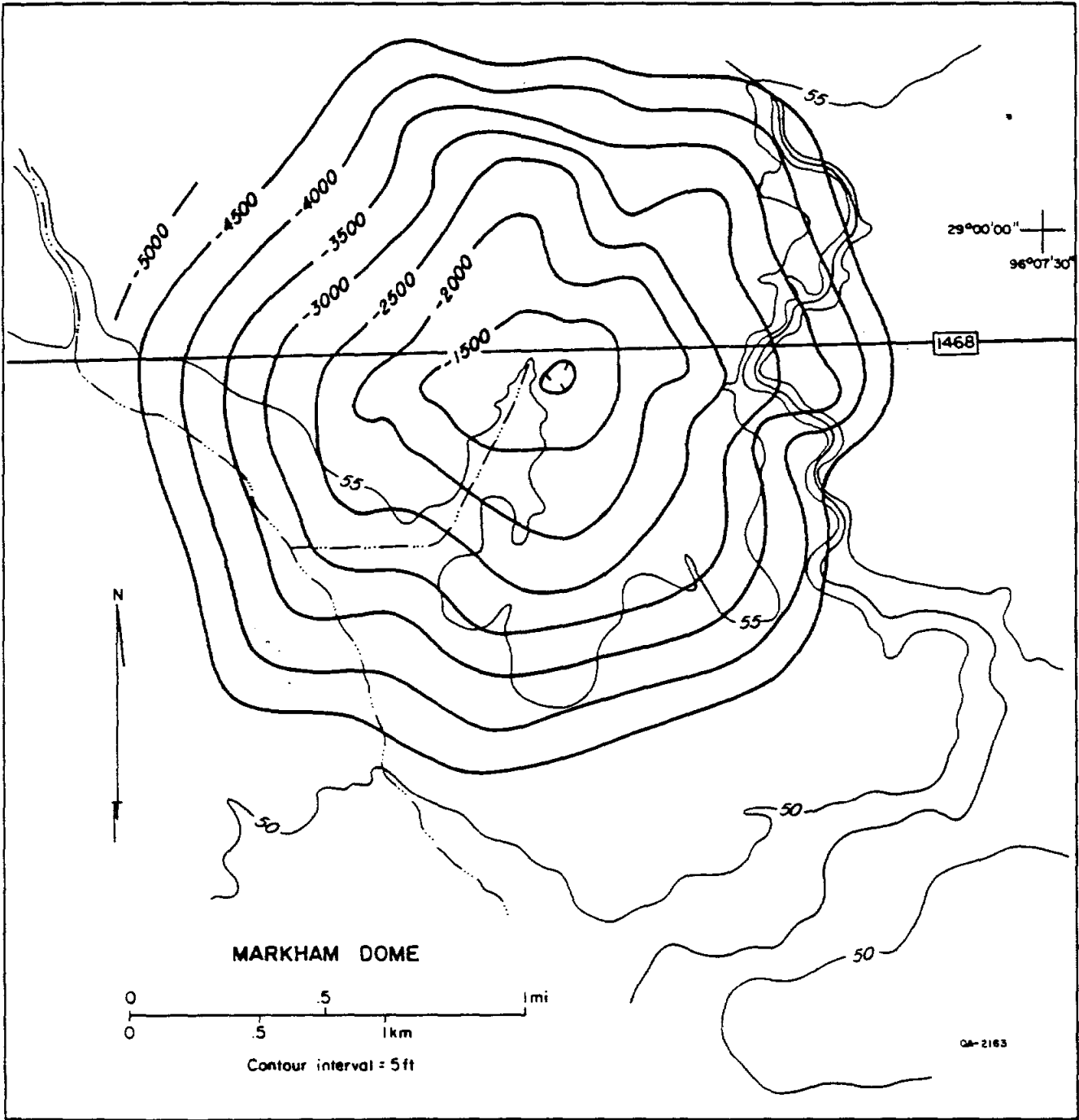


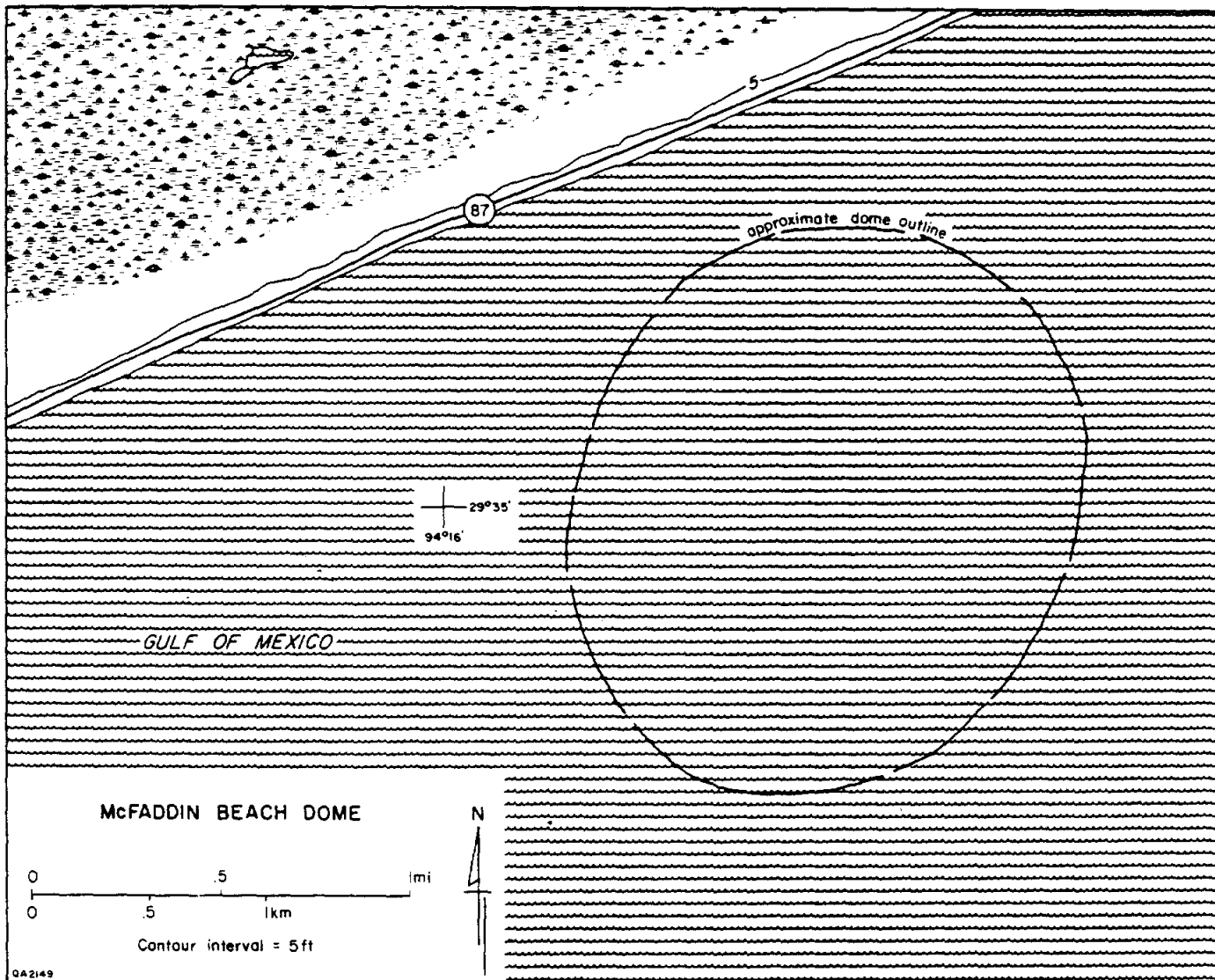


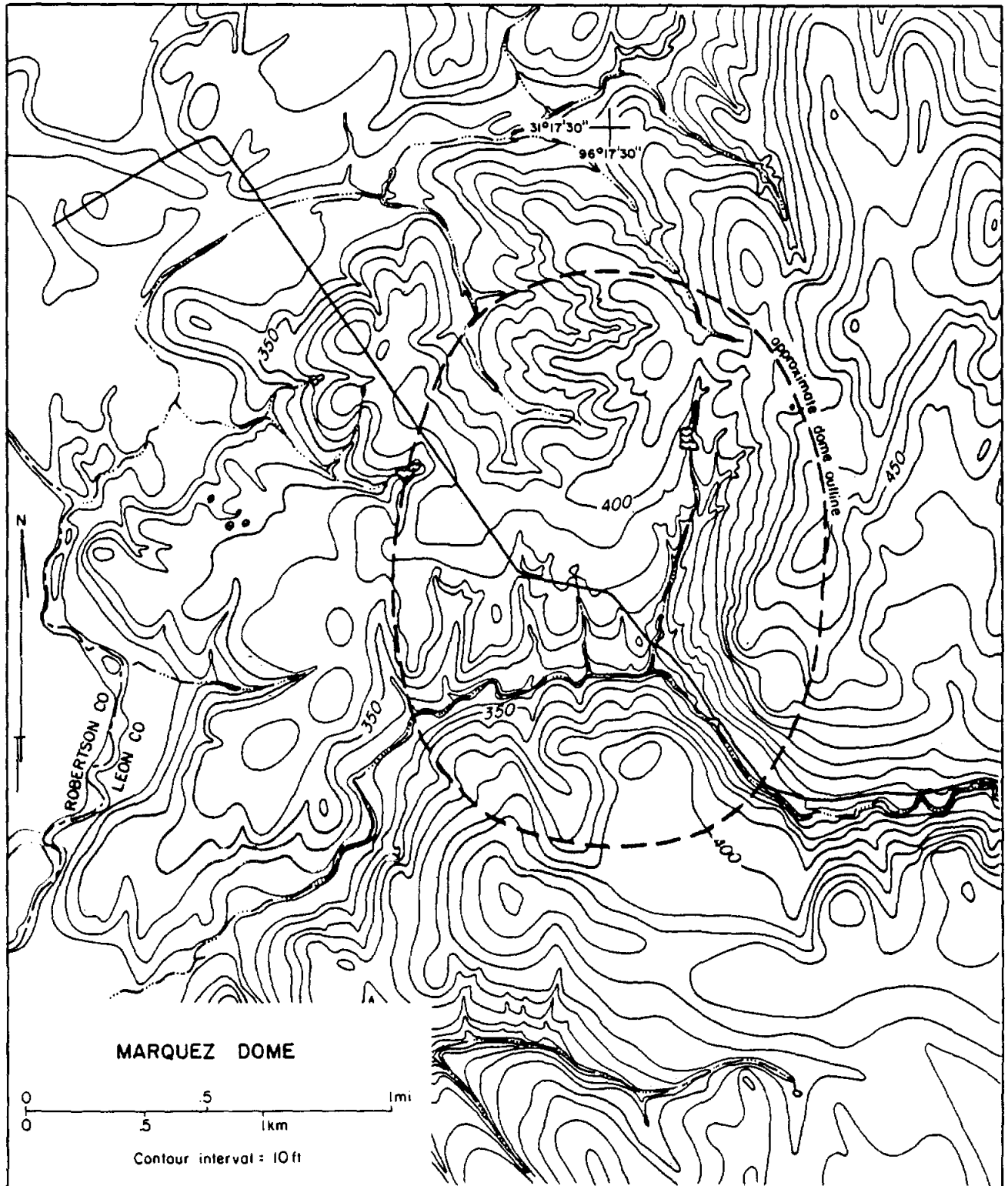


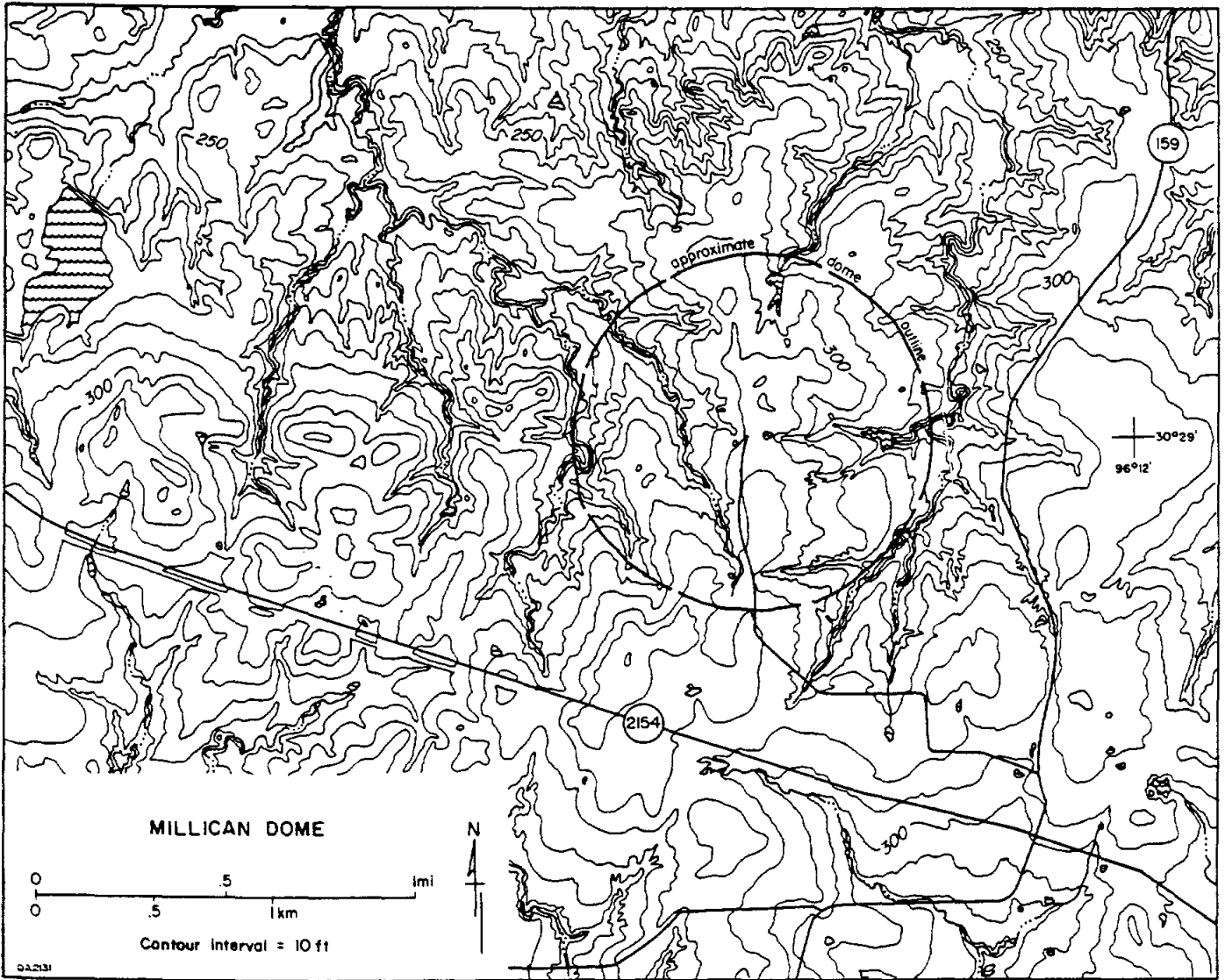


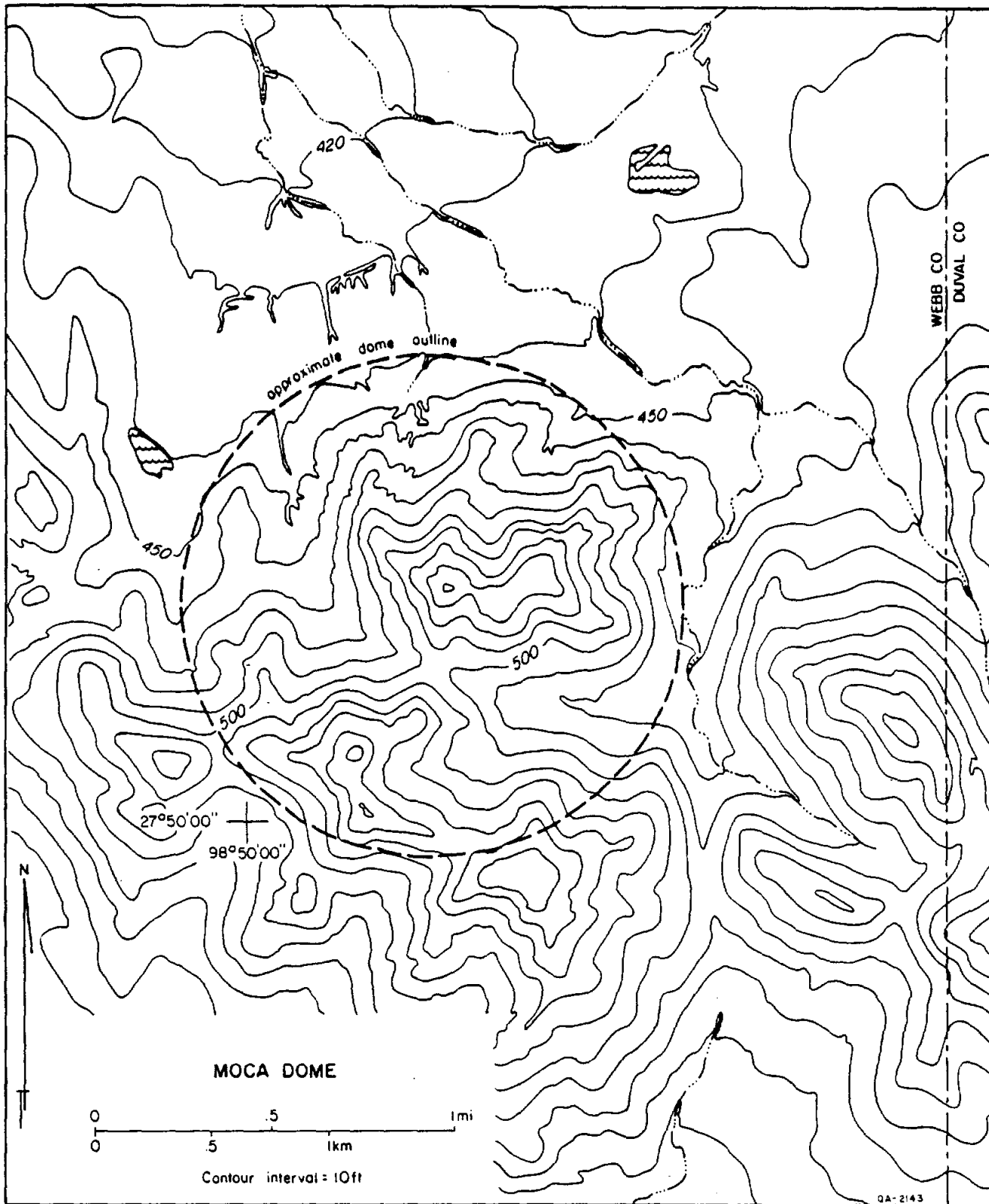


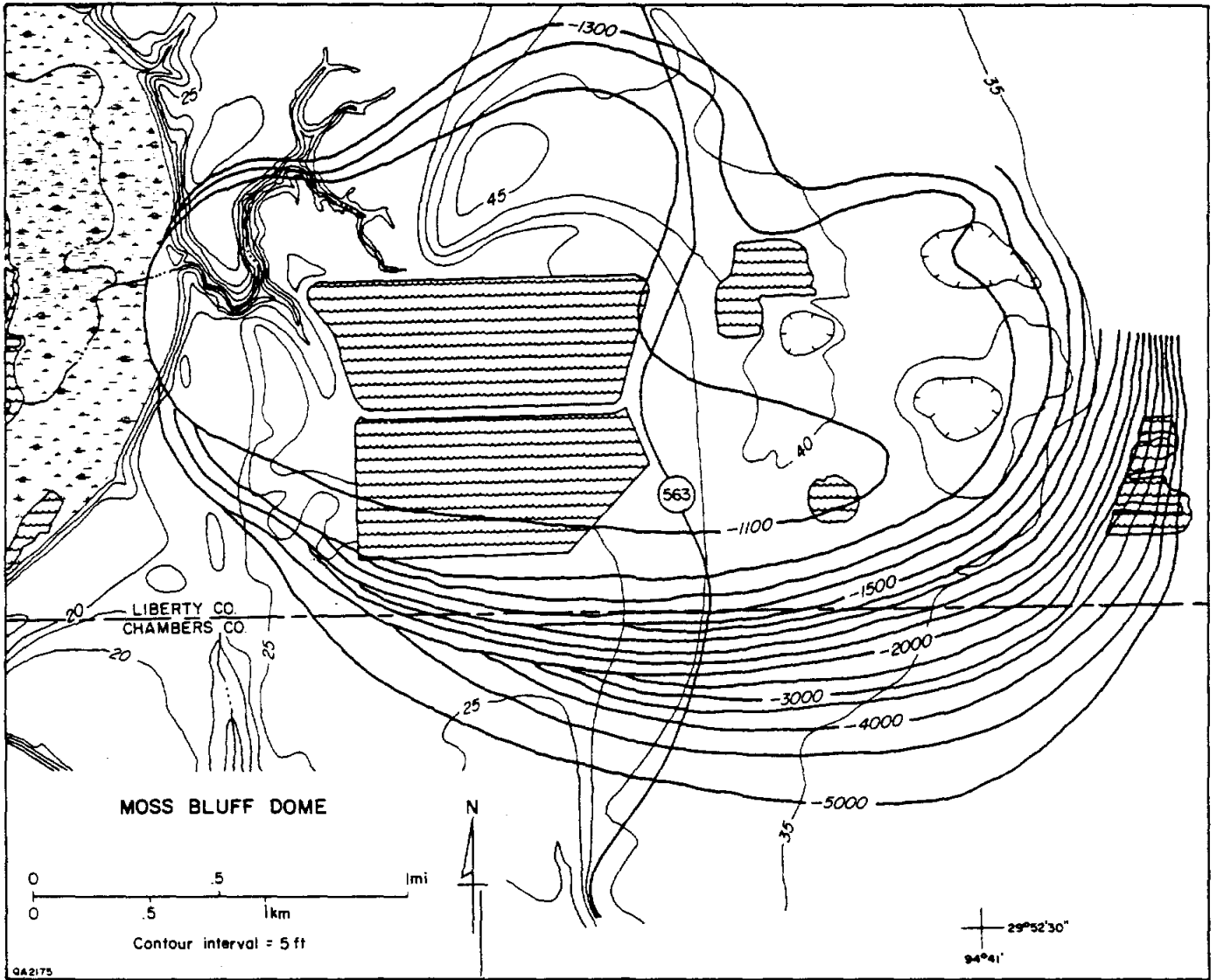


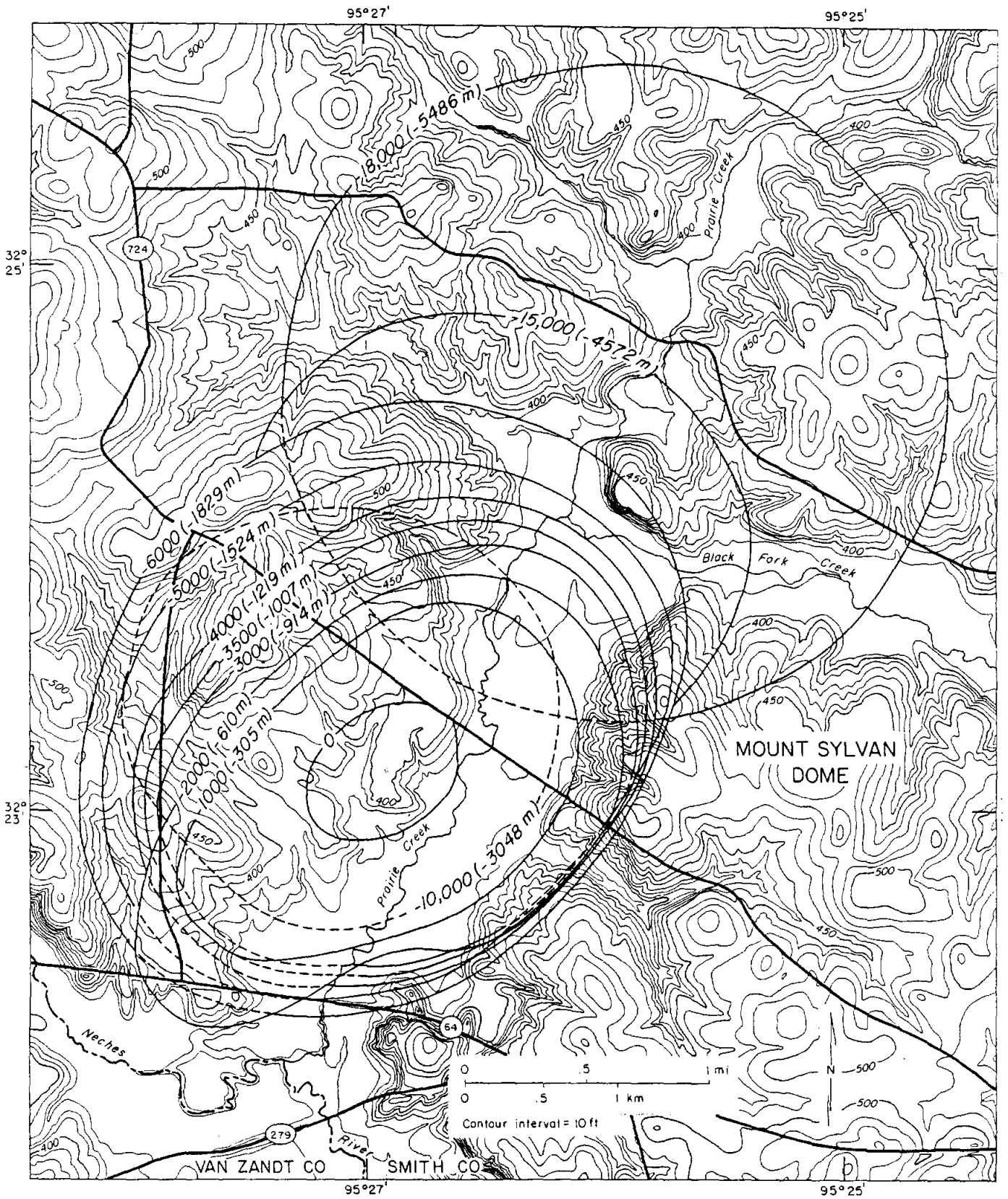


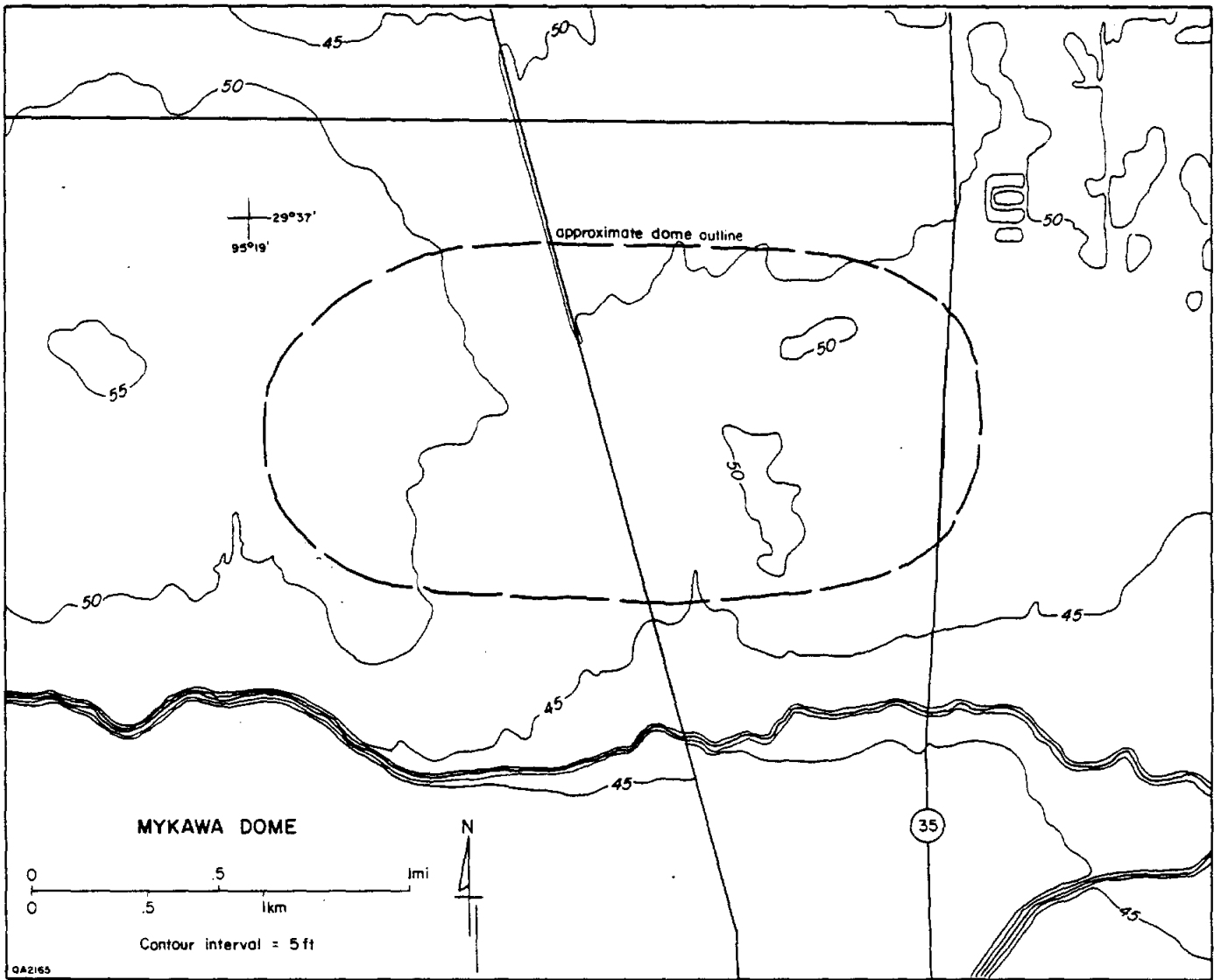


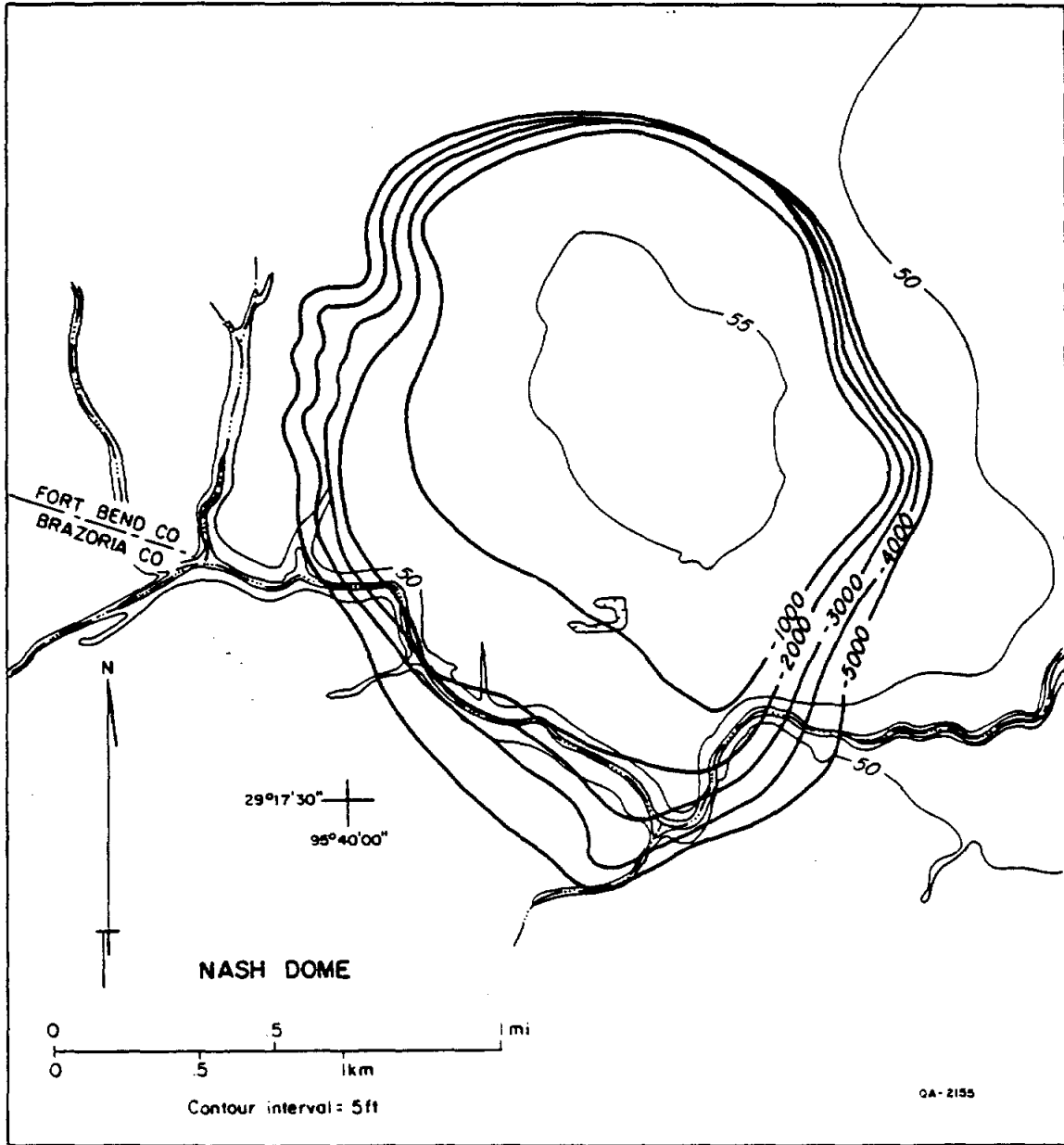


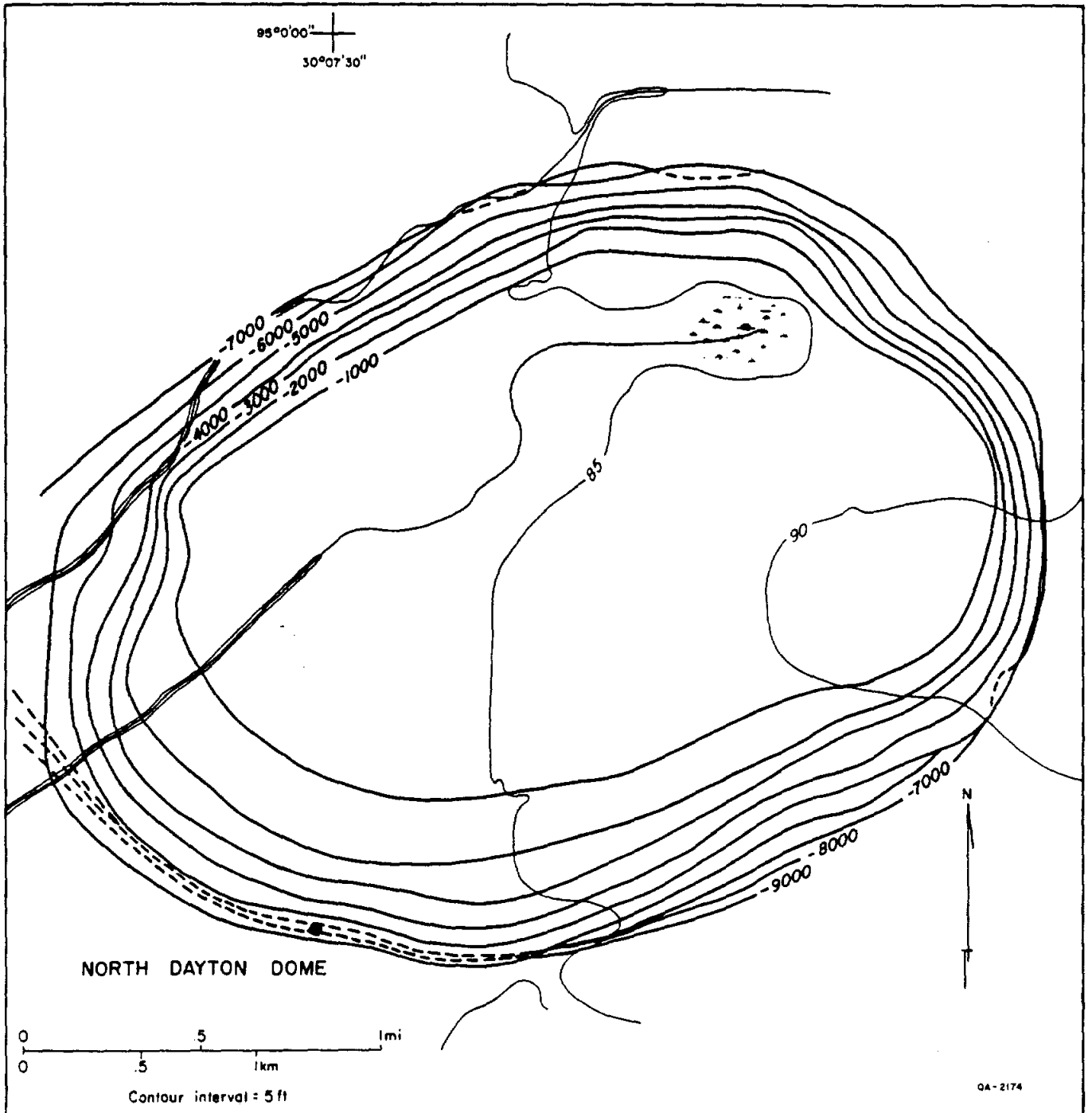


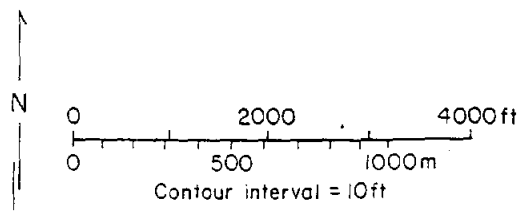
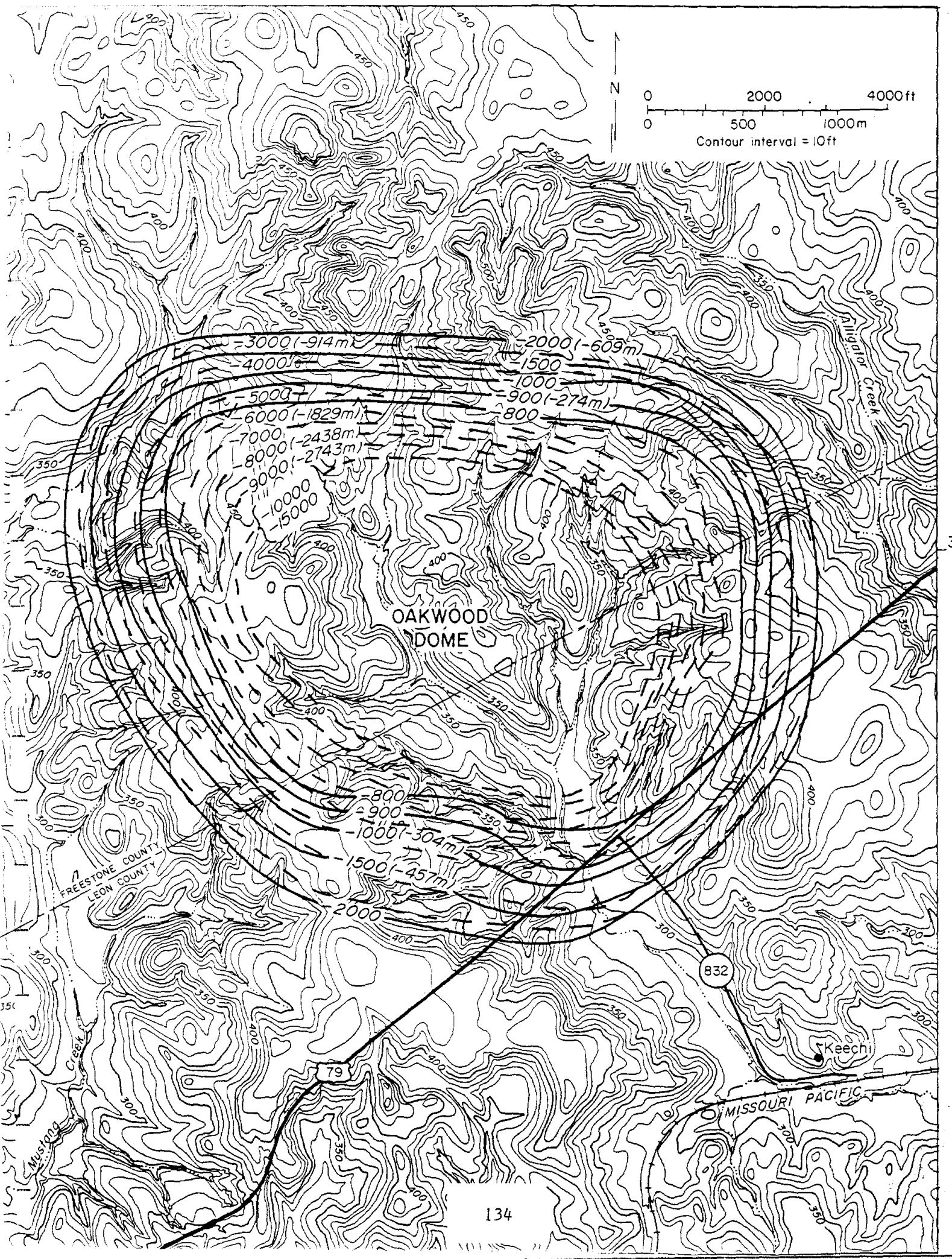












OAKWOOD
DOME

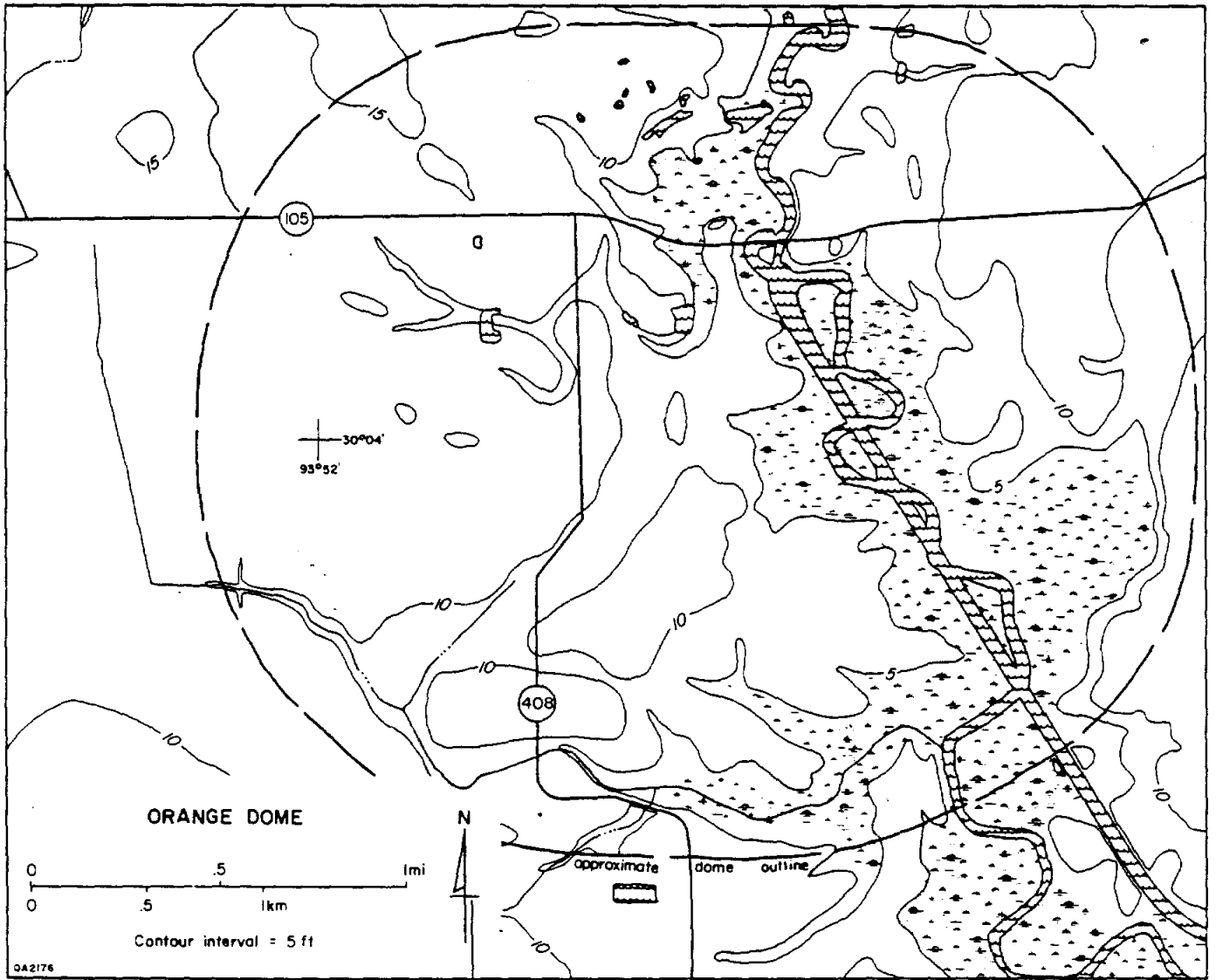
FREESTONE COUNTY
LEON COUNTY

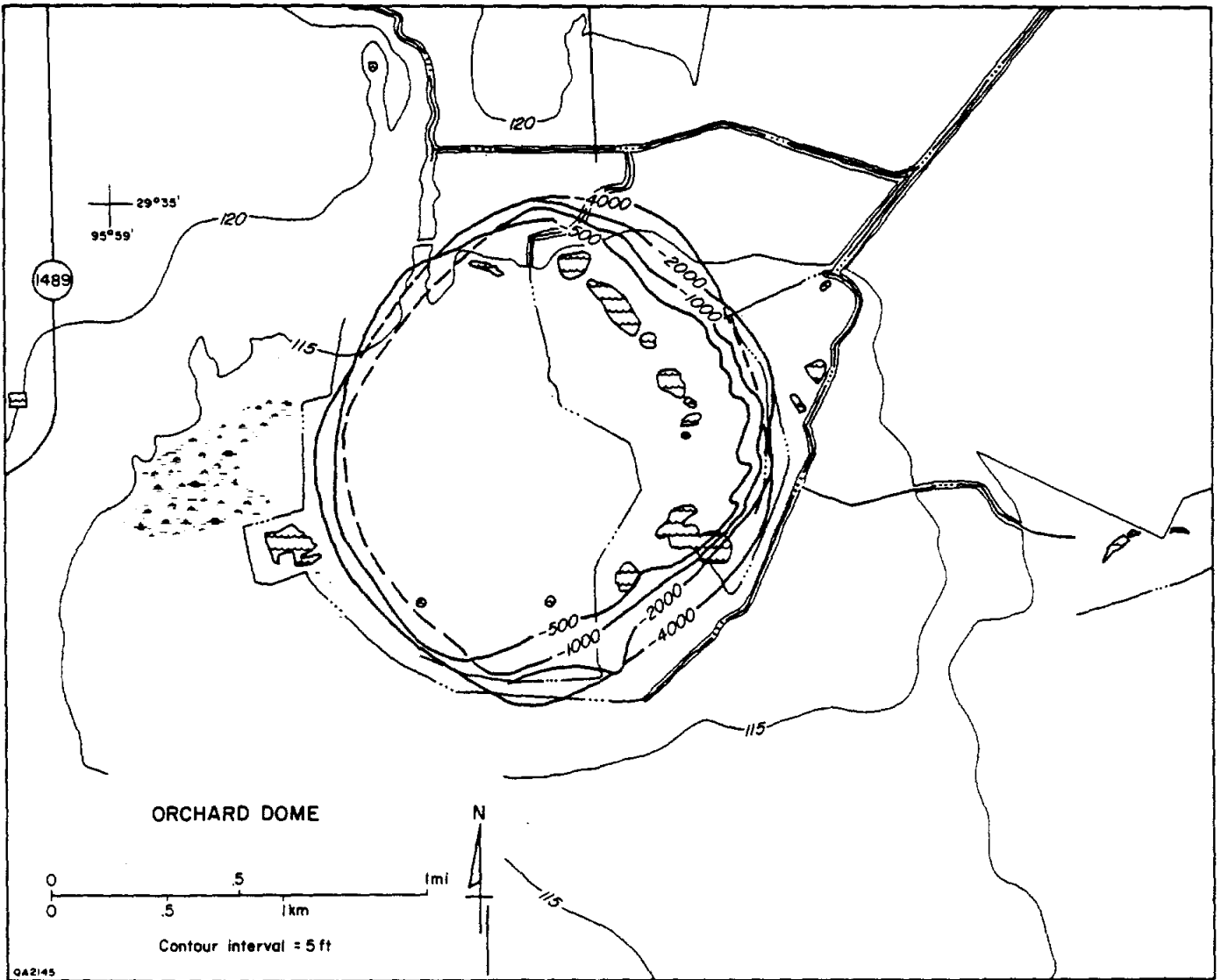
MISSOURI PACIFIC

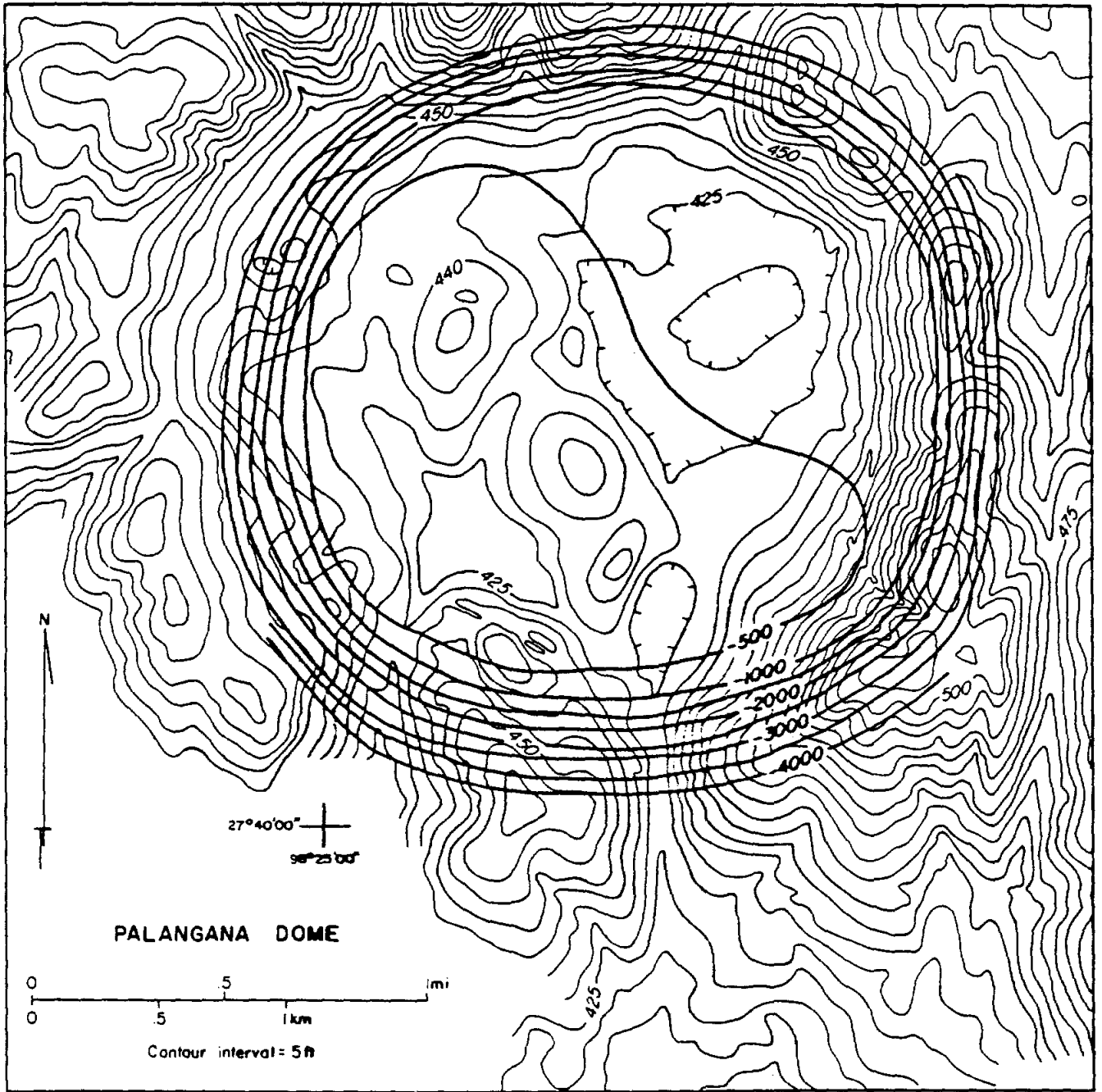
Keetchi

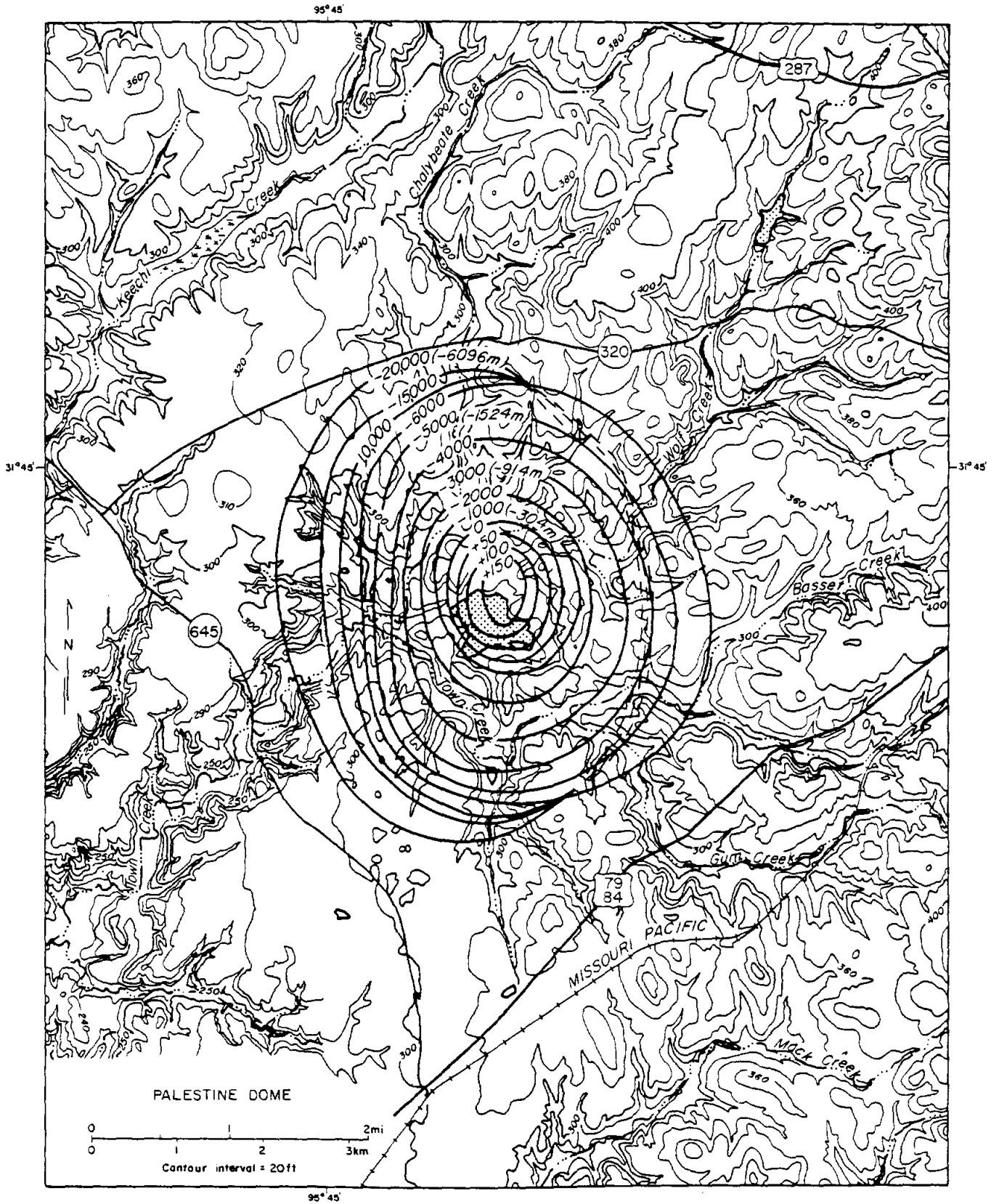
79

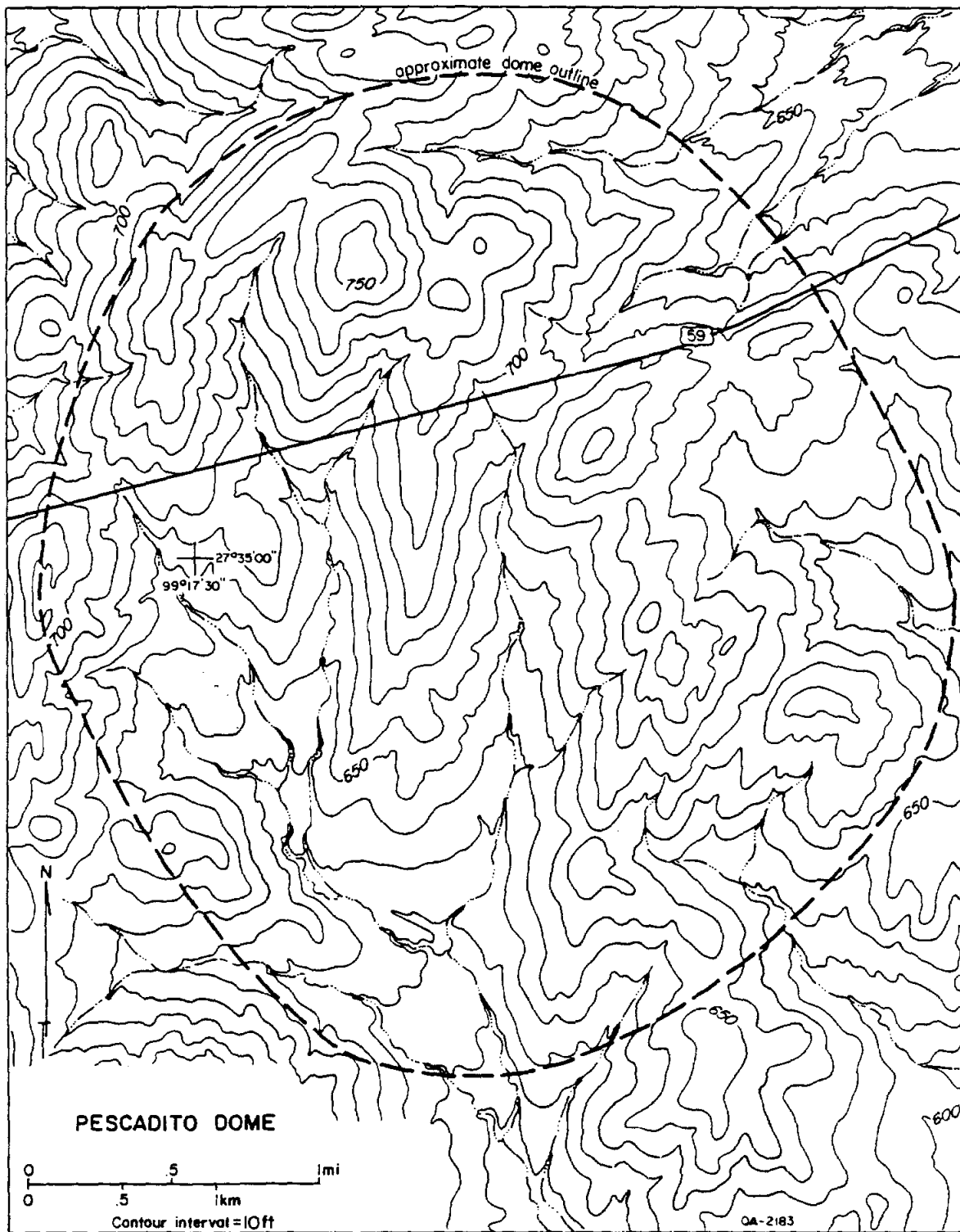
832

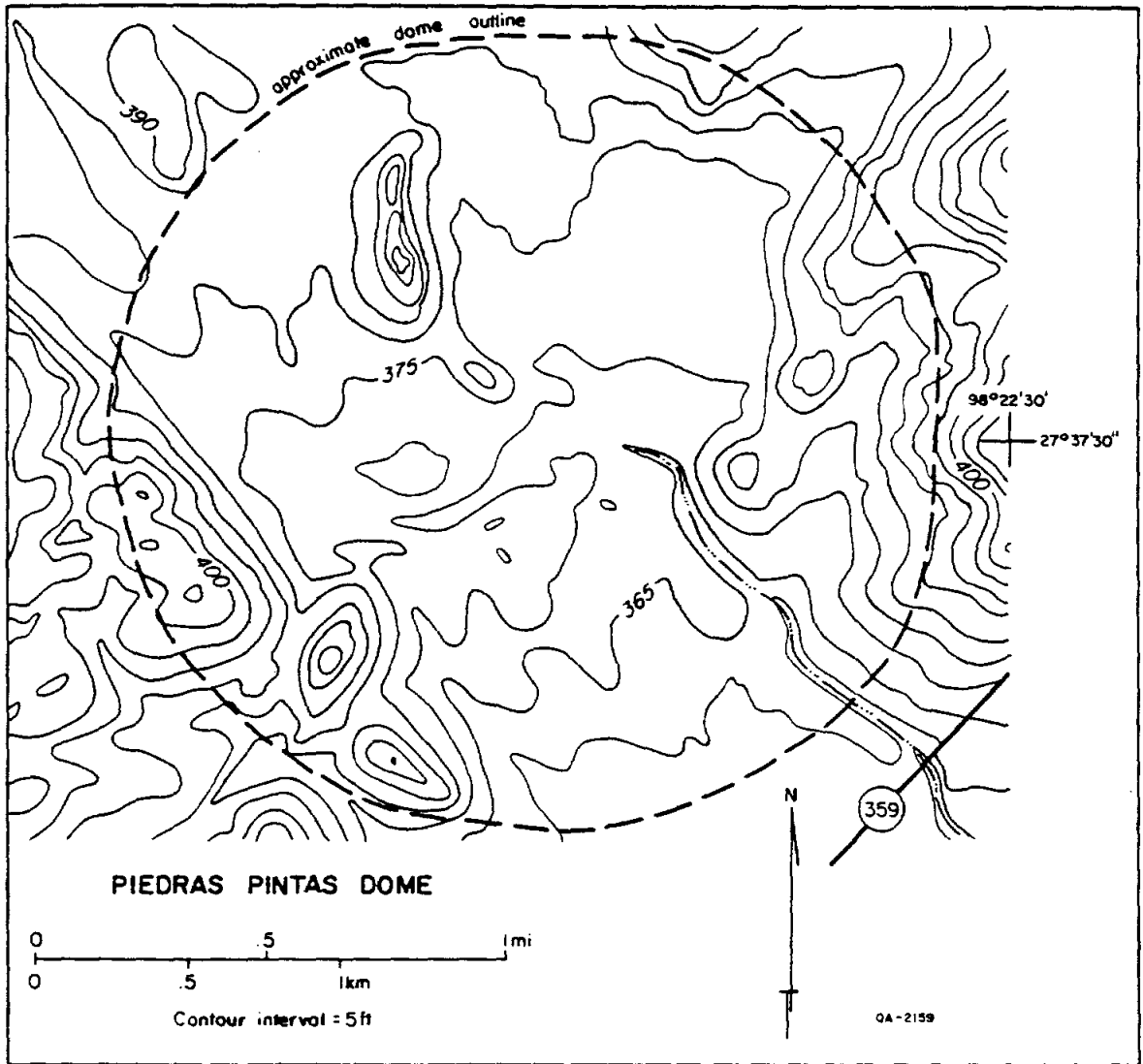


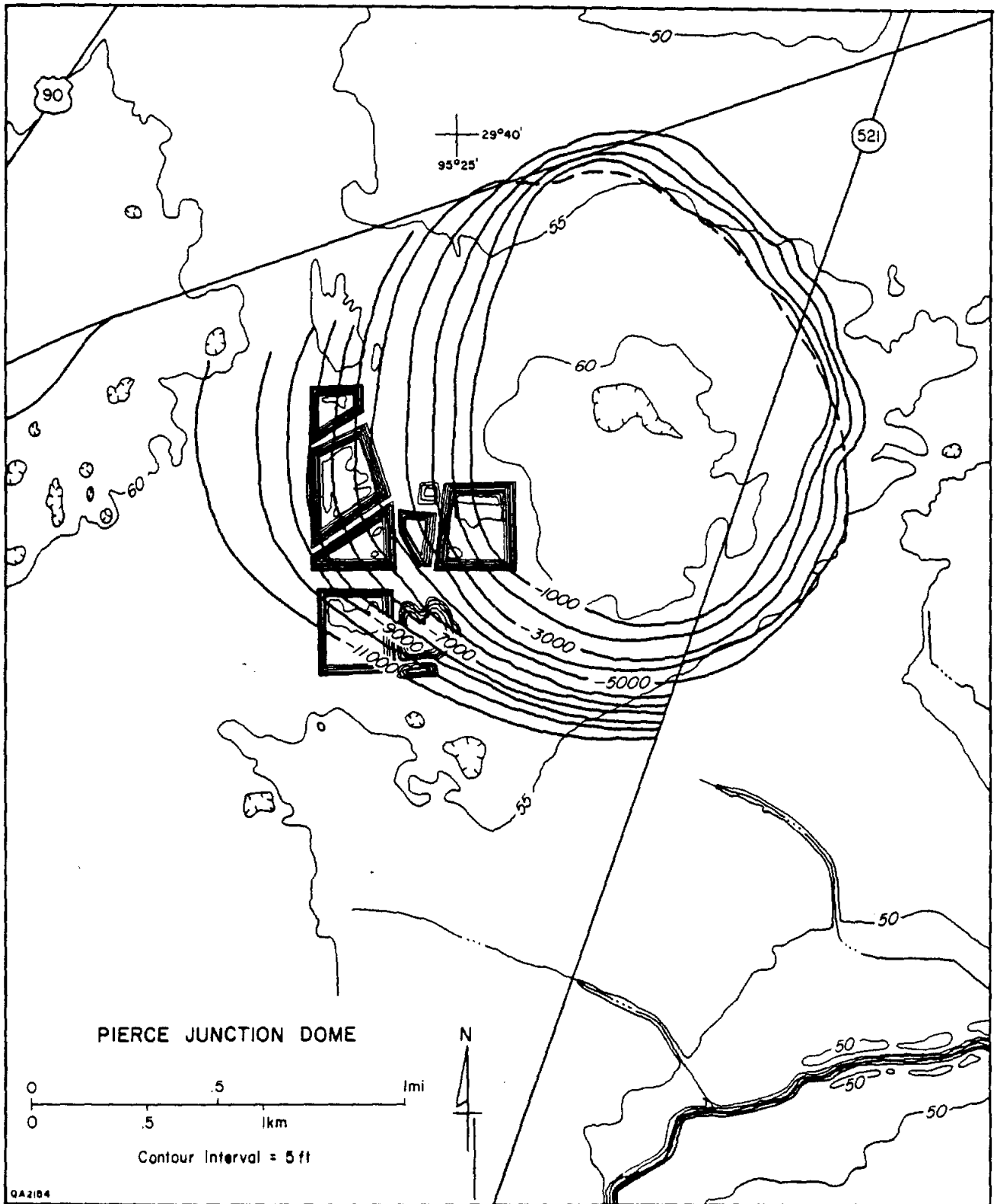


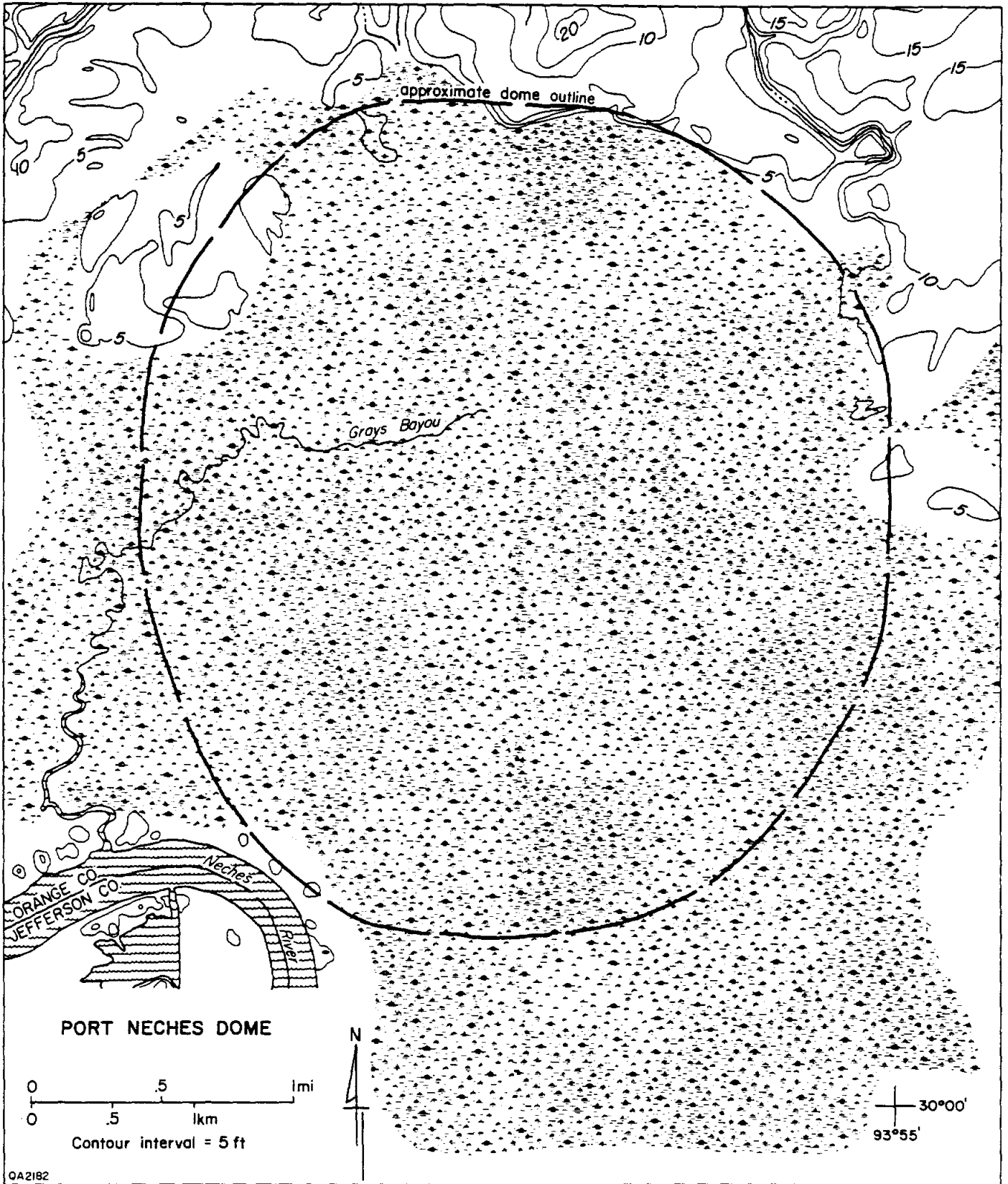


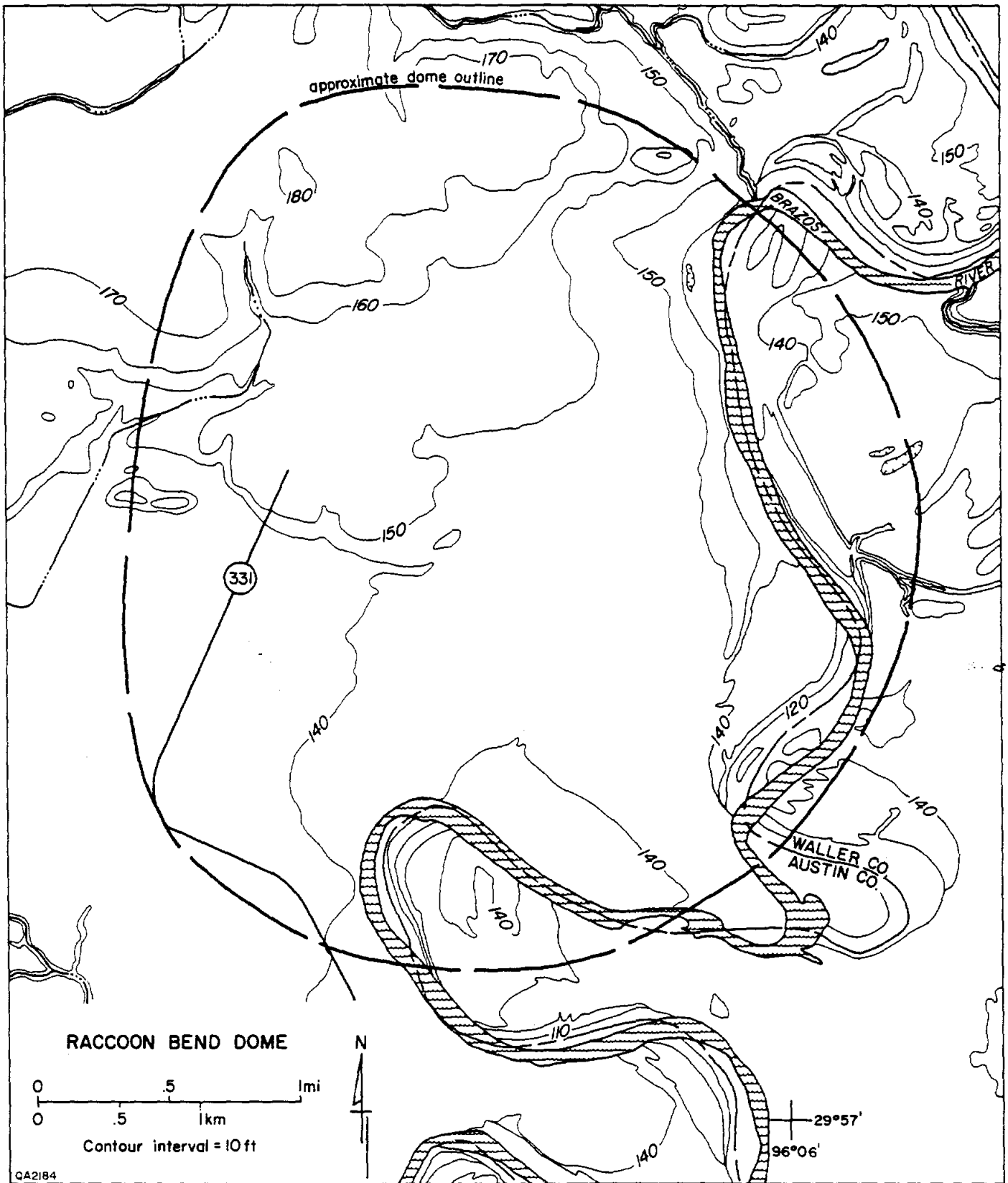


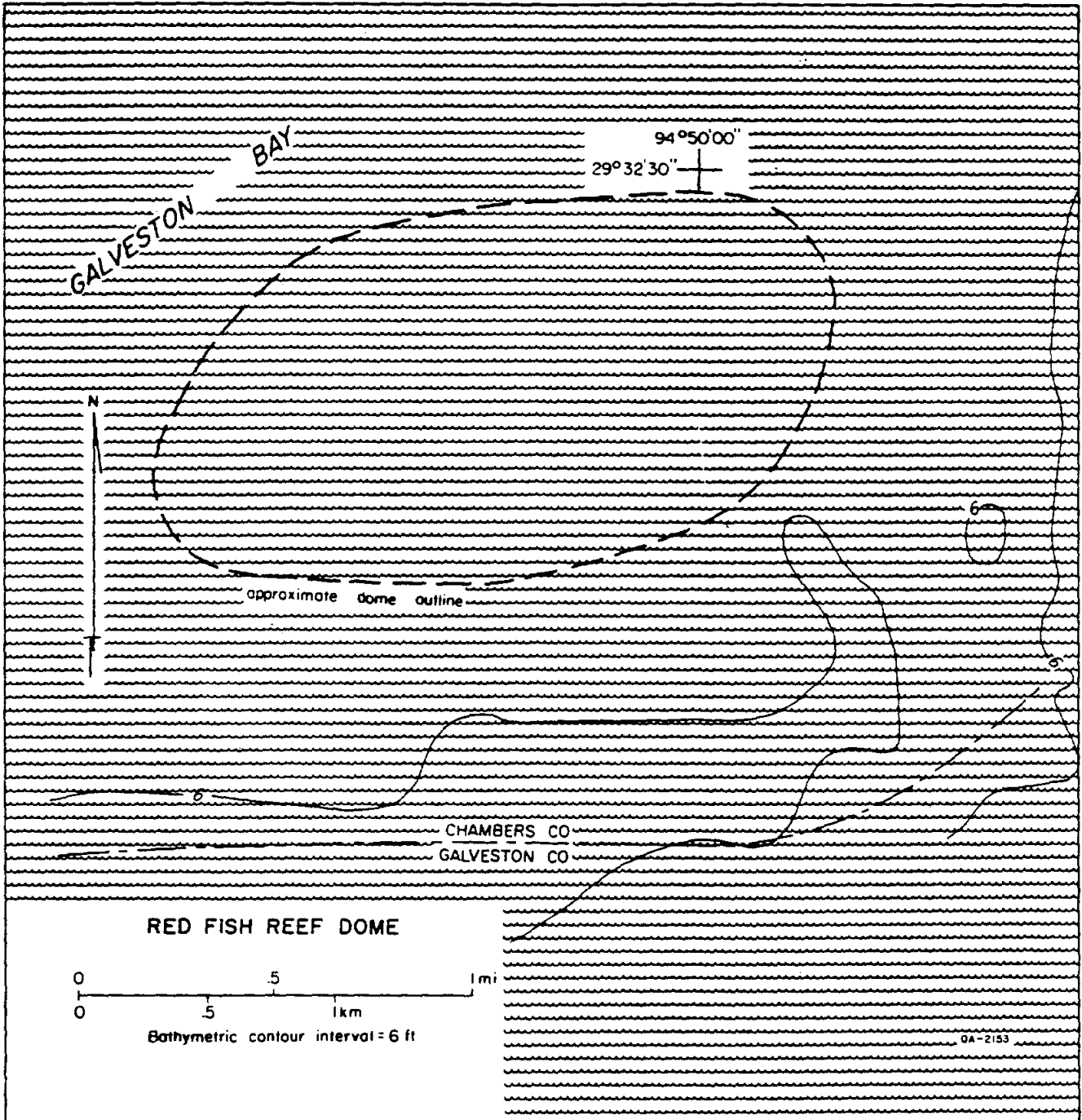


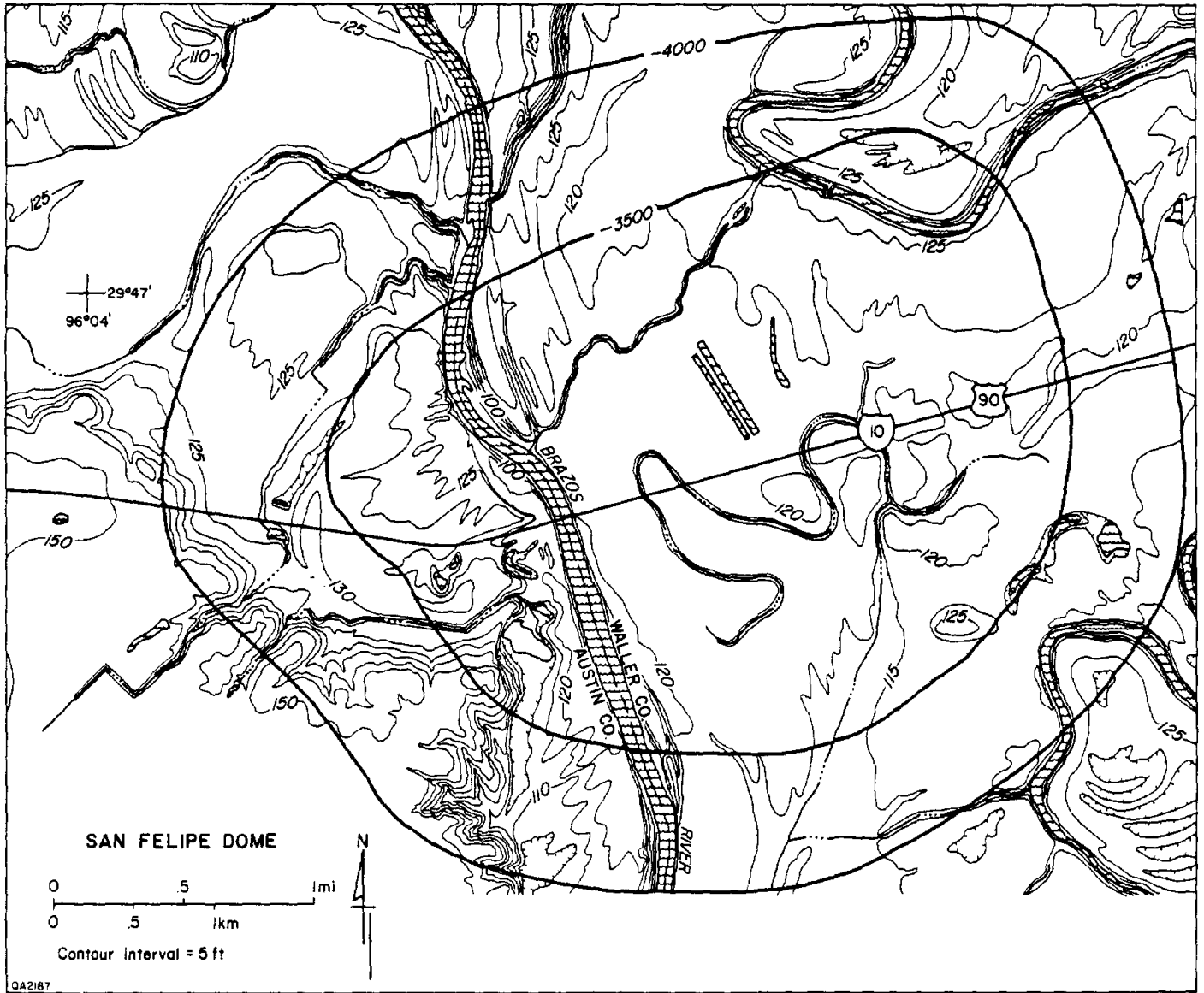


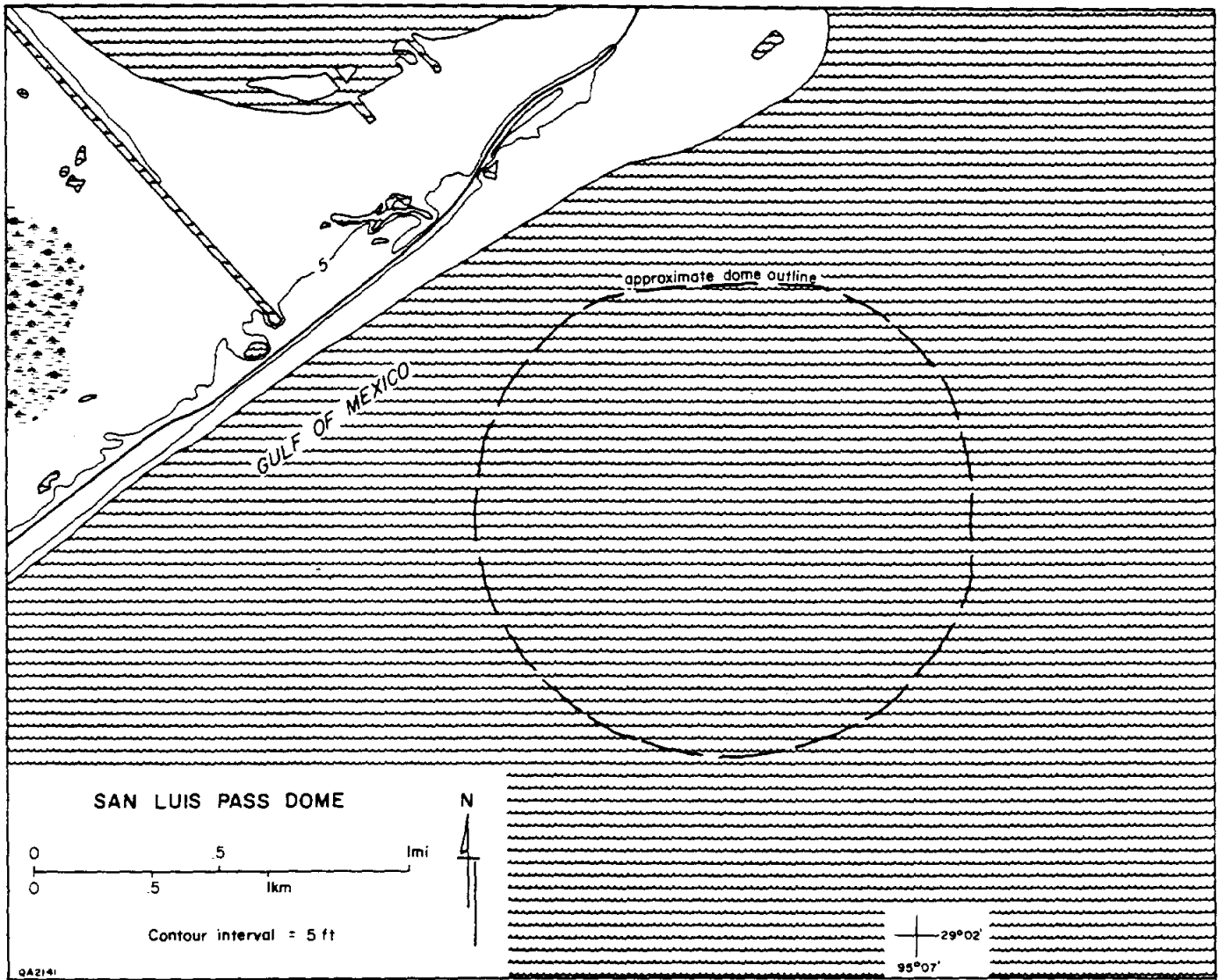


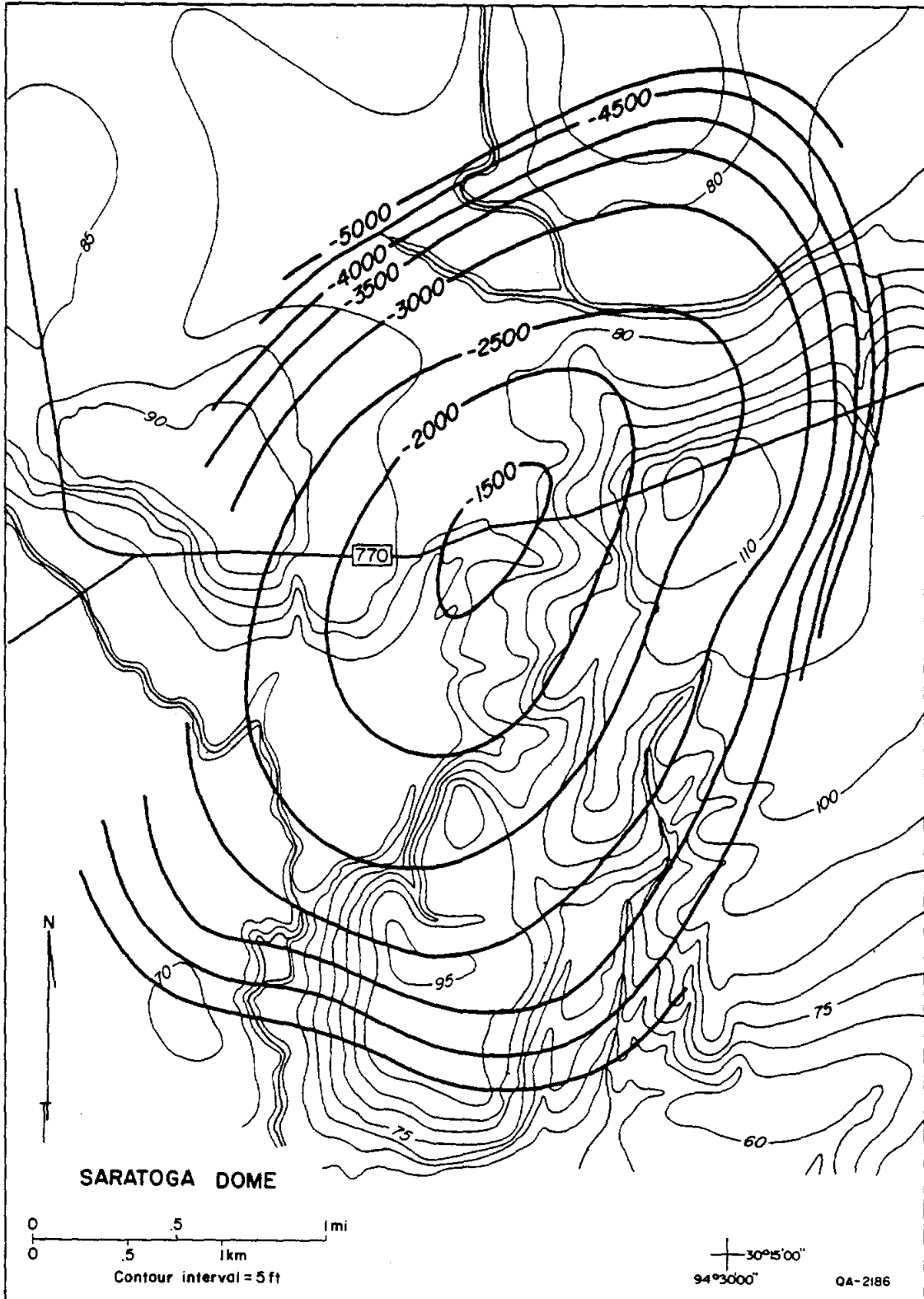


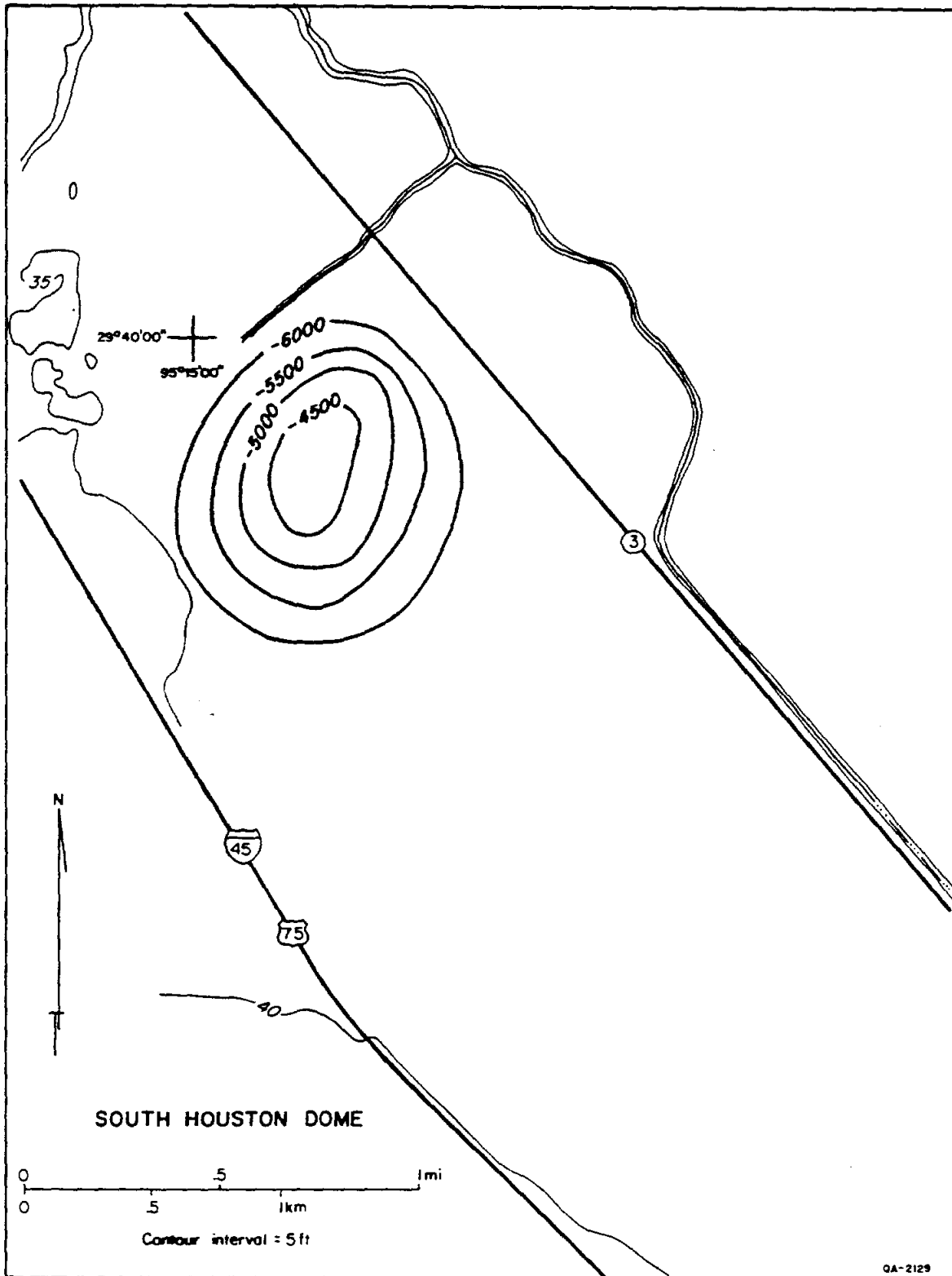


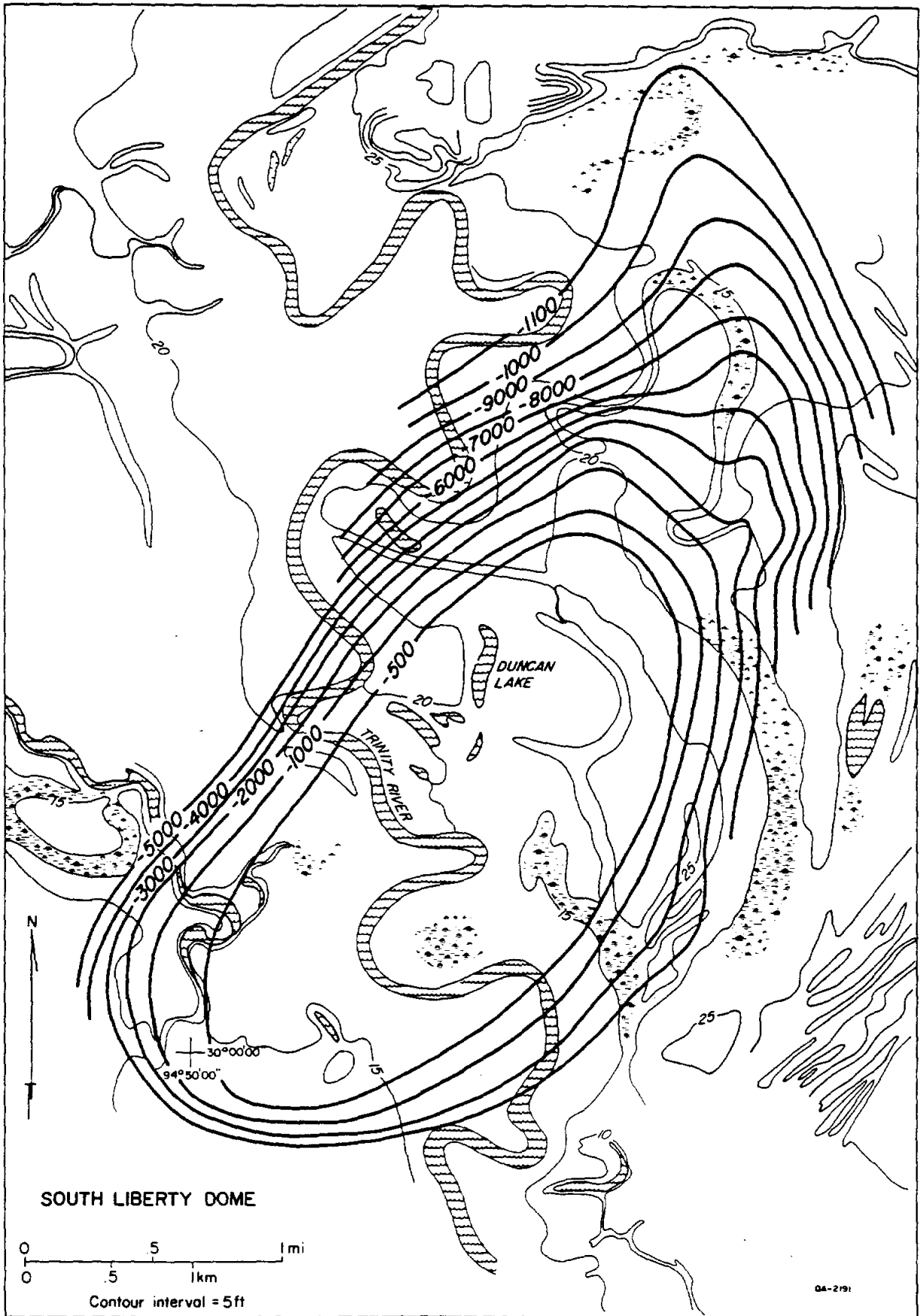


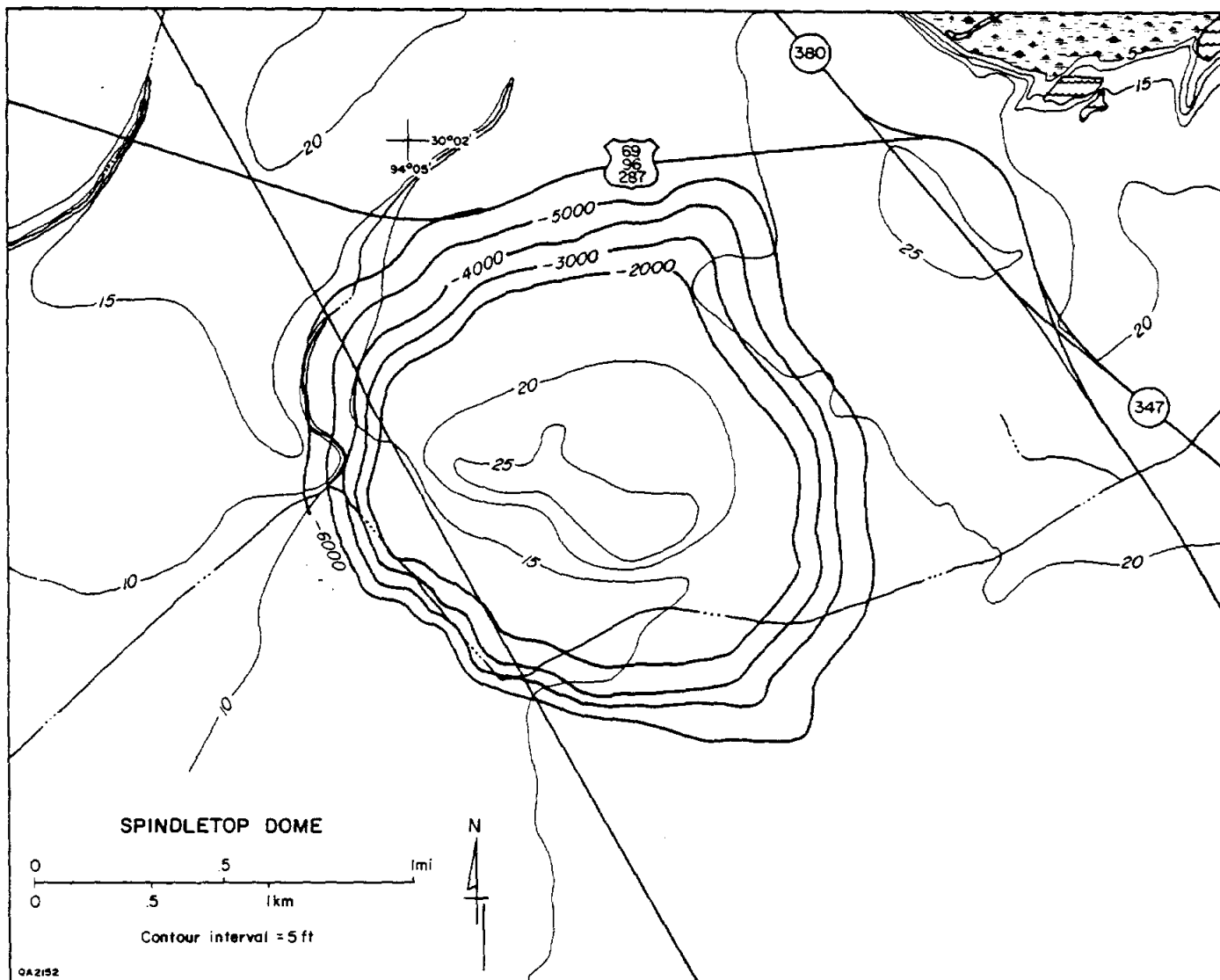


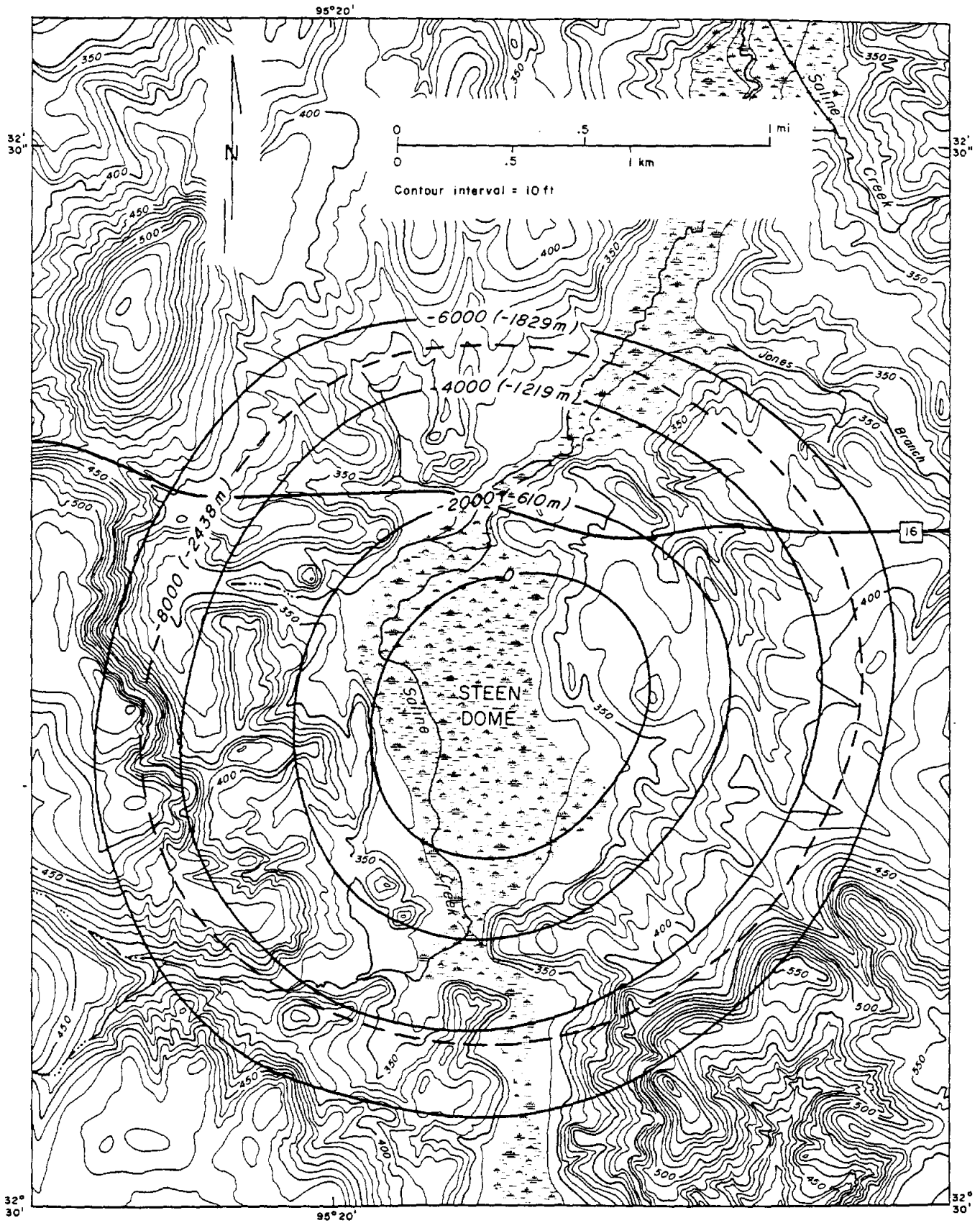


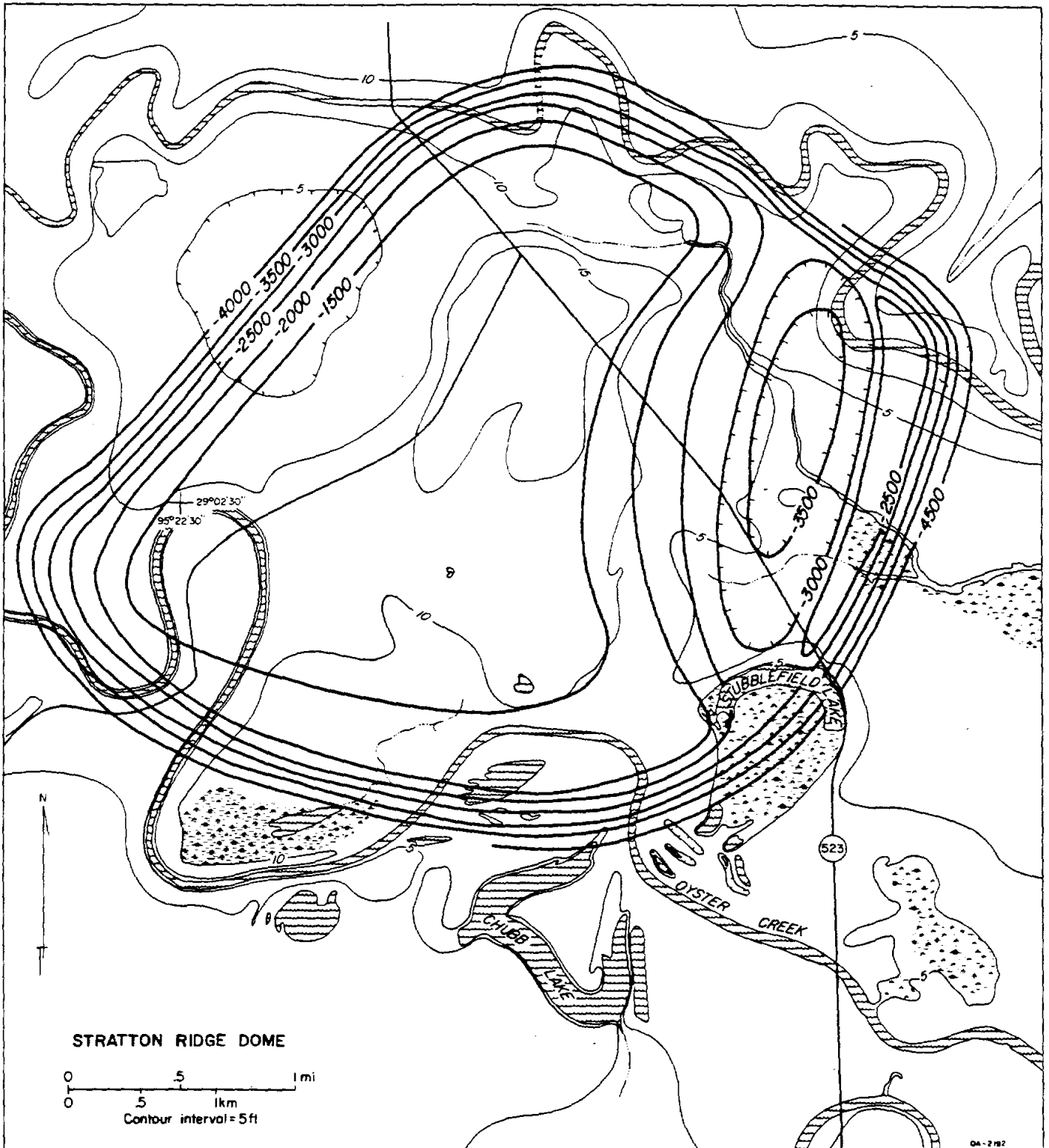


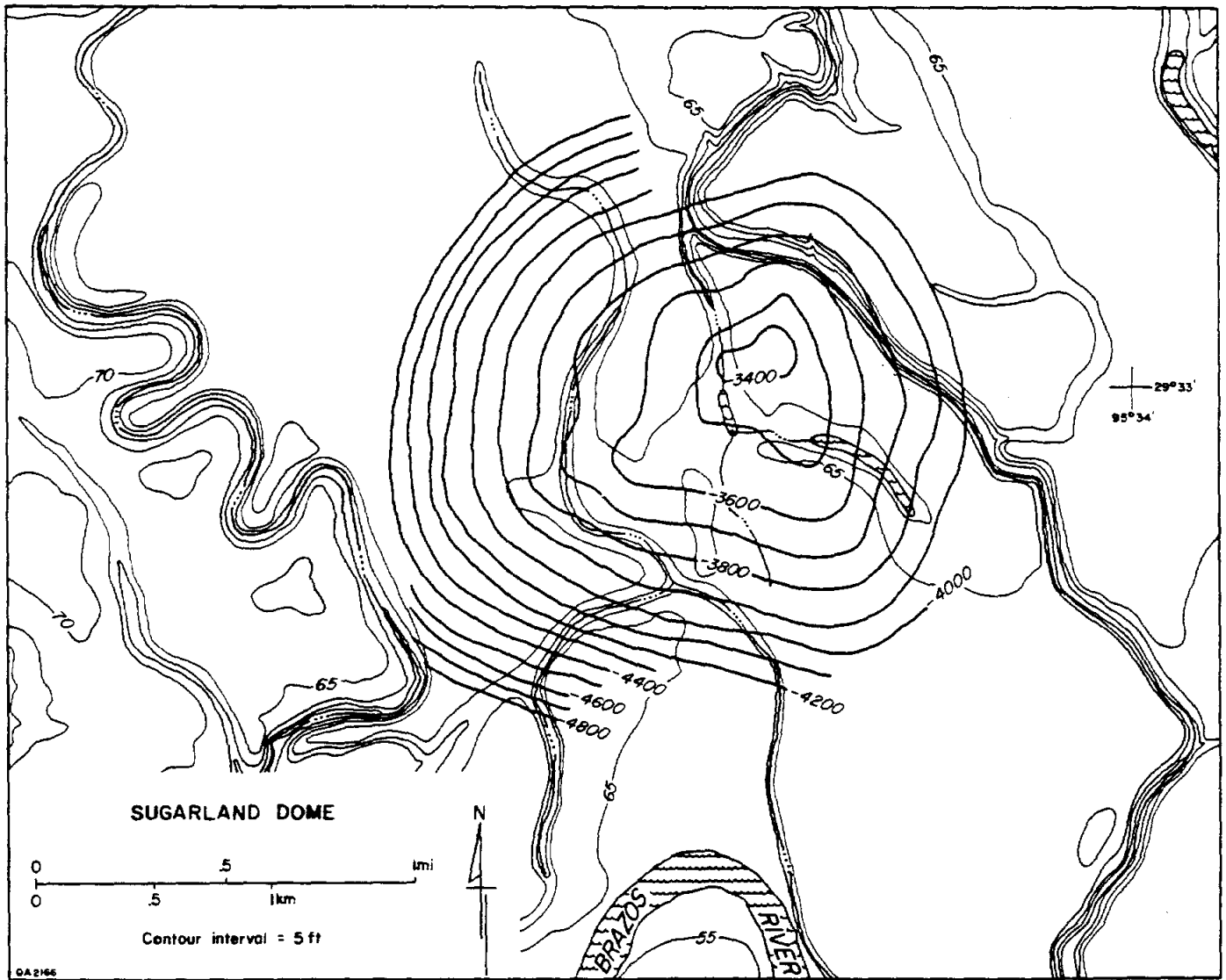


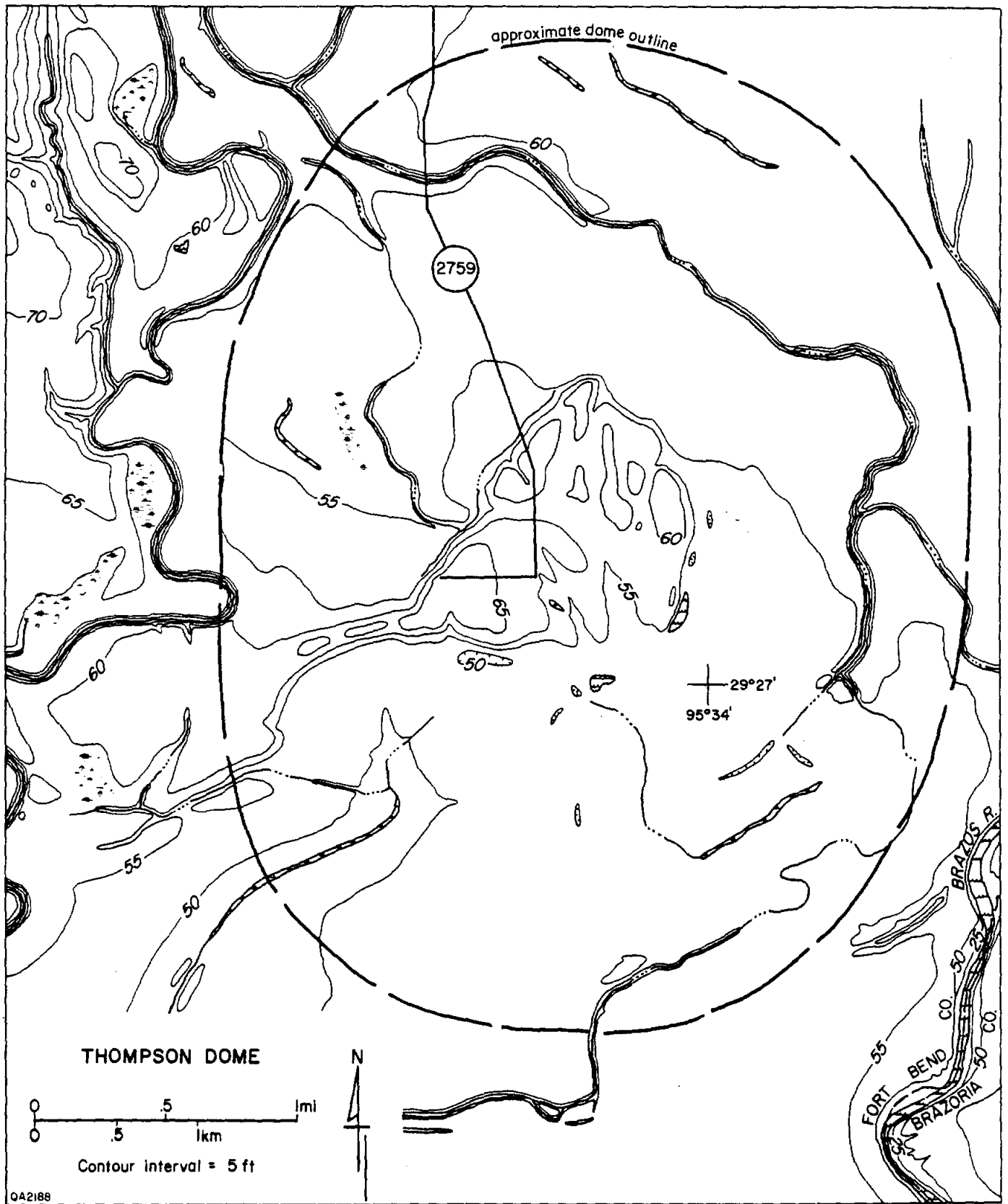


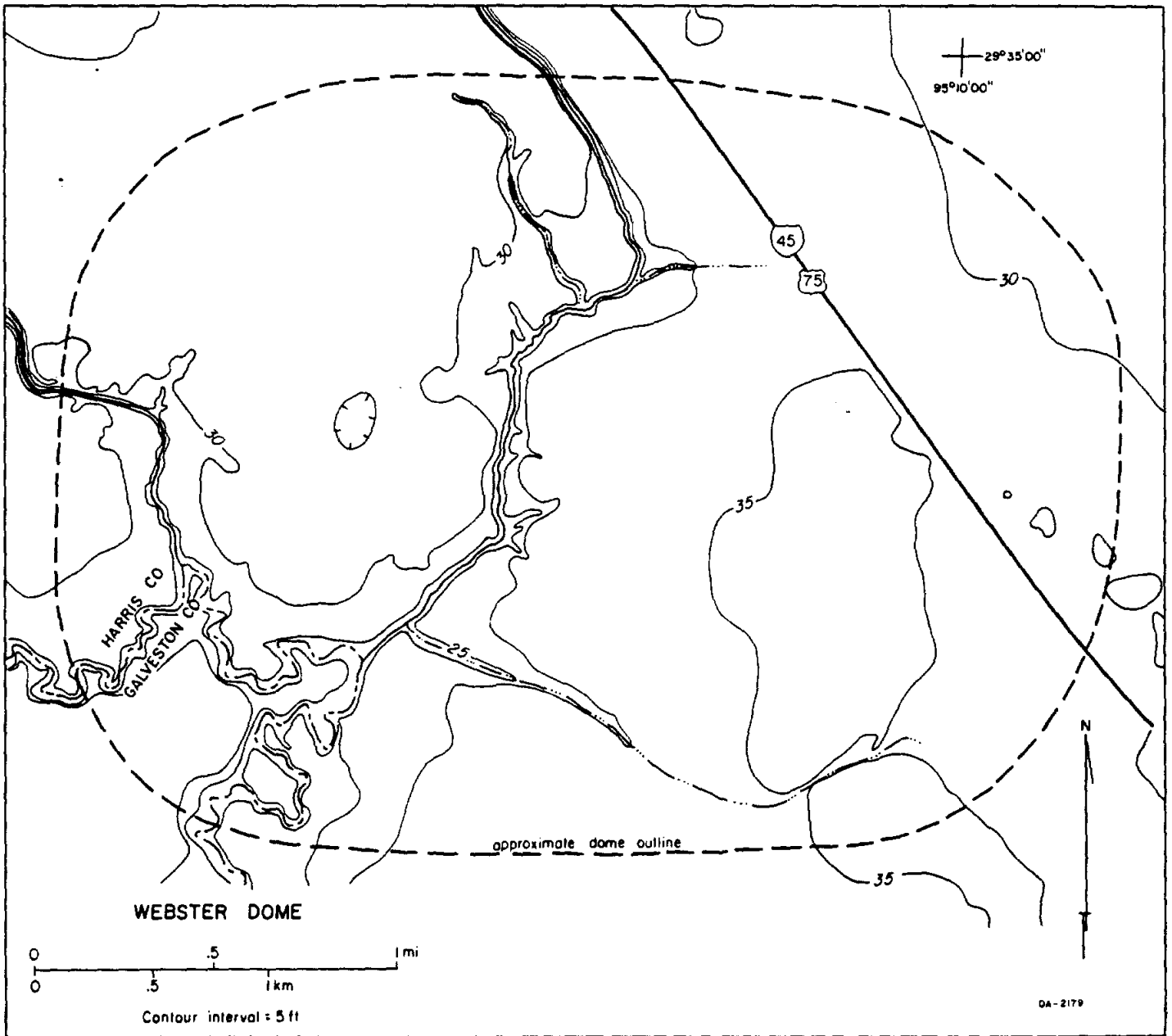


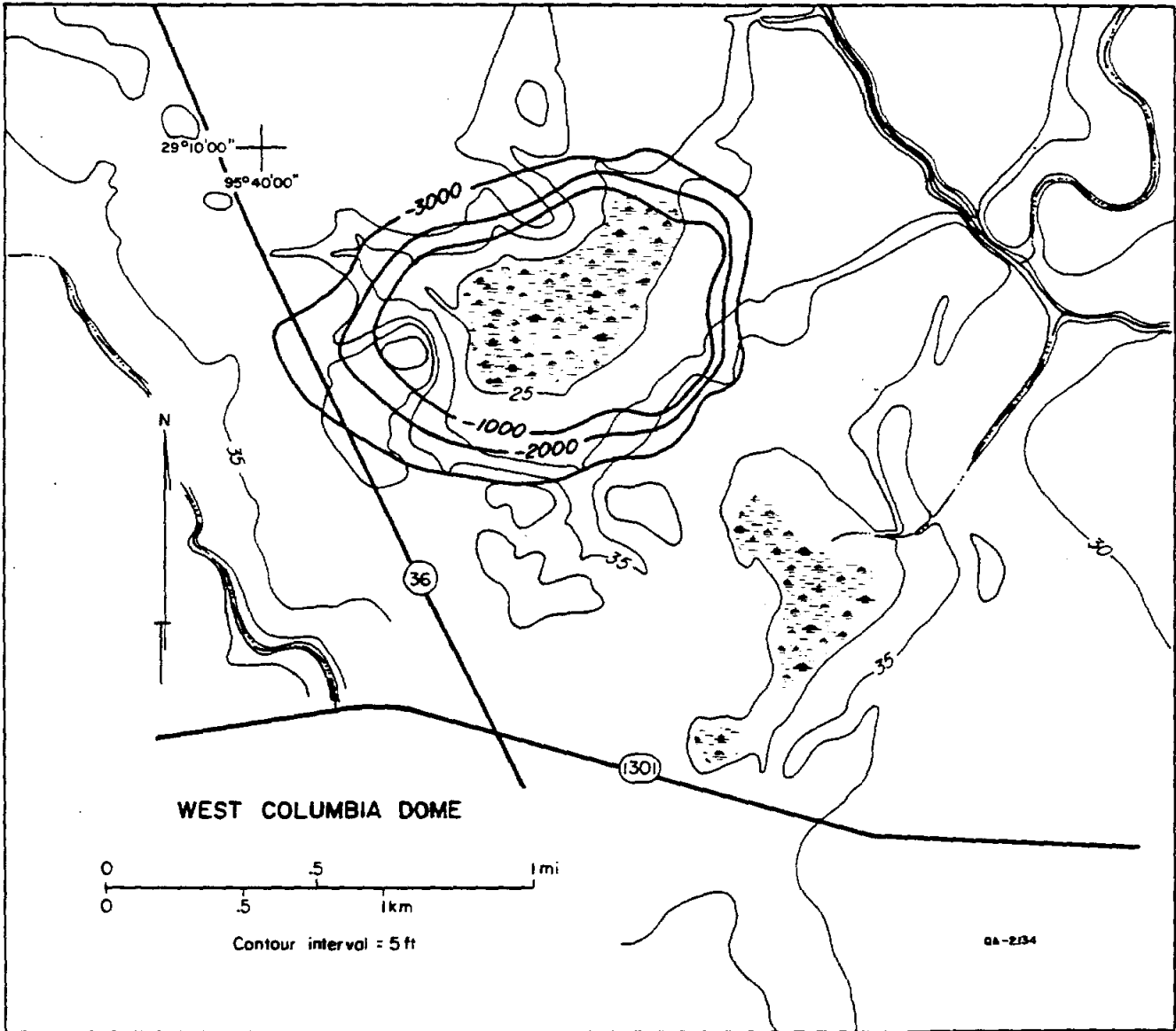


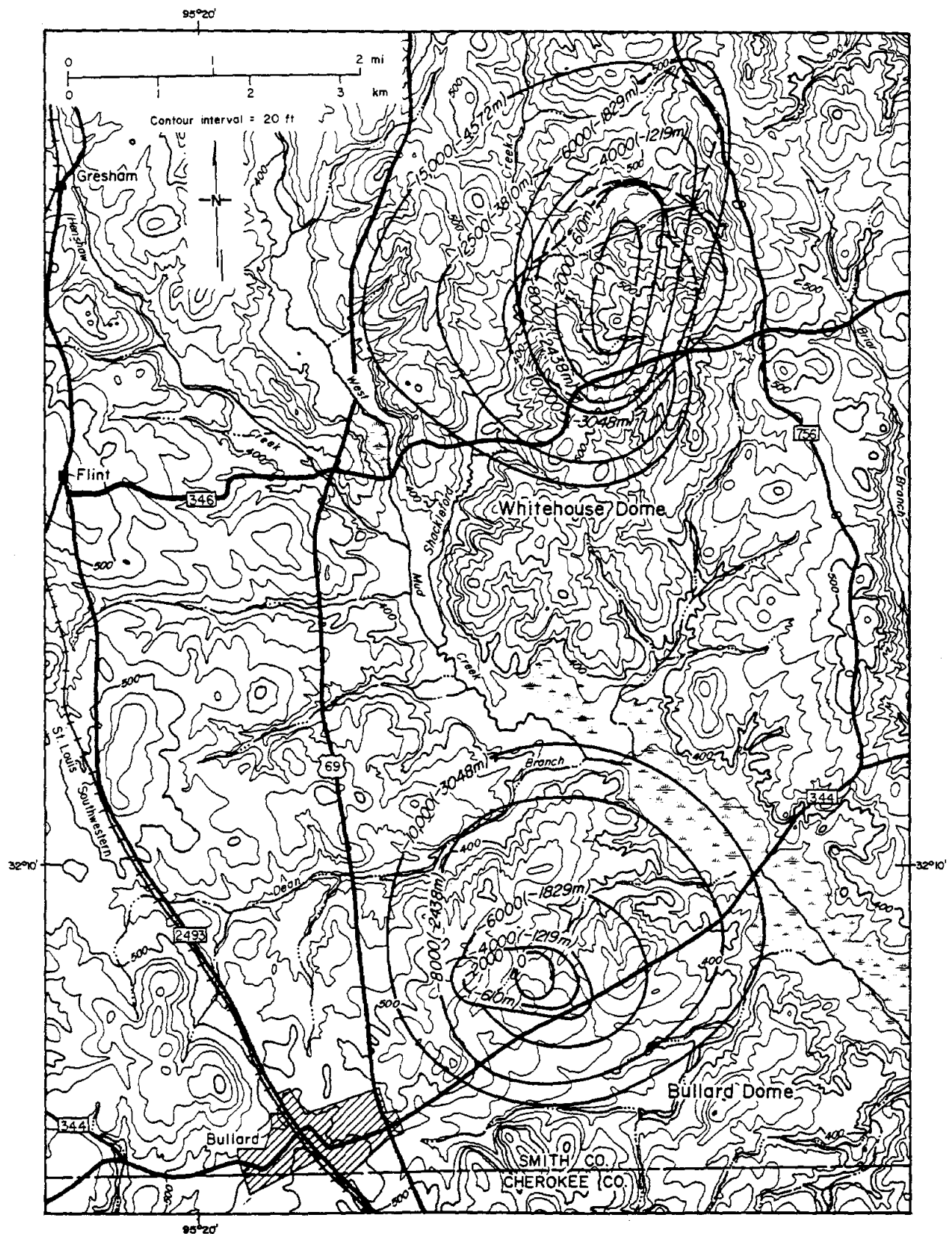












APPENDIX 2. Railroad Commission of Texas Authority Numbers for storage-well permits.

NAME OF SALT DOME	CURRENT OPERATOR OF STORAGE FACILITY	ORIGINAL APPLICANT	RAILROAD COMMISSION AUTHORITY NUMBERS

* BARBERS HILL	TEXAS EASTERN	TEXAS NATURAL GASOLINE	03-27865, 03-40761, 03-40760
* BARBERS HILL	DIAMOND SHAMROCK	DIAMOND SHAMROCK	03-59299
* BARBERS HILL	WARREN	WARREN	03-63536
* BARBERS HILL	X-RAL	X-RAL	03-64977
* BARBERS HILL	TENNECO	TENNESSEE GAS TRANSMISSION	03-33873, 03-77018, 03-77903, 03-32960
* BARBERS HILL	EXXON	HUMBLE OIL AND REFINING	03-45459, 03-65222
* BARBERS HILL	ENTERPRISE	ENTERPRISE	03-70198, 03-69531, 03-77044
* BARBERS HILL	CONOCO	CONOCO	03-68409, 03-76800
* BARBERS HILL	ARCO	TEXAS BUTADIENE AND CHEMICAL CORP.	03-33063
* BETHEL DOME	BI-STONE FUEL	BI-STONE FUEL	06-62759
* BIG HILL	UNION	PURE OIL CO.	03-34046, 03-33628
* BIG HILL	DEPARTMENT OF ENERGY	DEPARTMENT OF ENERGY	03-79466
* BLUE RIDGE	ABANDONED	TULONA-AMOCO	03-34676, 03-35658, 03-64673
* BOLING	VALERO	LO-VACA GATHERING CO.	03-73654
* BRENNHAM	SEMINOLE PIPELINE CO.	SEMINOLE PIPELINE CO.	03-76656
* BRYAN MOUND	DEPARTMENT OF ENERGY	DOW CHEMICAL	03-67782
* BRYAN MOUND	DEPARTMENT OF ENERGY	DEPARTMENT OF ENERGY	03-70337
* BUTLER DOME	U.P.G.	FREESTONE UNDERGROUND STOR.	05-23215
* CLEMENS	PHILLIPS PETROLEUM	PHILLIPS PETROLEUM	03-31930, 03-32483
* DAY	ABANDONED	PURE OIL	
* EAST TYLER	TEXAS EASTMAN	WARREN PETROLEUM	06-22995
* FANNETT	WARREN PETROLEUM	GULF OIL	03-23675, 03-29708, 03-30296, 03-31943
* HAINESVILLE	RUTANE SUPPLIES	ENTERPRISE PETROLEUM GAS CORP.	06-23529
* HULL	MOBIL	MAGNOLIA PETROLEUM CORP.	03-27186
* MARKHAM	TEXAS BRINE	TEXAS BRINE	03-64975
* MARKHAM	SEADRIFT PIPELINE	SEADRIFT PIPELINE	03-45456
* MOSS BLUFF	MOSS BLUFF STORAGE VENTURE	MOSS BLUFF STORAGE VENTURE	03-72099
* NORTH DAYTON	ENERGY STORAGE TERMINAL INC.	ENERGY STORAGE TERMINAL INC.	03-80865
* PIERCE JUNCTION	ENTERPRISE	WANDA PETROLEUM AND ELLIS TRANSPORT	03-33874, 03-60093
* PIERCE JUNCTION	COASTAL STATES CRUDE GATHERING	COASTAL STATES CRUDE GATHERING	03-26489, 03-64779
* SOUR LAKE	TEXACO	THE TEXAS CO.	03-23381, 03-23803, 03-30937, 03-23476
* STRATTON RIDGE	SEMINOLE PIPELINE	SEMINOLE PIPELINE	03-76306
* STRATTON RIDGE	AMOCO	FENIX AND SCISSON	03-62057
* STRATTON RIDGE	DOW	DOW	03-26779, 03-45413, 03-60633, 03-60845, 03-74630

LIST/TITLE L(17)NAME OF SALT DOME,B(1),R(30)CURRENT OPERATOR OF STORAGE FACILITY ,B(1),R(35)ORIGINAL APPLICANT ,B(1),R(48)RAILROAD COMMISSION AUTHORITY NUMBERS /

LIST/TITLE L(17)NAME OF SALT DOME,B(1),R(30)CURRENT OPERATOR OF STORAGE FACILITY ,B(1),R(35)ORIGINAL APPLICANT ,B(1),R(48)RAILROAD COMMISSION AUTHORITY NUMBERS /

C1,C226,C227,C230,OB LOW C1 WH C226 EXISTS:
C1,C226,C227,C230,OB LOW C1 WH C226 EXISTS:

APPENDIX 3. Railroad Commission of Texas Rule 74 procedures and requirements for storage-well operators.

Railroad Commission of Texas
Oil and Gas Division
051.02.02.074

Railroad Commission of Texas
Oil and Gas Division
051.02.02.074

051.02.02.074
-RULE 74. UNDERGROUND HYDROCARBON STORAGE-

Railroad Commission of Texas
Oil and Gas Division



RAILROAD COMMISSION OF TEXAS
OIL AND GAS DIVISION
CARTER STATION - P.O. BOX 1388 - AUSTIN, TEXAS 78766

NOTICE OF RULE AMENDMENT

Attached is an amendment to Rules 9 and 46, and a new Rule 74, adopted on December 21, 1981. These rules will become effective on April 1, 1982.

Glenn Jordan
Glenn Jordan
Legal Counsel
Underground Injection Control

FORM

(a) Permit required. No person may create, operate, or continue to use or maintain an underground hydrocarbon storage facility without obtaining a permit from the commission. Permits from the commission issued before the effective date of this rule shall continue in effect until revoked, modified, or suspended by the commission.

(b) Application.

(1) An application for a permit to dispose of saltwater or other mineralized water arising out of or incidental to the creation, operation, or maintenance of the underground storage facility shall be filed with the commission in accordance with the appropriate commission rules.

(2) An application for a permit to create, operate, or maintain an underground hydrocarbon storage facility shall be filed in the Austin office of the commission and shall contain the necessary information to demonstrate compliance with the laws of Texas and the rules of the commission.

(c) Geological requirement.

(1) Underground hydrocarbon storage facilities shall only be created, operated, or maintained in formations which are confined by impervious strata so as to prevent the waste of hydrocarbons, the uncontrolled escape of hydrocarbons to the surface, and the escape of hydrocarbons into freshwater formations.

(2) The applicant must submit a letter from the Texas Department of Water Resources, Austin, Texas, with the application, stating the depth to which freshwater strata occurs at each storage facility.

(d) Notice and hearing.

(1) The applicant shall give notice by mailing or delivering a copy of the application to the surface owner of the tract under which the

facility is located and to each adjoining offset operator, on or before the date the application is mailed to or filed with the commission.

(2) Notice of the application shall be published by the applicant in three consecutive publications in a newspaper of general circulation for the county where the facility will be located in a form approved by the director of underground injection control (hereinafter "director"). The applicant shall file in Austin proof of publication prior to the hearing or administrative approval.

(3) An application for a new underground hydrocarbon storage project will be considered for approval only after notice and hearing. After hearing, the examiner shall recommend a final action by the commission.

(4) An application for an expansion of a previously approved project may be considered for administrative approval if the commission receives no protest.

(A) If the commission receives a protest from a person notified pursuant to paragraph (1) or other interested person within 15 days of receipt of the application or after publication that the proposed plan as contained in the application will cause damage to oil, gas, geothermal resources, freshwater resources, or otherwise cause harm, then a hearing will be held on the application after the commission provides notice of hearing to all interested persons.

(B) If the commission receives no protest, the director may administratively approve the application. If the director denies administrative approval, the applicant shall have a right to a hearing on the matter. After hearing, the examiner shall recommend a final action by the commission.

(C) Subsequent commission action. A permit may be modified, suspended, or terminated after notice and opportunity for hearing if:

Railroad Commission of Texas
Oil and Gas Division
051.02.02.074

(1) A substantial change of conditions occurs in the operation, maintenance, or construction of the facility, or there are substantial changes in the information originally furnished;

(2) Freshwater is likely to be polluted as a result of continued operation of the facility;

(3) There are substantial violations of the terms and provisions of the permit or of commission rules;

(4) The applicant has misrepresented any material facts during the permit issuance process; or

(5) Injected fluids or gases are escaping from the storage facility.

(f) Transfer. An underground hydrocarbon storage permit may be transferred only upon written approval. The permitted operator shall file an application with the director for approval of the transfer of the permit for the facility. The director may require a hearing on the matter. After hearing, the examiner shall recommend a final action by the commission.

(g) Casing. Wells used for injection and removal of hydrocarbons from the storage facility shall be cased and the casing strings cemented to prevent stored hydrocarbons from escaping to the surface, into freshwater strata, or otherwise escaping and causing waste or endangering the public health.

(h) Monitoring and reporting.

(1) All operators of hydrocarbon storage wells shall monitor the injection pressure and volumes of fluids or gases injected and removed for each storage well on at least a monthly basis. Injection pressure and volumes injected shall be reported annually to the commission on the prescribed form. All monitoring records, including volumes withdrawn, shall be retained by the operator for at least five years. Operators storing crude

FORM

Railroad Commission of Texas
Oil and Gas Division
051.02.02.074

oil must also comply with other Commission rules including the filing of reports required under those rules.

(2) The operator shall report immediately to the appropriate district office any significant loss of fluids or gases, any significant mechanical failure or any other significant problem. The operator shall confirm this report in writing within five days.

(1) Testing.

(1) Each storage well shall be tested for mechanical integrity at least once every five years. The testing shall be in a manner approved by the director.

(2) The operator shall notify the appropriate district office at least five days prior to testing. Testing shall not commence before the end of the five-day period unless authorized by the district director.

(3) A complete record of all tests shall be filed in duplicate in the district office within 30 days after the testing.

(j) Plugging. Upon abandonment, all wells used for the injection or removal of hydrocarbons from the facility shall be plugged in accordance with Statewide Rule 14.

(k) Penalties.

(1) Violations of this rule will subject the operator to penalties and remedies specified in Title 3 of the Texas Natural Resources Code.

(2) The certificate of compliance for any underground hydrocarbon storage facility may be revoked in the manner provided in Statewide Rule 68 for violation of this rule.

H-10

PHASE I Report
July 1984

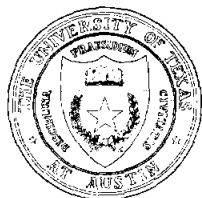
ROBERT L. BLUNTZER

BUREAU OF ECONOMIC GEOLOGY

THE UNIVERSITY OF TEXAS

AT AUSTIN

W. L. FISHER, DIRECTOR



TECHNICAL ISSUES FOR CHEMICAL WASTE
ISOLATION IN SOLUTION-MINED CAVERNS
IN SALT DOMES

Steven J. Seni, H. S. Hamlin, and W. F. Mullican III

Contract Report for the Texas Department of Water
Resources under Contract No. IAC (84-85)-1019

Bureau of Economic Geology
W. L. Fisher, Director
The University of Texas at Austin
University Station, P. O. Box X
Austin, Texas 78713-7508

CONTENTS

INTRODUCTION	1
DOMAL GEOLOGIC SYSTEM	1
Salt stock	2
Cavern stability	3
Cap rock.	4
Surrounding strata	5
DOME GEOHYDROLOGY	5
ENGINEERING CONSIDERATIONS	6
REFERENCES	8

INTRODUCTION

Many factors can be assessed to judge the technical merits of chemical waste isolation in solution-mined caverns in salt domes. Our investigation indicates that certain factors have primary importance, including the geohydrology, the engineering considerations, and the stability of the geologic isolation system, the cavern, the cap rock, and the surrounding strata. To a major extent, all these factors are interrelated and interdependent.

Initially, the domal system including cap rock, salt stock, and surrounding domed strata must be mapped to a level of detail generally not available in public sources and in the geologic literature. The most reasonable postulated release scenarios envision waste transport by ground water. Thus, the direction and rates of ground-water flow are critical. Ground-water flow is influenced by the rock matrix, which includes depositional systems, sand-body geometry, and fault patterns.

The cap rock is a focal point of many domal processes and is a particularly dynamic region of a salt dome. Studies on cap-rock properties may answer whether salt domes are undergoing uplift or dissolution. The cap rock plays a pivotal role in either promoting or retarding dome dissolution and cavern stability. Further domal studies must concentrate on defining (1) geometry and structure of cap rocks, (2) cap-rock lost-circulation zones, (3) geometry, structure, and stratigraphy of salt stocks and salt caverns, (4) salt-cavern stability, and (5) domal geohydrology. In the following sections, we discuss various issues that should be addressed to judge the technical merits of chemical waste isolation in solution-mined caverns in salt domes.

DOMAL GEOLOGIC SYSTEM

Definition of the geologic system is without doubt the first step in assessing the effectiveness of waste isolation in solution-mined caverns in salt. Precise mapping of the geometry of salt structures, their internal and external structure and stratigraphy, and the

domal geohydrology is mandatory. We intend to do detailed studies of domes on the basis of data availability and intrinsic interest. The program involves detailed mapping of the cap rock, salt stock, and surrounding strata. Geologic literature and data are abundant for certain domes, but characteristically only for the shallow zones of salt structures. It is often difficult to judge the quality of published literature and structural interpretations of original data for those domes in which the original sources of data are not provided.

Salt Stock

Assessing the suitability of salt domes for long-term isolation of toxic-chemical waste requires more than a literature search. Detailed mapping of salt structures requires investigations of borehole geophysical logs through salt, investigations of deep boreholes near the salt stock, and study of salt cores from individual domes.

In addition to better mapping of the whole domal geologic system, we intend to derive some statistical methods to place confidence limits, standard deviation, or both on the contours used to map various aspects of domal geology. This is especially critical for domal geometry because the accepted industry standard is to place caverns within 300 to 500 ft of the edge of the salt stock.

We intend to study salt cores collected by the Strategic Petroleum Reserve program from Bryan Mound and Big Hill salt domes. With these and other available salt cores, we hope to use salt structure and salt stratigraphy to aid in obtaining a better understanding of properties affecting salt-stock geometry, structure, cavern geometry, and cavern stability.

Recent model studies of salt domes and salt-stock stratigraphy have raised the possibility that the margins of salt domes may actually be large downturned overhangs perched on a relatively thin salt pedestal (M. P. A. Jackson, personal communication, 1984). On the basis of studies of the stratigraphy and structure of salt cores, especially of multiple sets of core from a single dome, we may be able to map the characteristic flow patterns within a salt stock that give rise to the large overhangs.

Conventional reflection seismic data are generally unable to sufficiently locate the margins of domes. A new tool, magneto-tellurics, is promising. By mapping telluric earth currents, the margins of salt stocks may be more precisely defined because of the large contrast in electrical properties between the salt stock and the surrounding strata (Geotronics, Inc., Austin, Texas).

Cavern Stability

The three primary factors that affect the stability of salt caverns are pressure, temperature, and cavern shape (Fenix and Scisson, Inc., 1976). Precise techniques for predicting cavern stability may still be beyond the state of the art. In many respects, the problem revolves around defining the in situ state of stress within a salt dome.

The difference between the hydrostatic pressure within and the lithostatic pressure outside the cavern is probably the primary parameter affecting cavern stability. The depth of the cavern determines lithostatic pressure. Lithostatic pressure increases at about twice the rate of hydrostatic pressure exerted by a cavern filled with brine. Natural gas caverns are prone to have stability problems because of their great depth (4,000 to 6,700 ft) and rapid changes in internal cavern pressure owing to gas cycling by pressure release. The first natural gas cavern in a salt dome was constructed in Eminence salt dome in Mississippi. According to SAI (1977) and Dreyer (1982), the cavern underwent unacceptable closure of 30 to 40 percent in the first year.

The plasticity and strain rate of rock salt increase with increasing temperature and depth (Carter and Heard, 1970; Dreyer, 1982; Heard, 1972). This increase in salt plasticity is generally cited as the rationale for requiring a lower cavern depth limit of about 5,000 ft to 7,000 ft.

Empirical parameters are used as guidelines when constructing most solution-mined caverns in salt. These parameters include the thickness of salt above the cavern, the thickness of salt between the cavern and the margin of the dome, the ratio of the thickness of salt (web)

between caverns and the diameter of the caverns, and the ratio of the height of the cavern to the diameter of the cavern.

Formulas have been devised to predict the convergence of caverns; these formulas include shape, depth, pressure, temperature, and dimensionless salt material constants (Dreyer, 1982). When a formula was applied to the gas storage cavern at Eminence salt dome, Mississippi, the predicted amount of closure was an order of magnitude less than the actual closure measured after one year. This illustrates that although mathematical models to predict cavern shape and stability exist, their usefulness is questionable.

Cap Rock

Cap rock influences dome and cavern stability in a complex fashion. A complete study of cap-rock thickness, mineralogy, hydrogeology, distribution and thickness of lost-circulation zones, distribution of faults, and cap-rock resources is necessary to assess reasonably the influence of cap rock on dome and cavern stability. Cap rocks of domes in the Houston Salt Basin contain lost-circulation zones characterized by vuggy to cavernous porosity and by loose accumulations of anhydrite sand. Wells are completed through these zones with difficulty. Once completed, well casings and cements are subject to attack by corroding circulating fluids.

Lost-circulation zones probably are indicators of active salt dissolution. Anhydrite dissolution and volume loss during hydration to gypsum may also be important. Loose anhydrite sand accumulates at the cap-rock - salt-stock interface where salt dissolution, if present, will be most active. The cap rock at Barbers Hill salt dome contains a 25-ft-thick lost-circulation zone of loose anhydrite sand at the cap-rock - salt-stock interface. Cap-rock lost-circulation zones are one facet of cap-rock hydrology. The flow systems within lost-circulation zones must be carefully assessed because the lost-circulation zone is a likely release point for waste discharging from a solution-mined cavern.

Cap-rock lost-circulation zones neither occur over all domes nor do they occur everywhere on a single cap rock. Core of cap rock at Oakwood salt dome reveals a tight cap-rock -

salt-stock interface (Kreitler and Dutton, 1983). Cap rocks without lost-circulation zones are likely barriers to dome dissolution.

Many cap rocks are highly fractured by radial faults inferred to result from lateral extension owing to present or past dome growth. Lost-circulation zones may develop preferentially along these fault zones. The result of the influence of radial faults on cap-rock hydrology may be open pathways for ground water to enter the salt stock.

Surrounding Strata

Cavern stability may be enhanced or degraded by the nature of the strata surrounding the salt dome. Structural attitude, sand-body geometry, ground-water flow directions and flux, ground-water chemistry, and permeability of surrounding strata are all factors that must be assessed. Depositional systems and three-dimensional sand-body geometry will influence classic ground-water and water chemistry parameters. The implications of ground-water data can be understood better with a thorough knowledge of depositional systems and the rock framework.

The structure and stratigraphy of strata surrounding a salt stock provide a means of deciphering dome-growth history. Domes with a younger growth history are less stable than older domes because domes characteristically undergo an exponential decline in the rate of growth with time. Salt domes in the Houston Salt Basin are generally thought to be much younger than those domes in the East Texas Basin. Detailed patterns of growth history for domes in the Houston Salt Basin are unknown. In contrast, dome-growth patterns are relatively well known in the East Texas Basin (Seni and Jackson, 1983; Jackson and Seni, 1984). Patterns and rates of dome growth, history of erosion over domes, and regional patterns and history of growth faults and radial faults all need to be considered in assessing dome stability.

DOMES GEOHYDROLOGY

Geohydrologic factors are a prime influence on both dome and cavern stability. Some geohydrologic variables that need to be quantified are three-dimensional analysis of hydraulic

head, pressure versus depth within an aquifer, aquifer permeability, aquifer heterogeneities, shallow- and deep-aquifer chemistry, and the age of ground water. Questions that need to be answered are (1) what is the direction of fluid flow, (2) what is the travel time of ground water within a given aquifer, and (3) what is the flux through the aquifer?

Studies of long-term waste isolation often assume worst-case scenarios. If the outcome of the worst-case scenario can be tolerated, then an important safety criterion is satisfied. For disposal of chemical waste in solution-mined caverns, a likely worst-case scenario would entail waste leakage into a cap-rock lost-circulation zone where rates of ground-water flux, permeabilities, and possibly recharge are high. Lost-circulation zones at Barbers Hill salt dome have accepted 1.5 billion barrels of salt water since the beginning of storage at that dome. This water has since begun to leak from plugged and abandoned oil-field boreholes.

Ideally a three-dimensional steady-state ground-water flow model based on conservative values for system variables should be constructed for a candidate dome. System variables should include the regional and local ground-water circulation patterns, leakage coefficients, recharge rates, and heterogeneities and anisotropies within aquifers to account for the effects of faults and sand-body distribution.

ENGINEERING CONSIDERATIONS

Engineered barriers may be the weak link in chemical-waste disposal systems in salt domes. The burden of stability rests largely on the cavern. Casing strings, casing cements, and cement plugs all serve to isolate the cavern from the surrounding surface, cap rock, and salt stock. Problems with leakage from plugged and abandoned oil-field drillholes in salt domes indicate that these borehole-plugging devices become ineffective with time. One problem is corrosion by sulfate-bearing and saline fluids in cap rocks.

Borehole closure around the casing and cements is expected to improve the seal between salt and cements. But the directions and magnitudes of salt flow within the salt mass are

unknown. Unidirectional lateral flow of salt within the salt mass could subject the plugged drillhole to unacceptable lateral shear stresses.

As currently conceived in the United States, nuclear waste isolation relies heavily on engineered barriers including resistant waste forms and encapsulation devices around the waste. Such barriers generally are not envisioned for chemical waste disposal. Solidifying chemical waste may be a desirable technique for preventing rapid ground-water transport of the waste; it could also minimize the potential for release of lithostatically pressurized waste liquids if drilling inadvertently breached the waste-filled cavern.

REFERENCES

- Carter, N. L., and Heard, H. C., 1970, Temperature and rate dependent deformation of halite: American Journal of Science, v. 269, p. 193-249.
- Dreyer, W., 1982, Underground storage of oil and gas in salt deposits and other non-hard rocks: in Beckman, H., ed., Geology of petroleum, v. 4: New York, Holsted Press, 207 p.
- Fenix and Scisson, Inc., 1976, Review of applicable technology--solution mining of caverns in salt domes to serve as repositories for radioactive wastes: Prepared for U.S. Energy Research and Development Administration, Office of Nuclear Waste Isolation, Oak Ridge, Tennessee, Contract No. Y/OWI/SUB-76/92880, 122 p.
- Heard, H. C., 1972, Steady-state flow in polycrystalline halite at pressure of 2 kilobars: in Heard, H. C., Borg, I. Y., Carter, N. L., and Raleigh, C. B., eds., Flow and fracture of rocks: American Geophysical Union, Geophysical Monograph 16, p. 191-210.
- Jackson, M. P. A., and Seni, S. J., 1984, The domes of East Texas: in Presley, M. W., ed., The Jurassic of East Texas: East Texas Geological Society, p. 163-239.
- Kreitler, C. W., and Dutton, S. P., 1983, Origin and diagenesis of cap rock, Gyp Hill and Oakwood salt domes, Texas: The University of Texas at Austin, Bureau of Economic Geology, Report of Investigations No. 131, 58 p.
- SAI, 1977, The mechanisms and ecological impacts of the collapse of salt dome oil storage caverns: McLean, Virginia, Science Applications, Inc., Report No. 5-210-00-567-04.
- Seni, S. J., and Jackson, M. P. A., 1983, Evolution of salt structures, East Texas diapir province, part 2: patterns and rates of halokinesis: American Association of Petroleum Geologists Bulletin, v. 67, no. 8, p. 1245-1274.

TABLES

1. List of salt domes with cavern failures, mechanisms, and consequences
2. List of salt domes with storage, operating company, RRC applicant, number of caverns, capacity, and product stored
3. List of salt domes with salt production, method, status, company, and history
4. List of salt domes with large oil fields and production status
5. List of salt domes with sulfide mineral occurrences and documentation

APPENDICES

1. Structure contour map of Texas salt domes constructed on a topographic base
2. Railroad Commission of Texas Authority Numbers for storage well permits
3. Railroad Commission of Texas Rule 74 procedures and requirements for storage well operations

PHASE I Report
July 1984

ROBERT L. BLUNTZER

BUREAU OF ECONOMIC GEOLOGY

THE UNIVERSITY OF TEXAS
AT AUSTIN

W. L. FISHER, DIRECTOR



COMPUTERIZED INVENTORY OF DATA
ON TEXAS SALT DOMES

Steven J. Seni, W. F. Mullican III,
and R. W. Ozment

Contract Report for the Texas Department of Water Resources
under Contract No. IAC (84-85)-1019

Bureau of Economic Geology
W. L. Fisher, Director
The University of Texas at Austin
University Station, P.O. Box X
Austin, Texas 78713-7508

CONTENTS

INTRODUCTION	1
DATA BASE	1
Organization of the data base	1
EXPLANATION OF GEOLOGIC TERMINOLOGY	2
Shape of the salt stock	2
Structure adjacent to the salt stock	5
SURFACE EXPRESSION	5
RESOURCES	8
DOCUMENTATION	8
REFERENCES	10
APPENDIX: data base for 84 Texas salt domes	separate document

FIGURES

1. Definition of diapir shape in plan view.	3
2. Parameters describing inclined diapirs in three dimensions.	4
3. Parameters describing diapir overhang.	6
4. Qualitative classification of drainage systems above domes into four ideal types as a guide to relative movement of the land surface	7

TABLES

1. List of computer program line number, data element, definition, and example	14
2. List of computer program line number, repeating group, definition, and example	20
3. Data base organization.	29
4. Information on storage operations in Texas domes.. . . .	32
5. Information on rock salt and brine mining in Texas domes.	33
6. Information on sulfur mining in Texas domes.	34

INTRODUCTION

On the basis of our initial investigations, a computerized spread sheet has been derived that summarizes information relevant to storing chemical wastes in salt domes in Texas. This inventory provides a ready reference source of dome-related data including location, physical dimensions and structure of the domes, surrounding strata, domal resources, and ground water. The data base is especially useful for manipulating data and creating lists and tables to compare individual domes and their potential uses and resources.

DATA BASE

The inventory is stored on System 2000 (S2K). S2K provides the user with a powerful tool for managing the data base. With S2K the user may define new data bases, modify definitions in existing data bases, and retrieve and update values within the data bases. S2K provides archival copies of data bases and records an audit trail to changes in the data base.

The structure of the data base is hierarchical. Basic components of the data base are data elements and repeating groups. Values (either numeric or text) are stored in data elements. Repeating groups are the structure for storing related sets of data elements. Repeating groups link hierarchical levels of the data base. Output in the form of tables and reports is generated with the "Report Writer."

Organization of the Data Base

Single data elements include 55 dome variables listed and defined in table 1. Repeating groups include 16 sets of data elements comprising 63 individual data elements listed and defined in table 2. The organization of the data base is shown in table 3; the entire data base as of May 1, 1984, constitutes appendix 1. The "Report Writer" feature of S2K facilitates preparation of charts and tables of data from the data base. Tables 4, 5, and 6 are examples of

output using the "Report Writer." The code needed to reproduce these tables is included at the bottom of the individual tables.

EXPLANATION OF GEOLOGIC TERMINOLOGY

Information on 84 salt diapirs in Texas is presented in the data base. Some salt pillows (nondiapiric salt structures) may also be included. Data for very deep salt structures is meager. The availability of data for each dome is variable. Structure-contour maps on top of domal material are available for 52 domes (62 percent of the total).

All data elements and repeating groups are listed by program line (pl) and defined in tables 1 and 2. Most geologic terms are self explanatory. The following sections and figures 1, 2, 3, and 4 provide an explanation of the geologic terminology. In the following sections parameters in the data base are keyed to a program line in parentheses. All documentation of the source of data is listed in Documentation Repeating Group (pl-500).

Shape of the Salt Stock

Several parameters describe the shape of the salt stock. Shape parameters are derived from structure-contour maps on top of the stock. Figure 1A illustrates how major-axis length (pl-31), major-axis orientation (pl-32), and minor-axis length (pl-33) were derived. Area of planar crest (pl-40) and planar crest percentage (pl-41) were calculated as shown in figure 1B. Axial ratio is a measure of the ellipticity of a diapir (fig. 1C).

The area (ft²) enclosed by each domal-structure contour was calculated by planimetry and is in Area Statistics Repeating Group (pl-34).

Salt-structure contour maps also yield data on the three-dimensional shape of the salt stock. Diapirs not having vertical axes are described in terms of axial tilt (pl-55), axial-tilt orientation (pl-56), and axial-tilt distance (pl-57) in figure 2. The presence and position of the salt-stock overhang determine whether the sides of the stock (pl-59) are parallel (no overhang),

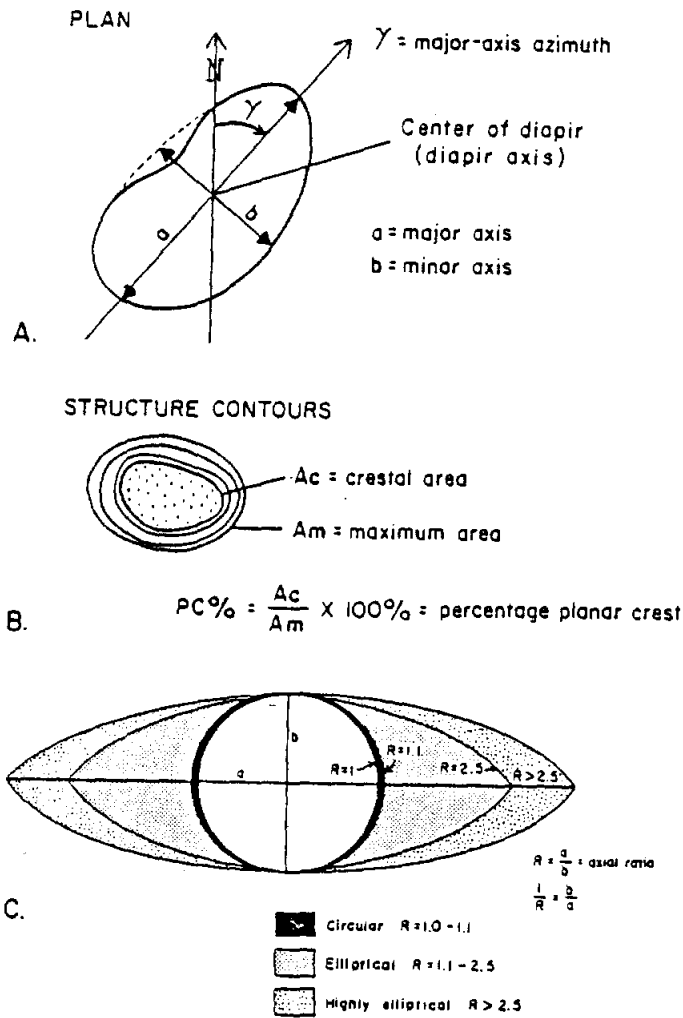
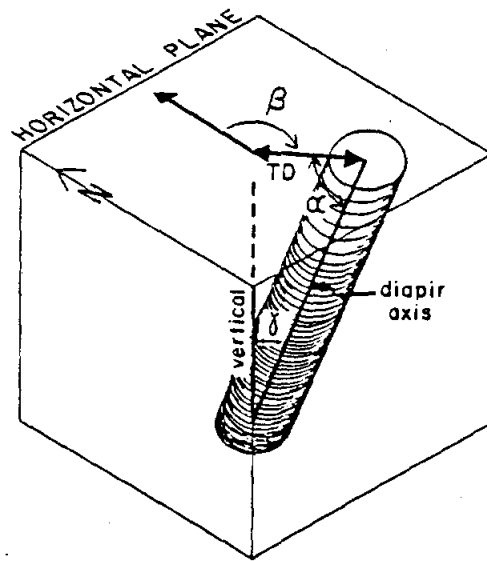


Figure 1. Definition of diapir shape in plan view. (A) Major axis, minor axis, and major-axis azimuth. (B) Crestal area and percentage planar crest. Area is measured by planimetry. (C) Three classes of diapir shape defined by different axial ratios.



- γ = axial tilt
- β = axial tilt azimuth
- TD = tilt distance
- α = axial plunge

Figure 2. Parameters describing inclined diapirs in three dimensions. These are calculated from structure-contour maps on top of salt.

upward diverging (below overhang), or upward converging (above overhang or no overhang). If an overhang is present, information is provided in Overhang Repeating Group (pl-60). If a partial overhang is present, the overhang arc is bracketed by the azimuth orientation of two lines--overhang orientation 1 (pl-62) and overhang orientation 2 (pl-63) (fig. 3B). Domes completely encircled by an overhang have an overhang orientation of 1 equal to 000° and an overhang orientation of 2 equal to 360°. Overhang azimuth (pl-64), lateral overhang (pl-65), and percentage overhang (pl-66) are illustrated in figure 3B.

Structure Adjacent to the Salt Stock

The dome data base is set to accept data on the structure of strata surrounding the salt stock. As of May 1, 1983, such data were not collected. Jackson and Seni (1984) provide definitions of terms used in the dome data base for terms applicable to strata surrounding the stock.

SURFACE EXPRESSION

The surface expression of strata over the dome is one indication of the relative structural and hydrologic stability of a dome. Subsidence above a dome is usually attributed to subsurface dissolution of salt by ground water or to solution-brining operations. Both natural and man-induced sinkholes and depressions are expressions of such processes (pl-120, 121). Uplift over a dome indicates that rates of upward dome growth exceed rates of dome-crest attrition by dissolution (pl-110).

Anomalous drainage patterns (Drainage Systems Repeating Group [pl-111]) over domes provide a way to assess the evidence for subsidence or uplift. Five ideal types of drainage patterns are recognized over Texas salt domes. Figure 4 shows a classification of four of these drainage types. Toroidal drainage (not included in figure 4) includes a central depression and a peripheral mound. Centrifugal drainage is radial drainage away from a central mound that

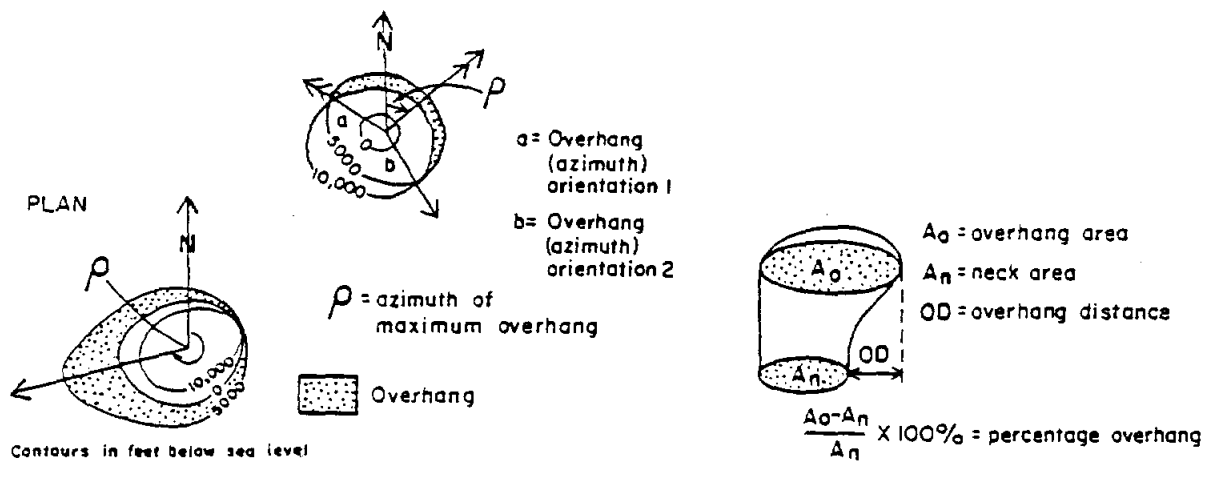


Figure 3. Parameters describing diapir overhang. Plan view (A) defines overhang and azimuth of maximum overhang on a structure-contour map on top of the salt. Plan view (B) defines partial overhang. Contours are elevation below sea level. Oblique view defines overhang area, neck area, overhang distance, and percentage overhang. Area is measured by planimetry.

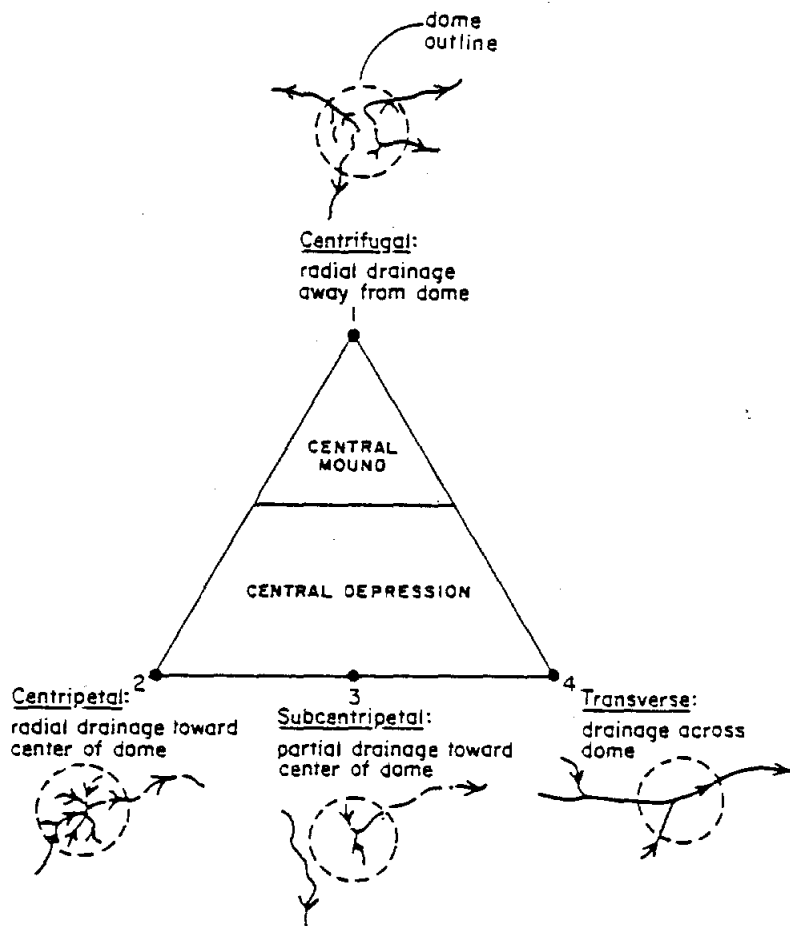


Figure 4. Qualitative classification of drainage systems above domes: four ideal types as a guide to relative movement of the land surface. Toroidal drainage is not shown.

occurs over domes rising faster than the overburden is being eroded or the crest is being dissolved. Centripetal drainage is drainage toward the central area over the salt stock. It provides evidence of collapse over the dome crest. Subcentripetal drainage suggests subsidence but is equivocal evidence. Transverse drainage indicates that any rise or subsidence of the dome is negligible compared with the rate of regional uplift or subsidence and stream incision or aggradation.

RESOURCES

Hydrocarbon production histories from producing salt domes are listed in Hydrocarbon Repeating Group (pl-150). These data are from the 1982 Railroad Commission Oil and Gas Annual Report. Other resources associated with diapirs include rock salt, brine, sulfur, and sulfide minerals. These resources and history of development are listed in Mineral Production Repeating Group (pl-190). Solution-mined storage caverns represent another domal resource. Data domes with a history of hydrocarbon storage, company, number of caverns, capacities, and products stored are listed in Hydrocarbon Storage Caverns Repeating Group (pl-225).

Ground-water resources around domes are listed in Aquifer Water Chemistry Repeating Group (pl-400). Water chemistry data are from Texas Department of Water Resources water chemistry wells. In addition to water chemistry, the following ground-water parameters are listed; regional depth of slightly saline ground water (pl-420), depth of slightly saline ground water near the dome (pl-421), ground-water irrigation near the dome (pl-435), municipalities using ground water near the dome (Repeating Group pl-425), and industries using ground water near the dome (Repeating Group pl-430).

DOCUMENTATION

Each dome includes a Documentation Repeating Group indicating the source of data. The information on each dome can be divided into three major classes of related data--dome

geometry, dome resources, and ground-water chemistry. Most of the data in these classes were derived from outside sources. All other data were generated at the Bureau of Economic Geology for this report.

Data on dome location and geometry were derived from salt-structure contour maps. Major sources of these contour maps are the Railroad Commission of Texas Hearing Files, Jackson and Seni (1984), Halbouty (1979), Geomap, and numerous articles on individual domes. Resource data include oil and gas, sulfur, sulfides, salt, brine, and storage. All oil and gas data are from the Railroad Commission of Texas 1982 Oil and Gas Annual Report. Most data on sulfur, salt, and brine are from Hawkins and Jirik (1966) and Jirik and Weaver (1976). Data on sulfide minerals are from Smith (1970a, b) and Price and others (1983). Data on storage in salt domes are from the Railroad Commission of Texas Hearing Files and Gas Processors Association (1983). The Texas Department of Water Resources provided data on ground-water chemistry and uses of ground water.

REFERENCES

- Barton, D. C., 1920, The Palangano salt dome, Duval County, Texas: *Economic Geology*, v. 6, p. 497-510.
- Behrman, R. G., Jr., 1953, Thompson Field, Fort Bend County, Texas: in McNaughton, D. A., ed., Typical oil and gas fields of southeast Texas: Houston Geological Society, Guidebook, Joint Annual Meeting, 1953, Houston, Texas, American Association of Petroleum Geologists, Society of Economic Paleontologists and Mineralogists, and Society of Exploration Geophysicists, p. 156-160.
- Burford, S. O., 1935, Structural features of Brenham salt dome, Washington and Austin Counties, Texas: *American Association of Petroleum Geologists Bulletin*, v. 9, no. 9, p. 1330-1338.
- Canada, W. R., 1953, Hockley Oil Field, Harris County, Texas: in McNaughton, D. A., ed., Typical oil and gas fields of southeast Texas: Houston Geological Society, Guidebook, Joint Annual Meeting, 1953, Houston, Texas, American Association of Petroleum Geologists, Society of Economic Paleontologists and Mineralogists, and Society of Exploration Geophysicists, p. 76-79.
- Davies, W. J., 1953, Brookshire (San Felipe) Field, Waller County, Texas: in McNaughton, D. A., ed., Typical oil and gas fields of southeast Texas: Houston Geological Society, Guidebook, Joint Annual Meeting, 1953, Houston, Texas, American Association of Petroleum Geologists, Society of Economic Paleontologists and Mineralogists, and Society of Exploration Geophysicists, p. 97-99.
- Ferguson, W. B., and Minton, J. W., 1936, Clay Creek salt dome, Washington County, Texas: *American Association of Petroleum Geologists Bulletin*, v. 20, no. 1, p. 68-90.
- Gas Processors Association, 1983, North American storage capacity for light hydrocarbons and U.S. LP-gas import terminals 1983: Tulsa, Oklahoma, 26 p.

- Halbouty, M. T., 1979, Salt domes, Gulf Region, United States and Mexico, 2nd ed.: Houston, Texas, Gulf Publishing, 561 p.
- Halbouty, M. T., and Hardin, G. C., Jr., 1951, Types of hydrocarbon accumulation and geology of South Liberty salt dome, Liberty County, Texas: American Association of Petroleum Geologists Bulletin, v. 35, no. 9, p. 1939-1977.
- Hart, R. J., Ortiz, T. S., and Magorian, T. R., 1981, Strategic petroleum reserve (SPR) geological site characterization report, Big Hill salt dome: Sandia National Laboratories, Albuquerque, New Mexico, SAND 81-1085.
- Hawkins, M. E., and Jirik, C. J., 1966, Salt domes in Texas, Louisiana, Mississippi, Alabama, and offshore tidelands--a survey: U.S. Bureau of Mines Information Circular 8313, 78 p.
- Hinson, H., 1953, Blue Ridge field, in McNaughton, D. A., ed., Typical oil and gas fields in southeast Texas: Houston Geological Society, Joint Annual Meeting, 1953, Houston, Texas, American Association of Petroleum Geologists, Society of Economic Paleontologists and Mineralogists, and Society of Exploration Geophysicists, p. 82-85.
- Houston Geological Society, 1951, Typical oil and gas fields in southeast Texas, McNaughton, D. A., ed.: Joint Annual Meeting, 1953, American Association of Petroleum Geologists, Society of Economic Paleontologists and Mineralogists, and Society of Exploration Geophysicists, 168 p.
- Jackson, M. P. A., and Seni, S. J., 1984, The domes of East Texas, in Presley, M. W., ed., The Jurassic of East Texas: East Texas Geological Society, p. 163-239.
- Jirik, C. J., and Weaver, L. K., 1976, A survey of salt deposits and salt caverns, their relevance to the Strategic Petroleum Reserve: Federal Energy Administration Report FEA/S-76/310, 64 p.
- Marshall, R. P., Jr., 1976, Gyp Hill Dome, in Typical oil and gas fields of South Texas: Corpus Christi Geological Society, p. 64-68.
- Martinez, J. D., Thoms, R. L., Kupfer, D. H., Smith, C. J., Jr., Kolb, C. R., Newchurch, E. J., Wilcox, R. E., Manning, T. A., Jr., Romberg, M., Lewis, A. J., Rovik, J. E., 1976, An

investigation of the utility of Gulf Coast salt domes for isolation of nuclear wastes: Louisiana State University Institute for Environmental Studies, Baton Rouge, Louisiana, Report No. ORNL-Sub-4112-25, prepared for U.S. Department of Energy, 329 p.

Marx, A. H., 1936, Hoskins Mound salt dome, Brazoria County, Texas: American Association of Petroleum Geologists Bulletin, v. 20, no. 2, p. 155-178.

Miller, J. C., 1942, Well spacing and production interference in West Columbia Field, Brazoria County, Texas: American Association of Petroleum Geologists Bulletin, v. 16, no. 9, p. 1441-1466.

Patrick, W. W., 1953, Salt dome statistics: in McNaughton, D. A., ed., Typical oil and gas fields of southeast Texas: Houston Geological Society, Guidebook, Joint Annual Meeting, Houston, Texas, American Association of Petroleum Geologists, Society of Economic Paleontologists and Mineralogists, and Society of Exploration Geophysicists, p. 13-20.

Pollack, J. M., 1953, Sugarland oil field, Fort Bend County, Texas: in McNaughton, D. A., ed., Typical oil and gas fields of southeast Texas: Houston Geological Society, Guidebook, Joint Annual Meeting, Houston, Texas, American Association of Petroleum Geologists, Society of Economic Paleontologists and Mineralogists, and Society of Exploration Geophysicists, p. 153-156.

Porter, R. L., and Seren, G. W., 1953, Damon Mound Field, Brazoria County, Texas: in McNaughton, D. A., ed., Typical oil and gas fields of southeast Texas: Houston Geological Society, Guidebook, Joint Annual Meeting, Houston, Texas, American Association of Petroleum Geologists, Society of Economic Paleontologists and Mineralogists, and Society of Exploration Geophysicists, p. 107-109.

Price, P. E., Kyle, J. Richard, and Wessel, G. R., 1983, Salt dome related zinc-lead deposits: in Kisarsanyi, G., and others, Proceedings, International Conference on Mississippi Valley type lead-zinc deposits: University of Missouri-Rolla, p. 558-571.

Smith, A. E., Jr., 1970a, Minerals from Gulf Coast salt domes, part 1: rocks and minerals, v. 45, no. 5, p. 299-303.

_____, 1970b, Minerals from Gulf Coast salt domes, part 2: rocks and minerals, v. 45, no. 6, p. 371-380.

Teas, L. P., and Miller, C. R., 1933, Raccoon Bend oil field, Austin County, Texas: American Association of Petroleum Geologists Bulletin, v. 17, no. 12, p. 1459-1491.

URM, 1982, Hydrogeologic investigation in the vicinity of Barbers Hill salt dome: Underground Resource Management, Austin, Texas, Job No. 82-807, 104 p.

URR, 1983, Application of United Resource Recovery, Inc., to dispose of waste by well injection at the Boling salt dome: Submitted to Texas Department of Water Resources by Keysmith Corp., Austin, Texas.

TABLE 1. List of computer program line number, data element, definition, and example.

PROGRAM LINE NUMBER	DATA ELEMENT	DEFINITION	EXAMPLE
1	DOME NAME	Name of dome	Barbers Hill
2	DOME CODE	Two letter/two number code for documentation	BB-28
3	LATITUDE	Latitude of center point of salt dome--degrees, minutes, and seconds north of equator	29D50M56S
4	LONGITUDE	Longitude of center point of salt dome--degrees, minutes, and seconds west of central meridian	94D54M37S
5	GRID LATITUDE-NORTH	Latitude located 2.5 mi north of deepest salt contour	29D54M19S
6	GRID LATITUDE-SOUTH	Latitude located 2.5 mi south of deepest salt contour	29D47M35S
7	GRID LONGITUDE-WEST	Longitude located 2.5 mi west of deepest salt contour	94D57M20S
8	GRID LONGITUDE-EAST	Longitude located 2.5 mi east of deepest salt contour	94D49M55S
21	SHALLOWEST CAP-ROCK DEPTH (in feet)	Minimum depth (feet) of cap rock below surface	320
22	SHALLOWEST SALT DEPTH (in feet)	Minimum depth (feet) of salt below surface	1300
23	DEEPEST CONTROL ON SALT (in feet)	Deepest depth (feet) of salt below surface penetrated by drill or seismic	6500

TABLE 1 (cont.)

PROGRAM LINE NUMBER	DATA ELEMENT	DEFINITION	EXAMPLE
31	MAJOR-AXIS LENGTH (in feet)	Length (feet) of major axis of salt dome, from structure-contour map; measured between shoulders of dome (see figure 1A)	11600
32	MAJOR-AXIS ORIENTATION (in degrees)	Azimuth orientation (range 0 to 180 degrees) of major axis (see figure 1A)	163
33	MINOR-AXIS LENGTH (in feet)	Length (feet) of minor axis of salt dome, from structure-contour map; measured between shoulders of dome perpendicular to major axis (see figure 1A)	9000
15 40	AREA OF PLANAR CREST	Area (feet ²) enclosed within highest structure contour of salt stock as measured by planimeter (see figure 1B)	41714286
41	PLANAR CREST PERCENTAGE	Percentage planar crest equals area of planar crest divided by maximum area of salt stock times 100 (see figure 1B)	56%
50	GENERAL SHAPE	Text description of salt stock	Piercement diapir
51	AXIAL RATIO	Major axis divided by minor axis (see figure 1C)	1.29
52	PLAN SHAPE	Text description of ellipticity salt stock (see figure 1C)	Circular

TABLE 1 (cont.)

PROGRAM LINE NUMBER	DATA ELEMENT	DEFINITION	EXAMPLE
53	DOMES SYMMETRY	Text description of three-dimensional symmetry of dome	Orthorhombic
54	AXIS	Text description of straight "line of best fit" joining centers of salt dome at individual structure-contour horizons	Inclined
55	AXIAL TILT ANGLE (in degrees)	Inclination angle (degrees) of diapir with respect to vertical (see figure 2)	13
56	AXIAL TILT ORIENTATION (in degrees)	Azimuth angle (degrees) in horizontal plane of line connecting diapir axis and center of dome at deepest structure-contour horizon (see figure 2)	226
57	AXIAL TILT DISTANCE (in feet)	Length (feet) of line connecting diapir axis and center of dome at deepest structure-contour horizon (see figure 2)	300
58	CREST	Text description of shape of crest of dome	Planar
59	SIDES	Text description of shape of flanks of dome	Upward converging above -3000 ft
70	MAXIMUM TRUE THICKNESS OF CAP ROCK (in feet)	Maximum true (isopach) thickness (feet) of cap rock	750
71	MINIMUM TRUE THICKNESS OF CAP ROCK (in feet)	Minimum true (isopach) thickness (feet) of cap rock	50

TABLE 1 (cont.)

PROGRAM LINE NUMBER	DATA ELEMENT	DEFINITION	EXAMPLE
72	CAP-ROCK MINERALOGY	Text description of mineralogy of cap rock	Calcite and anhydrite
73	CAP-ROCK LOST-CIRCULATION ZONES PA	Present/absent key of lost-circulation zones in cap rock	Present
74	CAP-ROCK LOST-CIRCULATION ZONES INFO	Text description of lost-circulation zones in cap rock	Lost-circulation zone at cap-rock-salt-stock interface
75	SULFIDE MINERALS	Present/absent key of sulfide occurrences in cap rock	Absent
76	GENERAL DOME INFORMATION	Text description suitable as storage buffer for any dome information	Drill rig collapsed while drilling through cap rock
81	LATERAL EXTENT OF RIM SYNCLINE (in feet)	Lateral distance (feet) between crest points of rim syncline	13000
82	LATERAL EXTENT OF DRAG ZONE (in feet)	Lateral distance (feet) between trough points (axial trace of rim syncline) around dome	2000
83	MAXDIPVERTVARI (in degrees feet)	Maximum dip (degrees) of strata that dip away from dome; depth (feet)	+70°, 2000
84	MAXDIPVERTVARZ (in degrees feet)	Minimum dip (degrees) of strata that dip toward dome; depth (feet)	0°, 4000
85	MAXDIPVERTVAR3 (in degrees feet)	Maximum dip (degrees) of strata that dip toward the dome; depth	20°, 8000

TABLE 1 (cont.)

PROGRAM LINE NUMBER	DATA ELEMENT	DEFINITION	EXAMPLE
102	YOUNGEST FAULTED STRATA	Formation and age of youngest faulted strata over dome	Lissie, Pleistocene
103	OLDEST STRATA ON SURFACE	Formation and age of strata exposed over dome	Austin Chalk, Cretaceous
110	RELIEF OVER DOME	See Repeating Group III	
120	SINKHOLES	Present/absent key of occurrence of sinkholes over dome	Present
121	SINKHOLE INFO	Text description of sinkhole	300 ft diameter sinkhole; water depth 30 ft; formed 1984 over old brine well
122	SURFACE SALINES	Present/absent key of occurrence of surface salines around dome	Absent
123	CONFIGURATION OF OVERBURDEN	Descriptive text of attitude of overburden	Homothetic faults in uplifted Pleistocene strata
220	PRODUCT STORAGE STATUS	Status key for storage operations in domes--active, abandoned, under construction	Active
221	STORAGE METHOD	Method key for construction method of cavern--cavern or mine	Cavern

TABLE 1 (cont.)

PROGRAM LINE NUMBER	DATA ELEMENT	DEFINITION	EXAMPLE
222	NUMBER OF CAVERNS	See Repeating Group 225	
223	TOTAL STORAGE CAPACITY (in barrels)	Reported product storage capacity (bbls) in 1983	2500000
420	REGIONAL DEPTH OF BASE OF SLIGHTLY SALINE GROUND WATER IN FEED	Average regional depth (feet) to base of slightly saline ground water defined as ≤ 3000 mg/l total dissolved solids in area not affected by dome growth	500
421	DEPTH OF BASE OF SLIGHTLY SALINE GROUND WATER OVER DOME	Depth (feet) to base of saline ground water defined as ≤ 3000 mg/l total dissolved solids over dome	200
422	SALINE ANOMALIES IN GROUND WATER	Present/absent/insufficient data key on occurrence of saline anomalies in ground water	Present
435	GROUND-WATER IRRIGA- TION NEAR DOME (in acres)	Present/absent/none indicated key on occur- rence of irrigation and coverage (in acres)	Present 500
445	SURVEY NAME FOR CENTER OF DOME	Survey name where center of dome coordi- nates are located	J. Miller A-232
446	SALT BASIN	Salt basin in which diapir is located	Houston salt basin

TABLE 2. List of computer program line number, repeating group, definition, and example.

PROGRAM LINE NUMBER	REPEATING GROUP	DEFINITION	EXAMPLE
10	COUNTIES	<u>Repeating Group</u> for county or counties where dome is located	-
10 - 11	COUNTY NAME	County name	Harris
34	AREA STATISTICS	<u>Repeating Group</u> for area and depth of dome from structure-contour map	-
34 - 35	DEPTH OF AREA CALCULATION (in feet)	Depth (feet) of salt dome for which subsequent area is calculated in program line (pl) -36	1000
34 - 36	AREA IN SQUARE FEET FOR DEPTH OF 35	Area (ft ²) at depth listed in pl-35	55809524
60	OVERHANG	<u>Repeating Group</u> for data on overhang	-
60 - 61	OVERHANG INFO	Text description of general characteristics of overhang	Overhang on NW corner of dome
60 - 62	OVERHANG ORIENTATION I (in degrees)	Azimuth orientation (degrees) of line from center of dome at overhang depth to margin of dome where overhang is initiated (see figure 3B)	300°

TABLE 2 (cont.)

PROGRAM LINE NUMBER	REPEATING GROUP	DEFINITION	EXAMPLE
60 - 63	OVERHANG ORIENTATION II (in degrees)	Azimuth orientation (degrees) of line from center of dome at overhang depth to margin of dome where overhang is terminated; overhang orientation II is the line that brackets overhang and is clockwise from overhang orientation I; for those domes with complete overhang--overhang orientation I = 0 degrees overhang orientation II = 360 degrees (see figure 3B)	52
60 - 64	OVERHANG AZIMUTH (in degrees)	Azimuth orientation from center of dome to maximum overhang (see figure 3B)	356
60 - 65	LATERAL OVERHANG (in feet)	Lateral extent (feet) overhang projects over dome flanks (see figure 3A)	400
60 - 66	PERCENTAGE OVERHANG	Percentage of overhang area over neck area (see figure 3A)	50
90	ANGLE BETWEEN SALT STOCK-STRATA	<u>Repeating Group</u> for angles and depths formed at contact between salt stock and strata	-
90 - 91	ANGLE (in degrees)	Angle between salt stock and strata	20
90 - 91	DEPTH (in feet)	Depth for angle measured in pl-91	2000

TABLE 2 (cont.)

PROGRAM LINE NUMBER	REPEATING GROUP	DEFINITION	EXAMPLE
100	ADJACENT STRATA FAULTING	<u>Repeating Group</u> for describing style of faulting and units faulted around salt domes	-
100 - 101	FAULT DESCRIPTOR	Text description of fault type-- homothetic and antithetic, dip of fault plane, strata faulted, and depth	Homothetic, toward dome, Frio, 2000
111	DRAINAGE SYSTEMS	<u>Repeating Group</u> for drainage system over crest of dome	-
111 - 112	DRAINAGE TYPE	Drainage systems are Centrifugal - Type 1 Centripetal - Type 2 Subcentripetal - Type 3 Transverse - Type 4 Toroidal - Type 5	Centrifugal - Type 1
150	HYDROCARBON RESOURCES	<u>Repeating Group</u> for maintaining current and cumulative production statistics on hydrocarbons from salt domes as reported by Railroad Commission of Texas	-
150 - 151	FIELD NAME PRODUCING HORIZON	Name of field and producing horizon	Sour Lake - 6700 Sand
150 - 152	RRC DISTRICT	Railroad Commission of Texas District where field is located	3

TABLE 2 (cont.)

PROGRAM LINE NUMBER	REPEATING GROUP	DEFINITION	EXAMPLE
150 - 153	COUNTY RESIDENCE	Texas county where field is located	
150 - 154	DISCOVERY DATE	Date of operator's request for field rules on new field discovery	1949
150 - 155	FIELD DEPTH (in feet)	Field depth (feet)	5200
150 - 156	GRAV API	API gravity of crude oil	
150 - 157	ENVIRONMENTAL CODE	Text description for environmental aspects	
23 150 - 158	ENV COMM 1	Text description for comments	
150 - 159	ENV COMM 2	Text description for comments	
150 - 160	ENV COMM 3	Text description for comments	
150 - 161	ENV COMM 4	Text description for comments	
150 - 165	CUMULATIVE CRUDE OIL PRODUCTION IN BARRELS	Cumulative crude oil (bbls) production through 1982	150000

TABLE 2 (cont.)

PROGRAM LINE NUMBER	DATA ELEMENT	DEFINITION	EXAMPLE
170	FIELD PRODUCTIONS	<u>Repeating Group</u> for annual additions to production data	-
170 - 171	YEAR	Latest year of production data	1982
170 - 172	GAS GROSS (in thousands of cubic feet)	Gas (MCF) produced in latest year of production	18000
170 - 173	CONDENSATE (in barrels)	Condensate (bbls) produced in latest year of production	5050
170 - 174	CASINGHEAD GAS (in thousands of cubic feet)	Casinghead gas (MCF) produced in latest year of production	200
170 - 175	CRUDE OIL (in barrels)	Crude oil (bbls) produced in latest year of production	24500

TABLE 2 (cont.)

PROGRAM LINE NUMBER	DATA ELEMENT	DEFINITION	EXAMPLE
190	MINERAL PRODUCTION	<u>Repeating Group</u> for data on minerals produced from salt domes and cap rocks	-
190 - 199	MINERAL NAME	Mineral name	Sulfur
190 - 200	PROD STATUS	Production status for each mineral	Abandoned
190 - 201	METHOD	Mining method; for minerals without production literature reference is cited	Frasch
25 190 - 202	COMPANY	Mining company	Hooker Chemical
190 - 203	HISTORY	Chronology of mining	1945-1965
190 - 204	ENV CODE	Text description for environmental aspects	
190 - 205	ENV COMM 1	Text description for comments	
190 - 206	ENV COMM 2	Text description for comments	

TABLE 2 (cont.)

PROGRAM LINE NUMBER	DATA ELEMENT	DEFINITION	EXAMPLE
225	HYDROCARBON STORAGE CAVERNS	<u>Repeating Group</u> for data on hydrocarbon storage operations	-
225 - 226	COMPANY	Current operator for storage operation	Texaco
225 - 227	ORIGINAL APPLICANT	Original applicant for storage operation	Texas Co.
225 - 228	TOTAL NUMBER OF CAVERNS	Total number of caverns created by operator; may include brine caverns	20
225 - 229	TOTAL CAVERN STORAGE CAPACITY IN BARRELS	Sum of storage capacity (bbls) used in 1983	2000000
225 - 230	RRC SPECIAL ORDER NUMBER	Railroad Commission authorization number for cavern creation and use	03-29667
235	STORED PRODUCT	<u>Repeating Group</u> for various products stored by operator	-
235 - 236	PRODUCT STORED	Name or type of hydrocarbon stored	Natural gas

TABLE 2 (cont.)

PROGRAM LINE NUMBER	DATA ELEMENT	DEFINITION	EXAMPLE
400	AQUIFER WATER CHEMISTRY	<u>Repeating Group</u> for aquifer data; all data compiled by Texas Department of Water Resources	-
400 - 401	AQUIFER	Name of aquifer for which data applies; area of interest is within grid boundaries in program lines 5, 6, 7, and 8	Sparta
400 - 402	TOTAL NUMBER OF WELLS SURVEYED	Number of wells with water chemistry available	8
27 400 - 403	LOWER NA IONS	Lowest value of Na (mg/L) reported for wells surveyed	20
400 - 404	HIGHER NA IONS	Highest value of Na ⁺ (mg/L) reported for wells surveyed	50
400 - 405	LOWER SO ₄ IONS	Lowest value of SO ₄ (mg/L) reported for wells surveyed	10
400 - 406	HIGHER SO ₄ IONS	Highest value of SO ₄ (mg/L) reported for wells surveyed	30
400 - 407	LOWER CL IONS	Lowest value of Cl (mg/L) reported for wells surveyed	10
400 - 408	HIGHER CL IONS	Highest value of Cl (mg/L) reported for wells surveyed	80
400 - 409	LOWER TDS	Lowest value of TDS (mg/L) reported for wells surveyed	2000
400 - 410	HIGHER TDS	Highest value of TDs (mg/L) reported for wells surveyed	35000

TABLE 2 (cont.)

PROGRAM LINE NUMBER	DATA ELEMENT	DEFINITION	EXAMPLE
425	MUNICIPALITIES PUBLIC GROUND-WATER USE NEAR DOME	<u>Repeating Group</u> listing all municipalities using ground water near dome	-
425 - 426	USER	Name of municipality using ground water	Mount Belvieu
430	INDUSTRIES USING GROUND WATER NEAR DOME	<u>Repeating Group</u> listing all industries using ground water near dome	-
28 430 - 431	INDUSTRIAL USER	Name of industrial user	Exxon
440	POPULATION CENTERS NEAR DOME	<u>Repeating Group</u> listing all population centers near dome with grid defined in program lines 5, 6, 7, and 8	
440 - 441	TOWN NAME	Name of population center	Port Neches
440 - 442	DISTANCE FROM DOME CENTER	Distance (feet) from center of population center to center of dome	8500
500	SALT-DOME DATA BASE DOCUMENTATION	<u>Repeating Group</u> with documentation of data base	-
500 - 501	DOCUMENTATION	Source of data	RRC
500 - 502	REPORTING YEAR	Date of referenced documentation	1984

Table 3. Data base organization.

```

DESCRIBE:
SYSTEM RELEASE NUMBER      2.60F
DATA BASE NAME IS DOMES
DEFINITION NUMBER        13
DATA BASE CYCLE           598
1* DOME NAME (TEXT X(20))
2* DOME CODE (NAME X(6) WITH SOME FUTURE ADDITIONS)
3* LATITUDE (NAME X(15))
4* LONGITUDE (NAME X(15))
5* GRID LATITUDE-NORTH (NAME X(15))
6* GRID LATITUDE-SOUTH (NAME X(15))
7* GRID LONGITUDE-WEST (NAME X(15))
8* GRID LONGITUDE-EAST (NAME X(15))
21* SHALLOWEST CAP ROCK DEPTH-IN FEET (INTEGER NUMBER 9(5))
22* SHALLOWEST SALT DEPTH-IN FEET (INTEGER NUMBER 9(5))
23* DEEPEST DEPTH CONTROL ON SALT-IN FEET (INTEGER NUMBER 9(5))
31* MAJOR AXIS LENGTH-IN FEET (INTEGER NUMBER 9(9))
32* MAJOR AXIS ORIENTATION-IN DEGREES (INTEGER NUMBER 999)
33* MINOR AXIS LENGTH-IN FEET (INTEGER NUMBER 9(9))
40* AREA OF PLANAR CREST-IN SQUARE FEET (DECIMAL NUMBER 9(9).9)
41* PLANAR CREST PERCENTAGE (DECIMAL NUMBER 99.9)
50* GENERAL SHAPE (TEXT X(80))
51* AXIAL RATIO (DECIMAL NUMBER 99.999)
52* PLAN SHAPE (TEXT X(80))
53* DOME SYMMETRY (TEXT X(12))
54* AXIS (TEXT X(80))
55* AXIAL TILT ANGLE-IN DEGREES (INTEGER NUMBER 99)
56* AXIAL TILT ORIENTATION-IN DEGREES (INTEGER NUMBER 999)
57* AXIAL TILT DISTANCE-IN FEET (INTEGER NUMBER 9(5))
58* CREST (TEXT X(80))
59* SIDES (NON-KEY TEXT X(200))
70* MAXIMUM TRUE THICKNESS OF CAP ROCK-IN FEET (INTEGER NUMBER 9999
)
71* MINIMUM TRUE THICKNESS OF CAP ROCK-IN FEET (INTEGER NUMBER 9999
)
72* CAP ROCK MINERALOGY (NON-KEY TEXT X(100))
73* CAP ROCK LOST-CIRCULATION ZONES PA (TEXT X(7))
74* CAP ROCK LOST-CIRCULATION ZONES INFO (NON-KEY TEXT X(100))
75* SULFIDE MINERALS (TEXT X(7))
76* GENERAL DOME INFORMATION (NON-KEY TEXT X(100))
81* LATERAL EXTENT OF RIM SYNCLINE-IN FEET (TEXT X(10))
82* LATERAL EXTENT OF DRAG ZONE-IN FEET (TEXT X(10))
83* MAXDIPVERTVAR1-IN DEGREES FEET (TEXT X(10))
84* MINDIPVERTVAR2-IN DEGREES FEET (TEXT X(10))
85* MAXDIPVERTVAR3-IN DEGREES FEET (TEXT X(10))
102* YOUNGEST FAULTED STRATA (TEXT X(30))
103* OLDEST STRATA ON SURFACE (NON-KEY TEXT X(100))
110* RELIEF OVER DOME (NON-KEY TEXT X(50))
120* SINKHOLES (TEXT X(7))
121* SINKHOLE INFO (NON-KEY TEXT X(100))
122* SURFACE SALINES (TEXT X(10))
123* CONFIGURATION OF OVERBURDEN (NON-KEY TEXT X(100))
220* PRODUCT STORAGE STATUS (NAME X(10) WITH MANY FUTURE ADDITIONS)
221* STORAGE METHOD (NAME X(10) WITH MANY FUTURE ADDITIONS)
222* NUMBER OF CAVERNS (INTEGER NUMBER 99)
223* TOTAL STORAGE CAPACITY-IN BARRELS (INTEGER NUMBER 9(9))
420* REGIONAL DEPTH OF BASE OF SLIGHTLY SALINE GROUNDWATER -IN FEET
(INTEGER NUMBER 9(5))
421* DEPTH OF BASE OF SLIGHTLY SALINE GROUNDWATER OVER DOME-IN FEET
(INTEGER NUMBER 9(5))
422* SALINE ANOMALIES IN GROUNDWATER (TEXT X(20))
435* GROUNDWATER IRRIGATION NEAR DOME-IN ACRES (TEXT X(50))
445* SURVEY NAME FOR CENTER OF DOME (TEXT X(100))
446* SALT BASIN (TEXT X(20))

```

10* COUNTIES (RG)
 11* COUNTYNAME (NAME X(20) IN 10 WITH SOME FUTURE ADDITIONS)
 34* AREA STATISTICS (RG)
 35* DEPTH OF AREA CALCULATION-IN FEET (INTEGER NUMBER 9(9) IN 34)
 36* AREA IN SQUARE FEET FOR DEPTH OF 35 (DECIMAL NUMBER 9(9).9 IN 34)
 60* OVERHANG (RG)
 61* OVERHANG INFO (NON-KEY TEXT X(200) IN 60)
 62* OVERHANG ORIENTATION 1-IN DEGREES (INTEGER NUMBER 999 IN 60)
 63* OVERHANG ORIENTATION 2-IN DEGREES (INTEGER NUMBER 999 IN 60)
 64* OVERHANG AZIMUTH-IN DEGREES (INTEGER NUMBER 999 IN 60)
 65* LATERAL OVERHANG-IN FEET (INTEGER NUMBER 9999 IN 60)
 66* PERCENTAGE OVERHANG (DECIMAL NUMBER 9999.9 IN 60)
 90* ANGLE BETWEEN SALT STOCK-STRATA (RG)
 91* ANGLE-IN DEGREES (INTEGER NUMBER 999 IN 90)
 92* DEPTH-IN FEET (INTEGER NUMBER 9(5) IN 90)
 100* ADJACENT STRATA FAULTING (RG)
 101* FAULT DESCRIPTION (TEXT X(50) IN 100 WITH MANY FUTURE ADDITIONS)
 111* DRAINAGE SYSTEMS (RG)
 112* DRAINAGE TYPE (TEXT X(100) IN 111 WITH MANY FUTURE ADDITIONS)
 150* HYDROCARBON RESOURCES (RG)
 151* FIELD NAME PRODUCING HORIZON (TEXT X(100) IN 150)
 152* RRC DISTRICT (NAME X IN 150 WITH SOME FUTURE ADDITIONS)
 153* COUNTY (NAME X(20) IN 150)
 154* DISCOVERY DATE (NAME XXXX IN 150 WITH MANY FUTURE ADDITIONS)
 155* FIELD DEPTH-IN FEET (INTEGER NUMBER 9(5) IN 150 WITH SOME FUTURE ADDITIONS)
 156* API GRAVITY (NAME XXXX IN 150 WITH SOME FUTURE ADDITIONS)
 157* ENVIRONMENTAL CODE (NAME X(5) IN 150 WITH MANY FUTURE ADDITIONS)
 158* ENV COMM 1 (NON-KEY TEXT X(250) IN 150)
 159* ENV COMM 2 (NON-KEY TEXT X(250) IN 150)
 160* ENV COMM 3 (NON-KEY TEXT X(250) IN 150)
 161* ENV COMM 4 (NON-KEY TEXT X(250) IN 150)
 165* CUMULATIVE CRUDE OIL PRODUCTION-IN BARRELS (INTEGER NUMBER 9(11) IN 150)
 170* FIELD PRODUCTION (RG IN 150)
 171* YEAR (NAME XXXX IN 170 WITH MANY FUTURE ADDITIONS)
 172* GAS GROSS-IN THOUSANDS OF CUBIC FEET (INTEGER NUMBER 9(10) IN 170)
 173* CONDENSATE-IN BARRELS (INTEGER NUMBER 9(10) IN 170)
 174* CASINGHEAD GAS-IN THOUSANDS OF CUBIC FEET (INTEGER NUMBER 9(10) IN 170)
 175* CRUDE OIL-IN BARRELS (INTEGER NUMBER 9(10) IN 170)
 190* MINERAL PRODUCTION (RG)
 199* MINERAL NAME (NAME X(10) IN 190 WITH MANY FUTURE ADDITIONS)
 200* PROD STATUS (NAME X(20) IN 190 WITH MANY FUTURE ADDITIONS)
 201* METHOD (NAME X(50) IN 190 WITH MANY FUTURE ADDITIONS)
 202* COMPANY (NAME X(50) IN 190 WITH SOME FUTURE ADDITIONS)
 203* HISTORY (NON-KEY TEXT X(100) IN 190)
 204* ENV CODE (NAME X(10) IN 190 WITH MANY FUTURE ADDITIONS)
 205* ENV COMM1 (NON-KEY TEXT X(250) IN 190)
 206* ENV COMM2 (NON-KEY TEXT X(250) IN 190)
 225* HYDROCARBON STORAGE CAVERNS (RG)
 226* COMPANY NAME (TEXT X(150) IN 225 WITH MANY FUTURE ADDITIONS)
 227* ORIGINAL APPLICANT (TEXT X(150) IN 225)
 228* TOTAL NUMBER OF CAVERNS (INTEGER NUMBER 9(5) IN 225)
 229* TOTAL CAVERN STORAGE CAPACITY-IN BARRELS (INTEGER NUMBER 9(9) IN 225)
 230* RRC SPECIAL ORDER NUMBER (NON-KEY TEXT X(150) IN 225)
 235* STORED PRODUCT (RG IN 225)
 236* PRODUCT STORED (TEXT X(30) IN 235 WITH SOME FUTURE ADDITIONS)
 400* AQUIFER WATER CHEMISTRY (RG)
 401* AQUIFER (TEXT X(40) IN 400 WITH MANY FUTURE ADDITIONS)
 402* TOTAL NUMBER OF WELLS SURVEYED (INTEGER NUMBER 9(5) IN 400)

- 403* LOWER NA IONS-IN MILLIGRAMS PER LITER (INTEGER NUMBER 9(5) IN 400)
- 404* HIGHER NA IONS-IN MILLIGRAMS PER LITER (INTEGER NUMBER 9(5) IN 400)
- 405* LOWER SO4 IONS-IN MILLIGRAMS PER LITER (INTEGER NUMBER 9(5) IN 400)
- 406* HIGHER SO4 IONS-IN MILLIGRAMS PER LITER (INTEGER NUMBER 9(5) IN 400)
- 407* LOWER CL IONS-IN MILLIGRAMS PER LITER (INTEGER NUMBER 9(5) IN 400)
- 408* HIGHER CL IONS-IN MILLIGRAMS PER LITER (INTEGER NUMBER 9(5) IN 400)
- 409* LOWER TDS-IN MILLIGRAMS PER LITER (INTEGER NUMBER 9(5) IN 400)
- 410* HIGHER TDS-IN MILLIGRAMS PER LITER (INTEGER NUMBER 9(5) IN 400)
- 425* MUNICIPALITIES USING GROUND WATER NEAR DOME (RG)
- 426* USER (NON-KEY TEXT X(100) IN 425)
- 430* INDUSTRIES USING GROUND WATER NEAR DOME (RG)
- 431* INDUSTRIAL USERS (NON-KEY TEXT X(100) IN 430)
- 440* POPULATION CENTERS NEAR DOME (RG)
- 441* TOWN NAME (TEXT X(50) IN 440 WITH MANY FUTURE ADDITIONS)
- 442* DISTANCE FROM DOME CENTER (INTEGER NUMBER 9(5) IN 440 WITH MANY FUTURE ADDITIONS)
- 500* SALT DOME DATA BASE DOCUMENTATION (RG)
- 501* DOCUMENTATION (NAME X(50) IN 500)
- 502* REPORTED YEAR (TEXT X(10) IN 500)

Table 4. Information on storage operations in Texas domes. Computer code to produce table shown at bottom.

NAME OF SALT DOME	CURRENT OPERATOR OF STORAGE FACILITIES	ORIGINAL APPLICANT	NUMBER OF CAVERNS	STORAGE CAPACITY IN BARRELS	PRODUCT STORED

* BARBERS HILL	TEXAS EASTERN	TEXAS NATURAL GASOLINE	27	30978000	LIGHT HYDROCARBONS
* BARBERS HILL	DIAMOND SHAMROCK	DIAMOND SHAMROCK	10	34700000	LIGHT HYDROCARBONS
* BARBERS HILL	WARREN	WARREN	29	45032000	LIGHT HYDROCARBONS
* BARBERS HILL	X-RAL	X-RAL	16	22065000	LIGHT HYDROCARBONS
* BARBERS HILL	TENNECO	TENNESSEE GAS TRANSMISSION	18	9823000	LIGHT HYDROCARBONS
* BARBERS HILL	EXXON	HUMBLE OIL AND REFINING	7	5710000	LIGHT HYDROCARBONS
* BARBERS HILL	ENTERPRISE	ENTERPRISE	13	13300000	LIGHT HYDROCARBONS
* BARBERS HILL	CONOCO	CONOCO	3	1200000	LIGHT HYDROCARBONS
* BARBERS HILL	ARCO	TEXAS BUTADIENE AND CHEMICAL CORP.	14	4914000	LIGHT HYDROCARBONS
* BETHEL DOME	BI-STONE FUEL	BI-STONE FUEL	3	9000000	NATURAL GAS
* BIG HILL	UNION	PURE OIL CO.	2	640000	LIGHT HYDROCARBONS
* BIG HILL	DEPARTMENT OF ENERGY	DEPARTMENT OF ENERGY	14	0	CRUDE OIL
* BLUE RIDGE	ABANDONED	TULOHY-AMOCO	3	0	LIGHT HYDROCARBONS
* BOLING	VALERO	LO-VACA GATERING CO.	4	10000000	NATURAL GAS
* BRENHAM	SEMINOLE PIPELINE CO.	SEMINOLE PIPELINE CO.	1	49000	LIGHT HYDROCARBONS
* BRYAN MOUND	DEPARTMENT OF ENERGY	DOW CHEMICAL	4	56800000	CRUDE OIL
* BRYAN MOUND	DEPARTMENT OF ENERGY	DEPARTMENT OF ENERGY	12	0	CRUDE OIL
* BUTLER DOME	U.P.G.	FREESTONE UNDERGROUND STOR.	3	490000	LIGHT HYDROCARBONS
* CLEMENS	PHILLIPS PETROLEUM	PHILLIPS PETROLEUM	17	5360000	LIGHT HYDROCARBONS
* DAY	ABANDONED	PURE OIL	1	0	LIGHT HYDROCARBONS
* EAST TYLER	TEXAS EASTMAN	WARREN PETROLEUM	10	4900000	LIGHT HYDROCARBONS
* FANNETT	WARREN PETROLEUM	GULF OIL	5	2428000	LIGHT HYDROCARBONS
* HAINESVILLE	BUTANE SUPPLIES	ENTERPRISE PETROLEUM GAS CORP.	3	1742000	LIGHT HYDROCARBONS
* HULL	MOBIL	MAGNOLIA PETROLEUM CORP.	11	8680000	LIGHT HYDROCARBONS
* MARKHAM	TEXAS BRINE	TEXAS BRINE	9	1900000	LIGHT HYDROCARBONS
* MARKHAM	SEADRIFT PIPELINE	SEADRIFT PIPELINE	6	7455000	LIGHT HYDROCARBONS
* MOSS BLUFF	MOSS BLUFF STORAGE VENTURE	MOSS BLUFF STORAGE VENTURE	5	0	LIGHT HYDROCARBONS
* NORTH DAYTON	ENERGY STORAGE TERMINAL INC.	ENERGY STORAGE TERMINAL INC.	2	0	LIGHT HYDROCARBONS
* PIERCE JUNCTION	ENTERPRISE	WANDA PETROLEUM AND ELLIS TRANSPORT	10	4060000	LIGHT HYDROCARBONS
* PIERCE JUNCTION	COASTAL STATES CRUDE GATHERING	COASTAL STATES CRUDE GATHERING	7	12734000	LIGHT HYDROCARBONS
* SOUR LAKE	TEXACO	THE TEXAS CO.	8	1196000	LIGHT HYDROCARBONS
* STRATTON RIDGE	SEMINOLE PIPELINE	SEMINOLE PIPELINE	4	152000	LIGHT HYDROCARBONS
* STRATTON RIDGE	AMOCO	FENIX AND SCISSON	7	5257000	LIGHT HYDROCARBONS
* STRATTON RIDGE	DOW	DOW	22	7000000	LIGHT HYDROCARBONS

```

LIST/TITLE L(18)NAME OF SALT DOME,B(1),R(30)CURRENT OPERATOR OF
LIST/TITLE L(18)NAME OF SALT DOME,B(1),R(30)CURRENT OPERATOR OF
STORAGE FACILITIES ,B(1),R(36)ORIGINAL APPLICANT ,B(1),
STORAGE FACILITIES ,B(1),R(36)ORIGINAL APPLICANT ,B(1),

R(7)NUMBER +OF +CAVERNS,B(1),R(10)STORAGE +CAPACITY +IN BARRELS,B(3),
R(7)NUMBER +OF +CAVERNS,B(1),R(10)STORAGE +CAPACITY +IN BARRELS,B(3),

R(18)PRODUCT STORED /C1,C226,C227,C229,C235,OB LOW C1 WH C226 EXISTS:
R(18)PRODUCT STORED /C1,C226,C227,C229,C235,OB LOW C1 WH C226 EXISTS:
    
```


Table 5. Information on rock salt and brine mining in Texas domes. Computer code to produce table shown at bottom.

NAME OF SALT DOME	MINERAL	STATUS OF PRODUCTION	REPORTING ORGANAZATION OR MINING METHOD	NAME OF COMPANY	MINING HISTORY

* BARBERS HILL	BRINE	ACTIVE	BRINE WELLS	DIAMOND SHAMROCK	
* BLUE RIDGE	BRINE	ACTIVE	BRINE WELLS	UNITED SALT	
* BLUE RIDGE	ROCK SALT	ABANDONED	SALT MINE	UNITED SALT	
* BROOKS DOME	BRINE	ABANDONED	L.S.U.-1976	UNKNOWN	1865
* BRYAN MOUND	BRINE	ABANDONED	BRINE WELLS	DOW CHEMICAL	
* GRAND SALINE DOME	ROCK SALT	ACTIVE	SALT MINE	MORTON SALT	
* GRAND SALINE DOME	BRINE	ABANDONED	BRINE WELLS	MORTON SALT	1845
* HOCKLEY	ROCK SALT	ACTIVE	SALT MINE	UNITED SALT	1929-PRESENT
* MARKHAM	BRINE	ACTIVE	BRINE WELLS	TEXAS BRINE CORP.	
* PALANGANA DOME	BRINE	ACTIVE	BRINE WELLS	P.P.G. IND. INC.	
* PALESTINE DOME	BRINE	ABANDONED	L.S.U.-1976	UNKNOWN	1865
* PIERCE JUNCTION	BRINE	ACTIVE	BRINE WELLS	TEXAS BRINE CORP.	
* SPINDLETOP	BRINE	ACTIVE	BRINE WELLS	TEXAS BRINE CORP.	
* STEEN DOME	BRINE	ABANDONED	L.S.U.-1976	UNKNOWN	1865
* STRATTON RIDGE	BRINE	ACTIVE	BRINE WELLS	DOW CHEMICAL	
* WHITEHOUSE DOME	BRINE	ABANDONED	L.S.U.-1976	UNKNOWN	

LIST/TITLE L(18)NAME OF SALT DOME,B(4),R(9)MINERAL ,B(4),R(10)

LIST/TITLE L(18)NAME OF SALT DOME,B(4),R(9)MINERAL ,B(4),R(10)

STATUS OF +PRODUCTION,B(4),R(22)REPORTING ORGANAZATION+

STATUS OF +PRODUCTION,B(4),R(22)REPORTING ORGANAZATION+

OR MINING METHOD ,B(4),R(18)NAME OF COMPANY ,B(4),R(14)MINING HISTORY/

OR MINING METHOD ,B(4),R(18)NAME OF COMPANY ,B(4),R(14)MINING HISTORY/

C1,C199,C200,C201,C202,C203,OB LOW C1 WH C199 EQ ROCK SALT OR C199 EQ BRINE:

C1,C199,C200,C201,C202,C203,OB LOW C1 WH C199 EQ ROCK SALT OR C199 EQ BRINE:

Table 6. Information on sulfur mining in Texas domes. Computer code to produce table shown at bottom.

NAME OF SALT DOME	MINERAL	STATUS OF PRODUCTION	MINING HISTORY	NAME OF COMPANY

* BIG CREEK	SULFUR	ABANDONED	1925-1926	UNION SULPHUR
* BOLING	SULFUR	ACTIVE	1929-PRESENT	TEXASGULF, INC
* BOLING	SULFUR	ABANDONED	1928-1929	UNION SULPHUR
* BOLING	SULFUR	ABANDONED	1935-1935	BAKER-WILLIAMS
* BOLING	SULFUR	ABANDONED	1935-1940	DUVAL SULPHUR AND POTASH
* BRYAN MOUND	SULFUR	ABANDONED	1967-1968	HOOVER CHEMICAL
* BRYAN MOUND	SULFUR	ABANDONED	1912-1935	FREEMONT SULPHUR
* CLEMENS	SULFUR	ABANDONED	1937-1960	JEFFERSON LAKE SULPHUR
* DAMON MOUND	SULFUR	ABANDONED	1953-1957	STANDARD SULPHUR
* FANNETT	SULFUR	ABANDONED	1958-1977	TEXASGULF
* GULF	SULFUR	ABANDONED	1910-1936	TEXAS GULF SULPHUR
* GULF	SULFUR	ABANDONED	1965-1970	TEXAS GULF SULPHUR
* HIGH ISLAND	SULFUR	ABANDONED	1968-1971	PAN AMERICAN PETROLEUM CO.
* HIGH ISLAND	SULFUR	ABANDONED	1960-1962	UNITED STATES SULPHUR
* HOSKINS MOUND	SULFUR	ABANDONED	1923-1955	FREEMONT SULPHUR
* LONG POINT	SULFUR	ABANDONED	1946-1982	JEFFERSON LAKE SULPHUR
* LONG POINT	SULFUR	ABANDONED	1930-1938	TEXAS GULF SULPHUR
* MOSS BLUFF	SULFUR	ABANDONED	1949-1982	TEXASGULF
* NASH	SULFUR	ABANDONED	1966-1969	PHILAN SULPHUR
* NASH	SULFUR	ABANDONED	1954-1956	FREEMONT SULPHUR
* ORCHARD	SULFUR	ABANDONED	1938-1970	DUVAL SALES
* PALANGANA DOME	SULFUR	ABANDONED	1929-1935	DUVAL SALES
* SPINDLETOP	SULFUR	ABANDONED	1952-1976	TEXASGULF

LIST/TITLE L(18)NAME OF SALT DOME,B(4),R(7)MINERAL,B(4),R(10)STATUS OF +
 LIST/TITLE L(18)NAME OF SALT DOME,B(4),R(7)MINERAL,B(4),R(10)STATUS OF +

PRODUCTION,B(4),R(15)MINING HISTORY,B(4),R(30)NAME OF COMPANY /
 PRODUCTION,B(4),R(15)MINING HISTORY,B(4),R(30)NAME OF COMPANY /

C1,C199,C200,C203,C202,08 LOW C1 WH C199 EQ SULFUR:
 C1,C199,C200,C203,C202,08 LOW C1 WH C199 EQ SULFUR: